Climate and environmental evolution in Late Pliocene and Quaternary sediments of coastal northwest Germany and Early–Middle Pleistocene of the Upper Jordan Valley, Israel

Der Fakultät Nachhaltigkeit der Leuphana Universität Lüneburg zur Erlangung des Grades Doktorin der Naturwissenschaften
-Dr. rer. nat.-

vorgelegte Dissertation von

Maria Sekar Proborukmi
geb. 29. Juli 1985 in: Yogyakarta, Indonesien

Eingereicht am:	29.03.2017
Betreuerin und Gutachterin:	Prof. Dr. Brigitte Urban
Betreuer und Gutachter:	Prof. Dr. Manfred Frechen
Gutachterin:	Prof. Dr. Naama Goren-Inbar
Tag der Disputation:	02.11.2017

„The past is the key to the present"

-Sir Charles Lyell-

Preface

This dissertation is based on the results and conclusions of the papers listed below. These papers are described and cited in the framework paper as follows:

Paper I

Proborukmi, M.S., Urban, B., Frechen, M., Grube, A. & Rolf, C. (2017): Late Pliocene–Pleistocene record of the Garding-2 research drill core, Northwest Germany. – Z. Dt. Ges. Geowiss., 168 (1): 141–167. DOI: 10.1127/zdgg/2017/0103.

Paper II

Proborukmi, M.S. & Urban, B. (2017): Palaeoenvironmental investigations of the Holocene sedimentary record of the Garding-2 research drill core, northwestern Germany. – Z. Dt. Ges. Geowiss., 168 (1): 39–51. DOI: 10.1127/zdgg/2017/0098.

Paper III

Proborukmi, M.S., Urban, B., Mischke, S., Mienis, H.K., Melamed, Y., Dupont-Nivet, G., Jourdan, F. & Goren-Inbar, N. (2018): Evidence for climatic changes around the Matuyama-Brunhes Boundary (MBB) inferred from a multi-proxy palaeoenvironmental study of the GBY#2 core, Jordan River Valley, Israel. – Palaeogeogr., Palaeoclimatol., Palaeoecol., 489 (C): 166–185. DOI: 10.1016/j.palaeo.2017.10.007.

Copyright notice

Declaration of originality

I hereby certify that this dissertation entitled: ”**Climate and environmental evolution in Late Pliocene and Quaternary sediments of coastal northwest Germany and Early–Middle Pleistocene of the Upper Jordan Valley, Israel**’’ is:

1. written by me without using unauthorised aids,
2. the result of my own work and includes nothing which is the outcome of work done in collaboration except as declared in Appendix A, specified in the text and acknowledged in citations,
3. neither as a whole nor in parts been submitted to any other degree assessments and purposes at Leuphana University of Lüneburg or at other universities and institutions.

Lüneburg, 29.03.2017

Maria Sekar Proborukmi

Acknowledgements

Firstly, I would like to thank God for all the graces, strength and protections.

Secondly, I would like to express my sincere gratitude to Prof. Dr. Brigitte Urban for her continuous support and encouragement for my doctoral study and related researches, her motivation, advice, patience, kindness and her immense knowledge. Her guidance has helped me through the whole doctoral study and I could not imagine having a better mentor and supervisor for my doctoral research.

Thirdly, I would also like to thank Prof. Dr. Manfred Frechen, who always provided time and options for stimulating discussions, for field trips and for assistance with production and publishing processes of my dissertation.

I would like to thank Prof. Dr. Naama Goren-Inbar for her insightful comments, the hard questions and support which have driven me to widen my research.

I am also indebted to DAAD-IGSP program and the DAAD-International Office Leuphana University of Lüneburg, which provided me with a scholarship for the first four years and three months of my doctoral study in Germany, which not only gave me the opportunities to upgrade my scientific knowledge and skills, but also enriched my perspective and life experiences.

I am honoured to get the chance to work with wonderful scientists in the Garding research group, Dr. Alf Grube (Ministry of Environment and Energy, Hamburg), Dr. Christian Rolf (Leibniz Institute for Applied Geophysics, Flintbeck), Dr. Tsumiko Sukamoto (Leibniz Institute for Applied Geophysics, Hannover), Dr. Jingran Zhang (Leibniz Institute for Applied Geophysics, Hannover) and Christel Adams, M.Sc. (Johannes Gutenberg University of Mainz), as well as the GBY#2 research group, Prof. Dr. Steffen Mischke (University of Iceland), Dr. Yoel Melamed (Bar Ilan University, Ramat Gan) and Dr. Guillaume Dupont-Nivet (Université de Rennes 1, University of Potsdam). Thank you for your hard work, and for the meetings, discussions, amazing results, co-operations and friendships.

My gratitude also goes to Prof. Dr. Peter Kershaw, (Monash University, Australia) for his valuable insights, comments and input in improving the manuscripts that comprise this dissertation.

I am sincerely grateful to Micha Edlich, Janine Murphy and Eoin Ryan (Writing Center for Academic English of Leuphana University of Lüneburg) for their helps and suggestions to f the English of this dissertation.

This dissertation could not have been completed without the great support I have received from so many people over the years, therefore my sincere thanks also goes to the following people:

- My fellow PhD students of Leuphana University of Lüneburg, who had struggled together with me: Khin Zarkyaw from Myanmar, Elizabeth Patricia Minaya Bedon from Peru, Frank Krüger, Zawzaw Latt from Myanmar, Emillio Tores from Chile, Silvia Materu from Tanzania, Emad Elba and Dalia Farghaly from Egypt, Yanyan Su from China, Tsany Ratna Dewi from Indonesia, Saifudin Saleh from Malaysia and Elaheh Nosratirad from Iran, thank you for all support and good times that we had together. I hope we can keep up with our works and making further steps to develop our research and home countries.

- The soil science research group member: Sabine Hansen, Mario Tucci, Karin Dziarski, Isa Schierholz, Caroline Thiem, Verena Küppers and Ligia Arias, thank you for your assistance with laboratory work, sampling and solving some administrative issues as well as your companion and help during our free times.

- Ernawita, Hasan Bashari, Irvan Yulianto, Siskha Prabawaningtyas and Lucia Dwi Krisnawati, who were fighting together with me during the past five years. Sincere gratitude for their kindness, support and for the fun chats that always brightened my days.

- My best friends: Yunita Theresia Gena, Wulandari Mandradewi, Tri Julinawati, Asep Indra Maulana, Dodo Pongpandin Paranoan, Diki Danil and Dendy Surya Fajar, thank you for the honest support, jokes and positivity you have brought to me.

Special thanks to the Dahling family: the late Mr. Dahling, Mrs. Ursel Dahling, Victoria Dahling and Cornelia Dahling for their kindness, for providing the best place to live in Lüneburg, offering strong support of my studies and sharing a lot of good times. They were always there during the difficult times and made my stay in Germany much easier and more enjoyable.

From the bottom of my heart I would like to thank my beloved family; Bapak Matheus Soebagjo, Ibu Kuria Tri Pirenohati, Gerardus Ario Condro Sasongko and Josephine Retno Padmaningrum. Words cannot express how grateful I am for their presence, inspiration, endless moral support and prayers that have been pushing me to carry on, especially in hard times.

Last but not least, I am grateful to Alexis Badai Samudra for his continuous and unconditional love, encouragement, prayers and sacrifices on my behalf, which has been carrying me this far.

Table of Contents

List of abbreviations and symbols

AMS	Accelerator Mass Spectrometry
AP	Arboreal Pollen
BC	Before Christ
BP	Before Present
Eu	European
GBY	Gesher Benot Ya‘aqov
ITM	Israeli Transverse Mercator
ka	Kilo-annum/thousand years
LPAZ	Local Pollen Assemblage Zone
Ma	Mega-annum/million years
MBB	Matuyama-Brunhes Boundary
MIS	Marine Isotope Stage
MPT	Mid-Pleistocene Transition
NAP	Non-Arboreal Pollen
OSL	Optically Stimulated Luminescence
PPB	Pliocene–Pleistocene Boundary
SI	International System of Units

^{14}C	Carbon-14/Radiocarbon
$^{40}Ar/^{39}Ar$	Argon-argon dating
(Ar+Am)/P	(*Artemisia*+Amaranthaceae)/Poaceae
C/N	Carbon/Nitrogen

List of figures

Summary

In this dissertation, a multi-proxy study, which included palaeoecological, lithological, geochemical and geochronological methods, was carried out to investigate climatic and environmental changes and their interaction during the Quaternary in formerly glaciated and non-glaciated areas. The information obtained will be used to provide a better understanding of the regional stratigraphic framework and to establish broader regional terrestrial correlations within the global marine isotope stage (MIS) framework. This study was conducted on two key drillings, the Garding-2 research drill core in the German North Sea coastal area of Schleswig-Holstein and the GBY#2 archaeological core at the Gesher Benot Ya'aqov (GBY) site, in the Upper Jordan Valley in Israel.

The results of this study are presented in three papers. Papers I and II focus on the study of the Garding-2 core, while the multi-proxy study of the GBY#2 core is presented in Paper III. The results of a variety of analyses conducted on the 240 m long Garding-2 sequence show interglacial-glacial cycles that are mainly controlled by variations in temperature. This sequence is composed of mainly fluvial-shallow marine sediments intercalated by muddy-peaty deposits. Based on the palynological and lithological findings, the Pliocene–Pleistocene transition was observed at 182.87 m. It is overlain by Praetiglian and the subsequent sediments of the Waalian and Bavelian Complexes. The boundary of either the second or third Cromerian Interglacial with younger sediments, which still belong to MIS 19, is marked by the last occurrence of *Tsuga* at 119.50 m and the development of mixed-deciduous forests. The palynologically equivalent sediments of the Bilshausen Interglacial were found below two Elsterian till layers, at 89.00 m–82.00 m. These sediments showed high and increased percentages of *Pinus* and *Picea* and scattered occurrences of *Abies* and *Carpinus*, which are similar to the features of the beginning of the Bilshausen or Rhume interglacial (Müller, 1992). An unconformity occurred at 80.29 m, at the bottom of late Holsteinian deposits, characterised by the occurrences of *Fagus* and *Pterocarya*, with low percentages of *Abies* and *Carpinus* and the absence of *Buxus*. These deposits are succeeded by sediments of the Fuhne cold period that shows higher percentages of NAP and occurrences of Ericales, *Helianthemum* and *Selaginella selaginoides*, which are unconformably overlain by Drenthian till at 73.00 m–71.00 m. A single peaty sample at 69.25 m with *Pinus-Picea-Abies* assemblage is correlated with the late Eemian Interglacial. This deposit is overlain by Weichselian glaciofluvial sediments.

Middle-late Holocene sediments occurred from 20 m upwards, following a hiatus, which was caused by the Early Holocene transgression. A subsequent thin layer of marine Atlantic

sediments is unconformably overlain by marine–tidal flat deposits up to 11.00 m. The first occurrence of *Fagus* (at 15.97 m) and *Carpinus* (at 15.03 m), which was optically stimulated luminescence (OSL)-dated to 3130±260 BP (at 16.22 m, Zhang et al., 2014), gives evidence for a Subboreal age for these deposits. Sandy sediments of the early Subatlantic, which were deposited between 11.00 m and the top of the Garding-2 sequence, indicate that local salt marshes, dunes and tidal flat vegetation expanded during this period. Due to regional features and the peculiarities of the local coastal environment, the expansions of *Fagus* and *Carpinus*, which are characteristic for the Subboreal–Subatlantic transition at about 2700 BP in northern Germany, are not clearly reflected in the Garding-2 pollen diagram.

In the Mediterranean area, a 50 m long core of GBY#2, was drilled at the Acheulian site of Gesher Benot Ya‘akov. The GBY#2 core provides a long Early–Middle Pleistocene geological, environmental and climatological record, which also enriches the knowledge of hominin-habitat relationships documented at the margins of the Hula Palaeo-lake. The sediment sequence of GBY#2 is under- and overlain by two basalt flows that are $^{40}Ar/^{39}Ar$ dated: two samples at the bottom of the core dated to 1195 ± 67 ka (at 48.30 m) and 1137 ± 69 ka (at 45.30 m), and another one at the top dated to 659 ± 85 ka (at 14.90 m). With the additional chronological identification of the Matuyama Brunhes Boundary (MBB) and the correlation with the GBY excavation sites, the sedimentary sequence of GBY#2 provides the climatic history during the late part of the mid-Pleistocene transition (MPT, 1.2 Ma–0.5 Ma). Multi-proxy analyses including those of pollen and non-pollen palynomorphs, macro botanical remains, molluscs, ostracods, fish, amphibians and micromammals provide evidence for lake and lake-margin environments during MIS 20 and MIS 19. During MIS 20, relatively cool semi-moist conditions were followed by a pronounced dry phase. During the subsequent MIS 19, warm and moist interglacial conditions were characterised by *Quercus-Pistacia* woodlands in this area. The depositional environment changed from an open water lake during MIS 20 to a lake margin environment in MIS 19. This finding is at odds with changing climate conditions from relatively dry to moist. This discrepancy could be explained by the prograding pattern of the lake shore due to the infilling of the basin, which resulted in shallower water.

Climatic changes during the Late Tertiary and the Quaternary in the high latitude regions in northwest Europe and during the Early–Middle Pleistocene in the mid latitude regions of the Middle East follow the patterns of global climatic changes, which are mainly controlled by orbital obliquity (±41 ka cycle) during the Early Pleistocene and by orbital eccentricity (±100 ka cycle) during the MPT (1.2 Ma–0.5 Ma) and the younger periods of the Quaternary. The results of this study also provide reliable evidence for long distance correlation of stratigraphic and climatic events of the Quaternary, which extends knowledge of regional and global impact of climatic fluctuations on the environment.

Kurzfassung

In dieser Dissertation wurde zur Untersuchung der klimatischen Veränderungen und ihrer Auswirkungen auf die Umweltbedingungen während des Quartärs in früher vergletscherten und in nicht vergletscherten Gebieten und um eine Korrelation mit den marinen Sauerstoffisotopenstadien (MIS) vorzunehmen, eine Multi-Proxy-Untersuchung, die verschiedene paläoökologische, lithologische, geochemische und geochronologische Methoden beinhaltet, durchgeführt. Diese Untersuchung wurde an den beiden Schlüsselbohrungen, der Garding-2-Forschungsbohrung aus dem deutschen Nordseeküstengebiet Schleswig-Holsteins und am archäologischen Standort Gesher Benot Ya'aqov (GBY), an der Kernbohrung GBY#2, im Oberen Jordan-Tal in Israel durchgeführt.

Die Ergebnisse dieser Arbeit werden in drei verschiedenen Artikeln diskutiert, wobei sich Paper I und II auf die Untersuchung des Garding-2 Kerns konzentrieren und die Multi-Proxy-Untersuchung des GBY#2 Kerns in Paper III diskutiert wird. Die Ergebnisse der umfänglichen Analysen, die an der 240 m langen Garding-2-Sequenz durchgeführt wurden, zeigen Interglazial-Glazial Zyklen, die hauptsächlich durch Temperaturschwankungen gesteuert werden. Diese Sequenz besteht aus überwiegend fluviatilen-, respektive flachmarinen Sedimenten, die von Einschaltungen mudde- und torfartiger Ablagerungen unterbrochen werden. Mithilfe der palynologischen und lithologischen Befunde konnte der Pliozän-Pleistozän-Übergang im Bereich von 182.87 m gelegt werden. Diese Sedimente werden von Ablagerungen des Prätiglium und diskordant denen des nachfolgenden Waalium- und Bavelium Komplex überlagert. Das Ende des vermutlich zweiten oder dritten Cromer Interglazials, welches in die MIS 19 gestellt wird, wird von Laubmischwaldelementen und dem letzten Auftreten von *Tsuga* in 119.50 m Tiefe charakterisiert. Die Sedimente des Bilshausen Interglazials wurden unterhalb von zwei Elster Moränen zwischen 89.00 m-82.00 m abgelagert. Diese Sedimente zeigen hohe und ansteigende Pollenanteile von *Pinus* und *Picea* und vereinzeltes Vorkommen von *Abies* und *Carpinus*, die den Merkmalen am Beginn des Interglazials Bilshausen oder Rhume ähneln (Müller, 1992). Eine Diskordanz tritt bei 80.29 m, am Ende der spätholsteinzeitlichen Ablagerungen auf. Die spätholsteinzeitlichen Sedimente ist durch das Auftreten von *Fagus* und *Pterocarya*, mit geringen Anteilen von *Abies* und *Carpinus*, und die Abwesenheit von *Buxus* gekennzeichnet. Diese Sedimente gehen in die nachfolgenden Ablagerungen der Fuhne-Kaltzeit, die wiederum von Drenthe-Grundmoräne zwischen 73.00 m-71.00 m diskordant überlagert werden, über. Eine einzelne Torfprobe bei 69.25 m, mit *Pinus-Picea-Abies* Zusammensetzung

korreliert mit der späten Eem Warmzeit, sie wird von weichselzeitlichen glaziofluvialen Ablagerungen überlagert.

Mittel- bis spätholozäne Sedimente treten von 20 m ab aufwärts nach einem Hiatus auf, der durch die frühholozäne Transgression verursacht wurde. Die sich anschließende gering mächtige marine atlantische Sedimentlage wird durch marine Ablagerungen bis zu 11.00 m diskordant überlagert. Das erste Auftreten von *Fagus* (bei 15.97 m) und *Carpinus* (bei 15.03 m), mit optisch stimulierter Lumineszenz (OSL) datiert auf 3130±260 BP (bei 16.22 m, Zhang et al., 2014), gibt Hinweis auf ein subboreales Alter dieser Ablagerungen. Sandige Sedimente des frühen Subatlantikums, die zwischen 11.00 m und dem oberen Teil der Garding-2-Sequenz abgelagert wurden, deuten darauf hin, dass sich in dieser Zeit lokal Salzmarschen, Dünen und Wattvegetation ausgebreitet haben. Aufgrund der regionalen Eigenschaften und Besonderheiten der Küstenlandschaft, lassen sich die in Norddeutschland bei etwa 2700 BP auftretenden und für den Übergang vom Subboreal zum Subatlantikum charakteristischen signifikanten anthropogenen Eingriffe in die Landschaft sowie der Anstieg von *Fagus* und *Carpinus* nicht eindeutig im Pollendiagramm erkennen.

Im Mittelmeerraum wurde ein 50 m langer Kern an der Acheulian Fundstelle Gesher Benot Ya'akov (GBY), GBY#2 erbohrt. Der GBY#2-Kern umfasst eine lange früh- bis mittelpleistozäne Abfolge, die das Wissen über die geologischen Bedingungen, Umwelt- und Klimaentwicklung und die Mensch-Lebensraum-Beziehungen am Rande des Hula-Paläosees, erweitern. Die GBY#2 Sedimentsequenz wird von zwei Basalt Schichten unter- beziehungsweise überlagert, die mit der $^{40}Ar/^{39}Ar$ Methode datiert wurden: diejenige an der Basis des Kerns wurde auf 1195 ± 67 ka (bei 48.30 m) und auf 1137 ± 69 ka (bei 45.30 m) und diejenige im Hangenden auf 659 ± 85 ka (bei 14.90 m) datiert. Mit der zusätzlichen chronologischen Identifizierung der Matuyama-Brunhes Boundary (MBB) und der Korrelation mit den „GBY Excavations", stellt die GBY#2 Sedimentsequenz die hochauflösende klimatische Geschichte des älteren Teils des Übergangs vom Alt- zum Mittelpleistozän (MPT, von 1.2 Ma bis 0.5 Ma) dar. Die Multi-Proxy-Untersuchung, einschließlich der Pollen- und Nicht-Pollen-Palynomorphen, makro-botanischen Reste, Mollusken, Ostrakoden, Fische, Amphibien und Mikromammalia zeigen See- und Seeuferrand Verhältnisse während MIS 20 und MIS 19 auf. Auf relativ kühle, gering feuchte Bedingungen der MIS 20, folgte eine ausgeprägte Trockenphase. Warme und feuchte interglaziale Bedingungen, die durch *Quercus-Pistacia* Wälder gekennzeichnet sind, herrschten während des anschließenden MIS 19 in der Region vor. Die Ablagerungsbedingungen am Untersuchungsort veränderten sich von einem offenen See während der MIS 20 zu Seeuferrandverhältnissen in MIS 19. Dieser Befund ist mit den wechselnden Klimabedingungen von relativ trocken bis feucht nicht in Übereinstimmung. Diese Diskrepanz kann durch die Seeuferverschiebung aufgrund von Sedimentakkumulation im Hula-Becken erklärt werden, was zu einem flacheren Wasserstand führte.

Die klimatischen Bedingungen und Veränderungen während des Spättertiärs und des Quartärs in Nordwesteuropa und während des späten Altpleistozäns und des frühen Mittelpleistozäns im Nahen Osten folgen dem Muster des globalen Klimawandels, der vor allem während des Frühpleistozäns durch die extraterrestrische Obliquität (Zyklus von 41 ka) und während des Früh-Mittelpleistozän Übergangs (MPT) und den jüngeren Abschnitten des Quartärs von der Exzentrizität (Zyklus von 100 ka) gesteuert wurde. Die Ergebnisse dieser Untersuchung liefern wichtige Datengrundlagen für weiterreichende Fernkorrelationen wichtiger stratigraphischer und klimatischer Quartärevents, die das Wissen über regionale und globale Auswirkungen von klimatischen Schwankungen erweitert haben.

Framework Paper

1. INTRODUCTION

1.1. Background

The earth is a dynamic system in which continuous changes of the atmosphere, geosphere and biosphere affect the environment to different degrees (Nesje and Dahl, 2016). Changes in environmental conditions are influenced strongly by climatic oscillations due to orbital forcing including eccentricity (±100 ka cycle), obliquity (±41 ka cycle) and precession (±20 ka cycle) (Raymo, 1997; Head and Gibbard, 2005; Lisiecki and Raymo, 2005; Ruddiman, 2006; Leroy et al., 2011). Climate changes, in terms of changes in temperature, seasonality, humidity as well as snow distribution, have been considered as a major impact factor on the Quaternary environmental dynamics as well as human evolution in general and human behaviour relating to expansion, migration and cultural development in particular (Jousse, 2006; Joannin et al., 2007a; Tzedakis et al., 2007; Elton, 2008; Bradtmöller et al., 2012). In the Quaternary, orbital obliquity was the main forcing during the Early Pleistocene, which progressively changed to eccentricity forcing. The period of this transition, between 1.2 Ma and 0.5 Ma is known as the mid-Pleistocene transition (MPT) (Berger and Jansen, 1996; Head and Gibbard, 2005). During the onset of this period, ice builts up slowly and melts rapidly. Glacial-interglacial oscillations are more and more forced by obliquity (100-ka cycle). During 0.9 Ma and 0.6 Ma, major glaciations in higher latitudes, a substantial increase of global ice volume at 940 ka as well as the increase of intensity and duration of cold periods were recorded. This change caused a rearrangement of the ocean circulation at the end of this transition, which triggered the increase of biomass production and the decrease of dissolved oxygen that drove some deep sea organisms to extinction. Vegetation in the terrestrial realm indicates cooler and dryer conditions at the beginning of the MPT and relatively warmer and moister ones towards the younger part of the MPT (Head and Gibbard, 2005).

Palaeoenvironmental studies, especially palynological analysis, play an important role when they come to reconstructing climatic and environmental conditions and changes and establishing biostratigraphical frameworks. They provide datasets of Quaternary stratigraphy and climatic and environmental features for broader correlation with other sites during the same chronological timeframe including the period of human migration and settlement. The impact of climatic changes varies depending on the geographical regions, which are more important between formerly glaciated and non-glaciated areas in the northern hemisphere and the lower latitude regions (Van der Wiel and Wijmstra, 1987). It is essential to understand the past climatic and environmental changes in different geographical regions with respect to the global climate picture, especially during the periods of human habitation. These insights are needed to develop sustainable adaptation and development strategies for ecosystems and people.

Many glacial and interglacial characteristics have been described for several Quaternary sediment sequences in Europe. These descriptions have been used to relate and compare regional effects of global climate change and events (Erd, 1970; Menke and Behre, 1973; Menke, 1975; Urban, 1983; Gibbard et al., 1991; Stephan and Menke, 1993; Hahne et al., 1994; Zagwijn, 1994; Zagwijn, 1996; Turner, 1998; Geyh and Müller, 2005; Litt et al., 2007; Hahne et al., 2008; Magri, 2010; Ehlers et al., 2011; Urban et al., 2011; Sirocko et al., 2013; Scheidt et al., 2015). In Germany, the correlations are mainly based on lithostratigraphy and climatostratigraphy that in particular use palynology, for climate reconstruction (Menke, 1968a; Frenzel, 1973; Menke, 1975; Menke, 1976; Urban, 1978a; Eissmann and Müller, 1979; Müller, 1986; Müller, 1992; Benda, 1995; Urban, 1995; Ehlers et al., 2004; Eissmann, 2004; Litt et al., 2007; Urban, 2007; Kleinmann et al., 2011; Urban et al., 2011; Stephan, 2014; Deutsche Stratigraphische Kommission, 2016). Palynological characteristics of the Late Pliocene and Early Pleistocene of the Lieth section, Schleswig-Holstein were described by Menke (1975, 1976). According to these sources, the Pliocene flora is no longer present in the Pleistocene sediments, which based on the climatic variations recorded from this section, are divided into cryomers and thermomers. The Gorleben section, which is partly overlapping with the Lieth section, the Bavelian- and Cromerian Complex of the late Early Pleistocene–Early Middle Pleistocene were palynologically described by Müller (1986, 1992). The sediments of the first ice advance of the Middle Pleistocene in northwestern Germany (Elsterian) are mainly dominated by coarse-grained material with angular quartz blocks and boulder-sized Scandinavian erratics (Ehlers et al., 1984; Ehlers, 1987; Von Hacht, 1987). In western Schleswig-Holstein, a marine transgression started during the Late Elsterian (Diehl, 2007). This transgression was followed by the deposition of Holsteinian sediments in Hamburg, in Hamburg-Hummelsbüttel (Hallik, 1960), Hamburg-Billbrock and -Dockenhuden (Linke and Hallik, 1993). Terrestrial-marine-terrestrial deposits that were found in Bossel dated to pollen zones VI to VIII (Müller and Höfle, 1994; Geyh and Müller, 2005). The onset of the Saalian

Complex is marked by the development of subarctic vegetation of the Fuhne Stadial (Knoth, 1964; Cepek, 1967; Erd, 1970, 1973; Urban et al., 1988) or Mehlbeck (Menke and Behre, 1973) and correlated with MIS 8 (Litt et al., 2007). Several intra Saalian warm periods were also studied: Wacken or Dömnitz (Menke, 1968a; Dücker, 1969; Erd, 1973), Schöningen (Urban et al., 2011), Nachtigall (Kleinmann et al., 2011) and Leck (Stephan et al., 2011; Urban et al., 2011). Menke and Tynni (1984) subdivided the subsequent Eemian Interglacial into seven pollen zones, which were based on the re-immigration sequence of the arboreal taxa in Dithmarschen. During the Weichselian cold period, several interstadials had been identified in surrounding areas (Menke, 1968b; Bock et al., 1985; Behre and Lade, 1986; Behre, 1989; Grüger, 1989; Merkt and Müller, 1999; Litt et al., 2001, 2007). A warming occurred during the end of the Weichselian Lateglacial. The transition from the Younger Dryas to the Preboreal was characterised by an expansion of *Betula* and *Pinus* (Firbas, 1949; Bos, 2001; Litt et al., 2001, 2007; Birks and Birks, 2008). Anthropogenic impact on the environment since the Late Atlantic (Neolithic) has been widely described for pollen records of Schleswig-Holstein (Wiethold, 1998; Behre, 2007; Nelle and Dörfler, 2008). In Mediterranean areas, the effects of climate changes of the Quaternary on vegetation have also been studied to define environmental and stratigraphical frameworks (Horowitz, 1975; Arias et al., 1979; Zohary, 1982; Suc, 1984; Van der Wiel and Wijmstra, 1987; Bertoldi et al., 1989; Horowitz, 1989; Van Zeist and Bottema, 1991; Combourieu-Nebout, 1993; Bottema, 1995; Subally et al., 1999; Suc and Popescu, 2005; Tzedakis et al., 2006; Joannin et al., 2007a; Joannin et al., 2007b, 2008; Langgut, 2008; Van Zeist et al., 2009; Van Zeist and Bottema, 2009; Bertini, 2010; Suc et al., 2010; Maiorano et al., 2016). Records in the Mediterranean generally conform to the global climatic pattern. However, vegetation of the Upper Jordan Valley during the Middle Pleistocene has not experienced major changes related to the glacial-interglacial fluctuations (Van Zeist and Bottema, 2009). Vegetation dynamics in the latter area are more closely related to the variations of humidity rather than temperature, which is characteristic of the Mediterranean climate (Suc, 1984; Van der Wiel and Wijmstra, 1987).

Two independent drillings, which promised great potential for multi-proxy palaeoenvironmental studies, were undertaken to characterise the climatic and environmental conditions of the Quaternary of two different geographical regions mentioned above and to correlate these features in local and regional scales. These drillings are: a) Garding (Garding-2 core), taken under the direction of the Leibniz Institute of Applied Geophysics (LIAG), Hannover, in the coastal area of northwestern Germany, and

b) an archaeological drilling undertaken at Gesher Benot Ya'aqov (GBY) in the Upper Jordan Valley Israel (GBY#2 core), which was initiated and directed by Prof. Dr. Naama Goren-Inbar, Hebrew University Jerusalem, Israel.

Garding Trough has been long investigated and a sequence of Late Tertiary and Quaternary sediments was expected to be found (Menke and Behre, 1973; Hinsc, 1974; Menke, 1976). The core from Oldenswort (OLW) that was taken in 2002 (Stephan, 2002), has not been investigated in a great detail concerning climatic and environmental aspects. Some drilling archives and geological maps of this area were examined and an intensive geophysical study was conducted in the study area. These studies had given evidence of thick and continuous Holocene sediments from a 36 m-long core of Garding-1 (Frechen et al., 2011). Based on these results, the location for a deeper drilling (240 m) of the Garding-2 core was selected. The Garding-2 core was chosen for this study because it offers a long continuous record of the Late Tertiary to Quaternary coastal and coastal-near sediments from the formerly glaciated area. This area has a great potential for a high resolution palynological analysis to characterise climatic patterns and establish climatostratigraphical framework and its effects on palaeoenvironmental conditions of the local area in western Schleswig-Holstein including changes in the composition of local vegetation, temperature, sea level, geomorphology and depositional environment. A comprehensive lithological description of the core (Grube, 2011) as well as geochronological study and sedimentation history of the top 16 ka sedimentary record of this core (Zhang et al., 2014) were carried out and used as important data for this dissertation.

Information on climatic and environmental conditions is also important in an archaeological site such as in the GBY site. The GBY site, and particularly its recent excavations, is part of a narrow embayment located at the south of a freshwater lake in a sedimentary and volcanic terrain (Belitzky, 2002; Feibel, 2001, 2004). The presence of the lake also provides variety of food plants (Melamed et al., 2016), aquatic taxa such as ostracods, molluscs, fish, crabs and amphibians (Ashkenazi et al., 2005, 2010; Mienis and Ashkenazi, 2011; Mischke et al., 2014; Rabinovich and Biton, 2011; Rosenfeld et al., 2004; Zohar et al., 2014; Biton et al., 2013, 2016), and a rich Mediterranean flora (Goren-Inbar et al., 2002a, 2002b) including macro- and micro-botanical remains (Kislev and Melamed, 2011; Van Zeist and Bottema, 2009). Well-preserved archaeological evidence of handaxes, cleavers and flakes of basalt, flint and limestone (Alperson-Afil et al., 2009; Goren-Inbar and Saragusti, 1996; Goren-Inbar and Sharon, 2006; Goren-Inbar et al., 1992, 2000, in press; Sharon et al., 2011), and wood artefacts (Goren-Inbar et al., 1994) were found at this site and assigned to the African Large Flake Acheulian Tradition (Sharon, 2007), which is characterised by modification of handaxes and cleavers made on large flakes. These remains were excavated from the lake sediments that were dated to MIS 20–18 (Goren-Inbar et al., 2000, Melamed et al., 2016). It shows that the GBY hominins had been present for a long duration in the Hula Valley and had exploited their environment to provide a stable and wide variation of subsistence sources. Low frequencies of heavily burned items that are normally produced by natural causes such as lightning, peat burning and volcanism, as well as clustered fire-damaged micro-artefacts possibly indicating hearths (Alperson-Afil, 2008; Alperson-Afil and Goren-Inbar, 2010; Alperson-Afil et al., 2009; Goren-Inbar et al., 2004) suggest that the occurrence of fire around the GBY site was caused by human activities. Based on these results, the first archaeological drilling in the Levant was carried out at the GBY site, and the GBY#2 core was taken about 300 m to the north of the GBY excavations. This core provides a shorter period of sedimentation than the Garding-2. However, it has a great possibility for high resolution palynological and multi-proxy investigations including plant macro-remains, molluscs, ostracods, micro-mammals, amphibian and fish, which were deposited together with the sediments of the Early–Middle Pleistocene age. These detailed multi-proxy palaeoenvironmental studies and micro-charcoal particle investigation of the GBY#2 core have also been conducted for the first time at the GBY archaeological site. Considering this promising information, this dissertation used palynology, which has also been applied by Suc and Zagwijn (1983) and Van der Wiel and Wijmstra (1987), as the main method to infer changes of vegetation in Western Europe and the Mediterranean with respect to the Quaternary glacial and interglacial features. Additional analyses of micro- and macro- biological remains, which are combined in a multi-proxy study, were used to further describe the environmental conditions.

Depending on the age and type of the sediments, suitable dating methods such as OSL, radiocarbon, palaeomagnetic and argon-argon dating ($^{40}Ar/^{39}Ar$) were carried out in these cores. The sediments of the Garding-2 core provide a Late Tertiary–Quaternary record including important climatic and chronological events such as Pliocene-Pleistocene Boundary (PPB) and the following Early-Middle Pleistocene transition (MPT). The Early−Middle Pleistocene boundary is important, especially for sediment records from Germany, as it is followed by three well-studied glaciations. The oldest known glaciation is the Elsterian (MIS 12/MIS 10), which is followed by the Saalian (MIS 8–MIS 6) and the Weichselian (MIS 4–MIS 2) (Litt et al., 2007; Gibbard and Cohen, 2008; Graham et al., 2011; Roskosch et al., 2015; Cohen and Gibbard, 2016; Deutsche Stratigraphische Kommission, 2016; Kunz et al., 2016). The MPT has been identified in the GBY#2 core by the Matuyama-Brunhes palaeomagnetic boundary (MBB) at 780 ka (MIS 19) (Head and Gibbard, 2005; Lisiecki and Raymo, 2005). This boundary can be used as a main reference point for the correlation and comparison of the climatic and environmental conditions of these two records as well as other important sites of the same depositional period.

Archaeological evidence of human activities and culture during the Early–Middle Pleistocene in the GBY area provides important information, in which Early Humans have reached the Levant at this period. A minor evidence of modern human settlement around Garding was found a long time later during the Holocene in the coastal North Sea area. The fact was inferred from the Garding-2 core. This data can be also used to compare favourable climatic and environmental conditions for human habitation during dispersion and settlement periods, which is potentially important for the development of future adaptation and sustainable development strategies.

The climatic changes that mark the shift from the Pliocene to the Pleistocene, and the subsequent interglacial and glacial periods during the latter period, are reflected in the Garding-2 core record. These changes are discussed in Paper I, whereas climatic and environmental conditions, as well as minor human impacts, of the same core during the Holocene are discussed in greater detail in Paper II. A multi-proxy palaeoenvironmental study was also carried out for the younger Early Pleistocene sediments of the GBY#2 core. The main findings of this investigation are presented in Paper III. The stratigraphic framework developed in the study traces the changing climatic and environmental conditions during the development of Acheulian culture in the Levant.

The results of the palynological and multi-proxy palaeoenvironmental analyses provide: (1) evidence for human migration in response to climatic and environmental changes, especially in the Upper Jordan Valley at the MBB, and in Eiderstedt Peninsula during the Holocene, (2) data to enrich knowledge of the local stratigraphic frameworks and (3) paleoclimatical and palaeoecological data that could be used to create more detailed stratigraphic frameworks for chronologically or archaeologically relevant nearby or farther sites.

1.2. Study areas

1.2.1. Location 1: Garding, northwest Germany

The Garding site is located in the Eider River estuary on the western coast of Schleswig-Holstein in northwestern Germany (Figs. 1a and b). The Garding-2 core drilling point is located at 3485562 (E) and 6019328 (N). It is approximately 700 m to the south of the pilot drilling location of the Garding-1 core (Frechen et al., 2011). This core penetrates the Garding Trough, which is located on the western flank of the Oldenswort North Salt Dome. The present morphology of the coastal area around the core site is dominated by marshlands and sand dunes with some barrier islands along the northwestern coast and in the vicinity of the Eider estuary (Falk, 2001). The potential natural vegetation of the surrounding area is mainly woodland and wetland vegetation. In open and wet lands, *Alnus* is a dominant arboreal taxon, while in the upland *Fagus sylvatica* is of greater importance (Nelle and Dörfler, 2008). Livestock husbandry and arable farming are common land use practices in this area.

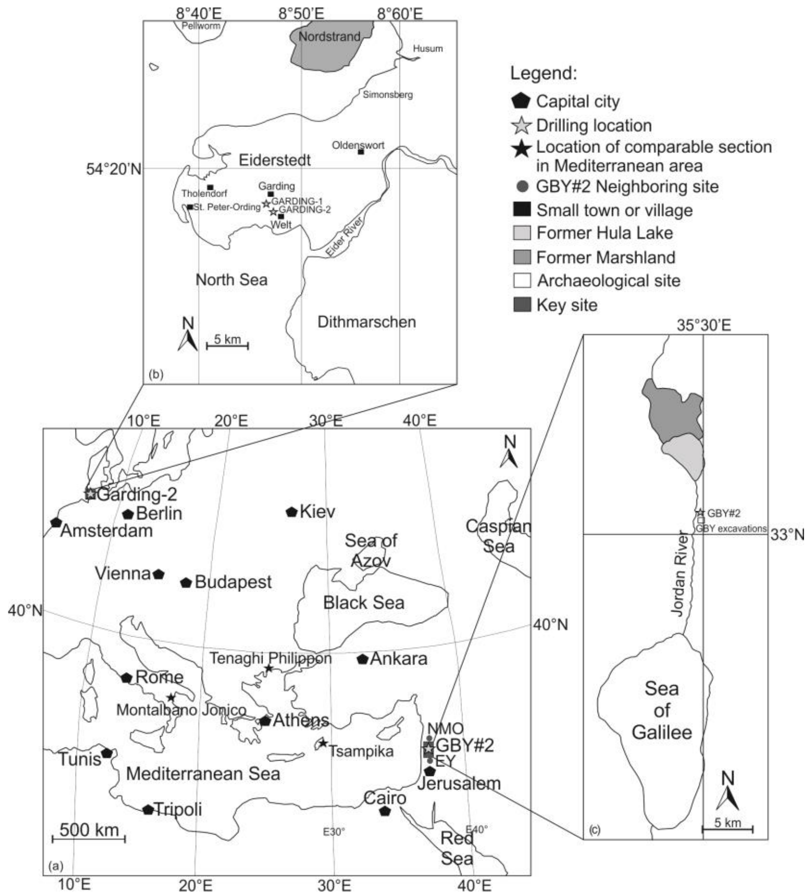

Figure 1. (a) Location map of the sites and drillings. (b) Garding-2 core, Eiderstedt Peninsula-Germany. (c) GBY#2 core, Hula Basin-Israel (modified after Van Zeist and Bottema (2009)).

1.2.2. Location 2: Gesher Benot Ya‘akov-Upper Jordan Valley, Israel

The GBY#2 core was drilled near the excavation site of the Acheulian culture, the so called GBY excavations (Figs. 1a and c), which is located in the Upper Jordan Valley, on the east bank of the Jordan River. It is about 4 km to the south of the recently drained Hula Lake at ITM E 200417 m and N 767274 m (Goren-Inbar et al., 2000). The core site is located about 300 m to the north of the GBY excavation site at ITM E 259080 m and N 768450 m (Figs. 1a and c). Geologically, this core is situated in a complex Quaternary tectonic setting of the Hula pull-apart basin (Horowitz, 1989; Belitzky, 2002). Sediments of the Benot Ya‘akov Formation, which are composed of sedimentary consolidated lacustrine materials including coquina, fine-grained calcareous and carbonate-free sediments, sands, mud and peat (Spiro and Sharon, 2008) were deposited between two basalt layers in the GBY#2 core. This area is characterised by a typical Mediterranean climate with hot and dry summers and cool and wet winters (Van Zeist et al., 2009; Van Zeist and Bottema, 2009). The potential natural vegetation around the study area is dominated by Eu-Mediterranean vegetation, which is mainly composed of evergreen species (Frey and Kürschner, 1989) and savannoid Mediterranean vegetation (Danin, 1992).

2. OBJECTIVES

The objectives of the research are:

1. To characterise different patterns of climatic and environmental changes during the Late Tertiary and the Quaternary in northwest Europe, and during the Early–Middle Pleistocene in the Middle East, which are represented by two research drill cores. The first core is Garding-2 in northwest Germany and another core is GBY#2 at the Gesher Benot Ya‘aqov, in Upper Jordan Valley, Israel.
2. To utilise the climatic and environmental characterisations in order to:
    - enrich the Quaternary stratigraphical framework of the study areas, mainly by establishing a regional climatostratigraphical frame;
    - provide a better understanding of the interaction between climatic changes and environmental conditions during the Quaternary;
    - establish a chronological framework based on the marine isotope stage (MIS), which is followed by palaeoclimatic correlation and palaeoenvironmental comparison of the correlable (same) period between the northwest German

coastal area (Garding) and the Near East (GBY) that are represented by the two key drillings.

3. To attempt to link the environmental and climatic evolution to changes in human behaviour during the diffusion of the hominins at the Early–Middle Pleistocene along the Upper Jordan Valley Israel and during the populating period of the Holocene on the coastal area of northwest Germany.

3. RESEARCH METHODS

Vegetation has undeniably been shown to provide a consistent response to climatic and environmental changes at terrestrial and transitional habitats and therefore, abundance and distribution of plants are considered to reflect these changes. For this reason, palynology was chosen as the main approach to meet the objectives and to answer the research questions (Fig. 2). In addition, physical and chemical analyses representing the abiotic characteristics, such as lithology, geochemistry, magnetic susceptibility and numerical dating as well as the analyses of other biological remains such as plant macro-remains, molluscs, ostracods, amphibians, micro-mammals and fish, which compose the biotic components of the palaeoenvironment, were carried out to describe the environmental development of the Garding-2 and GBY#2 cores (Fig. 2). These analyses were presented in three publications (Appendices A, B).

3.1. Palynology

Palynology is an interdisciplinary science including the study of modern and fossil pollen, spores and other palynomorphs. In this research, fossil palynomorphs were analysed to find some information about past composition of vegetation, which strongly relates to the climatic and environmental conditions in the region of the respective study areas. Pollen palynomorphs, as well as the non-pollen palynomorphs including micro-charcoal, foraminifera test linings, dinoflagellates, algae, water fern and diatom remains were extracted from the sediments of the two sections, which required high resolution sediment sampling. The samples were chemically treated and a quantitative palynological analysis was carried out. At least 300 grains of arboreal pollen (AP) were counted per sample, and a minimum of 350 grains of total AP and non-arboreal pollen (NAP) were counted in samples that contained very few AP. Some samples from the basal part of the GBY#2 core were poor in pollen; from these samples, at least 100 pollen grains were counted. The pollen basic sum (100%) was calculated based on the sum of AP and NAP, while pollen and spores of Cyperaceae, cryptogams, aquatic, and the locally over-represented terrestrial taxa were excluded. Raw data from the counts were processed by the TILIA software package (TILIA, TILIA GRAPH and TILIA VIEW) (Grimm, 1990). Important conclusions can be drawn by comparing the percentages of arboreal pollen (AP), and non-arboreal pollen (NAP) and interpreting changes in the taxa composition.

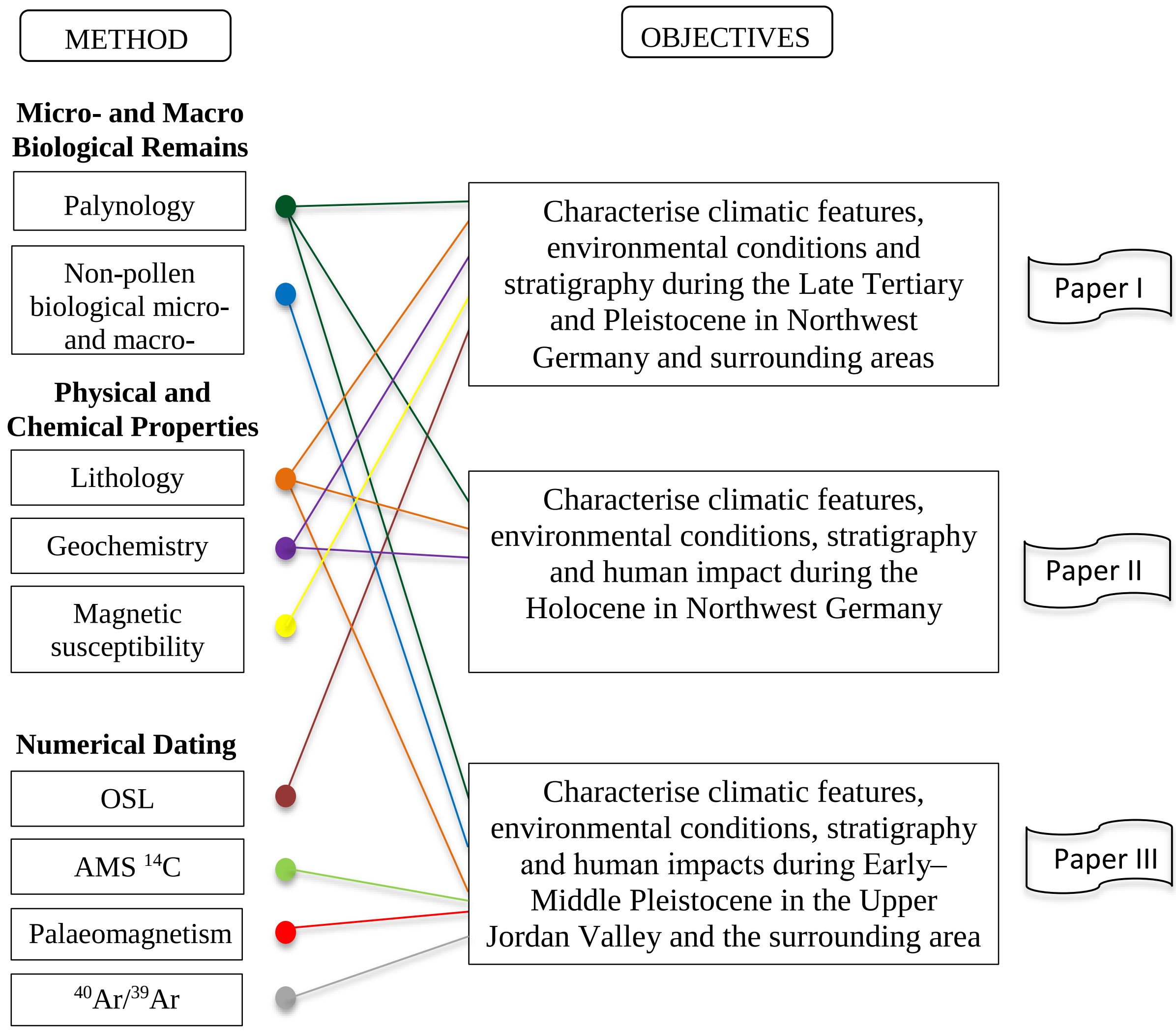

Figure 2. General scheme of applied methods.

Stratigraphically-constrained cluster analysis (Grimm, 1987) was carried out to group the samples in a stratigraphical order based on their similarity in the distribution and abundance of constrained taxa, mainly dryland vegetation that has stratigraphical and environmental significance. Locally, overrepresented taxa were excluded. The results of the cluster analysis help to define so-called local pollen assemblage zones (LPAZ), which enhance conventional palynological interpretation. The conventional observation of palynological characteristics also helps to better address the LPAZ boundaries.

3.1.1. Reconstruction of climatic changes

Papers I and II focus on climatic, environmental and biostratigraphical analyses during the Quaternary of the coastal area of northwest Germany near the village of Garding (Garding-2 core). In formerly glaciated areas, where e.g. Garding was situated, palynological criteria had primarily been used to characterise and correlate interglacial deposits, while lithological indicators such as glacial sediments provided the main evidence for the existence of cold periods (Litt et al., 2007; Stephan, 2014). Glacial periods are indicated by cool arctic conditions characterised by the deposition of glacial sediments such as tills and outwash sediments. Meanwhile, the interglacials in formerly glaciated Europe were characterised by terrestrial soil formation, peat bog development and a succession of vegetation with typical pioneer plants such as *Juniperus*, *Hippophae*, *Betula*, *Pinus* and heliophilous herbs during the early phase followed by an expansion of *Alnus*, *Corylus*, *Quercus*, *Ulmus*, *Tilia*, *Acer* and *Fraxinus*. This expansion characterised interglacial climax conditions, whereas late interglacial forest phases were mainly composed of *Carpinus*, *Abies*, (*Fagus*), *Picea*, *Pinus*, *Alnus* and *Quercus* (Iversen, 1958; Van der Wiel and Wijmstra, 1987; Lang, 1994). However, this general pattern does not entirely reflect the detailed vegetation succession and dominances that vary between investigated interglacial periods, which are discussed at length in Papers I and II.

Paper III identifies that the impacts of climatic changes on vegetation in the Upper Jordan Valley-Israel are specifically indicated by the fluctuations of the AP and steppe-like vegetation. Dry phases are characterised by steppes and steppic forests with low AP, which change into open pine-oak forests and development of evergreen oak forests during moister phases (Van der Wiel and Wijmstra, 1987; Van Zeist and Bottema, 2009). *Cedrus* is often used as an indicator of higher humidity, which is likely related to an increase in precipitation in a cooler Mediterranean climate (Van Zeist and Bottema, 2009). Species of *Ephedra*, on the other hand, are found in deserts, semi-deserts, desert steppes or seasonally dry habitats (Ickert-Bond and Renner, 2016). Calculation of an aridity index (*Artemisia*+Amaranthaceae)/Poaceae or (Ar+Am)/P ratio (Fowell et al., 2003) can also be used to interpret the aridity level by relative comparison of the ratios between samples. The higher the aridity index is, the drier the environmental conditions will be. This method is applicable in the GBY site because *Artemisia* (Danin, 1992) and Amaranthaceae are important components of dry steppe (Van Zeist and Bottema, 1991), while grasses are dominant in the more humid steppe, steppe shrub- and woodlands around the Hula area (Van Zeist et al., 2009).

3.1.2. Determination of relative age

According to the concept of climatostratigraphy, migration and extinction of certain plant taxa coincide with major environmental changes that are related to climatic conditions, particularly temperature. Identification of pollen assemblages, first occurrence, expansion and last occurrence of marker species has been used to identify the biostratigraphic boundaries and relative age of the sediments with respect to the local and regional (bio) stratigraphical framework. In Paper I, the assemblages of *Taxodium*, *Liquidambar*, *Nyssa*, *Sequoia* and *Sciadopitys* were used as Tertiary marker taxa (Zagwijn, 1960; Menke, 1975; Menke, 1976), whereby the last occurrence of *Pterocarya* occurred in the late Holsteinian (Reille et al., 1998; Litt et al., 2007) and the last occurrence of *Tsuga* marked the end of Cromerian Interglacial II or III (Müller, 1992).

Paper II provides an in-depth discussion of the Holocene period. Common features such as the *Ulmus* decline marking the Atlantic–Subboreal transition and the expansion of *Fagus* and *Carpinus* along with the rapid increase of anthropogenic indicators marking the beginning of the Subatlantic were used for subdivision (Firbas, 1949; Overbeck, 1975; Wiethold, 1998; Dörfler et al., 2012) .

3.1.3. Analysis of depositional environment

Local conditions inferred from pollen analyses can be used as a tool to define the depositional environment at the time of sediment deposition. In Papers I and II, coastal dynamics were indicated by the following certain taxa assemblages: (1) *Abies*, *Picea*, *Pinus*, *Taxodium* and *Tsug*a forming coniferous forests; (2) Ericaceae, heliophilous herbs and grasses indicating open terrestrial environments; (3) *Alnus*, *Pterocarya*, *Myrica*, *Fraxinus*, *Salix* and *Ulmus* suggesting a riparian setting; (4) *Nyssa*, *Myrica*, Ericaceae *Sphagnum*, *Taxodium*, Polypodiales and *Sequoia* indicating a backswamp environment; (5) Asteraceae, *Artemisia*, Caryophyllaceae, and Amaranthaceae representing marsh conditions; (6) wild grasses and Ericaceae indicating sand dunes vegetation and (7) dinoflagellate cysts and foraminifera test linings signifying a marine influence of inwashed reworked material in the basin.

Paper III illustrates that taxa indicative of steppe, woodland, local lake and wetland environments are important for the GBY#2 core. *Quercus* with the occurrence of some *Pistacia* and *Olea* are the main components of the woodland, while the assemblages of grasses, *Ephedra* species, *Artemisia* and Amaranthaceae indicate steppic and more open landscape conditions. In this paper, lake development is shown by an interchange of open water taxa such as *Salvinia*, *Myriophyllum spicatum*, *Myriophyllum verticillatum* and *Pediastrum simplex*, reed swamp components like *Ranunculus sceleratus*, *Typha latifolia* and Cyperaceae, and marsh communities with Amaranthaceae, Apiaceae, Poaceae and Cyperaceae.

3.1.4. Analysis of human impact

Human impact can also be seen in the pollen diagrams. During the Early Pleistocene at the Levantine Corridor, migration-related activities comprise the major constraints. Accordingly, Paper III investigates the impact of human-related activity. Micro-charcoal counting was applied to determine occurrence and intensity of burning activities at the sites and, with archaeological and other geological findings, it was used to interpret the origin of burning and whether such burning had been triggered by natural causes such as ignition by thunderstorms, a combination of drought and high temperature, volcanism or whether it had been the result of human activities.

In the younger Holocene period, which is discussed in Paper II, human activities were more complex. At the coastal area of Garding, agricultural and livestock grazing activities were the main concern. These can be analysed by the occurrences of cultivated taxa including cereals (Cerealia and *Secale cereale*) and weeds such as *Plantago lanceolata* and *Rumex acetosa* as well as *Artemisia* and Amaranthaceae. In the flooded areas, the settlers built dikes that can also be observed from local changes in the depositional processes towards shallower conditions.

3.1.5. Correlation

Results deduced from palynological analysis that were summarised above were used for near and long distance correlation. Garding-2 records of Paper I and II were compared to the Quaternary sites of Oldenswort and Lieth (Menke, 1975), as well as Tholendorf and Husum (Menke, 1969, 1986) (Fig. 1). Results from GBY#2 were correlated with the GBY excavation site (Van Zeist and Bottema, 2009) (Fig. 1) and other Mediterranean records such as the Tsampika section (Joannin et al., 2007a), the Montalbano Jonico section

(Maiorano et al., 2016), the Tenaghi Philippon profile (Tzedakis et al., 2006) (Fig. 1), among other important records (summarised in Almogi-Labin (2011). By the comparison of the climatic development and environmental evolution between Garding-2 and GBY#2 cores, and with other sites belonging to the same time period of deposition in the wider area of the GBY excavations and other Eastern Mediterranean records, scenarios of the impact of climate and environmental changes on human behaviour, in particular along the pathway through the Levant could be reconstructed.

3.2. Non-pollen biological micro- and macro-remains

The fresh water lake sediments of the GBY#2 core are composed mainly of fine-grained deposits, which offers possibilities of good preservation of diverse biological remains. In Paper III, plant macro remains were determined by Yoel Melamed (The Mina and Everard Goodman Faculty of Life Sciences, Bar-Ilan University), who is an expert in botany and archaeology to help reconstructing the composition of the local vegetation (Fig. 2) and Acheulian diet around the GBY site (Melamed et al., 2016). Additionally, the comparison of the results obtained using this approach with those from pollen analysis can give an assessment of whether the occurrences of some taxa in the vicinity of the site are under- or overrepresented.

Analyses of other palaeoenvironmental proxies such as molluscs and ostracods were conducted by Steffen Mischke (Faculty of Earth Sciences, University of Iceland), an expert in palaeontology of molluscs and ostracods, palaeolimatology and palaeoenvironment, and Henk K. Mienis (National Natural History Collections, Hebrew University of Jerusalem), an expert in malacology. Their study results describe useful data for determinations of depositional environments as well as the salinity and lake level fluctuations of the Hula Palaeo-lake (Fig. 2).

Fossils of amphibian and micro-mammals were also determined by an archaeozoology (osteology) expert, Rebecca Biton (Institute of Archaeology, Hebrew University of Jerusalem). These analyses provided additional information on depositional environment and ecology of the study area. Fish remains based on the publication of Zohar et al. (2014) have given useful basis for palaeoenvironmental including local water temperature and ecological interpretations.

3.3. Lithology, physical and chemical properties

Lithological descriptions of parameters such as texture, colour (Munsell Color, 2009), composition and sedimentary structure were explained in Papers I–III (Fig. 2). Detailed lithological descriptions of grain size, sedimentary structure, thickness and sediment compositions in Papers I and II were conducted by Alf Grube (Free and Hanseatic City of Hamburg, Ministry of Environment and Energy), while the colour determination was carried out in the soil laboratory of the Institute of Ecology in Leuphana University of Lüneburg. In Paper III, detailed lithological and sedimentological information of the GBY excavation and GBY#2 core were obtained from Feibel (2001, 2004 and 2009 personal communication), Goren-Inbar et al. (2002b) and from Spiro and Sharon, unpublished report (2008). The studied sections are mainly composed of sedimentary rocks. Therefore, grain size measurement is important in order to analyse the texture, sorting and porosity of the rock formation. Together with direct core observation of the lithological compositions, sedimentary structures and secondary geological structures, grain size distributions are essential in determining the sedimentation processes including the impact of post-depositional geological structural transformations and depositional environments of the sediments. Determination of mineralogy and structure of under- and over-lying basalt layers in Paper III provide valuable information to understand the formation processes and the source of these basalt flows. The overall additional information about the contact layers between lithological units and the degree of sediment weathering also provide evidence for interpretation of exposure and erosion in these three Papers. In Papers I and II, the identification of geochemical properties were conducted in soil laboratory of the Institute of Ecology of Leuphana University of Lüneburg. The carbonate content was measured using Scheibler aparatus and soluble salt contents were determined using an EC meter (VDLUFA, 1991). A CHNS/O 2400 series II analyser of PerkinElmer was used to measure the total Carbon (C) and Nitrogen (N), and a pH meter in 1:2.5 0.01 mol/l calcium chloride solution (Urban, 2002) was used to measure pH values of the sediments. These analyses were used to support the lithological interpretation of the depositional environments and conditions (Ad-Hoc-Arbeitsgruppe Boden, 2005; Plaster, 2009). Soluble salt and carbonate contents are important to infer the indications of salt water intrusion and the organic constituent of the sediments that reflect the depositional environmental conditions. pH of the sediments illustrates the acidity of the environments reflecting the chemical, physical and biological processes during and after the deposition. C/N ratios were calculated to define the source of the organic matter in the sediments, which might derive from terrestrial, transitional or marine environments (Meyers and Ishiwatari, 1993; Meyers, 1994; Thornton and McManus, 1994).

In Paper I, magnetic susceptibility measurement was conducted by Christian Rolf (LIAG Hannover) and was used to characterise the rock sequence of the Garding-2 core (Fig. 2). Low background susceptibility values (<10^{-5} SI) indicate sandy and silty sediments, while high susceptibility signal values represent sediments brought from other places by rivers or glaciers that likely indicate mixed sediment sources such as till.

3.4. Numerical dating

Depending on the age range and lithological compositions of the cores, several numerical dating methods were used to set up a solid chronological framework for correlation including optically stimulated luminescence (OSL), the radiocarbon, palaeomagnetism and argon-argon (^{40}Ar/^{39}Ar) methods. As Garding-2 is mainly composed of sandy deposits, the OSL method was used in Papers I and II (Fig. 2). OSL dating was conducted in Leibniz Institute for Applied Geophysics (LIAG), Hannover, Germany by Jingran Zhang. This method shows reliable results in determining the age of the Late Glacial and Holocene deposits that are in accordance with the radiocarbon dating results presented in Paper II (Fig. 2) (Zhang et al., 2014). However, the OSL method is limited in terms of dating the older sediments of the Garding-2 core.

To establish a more reliable time frame, palaeomagnetic studies were carried out on Tertiary and Quaternary sediments by Christian Rolf (LIAG Hannover) and examined in Paper I and on the GBY#2 core by Guillaume Dupont-Nivet (Rennes University palaeo-archaeomagnetic laboratory) in Paper III. Paper I shows that because of the coarse-grained dominated sediments of Garding-2, there were no clear palaeodirection trends observed in the core. On the other hand, the palaeomagnetic analysis was able to determine the MBB that is used as the correlation reference point between the GBY2# drill core and the GBY excavation site sequence, and other important sites in the Mediterranean area (Fig. 2) (Paper III). ^{40}Ar/^{39}Ar dating was also used to date the under- and over-lying basalt layers of the GBY#2 core in Paper III. This analysis was carried out in Western Australian Argon Isotope Facility, Department of Applied Geology and John de Laeter Centre for Isotope Research, Curtin University, Australia by Fred Jourdan.

4. OVERVIEW OF THE RESULTS

4.1. Paper I

Late Pliocene–Pleistocene record of the Garding-2 research drill core, Northwest Germany*. Maria Sekar Proborukmi, Brigitte Urban, Manfred Frechen, Alf Grube, Christian Rolf (2017). Zeitschrift der Deutschen Gesellschaft für Geowissenschaften (German Journal of Geology) 168 (1), 141–167. DOI: 10.1127/zdgg/2017/0103.*

Paper I focuses on the climatic, environmental and biostratigraphical analyses of the North-Sea coastal area near Garding, northwest Germany (Garding-2 core). It comprises 240 m of sediments of the Garding-2 core (Figs. 1a and b) consisting of Tertiary to Quaternary sediments of the Upper Pliocene, Pleistocene and Holocene. Although robust numerical dating results could not be obtained, palynological and lithological analyses provide considerable biostratigraphical, climatical and environmental evidence for establishing a stratigraphic framework of the Garding-2 core.

The sediments between 240.00 m and 182.87 m depth showed occurrences of *Carya* and *Sciadopitys*, *Liquidambar* and *Symplocos* and are correlated to the Late Pliocene (Zagwijn, 1963; Menke, 1975; Urban, 1978a; Urban, 1978b; Arias et al., 1984). The sediment sequence between 240.00 m and 199.00 m was assigned to the Brunssumian B (Menke, 1975) as it shows relatively high percentages of *Pterocarya*, *Liquidambar* and *Nyssa*, while the sediments between 199.00 m and 192.00 m were assigned to the Brunssumian C based on the predominance of conifers, especially *Sequoia* (Zagwijn, 1960; Menke, 1975; Andrew and West, 1977).

The coniferous forests, which are mainly composed of *Abies*, *Picea*, *Pinus*, *Taxodium* and *Tsuga*, had increased during the deposition of sediments between 192.00 m and 188.38 m, which can be correlated to the Reuverian A (Zagwijn, 1960; Menke, 1975). Thermophilous and Tertiary taxa subsequently decreased and an open landscape developed during the incipient climatic deterioration of the Reuverian B (Menke, 1975) at 188.38 m–182.87 m. On top of the Reuverian B sediments at 182.87 m, the Pliocene–Pleistocene boundary, which marks the beginning of a strong cooling and an erosional surface, was determined.

Correlative Praetiglian (Zagwijn, 1960; Menke, 1975) deposits were found between 182.87 m and 182.00 m, which showed the development of raised bogs in an open landscape that was mainly characterised by Ericaceae and heliophilous herbs. The coarse-grained sediments composed mainly of coarse sand between 182.00 m and 149.00 m. It indicates changes from swampy through fluvial to limnic conditions, which probably all belong to the Praetiglian period.

Pterocarya was found in the subsequent sediment layers between 149.00 m and 120.00 m suggesting that these deposits are of Holsteinian age or older (Litt et al., 2007; Reille et al., 1998). Based on their stratigraphical positions and the absence of the Tertiary and Early Pleistocene taxa such as *Sciadopitys*, *Sequoia*, *Carya* and *Nyssa*, these sediments are tentatively correlated to the Waalian-Bavelian periods. Meanwhile, its correlation to the Tiglian age is unlikely. The sediments between 149.00 m and 139.25 m showed a weak temperate forest phase characterised by *Quercus, Pinus, Picea*, *Alnus*, *Betula* and *Myrica*. The temperature change to a cooler and dryer climate at the top of this sediment sequence is characterised by the co-occurrence of heliophytes and *Larix*. Based on this evidence and their stratigraphic position, these sediments are correlated to the Tornesch Interglacial deposits of the Lieth section in Schleswig-Holstein (Menke, 1975; Menke, 1976; Litt et al., 2007) belonging to the Waalian Complex (Urban, 1997). The sediments between 139.25 m and 129.15 m showed interglacial optimum conditions with occurrences of *Quercus* and *Fraxinus* peaks. These sediments tentatively correlate to the Uetersen Interglacial of the Bavelian Complex of the Lieth section (Menke, 1975). The coarse-grained sediments between 129.15 m and 126.44 m indicated a relatively cool period with high NAP percentages, occurrences of *Selaginella selaginoides*, and low amounts of pollen of thermophilous taxa. Based on the evidence and their stratigraphical positions, these sediments can be correlated to the Dorst cool period of the Bavelian Complex (Zagwijn and De Jong, 1984; Müller, 1992; Litt et al., 2007; Deutsche Stratigraphische Kommission, 2016). A considerably warmer period between 126.44 m and 125.80 m was palynologically evidenced by increased percentages of *Quercus*, *Fraxinus* and *Tsuga* and the occurrence of *Ulmus* and *Carpinus* pollen, which can be tentatively correlated to the Osterholz Interglacial of the Cromerian Complex (Grüger, 1968; Müller, 1986; Müller, 1992).

The last occurrence of *Tsuga* was found at 119.50 m, in the coarse-grained sediment sequence between 125.80 m and 119.00 m. This event can be used as a stratigraphic marker to define the boundary to the second Cromerian Interglacial or the Hunteburg interglacial (Hahne et al., 1994), which coincides with the MBB as has been examined first in the Netherlands (Zagwijn et al., 1971). However, concerning the Quaternary stratigraphy of Germany, Litt et al. (2007) discussed whether the second Cromerian Interglacial might belong to the Matuyama Chron or to the Lishi Event of the Brunhes Chron (Fromm, 1994). *Tsuga* is still present in the third Cromerian Interglacial of the Gorleben section (Müller, 1992). Because there are no further discussion points made by the author to its occurrence in the sediments younger than Cromerian Interglacial I (Müller, 1992), *Tsuga* can be considered as autochthonous. Taking these former studies and the regional variations into account, the sediments at 125.80 m–119.50 m can be tentatively correlated to either Cromerian Interglacial II or III. Because of the unsuitable coarse-grained material, there are no useful palaeomagnetic directions that can be used to confirm the palynological interpretation of the Early–Middle Pleistocene boundary between 125.80 m and 115.00 m. Furthermore, the correlation of this boundary relies mainly on palynological interpretation. An oriented sample taken at 115.18 m was also a failure because of the chaotic behaviour of the magnetisation vectors. Three thin younger interglacial layers were identified between 119.00 m and 96.00 m. The youngest interglacial layer at 109.45 m–96.00 m likely correlates to the Cromerian V Bilshausen Interglacial (Müller, 1992). It is based on the palynological results showing an absence of *Tsuga*, high amounts of *Pinus* and the increased percentages of *Picea*, the low percentages of *Quercus*, *Fraxinus*, *Betula* and *Corylus*, and scattered occurrences of *Abies* and *Carpinus*.

Climatic deterioration of the early Elsterian glaciation was indicated by the sediments following the last thin interglacial layer, between 109.45 m and 96.00 m. The onset of this cooling was recorded palynologically at 92.11 m, while the Elsterian Glacial deposits were indicated by two till layers; at 89.00 m–85.50 m and at 85.50 m–82.00 m. These tills are composed of interbedded fine to coarse glaciofluvial sand that shows high magnetic susceptibility values indicating mixed sediment sources with higher magnetic susceptibility sediments brought in by glaciers or river.

Late Holsteinian deposits represented by a clayey layer at 81.00 m–79.20 m are characterised by the occurrence of *Fagus* and *Pterocarya* in a forest assemblage, which includes *Abies*, *Carpinus* and *Picea* (Erd, 1970; Müller, 1974; De Beaulieu et al., 2001) and is correlated to zone XIII of Müller (1974). This pollen zone shows a retreat of thermophilous trees and relatively high amounts of *Pinus* indicating the termination of the interglacial. Same pollen assemblage was recognised for the sediment sequence between 79.20 m and 73.00 m. However, higher NAP percentages occurred and more reworked marine and Tertiary–Early Pleistocene taxa were found from about 77.77 m upwards suggesting strong reworking activities. The occurrences of Ericales, *Helianthemum* and *Selaginella selaginoides* indicate subarctic conditions at the beginning of the Saalian-Complex, more specifically the onset of the Fuhne cold period (Dücker, 1969; Urban et al., 1988; Litt et al., 2007).

The Drenthian till was found between 73.00 m and 71.00 m. It is composed of sand with gravels and larger rock fragments with high values of magnetic susceptibility and has eroded most of the Lower Saalian deposits. A peaty layer was found at the subsequent depth around 69.25 m. This layer shows late interglacial conditions with a *Pinus-Picea-Abies* assemblage and the absence of *Pterocarya* that likely correlates to the Eemian zone VI (Menke and Tynni, 1984). This layer was then overlain by intercalation of fluvial and glaciofluvial deposits of mainly sandy and gravely sediments up to about 20.00 m, which were partly dated to the late Weichselian using the OSL method (Zhang et al., 2014).

4.2. Paper II

***Palaeoenvironmental investigations of the Holocene sedimentary record of the Garding-2 research drill core, northwestern Germany**. Maria Sekar Proborukmi, Brigitte Urban (2017). Zeitschrift der Deutschen Gesellschaft für Geowissenschaften (German Journal of Geology) 168 (1), 39–51. DOI: 10.1127/zdgg/2017/0098.*

Paper II presents the climatic conditions, biostratigraphical framework and environmental development of the coastal area near Garding, at the North Sea coast of northwest Germany during the Holocene, which comprises the depositional time span of the top 20 m sediments of the Garding-2 core. This part of the Garding-2 core is not included in Paper I. It was not only because of the higher resolution of the palynological record and the dense OSL- and accelerator mass spectrometry (AMS) ^{14}C- dating, but also because it aimed to specifically address human activities of the North Sea coastal area on the southern Eiderstedt Peninsula (Figs. 1a and b).

These youngest deposits of the Garding-2 core are composed of coastal sediments that were deposited during the Holocene. A hiatus, dated to between approximately 13000 BP and 8300 BP (Zhang et al., 2014) occurs at about 20.00 m. This hiatus was likely formed by the early Holocene transgression, which is also responsible for another erosional surface at about 19.60 m, dated to about 7000 BP (Zhang et al., 2014). Between these two unconformities, a thin Atlantic marine sediment layer, characterised by high amounts of *Pinus* and moderate values of *Betula* found together with an AP assemblage of *Corylus, Alnus, Quercus, Ulmus* and *Tilia,* was deposited. This layer can be correlated to pollen zone VI–VII of Firbas (1949) and pollen zone VIII^{WD} of Overbeck (1975).

On top of the younger unconformity, Subboreal (19.56 m–11.00 m) and early Subatlantic (10.85 m– 1.33 m) sediments were rapidly deposited. The *Ulmus* decline, which is a typical palynological feature of the Atlantic–Subboreal transition in northwestern

Europe (Overbeck, 1975; Wiethold, 1998; Dörfler, 2000; Parker et al., 2002; Kalis et al., 2003), is not recorded in the Garding-2 core. *Ulmus* shows low constant values throughout the whole pollen sequence. Numerical dating at around the first occurrence of *Fagus* at 16.22 m indicates an age of 3130±260 BP (Zhang et al., 2014). This age is not in agreement with the empirical occurrence of *Fagus* in the age model of Dörfler et al. (2012) and also with the age for the first appearance of *Fagus* in Tholendorf (Menke, 1969). This disagreement might be explained by erosion and redeposition processes, which are common in the study area. In a period of intensive erosion, even a thin sediment layer might represent considerable time spans. Taking these conditions of sedimentation into account, there is also a possibility that the Atlantic-Subboreal transitional sediments and older Subboreal sediments did contain *Fagus* pollen but have been eroded.

The Subboreal sediments between about 19.56 m and 16.90 m were deposited in an offshore marine environment which subsequently was followed by an unconformity marking a depositional environmental change into a foreshore (tidal flat) environment up to about 10.85 m. The subsequent more sandy sediments show increased pollen percentages of grasses, marsh and dune vegetation during the early Subatlantic, dated to around 2790±20 (Zhang et al., 2014). Depositional environment changed from sandy tidal flat, between 11.00 m and 6.00 m, to sandy barrier and spit, between 6.00 m and 3.72 m and was followed by the development of sand dunes in a backshore environment, between 3.72 m and the top of the core. The shallowing of the depositional environment was mainly caused by local conditions, due to a high rate of sediment accumulation as well as diking activities in this area in recent times, under the globally rising sea level.

The age of the onset of the Subatlantic in Garding-2 core is in very good agreement with the palynological record of Tholendorf , dated to 2800 BP (Menke, 1969; Meier, 2004). Although the oldest settlements in the German North Sea marshes were found during the Bronze Age, about 1000 BC (Behre, 1991), the well-known expansion of *Fagus* and *Carpinus* and rapid increase of anthropogenic indicators, which are characteristic of the beginning of the Subatlantic at about 2700 BP (Dörfler et al., 2012), were not clearly observed in the Garding-2 record. This might be caused by the low intensity of human settlement activities in the surrounding area of the core site, due to occasional storm floods (Menke, 1969), until the settlers began to build dikes around the 11^{th} century (Behre et al., 1979; Kühn and Panten, 1989; Zhang et al., 2014). However, this evidence is in agreement with the regional framework during the Subboreal–Subatlantic transition (Menke, 1969; Menke, 1986) and with the numerical dating results (Zhang et al., 2014).

4.3. Paper III

Climatic changes around the Matuyama-Brunhes Boundary (MBB) evidenced from a multi-proxy palaeoenvironmental study of the GBY#2 core, Jordan River Valley, Israel. *Maria Sekar Proborukmi, Brigitte Urban, Steffen Mischke, Henk K. Mienis, Yoel Melamed, Guillaume Dupont-Nivet, Fred Jourdan, Naama Goren-Inbar (2018). Palaeogeography, Palaeoclimatology, Palaeoecology 489 (C), 166–185. DOI: 10.1016/j.palaeo.2017.10.007.*

The multi-proxy palaeoenvironmental study of the GBY#2 core (Figs. 1a and c), which is presented in Paper III, reveals changes in climatic and environmental conditions around the MBB. The GBY#2 core is composed of a 50 m long sequence comprising 23 m of fine-grained calcareous and non-calcareous sediments, coquina and sand deposited between two basalt layers (Spiro and Sharon, 2008). These sediments belong to the Benot Ya‘akov Formation, which is composed of fluvio-lacustrine sedimentary rocks showing three dominant lithofacies: beach (coquina, sand and gravel), shallow lacustrine (calcareous mud) and fluvial channel (conglomerate) (Feibel, 2001, 2004; Goren-Inbar et al., in press). ^{40}Ar/^{39}Ar dating of these basalt layers shows a plateau age of 1.195 ± 0.067 Ma (at 48.30 m) and 1.137 ± 0.069 Ma (at 45.30 m) for the underlying layer and 0.659 ± 0.085 Ma (at 14.90 m) for the overlying layer (Goren-Inbar et al., 2009). These sediments provide diverse biological remains of plants, molluscs, ostracods, amphibians, micro-mammals and fishes, which were investigated forming a multi-proxy palaeoenvironmental study.

Sediments of the GBY#2 core show indications of shallow lake environments, from open water at the bottom to lake-margin conditions towards the top. Palynological results of pre-MBB sediments of the GBY#2 record indicate at least three climatic phases. Between 39.50 m and 32.60 m, the sediments were deposited during semi-moist and relatively cool conditions, which were indicated by relatively high percentages of AP, especially *Quercus calliprinos*-type, low percentages of pollen of steppic elements and occurrences of *Cedrus*. These conditions represent the newly defined climatic phase 1. The prevailing relatively deep open lake environment was indicated by high frequencies of micro- and macro-remains of the water ferns, *Azolla* cf. *filiculoides*, *Salvinia cf. natans* and *Salvinia* sp. in the older part of the sediment sequence, whereas the occurrence of Cyprinidae remains at 33.20 m, which suggests shallower lake environments, with a maximum depth of 5 m (Zohar et al., 2014) and ostracod *Candona neglecta*. Findings of amphibian and micromammalian remains also point to lake-margin environments. Comparison between the established MIS framework of the GBY excavation record (Van

Zeist and Bottema, 2009) and the palaeomagnetic results of the GBY#2 core lead to a correlation of the climatic phase 1 of the GBY#2 core with MIS 20d.

During the subsequent climatic phase 2, the depositional environment became even shallower from 32.60 m depth upwards, as indicated by higher numbers of pollen and macro-remains of reed, swamp and marsh taxa such as Cyperaceae, cf. *Typha*, grasses and Amaranthaceae, Apiaceae and Asteraceae up to about 20.15 m. These sediments were deposited under relatively arid and cool conditions that most likely relate to glacial stage MIS 20b. At the top of climatic phase 2, a transition to slightly warmer conditions was observed. The sediments between 20.15 m and 17.10 m showed the shallowest depositional environment of the entire record. It was indicated by deposition of the coquina layer and the occurrence of *Darwinula stevensoni* that are probably related to the accumulation of shells at or near the lake margin. A pronounced change of vegetation to *Quercus calliprinos*-, *Quercus ithaburensis*- and *Pistacia*-rich woodlands under a warm and relatively moist period of climatic cycle 3 was correlated to the interglacial stage, MIS 19c (Almogi-Labin, 2011; Maiorano et al., 2016). Two phases of slightly deeper depositional conditions, at 31.80 m–28.00 m and 25.30 m–20.15 m, are believed to be influenced by an interaction between climatic conditions and variations in sediment supply at the prograding lake shore.

In addition to the good correspondence of GBY#2 with the profile of the GBY excavation sites (Van Zeist and Bottema, 2009), palynological features and inferred climatic conditions recorded in GBY#2 core are also in good agreement with other pollen records from the central and eastern Mediterranean and related areas within the comparable time span of 900 ka and 700 ka (Almogi-Labin, 2011). These include the Early and Middle Pleistocene Tsampika section of Rhodes-Greece (Joannin et al., 2007a), the Montalbano Jonico section of southern Italy covering the MPT (Maiorano et al., 2016) and the Tenaghi Philippon profile in Eastern Macedonia, Greece (Fig. 1) (Tzedakis et al., 2006).

This research becomes the first study that applied high resolution palynology and micro-charcoal investigations to Early Pleistocene deposits of the GBY area. Depending on the frequency of the micro-charcoal findings in the samples, the existence of fire can be concluded in the study area. High frequencies of micro-charcoal particles were found in LPAZ GBY#2-2 (between 36.10 m and 32.60 m) pointing to human use of fire, which is also suggested by previous studies near the Hula Palaeo-lake shore (Goren-Inbar et al., 2004; Alperson-Afil, 2008; Alperson-Afil et al., 2009; Alperson-Afil and Goren-Inbar, 2010). This layer can be correlated with an artefact-containing layer of the GBY excavation sites, which also indicates fresh water conditions (Mienis and Ashkenazi, 2011).

5. CONCLUSIONS AND PERSPECTIVES

5.1. Climatic and environmental patterns

Quaternary glacial and interglacial events are reflected in vegetation variation in Western Europe and the Mediterranean (Suc and Zagwijn, 1983; Van der Wiel and Wijmstra, 1987). Climatic pattern of the Late Tertiary and the Quaternary in northwest Europe, which is represented by the Garding-2 core, and the Early–Middle Pleistocene in the Middle East, represented by the GBY#2 drill, is characterised by alternating glacial-interglacial periods. The climatic signals in both regions are generally aligned with the global climatic signals. Palynological analyses of Papers I–III show detailed climatic and environmental characteristics of both key drillings. The results of these papers indicate that vegetation distribution in Northwest Germany was predominantly controlled by changes in temperature and humidity while changes in humidity seem to have been more relevant for vegetation changes in the Levant. Glacial periods in Northwest Germany (Papers I and II) are characterised by open landscapes and heath formation as well as lower groundwater level with repeated ice advances and deposition of glacigenic sediments and till layers, while the interglacial periods are mainly indicated by the presence of substantial forest cover, which generally was accompanied by higher groundwater level and marine transgressions. In the Levant (Paper III), the Pleistocene glacial periods are characterised by more open landscape with steppic conditions, which are replaced by woodlands and shrublands during interglacial periods.

5.2. Stratigraphy and correlation

The detailed palynological records of the Garding-2 core has certainly enriched the knowledge of the local stratigraphy and the palynolgical characteristics of the Eiderstedt Peninsula with respect to the criteria of the north European Quaternary stratigraphy, especially at the important chronological and palaeoclimatical event boundaries PPB and Early–Middle Pleistocene transition and with global sea level changes during the optimum conditions of interglacial periods. This core is the first core that provides a long late Tertiary to Quaternary sediment record in this area, which reflects the local stratigraphy and global climatic events, and provides a correlating point to other records within the same period nearby. In Paper I, palynological and lithological findings from the Garding-2 core during the late Pliocene and Pleistocene provide evidence for PPB, Early–Middle Pleistocene transition and the interglacial and glacial periods during this time span, which are mainly in agreement with the Oldenswort and Lieth records (Menke, 1975). In Paper II, palynological evidence for thick Subboreal and Subatlantic sediments are found in the top 20 m of the Garding-2 core, which share similar features with the records of Tholendorf and Husum (Menke, 1969; Menke, 1986) that are located in the vicinity of the core. Multi-proxy studies, particularly of the palynological investigation of the GBY#2 sequence (Paper III) show climatic changes from relatively cool and dry to warmer and moister conditions shortly before the MBB, at about 780 ka (Head and Gibbard, 2005; Lisiecki and Raymo, 2005), which indicate similarities with the GBY excavation records (Van Zeist and Bottema, 2009). These conclusions allow a further distance correlation of the important stratigraphical events during the Quaternary of these sediment sequences to other important local and regional records with similar time spans providing additional information on the regional and global impacts of climatic fluctuations on environmental changes.

Impacts of the Quaternary climate fluctuation on the environment were also evident in the results of palaeoenvironmental study of the key cores. In the coastal area near Garding, the impact of the fluctuating Scandinavian ice caps volume was mainly represented by variation in sea level. In Papers I and II, changes of sea level influence the overall hydrological conditions and are reflected by shifting of depositional environment from limnic and glacio-fluvial during glacial periods to the alternating swampy and marshy wetlands, tidal flats and open marine conditions during the interglacial periods. Similar impacts were recorded in the lake sediment sequence at GBY site. Increased precipitation was generally observed by rising lake level. On the other hand, during periods of higher aridity, lake level falls and lake-margin environments such as marshes, reed-swamp and lake beach emerge. Additionally, Papers II and III, in particular, show that local conditions related to morphology and depositional systems are also important for understanding environmental developments. Paper II indicates that complex depositional processes in a coastal area such as spit formation, storm flood and constant erosion-deposition mechanism have significantly changed the environment, not only in terms of morphological features but also in human behaviour, as people were forced to adapt by creating mounds or even to leave the flooded area. In Paper III, the impact of the high sedimentation rate caused a progressive shallowing of depositional environment, predominantly as a result of the core's position at the lake margin, where prograding patterns of deposition occur due to the high amounts of sediment supply. These publications therefore suggest that in addition to the climatic conditions, local depositional processes and morphology should also be considered in palaeoenvironmental analyses.

The palynological record of the GBY#2 core shows relatively cool and moist conditions during MIS 20d that changed into relatively arid conditions during MIS 20b. Transition towards the warm and moister interglacial of MIS 19c was recorded in the topmost sediments of GBY#2, shortly before the MBB. Although palaeomagnetic measurements were not able to define the MBB in the Garding-2 core, the last occurrence of *Tsuga* indicates the end of the Cromerian II and/or III interglacial, which coincides with the MBB, during MIS 19. The palynological record also indicates warmer and relatively moist conditions shortly before the MBB in northern Germany, which are generally similar to the climatic conditions during the same period in the Levant. Based on these results, the Early–Middle Pleistocene boundary seems to be a globally important event in terms of climatic change showing strong regional differences. Accordingly, a more precise assignment of the Early–Middle Pleistocene boundary is necessary for a more detailed characterisation of environmental conditions and broader correlation of this event. From the Garding-2 record, further detailed identification of the MBB and palynological characteristics of the respective deposits at the area around Garding would be valuable to refine the knowledge of the Early-Middle Pleistocene transition in Schleswig-Holstein, rendering comparison with other areas and regional correlation possible. However, to improve the quality of the palaeomagnetic measurements, analyses of finer-grained material is necessary.

5.3. Climate, environment and human

Papers II and III discuss environmental and climatic conditions during the Early–Middle Pleistocene in the Levant and during the Holocene in northwest Germany. Multi-proxy palaeoenvironmental analysis shows diverse biological remains and evidence of human-induced fire at the Hula Palaeo-Lake. This freshwater lake had provided an ideal niche for flora, fauna and hominins during the Early-Middle Pleistocene. Micro-charcoal analysis could be refined in future research and a more detailed and comprehensive research to understand the role of fire around the GBY#2 core site, which will be valuable to complement the former conclusion of human-induced fire at the GBY excavations site, could be carried out. In Paper III, the age of the overlying basalt (659 ± 85 ka; MIS 16) shows that the artefact containing layers below this basalt still belong to the Acheulian Culture. Therefore, another possible continuation of this research is to further correlate the duration of the Acheulian habitation of the GBY#2 with other Acheulian sites such as Nahal Mahanayeem Outlet (NMO) (Aharonovich et al., 2014; Kalbe et al., 2014; Sharon and Oron, 2014) and Eshel Ya'akov (EY) (Fig. 1), to understand the geological processes that occurred between the MBB and MIS 16 deduced from the GBY#2 section.

The palynological and lithological records of the Garding-2 core indicate minor anthropogenic activities such as agriculture, animal husbandry and dike building in this Northern German coastal area during the Middle and Late Holocene (MIS 1). Temperature increases at the end of the Late Glacial and beginning of the Holocene caused a major sea level rise, which consistently changed the local morphology of the coastal area of the Eiderstedt Peninsula. Additionally, occasional storm floods also limited settling, land use, human activities and movements during the Late Holocene.

References

Ad-Hoc-Arbeitsgruppe Boden, 2005, Bodenkundliche Kartieranleitung: Schweizerbart'sche Verlagsbuchhandlung, Stuttgart.

Aharonovich, S., Sharon, G., and Weinstein-Evron, M., 2014, Palynological investigations at the Middle Palaeolithic site of Nahal Mahanayeem Outlet, Israel: Quaternary International, v. 331, p. 149–166.

Almogi-Labin, A., 2011, The paleoclimate of the Eastern Mediterranean during the transition from early to mid Pleistocene (900 to 700ka) based on marine and non-marine records: An integrated overview: Journal of Human Evolution, v. 60, no. 4, p. 428–436, doi: 10.1016/j.jhevol.2010.03.007.

Alperson-Afil, N., 2008, Continual fire-making by Hominins at Gesher Benot Ya'aqov, Israel: Quaternary Science Reviews, v. 27, no. 17–18, p. 1733–1739, doi: 10.1016/j.quascirev.2008.06.009.

Alperson-Afil, N., and Goren-Inbar, N., 2010, The Acheulian site of Gesher Benot Ya'aqov Volume II: Ancient flames and controlled use of fire: Springer, New York.

Alperson-Afil, N., Sharon, G., Kislev, M., Melamed, Y., Zohar, I., Ashkenazi, S., Rabinovich, R., Biton, R., Werker, E., Hartman, G., Feibel, C., and Goren-Inbar, N., 2009, Spatial organization of hominin activities at Gesher Benot Ya'aqov, Israel.: Science, v. 326, no. 5960, p. 1677–1680, doi: 10.1126/science.1180695.

Andrew, R., and West, R.G., 1977, Pollen Spectra from Pliocene crag at Orford, Suffolk: New Phytologist, v. 78, no. 3, p. 709–714.

Arias, C., Bigazzi, G., Bonadonna, F., Brunnacker, K., and Urban, B., 1984, Correlation of Plio-Pleistocene deposits of the Lower Rhine Basin (North-West Germany) and the Valle Ricca Pits (Central Italy): Quaternary Science Reviews, v. 3, p. 73–89, doi: 10.1016/0277-3791(84)90005-2.

Arias, C., Bigazzi, G., Bonadonna, F.P., and Urban, B., 1979, Tentative correlations among Quater-nary series of Central and Southern Europe: Acta Geologica Academie Scientific Hungaricae, v. 22, no. 1–4, p. 81–88.

Ashkenazi, S., Motro, U., Goren-Inbar, N., Biton, R., and Rabinovich, R., 2005, New morphometric parameters for assessment of body size in the fossil freshwater crab assemblage from the Acheulian site of Gesher Benot Ya‘aqov, Israel: Journal of Archaeological Science, v. 32, p. 675–689. doi:10.1016/j.jas.2004.12.003.

Ashkenazi, S., Klass, K., Mienis, H.K., Spiro, B., and Abel, R., 2010, Fossil embryos and adult Viviparidae from the Early-Middle Pleistocene of Gesher Benot Ya‘aqov, Israel: Ecology, longevity and fecundity: Lethaia, v. 43, p. 116–127. doi:10.1111/j.1502-3931.2009.00178.x.

Behre, K.-E., 1989, Biostratigraphy of the last glacial period in Europe: Quaternary Science Review, v. 8, no. 1, p. 25–44.

Behre, K.-E., 1991, Veränderungen von Landschaft und Umwelt in der Wesermarsch in den vergangenen Jahrtausenden: Archäologische Mitteilungen aus Nordwestdeutschland, v. 5, p. 33–36.

Behre, K.-E., 2007, Evidence for Mesolithic agriculture in and around central Europe? : Vegetation History and Archaeobotany, v. 16, no. 2, p. 203–219.

Behre, K.-E., and Lade, U., 1986, Eine Folge von Eem und 4 Weichsel-Interstadialen in Oerel/Niedersachsen und ihr Vegetationsablauf: Eiszeitalter und Gegenwart, v. 36, p. 11–36.

Behre, K.-E., Menke, B., and Streif, H., 1979, The Quaternary geological development of the German part of the North Sea, *in* Oele, E., Schüttenhelm, R.T.E., and Wiggers, A.J. eds., The Quaternary history of the North Sea, p. 85–115.

Belitzky, S., 2002, The structure and morphotectonics of the Gesher Benot Ya‘aqov area, Northern Dead Sea Rift, Israel: Quaternary Research, v. 58, p. 372–380, doi: 10.1006/qres.2002.2347.

Benda, L., 1995, Das Quartär Deutschland: Gebrüder Borntraeger Berlin, Stuttgart.

Berger, W.H., and Jansen, E., 1996, Climate, Mid-Pleistocene Connection, shift: the Nansen, *in* Johannessen, O.M., Muench, R.D., and Overlan, J.E. eds., The Polar Oceans and Their Role in Shaping the Global Environmen. AGU Geophysical Monograph, AGU, Washington D.C., p. 295–311.

Bertini, A., 2010, Pliocene to Pleistocene palynoflora and vegetation in Italy: State of the art: Quaternary International, v. 225, no. 1, p. 5–24, doi: 10.1016/j.quaint.2010.04.025.

Bertoldi, R., Rio, D., and Thunell, R., 1989, Pliocene-pleistocene vegetational and climatic evolution of the south-central mediterranean: Palaeogeography, Palaeoclimatology, Palaeoecology, v. 72, no. C, p. 263–275, doi: 10.1016/0031-0182(89)90146-6.

Birks, H.J.B., and Birks, H.H., 2008, Biological responses to rapid climate change at the Younger Dryas-Holocene transition at Kråkenes, western Norway: The Holocene, v. 18, no. 1, p. 19–30.

Biton, R., Geffen, E., Vences, M., Cohen, O., Bailon, S., Rabinovich, R., Malka, Y., Oron, T., Boistel, R., Brumfeld, V., and Gafny, S., 2013, The rediscovered Hula painted frog is a living fossil: Nature Communications, v. 4, no. 1959. doi: 10.1038/ncomms2959.

Biton, R., Boistel, R., Rabinovich, R., Gafny, S., and Bailon, S., 2016, Osteological observations on the Alytid Anura Latonia nigriventer with comments on functional morphology, biogeography, and evolutionary history: Journal of Morphology, v. 227, no. 9, p. 1131–1145.

Bock, W., Menke, B., Strehl, E., and Ziemus, H., 1985, Neue Funde des Weichsel-Spätglazials in Schleswig-Holstein: Eiszeitalter und Gegenwart, v. 35, p. 161–180.

Bos, J.A.A., 2001, Lateglacial and Early Holocene vegetation history of the northern Wetterau and the Amöneburger Basin (Hessen), central Germany: Review of Palaeobotany and Palynology, v. 115, no. 3–4, p. 177–204.

Bottema, S., 1995, The Younger Dryas in the Eastern Mediterranean: Quaternary Science Reviews, v. 14, no. 9, p. 883–891, doi: 10.1016/0277-3791(95)00069-0.

Bradtmöller, M., Pastoors, A., Weninger, B., and Weniger, G.C., 2012, The repeated replacement model - Rapid climate change and population dynamics in Late Pleistocene Europe: Quaternary International, v. 247, no. 1, p. 38–49, doi: 10.1016/j.quaint.2010.10.015.

Cepek, A.G., 1967, Stand und Probleme der Quartärstratigraphie im Nordteil der DDR: Berichte der Deutschen Gesellschaft für Geologische Wissenschaft, Reihe A, v. 12, no. 3–4, p. 375–404.

Cohen, K.M., and Gibbard, P.L., 2016, Global chronostratigraphical correlation table for the last 2.7 million years v. 2016a, International Commission on Stratigraphy. Available online: http://www.stratigraphy.org/index.php/ics-chart-timescale (accessed 9 February 2017).

Combourieu-Nebout, N., 1993, Vegetation response to Upper Pliocene glacial/interglacial cyclicity in the Central Mediterranean: Quaternary Research, v. 40, p. 228–236.

Danin, A., 1992, Flora and vegetation of Israel and adjacent areas: Bocconea, , no. 3, p. 18–42.

De Beaulieu, J.L., Andrieu-Ponel, V., Reille, M., Grüger, E., Tzedakis, C., and Svobodova, H., 2001, An attempt at correlation between the Velay pollen sequence and the Middle Pleistocene stratigraphy from central Europe: Quaternary Science Reviews, v. 20, no. 16–17, p. 1593–1602, doi: 10.1016/S0277-3791(01)00027-0.

Deutsche Stratigraphische Kommission, 2016, Stratigraphischen Tabelle von Deutschland 2016.

Diehl, M., 2007, Palynologie und Sedimentologie der Interglazialprofile Döttingen, Bonstorf, Munster and Bilshausen, Dissertation: University of Mainz, 310 p.

Dörfler, W., 2000, Palynologische Untersuchungen zur Vegetations- und Landschaftsentwicklung von Joldelund, Kr. Nordfriesland, *in* Haffner, A., Jöns, H., and Reichstein, J. eds., Frühe Eisengewinnung in Jodelund, Kr. Nordfriesland. Universitätsforschungen zur Prähistorischen Archäologie Band: 59, Verlag Dr. Rudolf Habelt GmbH., Bonn, p. 147–216.

Dörfler, W., Feeser, I., Van den Bogaard, C., Dreibrodt, S., Erlenkeuser, H., Kleinmann, A., Merkt, J., and Wiethold, J., 2012, A high-quality annually laminated sequence from Lake Belau, Northern Germany: Revised chronology and its implications for palynological and tephrochronological studies: The Holocene, v. 22, p. 1413–1426.

Dücker, A., 1969, Der Ablauf der Holstein-Warmzeit in Westholstein: Eiszeitalter und Gegenwart, v. 20, p. 46–57.

Ehlers, J., 1987, Die Entstehung des Kaolinsandes von Sylt, *in* Von Hacht, U. ed., Fossilien von Sylt, II, Von Hacht, Hamburg, p.249–267.

Ehlers, J., Meyer, K.-D., and Stephan, H.-J., 1984, The pre-Weichselian glaciations of North-West Europe: Quaternary Science Review, v. 3, no. 1, p. 1–40.

Ehlers, J., Eissmann, L., Lippstreu, L., Stephan, H.-J., and Wansa, S., 2004, Pleistocene Glaciations of North Germany, *in* Ehlers, J., Gibbard, P.L., and Hughes, P.D. eds., Quaternary Glaciations – Extent and Chronology; Part I: Europe; Vol. 2a:

Developments in Quaternary Science, Elsevier, Amsterdam, p. 135–146.

Ehlers, J., Grube, A., Stephan, H.-J., and Wansa, S., 2011, Pleistocene glaciations of North Germany – New Results, *in* Ehlers, J., Gibbard, P.L., and Hughes, P.D. eds., Developments in Quaternary Science 15: Quaternary Glaciations – Extent and Chronology, A closer look, Elsevier, Amsterdam, p. 149–162.

Eissmann, L., 2004, Reduced to the Maximum: Mitteleuropäisches Quartär im Spiegel hochverdichteter geologischer Schnitte: Mauritiana (Altenburg), v. 19, p. 1–16.

Eissmann, L., and Müller, A., 1979, Leitlinien der Quartärentwicklung im norddeutschen Tiefland: Zeitschrift für Geologische Wissenschaften Berlin, v. 7, no. 4, p. 451–462.

Elton, S., 2008, The environmental context of human evolutionary history in Eurasia and Africa: Journal of Anatomy, v. 212, no. 4, p. 377–393, doi: 10.1111/j.1469-7580.2008.00872.x.

Erd, K., 1970, Pollen-analytical classification of the Middle Pleistocene in the German Democratic Republic: Palaeogeography, Palaeoclimatology, Palaeontology, v. 8, p. 129–145.

Erd, K., 1973, Vegetationsentwicklung und Biostratigraphie der Dömnitz-Warmzeit (Fuhne/Saale) im Profil von Pritzwalk/Prignitz: Abhandlung des Zentralen Geologischen Instituts, v. 18, p. 9–48.

Falk, G.C., 2001, Die Paläogeomorphologie ausgewählter Standorte der schleswig-holsteinischen Nordseeküste im Früh- und Mittelholozän: Technical University of Berlin, 171 p.

Feibel, C.S., 2001, Archaeological sediments in lake margin environments, *in*: Stein, J.K., Farrand, W.R. eds., Sediments in Archaeological Context, The University of Utah Press, Salt Lake City, p. 127–148.

Feibel, C.S., 2004, Quaternary lake margins of the Levant Rift Valley, *in*: Goren-Inbar, N., Speth, J.D. eds., Human Paleoecology in the Levantine Corridor, Oxbow Books, Oxford, p. 21–36.

Firbas, F., 1949, Spät- und nacheiszeitliche Waldgeschichte Mitteleuropas nördlich der Alpen. Band 1: Allgemeine Waldgesichte: Fischer, Jena.

Fowell, S.J.B., Hansen, C.S., Peck, J.A., Khosbayar, P., and Ganbold, E., 2003, Mid to late Holocene climate evolution of the Lake Telmen Basin, North Central Mongolia, based on palynological data: Quaternary Research, v. 59, p. 353–363.

Frechen, M., Buness, H., Grube, A., Königer, P., Sirocko, F., Urban, B., and Wiederhold, H., 2011, The Garding Drilling Project – Unravelling the Quaternary Record in

Northern Germany by means of Palynology , Geology and Applied Geophysics, in Cologne.

Frenzel, B., 1973, On the Pleistocene vegetation history.: Eiszeitalter und Gegenwart Quarternary Science Journal, v. 23/24, p. 321–332.

Frey, W., and Kürschner, H., 1989, Tübinger Atlas des Vorderen Orients, Karte A VI 1, Vorderer Orient. Vegetation 1:8000000: Dr. Ludwig Reichert Verlag, Wiesbaden.

Fromm, K., 1994, Paläomagnetische Bestimmungen an Quartärsedimenten in Nordwest-Deutschland, *in* Meyer, K.-D. ed., Geologisches Jahrbuch A: 134 - Neuere Untersuchungen an Interglazialen in Niedersachsen, Schweizerbart'sche Verlagsbuchhandlung, Stuttgart, p. 229–257.

Geyh, M.A., and Müller, H., 2005, Numerical 230Th/U dating and a palynological review of the Holsteinian/Hoxnian Interglacial: Quaternary Science Reviews, v. 24, no. 16–17, p. 1861–1872, doi: 10.1016/j.quascirev.2005.01.007.

Gibbard, P.L., and Cohen, K.M., 2008, Global chronostratigraphical correlation table for the last 2.7 million years: Episodes, v. 31, no. 2, p. 243–247.

Gibbard, P., West, R., Zagwijn, W., Balson, P., Burger, A., Funnell, B., Jeffery, D., Dejong, J., Vankolfschoten, T., Lister, A., Meijer, T., Norton, P., Preece, R., Rose, J., et al., 1991, Early and Early Middle Pleistocene Correlations in the Southern North-Sea Basin: Quaternary Science Reviews, v. 10, p. 23–52.

Goren-Inbar, N., and Saragusti, I., 1996, An Acheulian biface assemblage from Gesher Benot Ya'aqov, Israel: indications of African affinities: Journal of Field Archaeology, v. 23, p. 15–30. doi:10.2307/530606.

Goren-Inbar, N., and Sharon, G., 2006, Invisible handaxes and visible Acheulian biface technology at Gesher Benot Ya'aqov, Israel, *in* Goren-Inbar, N., and Sharon, G. eds., Axe Age: Acheulian Tool-Making from Quarry to Discard, Equinox Publishing Ltd., London, p. 105–129.

Goren-Inbar, N., Belitzky, S., Verosub, K.L., Werker, E., Kislev, M.E., Heimann, A., Carmi, I., and Rosenfeld, A., 1992, New discoveries at the Middle Pleistocene Acheulian site of Benot Ya'aqov, Israel: Quaternary Research, v. 38, p. 117–128.

Goren-Inbar, N., Lister, A., Werker, E., and Chech, M., 1994, A butchered elephant skull and associated artifacts from the Acheulian site of Gesher Benot Ya'aqov, Israel: Paléorient, v. 20, p. 99–112. doi:10.3406/paleo.1994.4604.

Goren-Inbar, N., Feibel, C.S., Verosub, K.L., Melamed, Y., Kislev, M.E., Tchernov, E., and Saragusti, I., 2000, Pleistocene Milestones on the Out-of-Africa Corridor at

Gesher Benot Ya‘aqov, Israel: Science, v. 289, no. 5481, p. 944–947, doi: 10.1126/science.289.5481.944.

Goren-Inbar, N., Sharon, G., Melamed, Y., and Kislev, M., 2002a, Nuts, nut cracking, and pitted stones at Gesher Benot Ya‘aqov, Israel: Proceedings of the National Academy of Sciences of the United States of America, v. 99, p. 2455–2460. doi:10.1073/pnas.032570499.

Goren-Inbar, N., Werker, E., and Feibel, C.S., 2002b, The Acheulian Site of Gesher Benot Ya‘aqov, Israel, I The Wood Assemblage: Oxbow Books, Oxford.

Goren-Inbar, N., Alperson, N., Kislev, M.E., Simchoni, O., Melamed, Y., Ben-Nun, A., and Werker, E., 2004, Evidence of Hominin Control of Fire at Gesher Benot Ya‘aqov, Israel: Science, v. 304, no. 5671, p. 725–727, doi: 10.1126/science.1095443.

Goren-Inbar, N., Kislev, M., Melamed, Y., Rabinovich, R., Zohar, I., Biton, R., et al., 2009, The effect of climate change on the environment and hominins of the Upper Jordan Valley between ca. 800Ka and 700Ka ago as a basis for prediction of future scenarios. ISF Report. Jerusalem: Hebrew University (Israel Science Foundation grant).

Goren-Inbar, N., Alperson-Afil, N., Sharon, G., and Herzlinger, G., in press, The Acheulian Site of Gesher Benot Ya‘aqov: The Lithic Assemblages: Springer, Dordrecht.

Graham, A.G.C., Stoker, M.S., Lonergan, L., Bradwell, T., and Stewart, M.A., 2011: The Pleistocene glaciations of the North Sea basin, *in*: Ehlers, J., and Gibbard, P.L. eds., Quaternary glaciations – extent and chronology; 2nd ed., Elsevier, Amsterdam, p. 261–278.

Grimm, E.C., 1987, CONISS: A fortran 77 program for stratigraphically constrained cluster analysis by the method of incremental sum of squares: Computers and Geosciences, v. 13, no. 1, p. 13–35.

Grimm, E.C., 1990, Tilia, Tiliagraph & Tiliaview. PC spreadsheet and graphics software for pollen data.

Grube, A., 2011, Schichtansprache der Forschungsbohrung Garding-2, Landesamt für Landwirtschaft, Umwelt und ländliche Räume, Flintbek, unpublished.

Grüger, E., 1968, Vegetationsgeschichtliche Untersuchungen an cromerzeitlichen Ablagerungen im nördlichen Randgebiet der deutschen Mittelgebirge: Eiszeitalter und Gegenwart, v. 18, p. 204–235.

Grüger, E., 1989, Stratigraphy of the last interglacial/glacial cycle in Germany: Quaternary International, v. 3, p. 69–79.

Hahne, J., Mengeling, H., Merkt, J., and Gramann, F., 1994, Die Hunteburg-Warmzeit

("Cromer-Komplex") und Ablagerungen der Elster-, Saale- und Weichsel-Kaltzeit in der Forschungsbohrung Hunteburg GE 58 bei Osnabrück, *in* Meyer, K.-D. ed., Geologisches Jahrbuch A: 134 - Neuere Untersuchungen an Interglazialen in Niedersachsen, Schweizerbart'sche Verlagsbuchhandlung, Stuttgart, p. 117–166.

Hahne, J., Ellwanger, D., and Stritzke, R., 2008, Evidence for a Waalian thermomer pollen record from the research borehole Heidelberg UniNord , Upper Rhine Graben , Baden-Württemberg: Eiszeitalter und Gegenwart Quarternary Science Journal, v. 57, no. 3–4, p. 403–410.

Hallik, R., 1960, Die Vegetationsentwicklung der Holstein-Warmzeit in Nordwestdeutschland und die Altersstellung der Kieselgurlager der südlichen Lüneburger Heide: Zeitschrift der Deutschen Geologischen Gesellschaft, v. 112, p. 326–333.

Head, M.J., and Gibbard, P.L., 2005, Early-Middle Pleistocene transitions: an overview and recommendation for the defining boundary: Geological Society, London, Special Publications, v. 247, no. 1, p. 1–18, doi: 10.1144/GSL.SP.2005.247.01.01.

Hinsch, W., 1974, Geologisches Jahrbuch A: 24 - Das Tertiär im Untergrund von Schleswig-Holstein (Das Nordwestdeutsche Tertiärbecken, Beitrag 5): Schweizerbart'sche Verlagsbuchhandlung, Stuttgart.

Horowitz, A., 1975, The Quaternary Stratigraphy and Paleogeography of Israel: Paléorient, v. 3, p. 47–100, doi: 10.3406/paleo.1975.4190.

Horowitz, A., 1989, Palynological evidence for the Quaternary rates of accumulation along the Dead Sea Rift, and structural implications: Tectonophysics, v. 164, no. 1, p. 63–71, doi: 10.1016/0040-1951(89)90234-5.

Ickert-Bond, S.M., and Renner, S.S., 2016, The Gnetales: Recent insights on their morphology, reproductive biology, chromosome numbers, biogeography, and divergence times: Journal of Systematics and Evolution, v. 54, no. 1, p. 1–16, doi: 10.1111/jse.12190.

Iversen, J., 1958, The bearing of glacial and interglacial on the formation and extinction of plant taxa:

Joannin, S., Cornée, J.-J., Moissette, P., Suc, J.-P., Koskeridou, E., Lécuyer, C., Buisine, C., Kouli, K., and Ferry, S., 2007a, Changes in vegetation and marine environments in the eastern Mediterranean (Rhodes, Greece) during the Early and Middle Pleistocene: Journal of the Geological Society, London, v. 164, no. 2007, p. 1119–1131.

Joannin, S., Quillévéré, F., Suc, J.-P., Lecuyer, C., and Martineau, F., 2007b, Composite climate changes during the Early Pleistocene: continental and marine responses recorded in the Central Mediterranean region (Santa Lucia Section, Crotone, Italy): Quaternary Research,.

Joannin, S., Ciaranfi, N., and Stefanelli, S., 2008, Vegetation changes during the late Early Pleistocene at Montalbano Jonico (Province of Matera, southern Italy) based on pollen analysis: Palaeogeography, Palaeoclimatology, Palaeoecology, v. 270, no. 1–2, p. 92–101, doi: 10.1016/j.palaeo.2008.08.017.

Jousse, H., 2006, What is the impact of Holocene climatic changes on human societies? Analysis of West African Neolithic populations dietary customs: Quaternary International, v. 151, no. 1, p. 63–73.

Kalbe, J., Sharon, G., Porat, N., Zhang, C., and Mischke, S., 2014, Geological setting and age of the Middle Paleolithic site of Nahal Mahanayeem Outlet (Upper Jordan Valley, Israel); Quaternary International, v. 331, p. 139–148.

Kalis, A.J., Merkt, J., and Wunderlich, J., 2003, Environmental changes during the Holocene climatic optimum in central Europe – human impact and natural causes: Quaternary Science Reviews, v. 22, p. 33–79.

Kislev, M., and Melamed, Y., 2011, The first archaeobotanical record of environmental change and hominin diet in the Out-of-Africa Corridor during the Lower to Upper Paleolithic, Center of Excellence Project No. 858/09.

Kleinmann, A., Müller, H., Lepper, J., and Waas, D., 2011, Nachtigall: A continental sediment and pollen sequence of the Saalian Complex in NW-Germany and its relationship to the MIS-framework: Quaternary International, v. 241, p. 97–110.

Knoth, W., 1964, Zur Kenntnis der pleistozänen Mittelterrassen der Saale und Mulde nördlich von Halle: Geologie, v. 13, p. 598–616.

Kühn, H.J., and Panten, A., 1989, Der frühe Deichbau in Nordfriesland: Archäologisch-historische Untersuchungen: Nordfriisk Instituut, Bredstedt.

Kunz, A., Urban, B., and Tsukamoto, S., 2016, Chronological investigations of Pleistocene interglacial, glacial and aeolian deposits from Schöningen (Germany) using post-IR IRSL dating and pollen analysis: Zeitschrift der Deutschen Gesellschaft für Geowissenschaften, v. 168, no. 1, p. 81–104, doi: 10.1127/zdgg/2016/0080.

Lang, G., 1994, Quartäre Vegetationsgeschichte Europas. Methoden und Ergebnisse: Fischer, Jena.

Langgut, D., 2008, Late Quaternary palynological sequences from the Eastern

Mediterranean Sea. Report GSI/16/08, Geological Survey of Israel.:

Leroy, S.A.G., Arpe, K., and Mikolajewicz, U., 2011, Vegetation context and climatic limits of the Early Pleistocene hominin dispersal in Europe: Quaternary Science Reviews, v. 30, no. 11–12, p. 1448–1463, doi: 10.1016/j.quascirev.2010.01.017.

Linke, G., and Hallik, R., 1993, Die pollenanalytischen Ergebnisse der Bohrungen Hamburg-Dockenhuden (qho 4), Wedel (qho 2) und Hamburg-Billbrook, *in* Benda, L. ed., Geologisches Jahrbuch A: 138, Holstein-Interglazial: Schweizerbart'sche Verlagsbuchhandlung, Stuttgart, p. 169–184.

Lisiecki, L.E., and Raymo, M.E., 2005, A Pliocene-Pleistocene stack of 57 globally distributed benthic δ18O records: Paleoceanography, v. 20, no. 1, p. 1–17, doi: 10.1029/2004PA001071.

Litt, T., Brauer, A., Goslar, T., Merkt, J., Bałaga, K., Müller, H., Ralska-Jasiewiczowa, M., Stebich, M., and Negendank, J.F.W., 2001, Correlation and synchronisation of Lateglacial continental sequences in northern central Europe based on annually laminated lacustrine sediments: Quaternary Science Review, v. 20, p. 1233–1249.

Litt, T., Behre, K.-E., Meyer, K.-D., Stephan, H.-J., and Wansa, S., 2007, Stratigraphische Begriffe für das Quartär des norddeutschen Vereisungsgebietes: Eiszeitalter und Gegenwart Quarternary Science Journal, v. 56, no. 1, p. 7–65, doi: 10.3285/eg.56.1-2.

Magri, D., 2010, Persistence of tree taxa in Europe and Quaternary climate changes: Quaternary International, v. 219, no. 1–2, p. 145–151, doi: 10.1016/j.quaint.2009.10.032.

Maiorano, P., Bertini, A., Capolongo, D., Eramo, G., Gallicchio, S., Girone, A., Pinto, D., Toti, F., Ventruti, G., and Marino, M., 2016, Climate signatures through Marine Isotope Stage 19 in the Montalbano Jonico section (Southern Italy): A landsea perspective: Palaeogeography, Palaeoclimatology, Palaeoecology, v. 461, p. 341–361, doi: 10.1016/j.palaeo.2016.08.029.

Meier, D., 2004, Man and environment in the marsh area of Schleswig-Holstein from Roman until Medieval times. Quaternary International, v. 112, p. 55–69.

Melamed, Yoel, Kislev, M.E., Geffen, E., Lev-Yadun, S., and Goren-Inbar, N., 2016, The plant component of an Acheulian diet at Gesher Benot Ya'aqov, Israel. Proceedings of the National Academy of Sciences of the USA, v. 113, no. 51, p. 14674–14679.

Menke, B., 1968a, Beiträge zur Biostratigraphie des Mittelpleistozäns in Norddeutschland: Meyniana, v. 18, p. 35–42.

Menke, B., 1968b, Das Spätglazial von Glüsing: Eiszeitalter und Gegenwart, v. 19, p. 73–84.

Menke, B., 1969, Vegetationskundliche und vegetationsgeschichtliche Untersuchungen an Strandwällen: Mitteilungen der Foristisch-soziologischen Arbeitsgemeinschaft N. F., v. 14, p. 95–120.

Menke, B., 1975, Vegetationsgeschichte und Florenstratigraphie Nordwestdeutschlands im Pliozän und Frühquartär. Mit einem Beitrag zur Biostratigraphie des Weichselfrühglazials, *in* Lang, H.D. ed., Geologisches Jahrbuch A: 26 - Pliozän und Frühquartär in NW-Deutschland, Schweizerbart'sche Verlagsbuchhandlung, Stuttgart, p. 3–151.

Menke, B., 1976, Geologisches Jahrbuch A: 32 - Pliozäne und ältestquartäre Sporen- und Pollenflora von Schleswig-Holstein: Schweizerbart'sche Verlagsbuchhandlung, Stuttgart.

Menke, B., 1986, Beiträge zur Entwicklung des Holuzäns im Raum Husum-Simonsberg/Nordfriesland: Offa, v. 43, p. 265–272.

Menke, B., and Behre, K.-E., 1973, History of vegetation and biostratigraphy: Eiszeitalter und Gegenwart, v. 23/24, p. 251–267.

Menke, B., and Tynni, R., 1984, Geologisches Jahrbuch A: 76 - Das Eem-Interglazial und das Weichselfrühglazial von Redderstall/Dithmarschen und ihre Bedeutung für die mitteleuropäische Jungpleistozän-Gliederung: Schweizerbart'sche Verlagsbuchhandlung, Stuttgart.

Merkt, J., and Müller, H., 1999, Varve chronology and palynology of the Lateglacial in Northwest Germany from lacustrine sediments of Hämelsee in Lower Saxony: Quaternary International, v. 61, p. 41–59.

Meyers, P.A., 1994, Preservation of elemental and isotopic source identification of sedimentary organic matter: Chemical Geology, v. 114, p. 289–302, doi: 10.1016/0009-2541(94)90059-0.

Meyers, P.A., and Ishiwatari, R., 1993, Lacustrine organic geochemistry-an overview of indicators of organic matter sources and diagenesis in lake sediments: Organic Geochemistry, v. 7, p. 867–900.

Mienis, H.K., and Ashkenazi, S., 2011, Lentic Basommatophora molluscs and hygrophilous land snails as indicators of habitat and climate in the Early-Middle Pleistocene (0.78 Ma) at the site of Gesher Benot Ya'aqov (GBY), Israel: Journal of Human Evolution, v. 60, no. 4, p. 328–340, doi: 10.1016/j.jhevol.2010.03.009.

Mischke, S., Ashkenazi, S., Almogi-Labin, A., and Goren-Inbar, N., 2014, Ostracod evidence for the Acheulian environment of the ancient Hula Lake (Levant) during the early-mid Pleistocene transition: Palaeogeography Palaeoclimatology Palaeoecology, v. 412, p. 148–159. doi:10.1016/j.palaeo.2014.07.036.

Müller, H., 1974, Pollenanalytische Untersuchungen und Jahresschichtenzählungen an der holsteinzeitlichen Kieselgur von Munster-Breloh, *in* Lang, H.D. ed., Geologisches Jahrbuch A: 21, Kieselgur-Lagerstätten: Verbreitung, Diatomeen, Pollen-Analytische Studien und Jahresschichtenzählungen an Vorkommen in Niedersachsen, Schweizerbart'sche Verlagsbuchhandlung, Stuttgart, p. 107–140.

Müller, H., 1986, Alquartäre Sedimente im Deckgebirge des Salzstockes Gorleben: Zeitschrift der Deutschen Gesellschaft für Geowissenschaften, v. 137, p. 85–95.

Müller, H., 1992, Climatc changes during and at the end of the interglacials of the Cromerian Complex, *in* Kukla, G.J. and Went, E. eds., Start of a Glacial, Springer, Heidelberg, p. 51–70.

Müller, H., and Höfle, H.-C., 1994, Geologisches Jahrbuch A: 134, Die Holstein-Interglazialvorkommen bei Bossel westlich von Stade und Wanhöden nördlich Bremerhaven: Schweizerbart'sche Verlagsbuchhandlung, Stuttgart, p. 71 – 116.

Munsell Color, 2009, Munsell soil-color chart: Munsell color x.rite, Michigan.

Nelle, O., and Dörfler, W., 2008, A summary of the late- and post-glacial vegetation history of Schleswig-Holstein: Mitteilungen der Arbeitsgemeinschaft Geobotanik in Schleswig-Holstein und Hamburg, v. 65, p. 45–68, doi: ISSN 0344-8002.

Nesje, A., and Dahl, S.O., 2016, Glaciers and environmental change: Routledge, New York.

Overbeck, F., 1975, Botanisch-geologische Moorkunde, unter besonderer Berücksichtigung der Moore, Nordwestdeutschlands als Quellen zur Vegetations-, Klima- und Siedlungsgeschichte: Karl Wachholtz Verlag, Neumünster.

Parker, A.G., Goudie, A.S., Anderson, D.E., Robinson, M.A., and Bonsall, C., 2002, A review of the mid-Holocene elm decline in the British Isles: Progress in Physical Geography, v. 26, p. 1–45.

Plaster, E.J., 2009, Soil Science and Management: Cengage Learning, Delmar.

Rabinovich, R., and Biton, R., 2011, The Early-Middle Pleistocene faunal assemblages of Gesher Benot Ya'aqov: Inter-site variability: Journal of Human Evolution, v. 60, p. 357–374. doi:10.1016/j.jhevol.2010.12.002.

Raymo, M.E., 1997, The timing of major climate terminations: Paleoceanography, v. 12, no. 4, p. 577, doi: 10.1029/97PA01169.

Reille, M., Andrieu, V., De Beaulieu, J.-L., Guenet, P., and Goeury, C., 1998, A long pollen record from Lac du Bouchet, Massif Central, France: for the period ca. 325 to 100 ka BP (OIS 9c to OIS 5e): Quaternary Science Reviews, v. 17, no. 12, p. 1107–1123, doi: 10.1016/S0277-3791(97)00093-0.

Rosenfeld, A., Nathan, Y., Feibel, C.S., Schilman, B., Halicz, L., Goren-Inbar, N., and Siman-Tov, R., 2004, Palaeoenvironment of the Acheulian Gesher Benot Ya‘aqov Pleistocene lacustrine strata, Northern Israel - lithology, ostracod assemblages and ostracod shell geochemistry: Journal of African Earth Sciences, v. 38, p. 169–181. doi:10.1016/j.jafrearsci.2003.10.008.

Roskosch, J., Winsemann, J., Polom, U., Brandes, C., Tsukamoto, S., Weitkamp, A., Bartholomäus, W.A., Henningsen, D., and Frechen, M., 2015, Luminescence dating of ice-marginal deposits in northern Germany: evidence for repeated glaciationsduring the Middle Pleistocene (MIS 12 to MIS 6): Boreas, v. 44 no. 1 p. 103–126.

Ruddiman, W.F., 2006, Orbital changes and climate: Quaternary Science Reviews, v. 25, p. 3092–3112.

Scheidt, S., Hambach, U., and Rolf, C., 2015, A consistent magnetic polarity stratigraphy of late Neogene to Quaternary fluvial sediments from the Heidelberg Basin (Germany): A new time frame for the Plio–Pleistocene palaeoclimatic evolution of the Rhine Basin: Global and Planetary Change, v. 127, p. 103–116.

Sharon G., 2007, Acheulian large flake industries: Technology, chronology, and significance: BAR International Series, Oxford.

Sharon, G., and Oron, M., 2014, The lithic tool arsenal of a Mousterian hunter; Quaternary International, v. 331, p. 167–185.

Sharon, G., Alperson-Afil, N., and Goren-Inbar, N., 2011, Cultural conservatism and variability in the Acheulian sequence of Gesher Benot Ya‘aqov: Journal of Human Evolution, v. 60, p. 387–397. doi:10.1016/j.jhevol.2009.11.012.

Sirocko, F., Dietrich, S., Veres, D., Grootes, P.M., Schaber-Mohr, K., Seelos, K., Nadeau, M.J., Kromer, B., Rothacker, L., Röhner, M., Krbetschek, M., Appleby, P., Hambach, U., Rolf, C., et al., 2013, Multi-proxy dating of Holocene maar lakes and Pleistocene dry maar sediments in the Eifel, Germany: Quaternary Science Reviews, v. 62, p. 56–76, doi: 10.1016/j.quascirev.2012.09.011.

Spiro, B., and Sharon, G., 2008, Preliminary report on the handling, sampling and storing of the geological core #2-2006 from Gesher Benot Ya‘aqov, unpublished.

Stephan, H.-J-, 2002, Forschungsbohrung Oldenswort (OLW), Landesamt für Natur und Umwelt, Abteilung Geologie/Boden, unpublished.

Stephan, H.-J., 2014, Climato-stratigraphic subdivision of the Pleistocene in Schleswig-Holstein, Germany and adjoining areas: Quaternary Research, v. 63, no. 1, p. 3–18, doi: 10.3285/eg.63.1.01.

Stephan, H.-J., and Menke, B., 1993, Das Pleistozän in Schleswig-Holstein: GLA SH (Geologisches Landesamt Schleswig-Holstein), v. 3, p. 19–62.

Stephan, H.-J., Urban, B., Lüttig, G., Menke, B., and Sierralta, M., 2011, Geologisches Jahrbuch A: 160, Palynologische, petrographische und geochronologische Untersuchungen an Ablagerungen der Leck-Warmzeit (spätes Mittelpleistozän) und begleitender Sedimente: Schweizerbart'sche Verlagsbuchhandlung, Stuttgart.

Subally, D., Bilodeau, G., Tamrat, E., Ferry, S., Debard, E., and Hillaire-Marcel, C., 1999, Cyclic climatic records during the Olduvai Subchron (uppermost Pliocene) on Zakynthos Island (Ionian Sea): Geobios, v. 32, no. 6, p. 793–803.

Suc, J.-P., 1984, Origin and evolution of the Mediterranean vegetation and climate in Europe: Nature, v. 307, no. 5950, p. 429–432, doi: 10.1038/307429a0.

Suc, J.-P., and Zagwijn, W.H., 1983, Plio-Pleistocene correlations between the northwestern Mediterranean region and northwestern Europe according to recent biostratigraphic and palaeoclimatic data: Boreas, v. 12, no. 3, p. 153–166.

Suc, J.-P., and Popescu, S.-M., 2005, Pollen records and climatic cycles in the North Mediterranean region, *in* Head, M.J. and Gibbard, P.L. eds., Early– Middle Pleistocene Transitions: The Land–Ocean Evidence, Geological Society of London, p. 147–158.

Suc, J.-P., Combourieu-Nebout, N., Seret, G., Popescu, S.M., Klotz, S., Gautier, F., Clauzon, G., Westgate, J., Insinga, D., and Sandhu, A.S., 2010, The Crotone series: A synthesis and new data: Quaternary International, v. 219, no. 1–2, p. 121–133, doi: 10.1016/j.quaint.2010.01.008.

Thornton, S.F., and McManus, J., 1994, Application of Organic Carbon and Nitrogen Stable Isotope and C/N Ratios as Source Indicators of Organic Matter Provenance in Estuarine Systems: Evidence from the Tay Estuary, Scotland: Estuarine, Coastal and Shelf Science, v. 38, no. 3, p. 219–233, doi: 10.1006/ecss.1994.1015.

Turner, C., 1998, Volcanic Maars, Long Quaternary Sequences and the Work of the Inqua Subcommission on European Quaternary Stratigraphy: Quaternary International, v. 47–48, no. 97, p. 41–49, doi: 10.1016/S1040-6182(97)00069-4.

Tzedakis, P.C., Hooghiemstra, H., and Pälike, H., 2006, The last 1.35 million years at Tenaghi Philippon: revised chronostratigraphy and long-term vegetation trends: Quaternary Science Reviews, v. 25, no. 23–24, p. 3416–3430.

Tzedakis, P.C., Hughen, K.A., Harvati, I., and Cacho, K., 2007, Placing late Neanderthals in a climatic context: Nature, v. 449, p. 206–208.

Urban, B., 1978a, The Interglacial of Frechen I/Rheinland – A section of the Tiglian A-type: Geologie en Mijnbouw/Netherlands Journal of Geosciences, v. 57, no. 3, p. 401–406.

Urban, B., 1978b, Vegetationsgeschichtliche Untersuchungen zur Gliederung des Altquartärs der Niederrheinischen Bucht, Dissertation: University of Cologne, 165 p.

Urban, B., 1983, Biostratigraphic correlation of the Kärlich interglacial, Northwestern Germany: Boreas, v. 12, p. 83–90.

Urban, B., 1995, Younger Middle Pleistocene Interglacials (Holsteinian, Reinsdorf, Schöningen) in the Schöningen open cast lignite mine (Eastern Lower Saxony/Germany): Mededelingen Rijks Geologische Dienst, v. 52, p. 175–186.

Urban, B., 1997, Grundzüge der eiszeitlichen Klima- und Vegetationsgeschichte in Mitteleuropa, *in* Wagner, G.A. and Beinhauer, K.W. eds., Homo heidelbergensis von Mauer-Das Auftreten des Menschen in Mitteleurop, Universitätsverlag C.Winter, Heidelberg, p. 241–265.

Urban, B., 2002, Manual for analysis of soil and related materials, *in* Kunst, S., Kruse, T. and Burmester, A. eds., Sustainable water and soil management, Springer, Berlin, p. 321–370.

Urban, B., 2007, Quartäre Vegetations- und Klimaentwicklung im Tagebau Schöningen, *in* Thieme, H. ed., Die Schöninger Speere: Mensch und Jagd vor 400.000 Jahren, Theiss, Stuttgart, p. 66–75.

Urban, B., Thieme, H., and Elsner, H., 1988, Biostratigraphie, quartärgeologische und urgeschichtliche Befunde aus den Tagebau „Schöningen", Ldkr. Helmstedt: Zeitschrift der Deutschen Gesellschaft für Geowissenschaften, v. 139, p. 123–154.

Urban, B., Sierralta, M., and Frechen, M., 2011, New evidence for vegetation development and timing of Upper Middle Pleistocene interglacials in Northern Germany and tentative correlations: Quaternary International, v. 241, no. 1–2, p. 125–142, doi: 10.1016/j.quaint.2011.02.034.

Van der Wiel, A.M., and Wijmstra, T.A., 1987, Palynology of the lower part (78-120m) of the core Tenaghi Philippon, Middle Pleistocene of Macedonia, Greece: Review of

Palaeobotany and Palynology, v. 52, p. 73–88.

Van Zeist, W., and Bottema, S., 1991, Late Quaternary vegetation of the Near East. Beihefte zum Tübinger Atlas des Vorderen Orients. Reihe A (Naturwissenschaften) Nr. 18.: Dr. Ludwig Reichert Verlag, Wiesbaden.

Van Zeist, W., and Bottema, S., 2009, A palynological study of the Acheulian site of Gesher Benot Ya'aqov, Israel: Vegetation History and Archaeobotany, v. 18, no. 2, p. 105–121, doi: 10.1007/s00334-008-0167-5.

Van Zeist, W., Baruch, U., and Bottema, S., 2009, Holocene Palaeoecology of the Hula Area , Northeastern Israel, *in* Kaptijn, E. and Petit, L.P. eds., A timeless vale. Archaeological and related essays on the Jordan Valley in honour of Gerrit van der Kooij on the occasion of his sixty-fifth birthday, Leiden University Press, Leiden, p. 29–64.

VDLUFA, 1991, Methodenbuch, Band 1: Die Untersuchung der Böden, VDLUFA-Verlag, Darmstadt.

Von Hacht, U., 1987, Fossilien von Sylt, II: Von Hacht, Hamburg.

Wiethold, J., 1998, Studien zur jüngeren postglazialen Vegetations- und Siedlungsgeschichte im östlichen Schleswig-Holstein, Dissertation: University of Kiel, 365 p.

Zagwijn, W.H., 1960, Aspects of the Pliocene and Early Pleistocene vegetation in the Netherlands: Mededelingen van de Geologische Stichting, v. C–III, no. 5, p. 1–78.

Zagwijn, W.H., 1963, Pollen-analytic investigations in the Tiglian of the Netherlands: Mededelingen van de Geologische Stichting, v. 16, p. 49–71.

Zagwijn, W.H., 1994, Reconstruction of climate change during the Holocene in western and central Europe based on pollen records of indicator species: Vegetation History and Archaeobotany, v. 3, p. 65–88, doi: 10.1007/BF00189928.

Zagwijn, W.H., 1996, An analysis of Eemian climate in western and central Europe: Quaternary Science Reviews, v. 15, no. 5–6, p. 451–469, doi: 10.1016/0277-3791(96)00011-X.

Zagwijn, W.H., and De Jong, J., 1984, Die Interglaziale von Bavel und Leerdam und ihre stratigraphische Stellung im niederländischen Früh-Pleistozän: Mededelingen Rijks Geologische Dienst, v. 37, p. 155–169.

Zagwijn, W.H., Van Montfrans, H.M., and Zandstra, J.G., 1971, Subdivision of the "Cromerian" in the Netherlands: pollen-analysis, palaeomagnetism and sedimentary petrology: Geologie en Mijnbouw/Netherlands Journal of Geosciences, v. 50, p. 41–

58.

Zhang, J., Tsukamoto, S., Grube, A., and Frechen, M., 2014, OSL and ^{14}C chronologies of a Holocene sedimentary record (Garding-2 core) from the German North Sea coast: Boreas, v. 43, p. 856–868.

Zohar, I., Goren, M., and Goren-Inbar, N., 2014, Fish and ancient lakes in the dead sea rift: The use of fish remains to reconstruct the ichthyofauna of Paleo-lake Hula: Palaeogeography, Palaeoclimatology, Palaeoecology, v. 405, p. 28–41, doi: 10.1016/j.palaeo.2014.04.006.

Zohary, M., 1982, Beihefte zum Tübinger Atlas des Vorderen Orients. Reihe A, No. 7: Vegetation of Israel and adjacent areas: Dr. Ludwig Reichert Verlag, Wiesbaden.

Appendix A

Overview of Articles

I avouch that all information given in the Appendix A is true in each instance and overall.

Lüneburg, 29.03.2017

Maria Sekar Proborukmi

List of publications according to Guideline of Cumulative Dissertation of Faculty of Sustainability Science §1–14

Paper	Title	Author(s)	Authorship (§12)	WF	Publication type	Publication status (§9)	Conference contribution (§9b)
I	Palaeoenvironmental investigations of the Holocene sedimentary record of the Garding-2 research drill core, Northwest Germany	MSP, BU	First author with predominant contribution	1	Journal article	published (2017) in Zeitschrift der Deutschen Gesellschaft für Geowissenschaften (ZDGG) - German Journal of Geology	9th European Palaeobotany-Palynology Conference (26–31 August 2014, Padova-Italy). Oral presentation. http://geo.geoscienze.unipd.it/eppc2014/Program_July-2014.pdf
II	Late Pliocene–Quaternary record of the Garding-2 research drill core, Northwest Germany	MSP, BU, MF, AG, CR	First author with predominant contribution	1	Journal article	published (2017) in Zeitschrift der Deutschen Gesellschaft für Geowissenschaften (ZDGG) - German Journal of Geology	The Quaternary of the Urals: global trend and Pan-European Quaternary records. INQUA-SEQS 2014 (10–16 September 2014, Ekaterinburg-Russia. Abstract. http://inqua-seqs2014.ecology.uran.ru/
							XIX INQUA Congress. Quaternary perspectives on climate change, natural hazards and civilization (26 July–2 August 2015, Nagoya-Japan). Oral presentation. http://inqua2015.jp/
							LIAG Austauschsitzung 2015 (4–5 November 2015, Hannover-Germany). Oral Presentation. https://www.liag-hannover.de/fileadmin/user_upload/dokumente/forschungsberichte/fb2015.pdf
III	Evidence for climatic changes around the Matuyama-Brunhes Boundary (MBB) inferred from a multi-proxy palaeoenvironmental study of the GBY#2 core, Jordan River Valley, Israel	MSP, BU, SM, HKM, YM, GDN, FJ, NGI	First author with predominant contribution	1	Journal article	published (2018, 2017-online version) in Palaeogeography, Palaeoclimatology, Palaeoecology, Elsevier publishing company	
Total WF:				**3**			

WF: weighting factor

Contributions of authors according to the Guideline of Cumulative Dissertation of Faculty Sustainability Science §12

Type of contributions	Paper I	Paper II	Paper III
Conception of research approach	MSP, BU	MSP, BU, MF	MSP, BU
Development of research methods	MSP, BU	MSP, BU	MSP, BU, NGI
Data collection and data preparation	MSP, BU	MSP, BU, MF, AG, CR	MSP, BU, NGI
Execution of research	MSP, BU	MSP, BU, MF, AG, CR	MSP, BU, NGI, SM, YM, GDN, FJ
Analysis/Interpretation of data or preliminary results	MSP, BU	MSP, BU, MF, AG, CR	MSP, BU, NGI, SM, YM, GDN, FJ, HKM
Writing or substantive rewriting of the manuscript	MSP, BU	MSP, BU	MSP, BU, NGI, SM, YM, GDN, FJ

Name of the authors:
Maria Sekar Proborukmi (MSP)[1], Brigitte Urban (BU)[1], Manfred Frechen (MF)[2], Alf Grube (AG)[3], Christian Rolf (CR)[2], Naama Goren-Inbar (NGI)[4], Steffen Mischke (SM)[5], Yoel Melamed (YM)[6], Guillaume Dupont-Nivet (GDN)[7,8], Fred Jourdan (FJ)[9], Henk K. Mienis (HKM)[10]

Affiliation of the authors:
1. Institute of Ecology, Subject Area Landscape Change, Leuphana University of Lüneburg, Scharnhorststraße 1, 21335 Lüneburg, Germany
2. Leibniz Institute for Applied Geophysics, Stilleweg 2, 30655 Hannover, Germany
3. Free and Hanseatic City of Hamburg, Ministry of Environment and Energy, Geological Survey, Neuenfelder Straße 19, 21109 Hamburg, Germany
4. Institute of Archaeology, Hebrew University of Jerusalem, Mount Scopus, Jerusalem, 9190501, Israel
5. Faculty of Earth Sciences, University of Iceland, Sturlugata, Iceland
6. The Mina and Everard Goodman Faculty of Life Sciences, Bar-Ilan University, Ramat- Gan, 5290002, Israel
7. UMR-CNRS 6118 OSUR-Geosciences Rennes, Université de Rennes 1, Campus de Beaulieu Bat. 15, 35042 Rennes Cedex, France
8. Institute of Earth and Environmental Science, University of Potsdam, Karl-Liebknecht-Str. 24-25, 14476 Potsdam-Golm, Germany
9. Western Australian Isotope Facility, Department of Applied Geology and John de Laeter Centre for Isotope Research, Curtin University, GPO Box U1987, Perth, WA 6845, Australia
10. National Natural History Collections, Hebrew University of Jerusalem, Edmond J. Safra Campus, Jerusalem, 9190401, Israel

Appendix B

Reprint of Articles

This dissertation is based on the following articles that are presented and referred in the framework paper.

Paper I

Late Pliocene–Pleistocene record of the Garding-2 research drill core, Northwest Germany

Reprinted from: Maria Sekar Proborukmi, Brigitte Urban, Manfred Frechen, Alf Grube, Christian Rolf (2017). Late Pliocene–Pleistocene record of the Garding-2 research drill core, Northwest Germany. Zeitschrift der Deutschen Gesellschaft für Geowissenschaften (German Journal of Geology) 168 (1), 141–167. DOI: 10.1127/zdgg/2017/0103.

Z. Dt. Ges. Geowiss. (German J. Geol.), **168 (1)**, p. 141–167, 7 figs. **Article**
Published online March 2017

Late Pliocene–Pleistocene record of the Garding-2 research drill core, Northwest Germany

Maria Sekar Proborukmi[1], Brigitte Urban[1], Manfred Frechen[2], Alf Grube[3] & Christian Rolf[2]*

Proborukmi, M.S., Urban, B., Frechen, M., Grube, A. & Rolf, C. (2017): Late Pliocene–Pleistocene record of the Garding-2 research drill core, Northwest Germany. – Z. Dt. Ges. Geowiss., 168: 141–167, Stuttgart.

Abstract: A multi-proxy study, including palaeoecological, lithological, geochemical and geochronological methods, has been carried out on the Garding-2 research drill core in the German North Sea coastal area at Garding, in Schleswig-Holstein to investigate the palaeoenvironmental and palaeoclimatic evolution and the Quaternary stratigraphy for a broader correlation of Quaternary sequences of formerly glaciated and non-glaciated areas and with Marine Isotope Stages (MIS).

The 240 m long sequence, composed mainly of fine- and coarse-grained fluvial–shallow marine sediments intercalated by muddy–peaty deposits, reveals interglacial–glacial cycles. Based on palynological and lithological findings, the Pliocene-Pleistocene transition lies at 182.87 m below the surface. It is succeeded by Praetiglian deposits and sediments of the Waalian and Bavelian Complex. The termination of the probably second or third Cromerian interglacial is marked by the development of mixed-deciduous forest and the last occurrence of *Tsuga* at 119.50 m depth. At about 109.45–96.00 m, another pre-Elsterian interglacial period is found and tentatively correlated with the Bilshausen Interglacial. The overlying glacigenic sediments between about 89.00 and 82.00 m are assigned to the Elsterian. An unconformity occurs below 80.29 m, at the base of late Holsteinian deposits, which are succeeded by sediments of the subsequent Fuhne cold period between 79.20 and 73.00 m. These deposits are unconformably overlaid by the Drenthian till at 73.00–71.00 m. A single sample of the late Eemian Interglacial is found at 69.25 m and overlain by the Weichselian glaciofluvial sediments. Middle–late Holocene sediments occur from 20 m depth upwards, following a hiatus that is caused by the early Holocene transgression. Optically stimulated luminescence and radio carbon dating results are in accordance (Zhang et al. 2014) and show that these sediments were deposited between around 8.3 and 1.5 ka.

Keywords: Late Pliocene, Early–Late Pleistocene, coastal sediments, palynology, optically stimulated luminescence dating, magnetic susceptibility

1. Introduction

The Quaternary stratigraphy of Northwest Germany has a long history of investigation (Menke 1968a, 1975, 1976a, Frenzel 1973, Urban 1978a, 1995, 2007, Eissmann & Müller 1979, Müller 1986, 1992, Benda 1995, Ehlers et al. 2004, Eissmann 2004, Litt et al. 2007, Kleinmann et al. 2011, Urban et al. 2011, Stephan 2014). The characteristics of the Quaternary glacial and interglacial deposits have been identified at several sites in Europe where researchers mainly focus on the correlation and comparison of regional effects of climatic change and events with the northwestern European stratigraphy (Erd 1970, Menke 1970, 1975, Menke & Behre 1973, Urban 1983, Arias et al. 1984, Gibbard et al. 1991, Stephan & Menke 1993, Zagwijn 1994, 1996, Turner 1998, Eissmann 2002, Kukla et al. 2002, Pross & Klotz 2002, Geyh & Müller 2005, Litt et al. 2007, Koutsodendris et al. 2010, Magri 2010, Ehlers et al. 2011, Urban et al. 2011, Kuneš et al. 2013, Sirocko et al. 2013, Scheidt et al. 2015).

The objectives of this paper are to contribute to a better understanding of northern German Quaternary stratigraphy and palaeoenvironmental and palaeoclimatic evolution, with a focus on providing a broader correlation between them.

A sequence of well-preserved late Tertiary and Quaternary sediments was expected to be found in the Garding Trough (Menke & Behre 1973, Hinsch 1974, Menke 1976a), located in the western coastal area of Schleswig-Holstein, Germany, and a joint research drilling project in the Garding area was initiated. Some drilling archives, unfortunately mainly of shallow drill holes, and geological maps were

*Addresses of the authors: [1]Institute of Ecology, Subject Area Landscape Change, Leuphana University of Lüneburg, Scharnhorststraße 1, 21335 Lüneburg, Germany; [2]Leibniz Institute for Applied Geophysics, Stilleweg 2, 30655 Hannover, Germany; [3]Free and Hanseatic City of Hamburg, Ministry of Environment and Energy, Geological Survey, Neuenfelder Straße 19, 21109 Hamburg, Germany / Maria.S.Proborukmi@stud.leuphana.de; b.urban@leuphana.de; Manfred.Frechen@liag-hannover.de; alf.grube@bue.hamburg.de; Christian.Rolf@liag-hannover.de.

DOI: 10.1127/zdgg/2017/0103 1860-1804/0103 $ 12.60

evaluated. The later intensive geophysical investigations in the area and the pilot drilling of a 36 m-long core of Garding-1 (Fig. 1) had given evidence of relatively thick and continuous Holocene sediments (Frechen et al. 2011). These results gave hints that a deeper-drilled core in the vicinity of the drilling point could provide a record of relatively thick Quaternary sediments. Based on these results, the location of the Garding-2 research drill hole was chosen and the drilling was performed in February 2011 under the direction of Leibniz Institute of Applied Geophysics (LIAG), Hannover.

The Garding-2 core is composed of 240 m of sediment (Figs. 2a, b) showing alternating fine-grained, partially organic, and coarse-grained deposits ranging from the late Tertiary to the Quaternary. These deposits offer numerous possibilities for high-resolution Quaternary studies. Palynological and lithological studies, together with geochronological measurements, such as optically stimulated luminescence (Zhang et al. 2014) and palaeomagnetic investigation were carried out to determine the environmental characteristics and climatic evolution of the study area and to establish a more reliable and robust stratigraphic and chronological framework. Additional data on sediment properties such as pH, carbon (C) and nitrogen (N) as well as soluble salt and carbonate ($CaCO_3$) contents were generated as these are important for reconstructing the depositional environment and climatic characteristics of coastal dynamics.

2. Regional setting

2.1 Location

The Garding-2 core drilling site is situated near the village of Welt, located in the Eider River estuary on the western coast of Schleswig-Holstein, Northern Germany (Fig. 1). Gauss-Krüger coordinates of the drilling point are 3485562 (E) and 6019328 (N). The Garding-2 core is situated about 700 m to the south of the Garding-1 core, both cores being named after the small village of Garding that is located approximately 2 km north of the drilling locations (Fig. 1).

2.2 Geological setting

The present morphology of the study area is dominated by tidal flats and marshes, which are characteristic for a coastal environment. Pastures and arable farming are commonly practiced in this area. The subsurface NW–SE cross-section (Fig. 3) shows that the Garding-2 core penetrates the eastern part of the Garding Trough, west of the Oldenswort North salt dome. The Cimmerian Orogeny generated an extensional stress regime, and this process was followed by a rifting of the North Sea and Ems area, which led to a diapirism of the Keuper evaporite and formation of the rim syncline

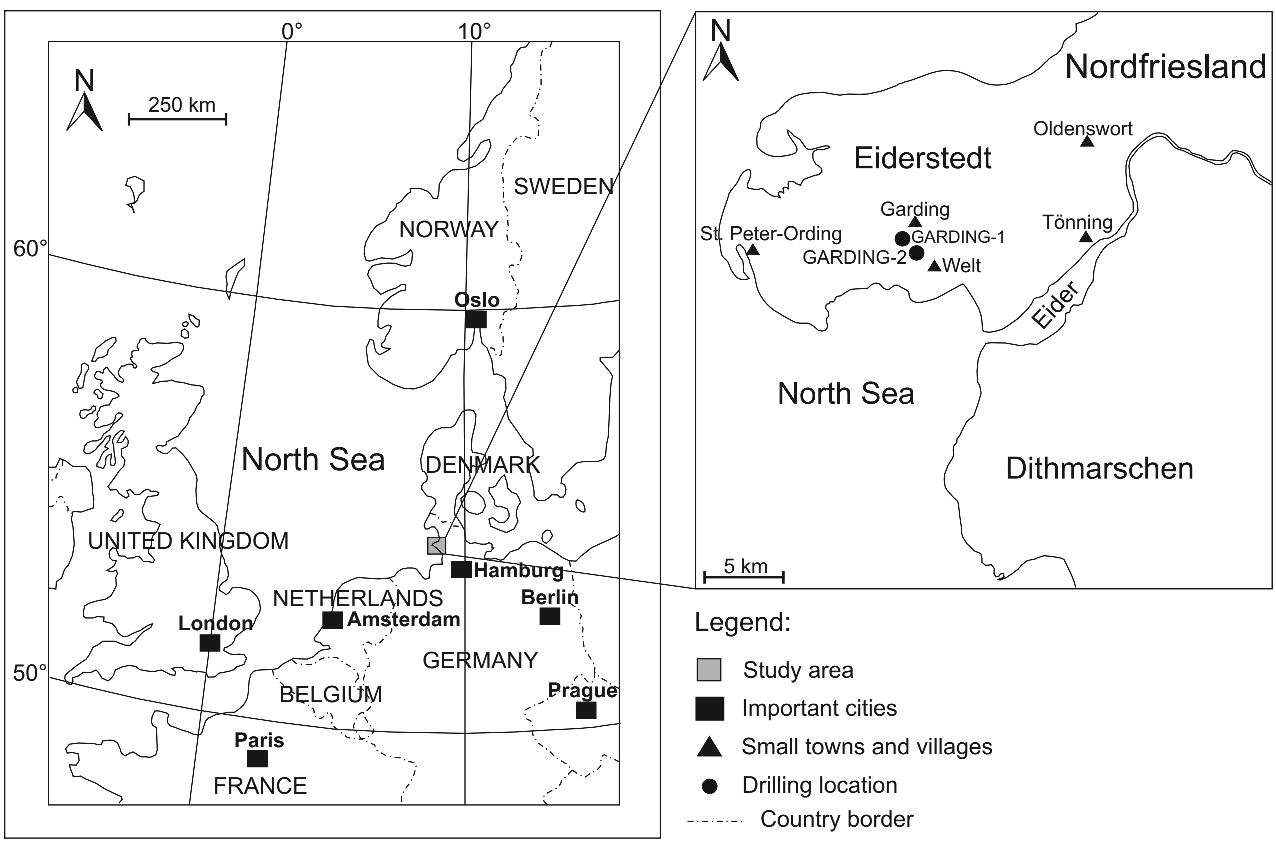

Fig. 1: Location of the Garding-1 and Garding-2 scientific drillings in the Garding Area, Schleswig-Holstein (modified from http://www.worldatlas.com/webimage/countrys/eu.htm and https://maps.google.de).

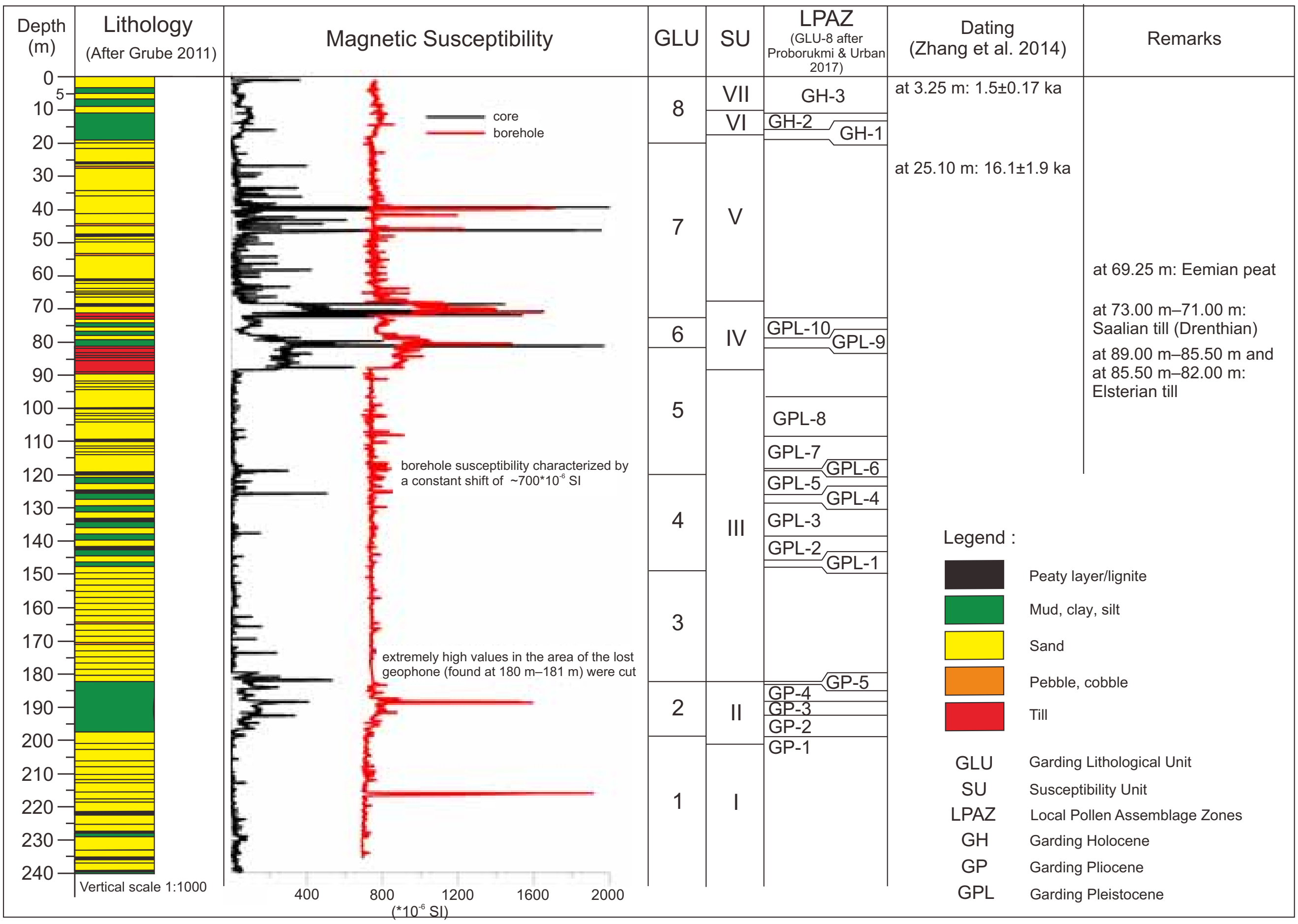

(a)

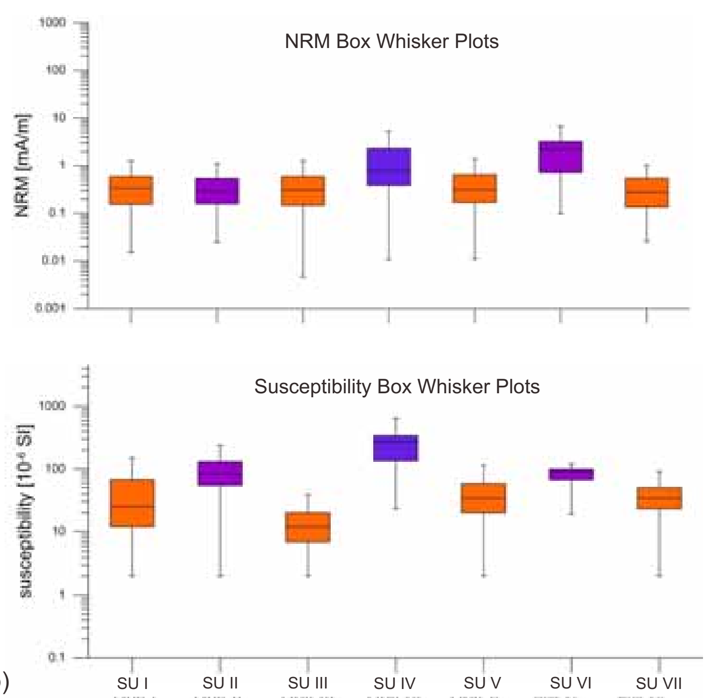

(b)

Fig. 2: (**a**) Simplified profile of the Garding-2 core showing eight lithological units, GLU-1–GLU-8 (modified after detailed description of Grube 2011), OSL dating results (Zhang et al. 2014), local pollen assemblage zones (LPAZ) including the Holocene sequence (Proborukmi & Urban 2017) and susceptibility units (SU I–SU VII) derived from core and borehole measurements. (**b**) Whisker plots of NRM and magnetic susceptibility of the Garding-2 core, showing seven susceptibility units (SU).

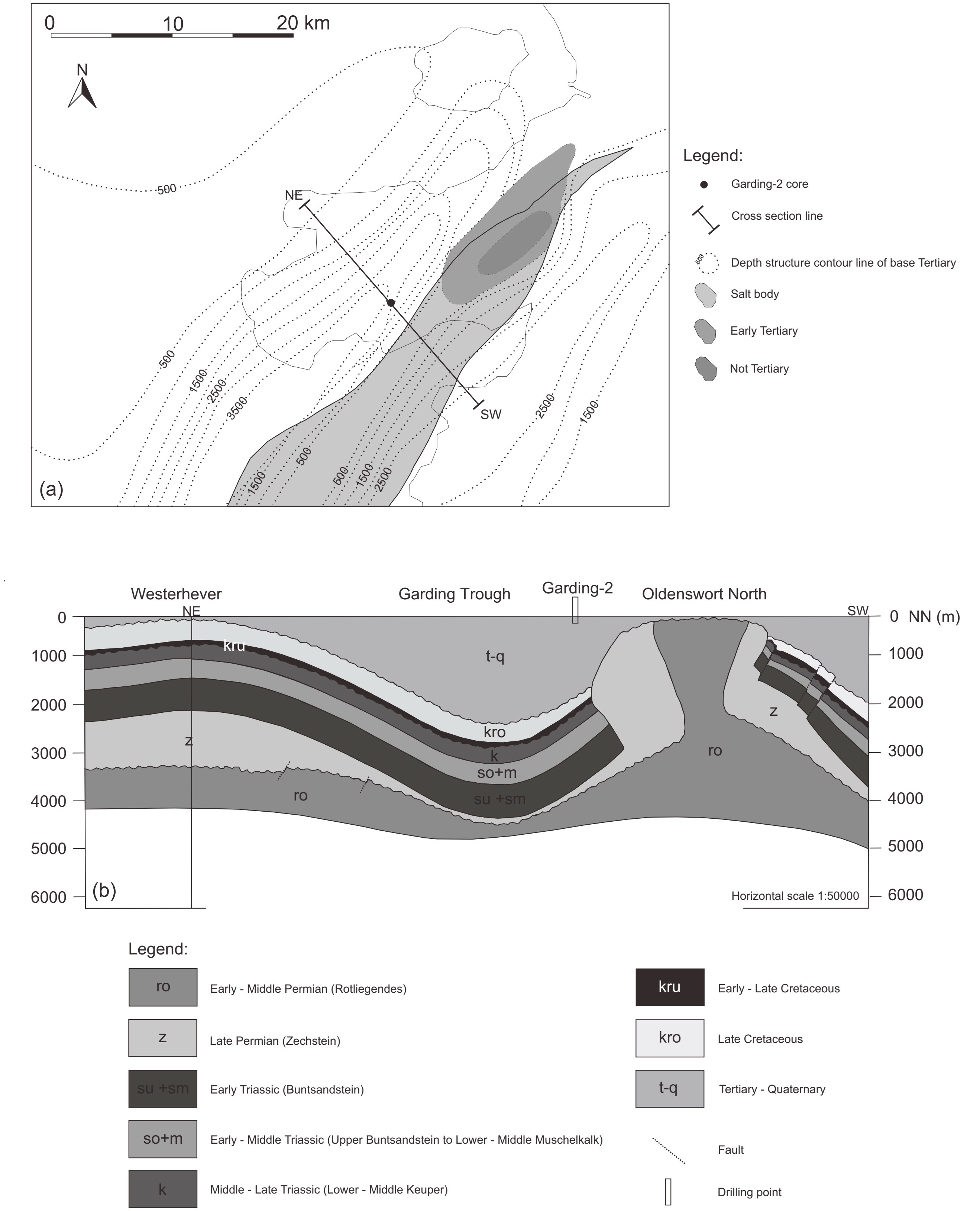

Fig. 3: (**a**) Base Tertiary depth structure map showing NE–SW salt diapir and thick Quaternary deposits (modified after Hinsch 1974). (**b**) NW–SE cross-section showing accumulation of Tertiary–Quaternary sediment sequences where the Garding-2 core was taken (modified after Baldschuhn et al. 2001).

with a greatest impact during the Late Jurassic (Frisch & Kockel 1999, Bald-schuhn et al. 2001). Subhercynian tectonic inversion reactivated the diapirism during the Late Cretaceous and Early Cenozoic (Baldschuhn et al. 1991, 2001). Due to tectonic activities and sea-level changes, the trough was primarily filled with clastic sediments of Tertiary and Quaternary age (Mohr et al. 2005; Fig. 3). The upper parts of the basin reshaped due to landscape changes caused by the ice advance during the Elsterian Glaciation, causing a deep vertical erosion and redeposition beneath the ice sheet (Ehlers & Linke 1989, Hinsch 1991). Composition of the Elsterian deposits varies greatly due to reworking and mixing of the local and regional materials. In North Germany, these deposits are mainly composed of reworked Tertiary sediments of a clayey, silty and sandy matrix of till with western Scandinavian pebbles and blocks, while the younger Saalian till is dominated by Swedish drifted materials, with more Baltic components in the Warthian compared to the Drenthian Stadium (Stephan 2014). The major sea-level rises in the Holsteinian and the beginning of the Holocene changed the morphological and geological setting into a deeper open marine depositional environment (Menke 1976b, Streif 2004).

2.3 Overview of the Quaternary stratigraphy and sea-level changes in Northwest Germany and adjacent areas

The subdivision of the Quaternary is predominantly based on climatic changes that have been revealed by the sediment record permitting a climatostratigraphical classification of characteristic units (Litt et al. 2008). Palynostratigraphical criteria have mainly been used in defining the warm phases and in correlating interglacial deposits, whereas lithostratigraphical indicators such as glacial sediments provide the main evidence for the existence of cold periods (Litt et al. 2007, Stephan 2014).

The onset of the Quaternary in northwestern Europe is marked by a cooling and the existence of an open landscape including boreal forest steppe (Zagwijn 1960, 1974, Menke & Behre 1973, Menke 1976a, Urban 1978a, Litt et al. 2007) in the Praetiglian. This is indicated by the extinction of Tertiary taxa such as *Taxodium*, *Aesculus*, *Zelkova* and *Liquidambar*, which were very common in the Reuverian (Zagwijn 1960, Hahne et al. 2008). The cooling at the Pliocene-Pleistocene transition coincides with the Gauss-Matuyama magnetic polarity change (Cande & Kent 1995, Partridge 1997, Suc et al. 1997, Pillans & Naish 2004), which is correlated with MIS 104 (Shackleton et al. 1990).

Examples of well-preserved Early Pleistocene deposits in Schleswig-Holstein occur in the Lieth and Oldenswort sections, as indicated by deposits of kaolin sand (Menke 1970, 1972, Menke & Behre 1973, Stephan & Menke 1993). The peaty and swampy sediments in these sections reflect an open landscape with subarctic vegetation. Non-arboreal pollen (NAP) of Poaceae and some *Artemisia* amongst others, Ericaceae and Cyperaceae dominate and reworked pollen of Tertiary taxa such as *Nyssa*, *Liquidambar* and Taxodiaceae (*Sequoia*, *Taxodium* and *Sciadopitys*) (Menke 1975, 1976a) occur. Similar characteristics were also found in the Meinweg profile in the Netherlands, which is assigned to the Praetiglian (Zagwijn 1960).

Forest started to expand again in the Tiglian: thermophilous taxa such as *Quercus*, *Ulmus*, *Carpinus*, some *Ostrya* and *Eucommia* emerged although Ericaceae, Poaceae, *Pinus*, *Betula*, *Alnus*, *Myrica* and terrestrial herbs are at this time still dominant (Menke 1975). The vegetation of the oldest part of the Tiglian, the Tiglian A, is distinctive, as it is characterised by a pronounced *Fagus*-*Pinus*-*Picea*-(*Carpinus*)-*Tsuga* rich vegetation documented only at very few sites (Zagwijn 1963, Menke 1975, Urban 1978a, b).

Arboreal pollen (AP) decreased during the subsequent Eburonian Glacial Complex, which is marked by the end of the Olduvai normal magnetic polarity subchron (Cande & Kent 1995, Urban 1997). Ericaceae, *Artemisia* and other heliophilous herbs dominated the landscape. However, *Myrica* was found in relatively high quantities, suggesting the presence of open boggy shrub-lands during part of the Eburonian (Menke 1975).

The reverse magnetisation of the Matuyama Chron was observed for the Waalian Interglacial Complex, when *Pinus*, *Betula*, *Alnus*, *Myrica* (Menke 1975, Urban 1997), *Tsuga* and *Eucommia ulmoides* increased substantially (Hahne et al. 2008), especially during Waalian A and C. The Menapian and the subsequent Bavelian Interglacial Complex are characterised by *Tsuga*, *Eucommia*, *Pterocarya*, *Ostrya*, *Carpinus*, *Quercus*, *Ulmus, Taxus*, *Picea* and *Abies* with minor importance of *Tilia* (Urban 1997), which is also observed in the Marleben Interglacial of Gorleben (Müller 1992). The latter was correlated with the Uetersen Interglacial following a description of Menke (1975) for the Lieth sequence (Litt et al. 2007, Deutsche Stratigraphische Kommission 2016).

The transition between the Early and Middle Pleistocene is marked by a long period of climatic oscillations with pronounced warm and cold phases and the Matuyama-Brunhes magnetic polarity change (Litt et al. 2007, Head et al. 2008). The Matuyama-Brunhes polarity change is dated to 780 ka BP and correlated with the middle part of MIS 19 (Shackleton et al. 1990, Bassinot et al. 1994, Channell et al. 2004, Head & Gibbard 2005). It is widely used as the palaeomagnetically defined boundary between the Early and the Middle Pleistocene (Richmond 1996).

At the Early to Middle Pleistocene transition, the climatostratigraphy shows five interglacials and cold stages in the Cromerian Complex, as described by Müller (1992) and the Deutsche Stratigraphische Kommission (2016). According to the same authors, the first interglacial, the Osterholz Interglacial (Grüger 1968), still shows reverse magnetisation and is correlated with the Matuyama Chron. It is palynologically characterized by *Pinus*, *Picea*, *Quercus*, *Carpinus*, *Ulmus* and *Tilia*, and the occurrence of *Eucommia*, *Celtis*, *Tsuga* and *Pterocarya*. This interglacial is then followed by the second interglacial (Hunteburg), which is characterised by an early and strong expansion of *Ulmus* and a distinct *Abies* and *Carpinus* phase (Müller 1992, Hahne et al. 1994). Similar palynological features are also found later in the youngest Cromerian interglacial, the Bilshausen or Rhume, when the *Abies* expansion is followed by the spreading of *Carpinus* (Menke & Behre 1973, Müller 1992). During the second interglacial phase, *Eucommia* was still part of the vegetation at Gorleben in Northeast Lower Saxony (Müller 1986, 1992), while it is missing in the Hunteburg section (Hahne et al. 1994). At Gorleben, three more interglacial periods succeeding the Hunteburg Interglacial including the Rhume (Bilshausen) Interglacial were established (Müller 1986, 1992, Deutsche Stratigraphische Kommission 2016). These interglacials show rare occurrences of *Pterocarya* and *Celtis*, while *Tsuga* is absent (Müller 1986). However, in the later publication of Müller (1992), the occurrence of *Tsuga* is presented in the pollen diagram up to the proposed third Cromerian interglacial. This fact was not further commented on by the author (Müller 1992).

Sediments of the Elsterian Glaciation generally overlie the Cromerian deposits. A cooling after the youngest Cromerian Interglacial marks the beginning of the Elsterian (Litt et al. 2007). The Elsterian Glacial advances are believed to have been the main force of erosion of some parts of the Early Pleistocene sediments and even older deposits in Northern Germany (Stephan 2014). In northwestern Germany, tills representing this cold phase are mainly dominated by coarse-grained material with angular quartz blocks and boulder-sized Scandinavian erratics (Ehlers et al. 1984, Ehlers 1987, Von Hacht 1987).

At the end of the Elsterian, a marine transgression following arctic-subarctic conditions marks the onset of the Holsteinian (Stephan 2014). At the North Sea in western Schleswig-Holstein, the transgression started during the Elsterian (Diehl 2007) and reached a maximum inundation around the beginning of the *Abies*-*Carpinus* phase, as found in Hamburg-Hummelsbüttel (Hallik 1960), Hamburg-Billbrock and -Dockenhuden (Linke & Hallik 1993). The superposition of terrestrial-marine-terrestrial deposits is found in Bossel between pollen zone VI and VIII (Müller & Höfle 1994, Geyh & Müller 2005).

The Holsteinian begins with an early expansion of *Picea* and *Alnus*, before the development of deciduous forest dominated by *Quercus* and *Ulm*us. Thermophilous taxa established in a shorter period compared to the Eemian Interglacial. It is followed by a phase of *Abies* and *Carpinus* spreading, with occurrences of *Buxus* and *Celtis*. The co-occurrence of *Pterocarya* and *Fagus* during terminal interglacial phases is a common feature and has been observed in Germany and in western and eastern Europe (Erd 1970, Müller 1974, Erd et al. 1987, De Beaulieu et al. 2001, Hahne et al. 2008, Hrynowiecka & Szymczyk 2011); however, this co-occurrence has not been recorded in the Netherlands (Zagwijn 1973), where this period is rather characterised by the expansion of *Abies* towards the north of its present day distribution limit (Zagwijn 1992). The age of the Holsteinian is still a matter of debate and the general correlation of the Holsteinian with MIS 11 (Nitychhoruk et al. 2005, Candy et al. 2014, Cohen & Gibbard 2016) or, alternatively, to MIS 9 (Geyh & Müller 2005, Geyh & Krbetschek 2012, Deutsche Stratigraphische Kommission 2016) remains controversial.

A transition from late Holsteinian boreal to Early Saalian subarctic vegetation marks the end of the Holsteinian and the onset of the Saalian Complex (Jerz & Linke 1987, Linke & Hallik 1993, Litt et al. 2007), more specifically the Fuhne Stadial (Knoth 1964, Cepek 1967, Erd 1970, 1973, Urban et al. 1988) or Mehlbeck (Menke & Behre 1973) that is correlated with MIS 8 (Litt et al. 2007). During the Saalian Complex, several distinct warm periods have been identified between the periglacial sediments of the Saalian, for example Wacken or Dömnitz (Menke 1968a, Dücker 1969, Erd 1973), Schöningen (Urban et al. 2011), Nachtigall (Kleinmann et al. 2011) and Leck (Stephan et al. 2011, Urban et al. 2011). The Saalian Complex is correlated to a time span between MIS 10 and MIS 6 (Gibbard & Cohen 2008, Cohen & Gibbard 2016, Graham et al. 2011) or to between MIS 8 and MIS 6 (Litt et al. 2007, Roskosch et al. 2015, Kunz et al. 2016).

At the beginning of the Eemian, sea level rose and caused flooding in most of the river valleys along the Baltic Sea and North Sea coasts (Höfle et al. 1985, Stephan 2014) with a maximal shifting of about 40 km landwards in the Rostock-Schwaan area (Müller 2004, Meng et al. 2009) as well as in the coastal area of Northwest Germany (Caspers et al. 2002). According to Winn et al. (2000), Th/U age determinations at Dagebuell, northwestern Germany, indicate an average age of this transgression of 132 ± 1 ka. According to Menke & Tynni (1984), the Eemian Interglacial can be subdivided into seven pollen zones based on the re-immigration sequence of the arboreal taxa in Dithmarschen (Fig. 1). It begins with the expansion of *Betula* (zone I) that is followed by *Pinus* forming *Pinus*-*Betula* woodlands (zone II). Thermophilous deciduous woodlands expanded (zone III) shortly after pollen zone II, coinciding with the beginning of the Eemian transgression (Caspers et al. 2002). A mixed-oak forest dominated by *Corylus* (zone IVa) succeeding this phase is followed by the expansion of *Taxus* and *Tilia* (zone IVb), which occur around the peak of transgression (Caspers et al. 2002). Subsequently, *Carpinus* expands and increasing amounts of *Picea* are observed (zone V). At the end of the Eemian, thermophilous taxa decrease and boreal woodlands dominated by *Pinus*, *Picea* and *Abies* were widely distributed (zone VI and VII). Fluvial sediments from the lower Peene Valley, Northeast Germany also show a sequence of mixed-oak forests dominated by *Corylus* (zone IVa) and the beginning of the subsequent *Corylus*-*Taxus*-*Tilia* phase (Zone IVb), with occurrences of the typical Eemian mollusc, *Theodoxus fluviatilis* (Meng et al. 2009). By taking the beginning of the Eemian at about 127.2 ka (Brauer et al. 2007, Litt & Gibbard 2008) and the determined duration of each pollen zone into account (Müller 1974), this sequence was deposited at about 125 ka (Meng et al. 2009), which also gives information about the time of the peak of the Eemian transgression in the Peene Valley. The Eemian Interglacial is correlated with MIS 5e (Litt et al. 2007).

During the subsequent Weichselian cold period, several interstadials have been identified (Menke 1968b, Bock et al. 1985, Behre & Lade 1986, Behre 1989, Grüger 1989, Merkt

& Müller 1999, Litt et al. 2001, 2007). These would have preceded the Fenno-Scandinavian ice sheet advance that covered parts of Northern Germany during the Weichselian Lateglacial. This Lateglacial begins with the Meiendorf Interstadial at approximately 14.7 ka BP, which is followed by two other interstadials, the Bølling and the strongest one Allerød, and ends with the cool phase of the Younger Dryas (Litt et al. 2007).

A warming occurred during the end of the Weichselian Lateglacial. It had already started at around 11,600 years BP, which was suggested by the varved sediments of the Eifel volcanic maars in Germany (Brauer et al. 1999, Litt & Stebich 1999, Litt et al. 2001). This warming is marked by a rapid sea-level rise during the early Holocene and the subsequent intra-interglacial climatic oscillations that continue to the present day (Pirazzoli 1991, Behre 2003, 2004), although interupted by multiple stagnant and regression phases (Menke 1968c, Behre 1991, Streif 2004). The transition from the Younger Dryas to the Preboreal is characterised by an expansion of *Betula* and *Pinus* (Firbas 1949, Bos 2001, Litt et al. 2001, 2007, Van der Plicht et al. 2004, Birks & Birks 2008). This expansion is followed by a spreading of *Corylus* in most areas in Germany, due to the development of warmer and dryer conditions during the Boreal (Firbas 1949, Bos 2001, De Klerk 2002). Mixed deciduous forests composed of *Quercus*, *Ulmus*, *Tilia*, *Fraxinus*, *Acer* and *Alnus* developed from the Atlantic period onwards. At the beginning of the Subboreal, *Fagus* and *Carpinus* emerge (Firbas 1949, Litt et al. 2009). A short period characterised by denser forests of *Fagus*, *Carpinus* and *Quercus* marks the beginning of the Subatlantic. Anthropogenic indicators since the Late Atlantic (Neolithic) have been widely observed in North Germany (Wiethold 1998, Behre 2007, Nelle & Dörfler 2008).

3. Material and methods

The Garding-2 drilling was entirely carried out as a cored bore hole (co. Ivers, Osterrönfeld) under the supervision of the Geological Survey Schleswig-Holstein between February and April 2011. The Garding-2 core consists of a sequence of 240 m of sediments that are diverse in terms of lithology and thickness. This core was cut in metre long sections, which were halved. One half was kept in LIAG, Hannover, while the other half has been sampled for palynological and lithological analyses and is kept in the LIAG storage in Grubenhagen. Lithological descriptions were carried out on approximately 1000 layers, and approximately 425 selected samples of clearly distinguishable horizons were collected throughout the core. The samples for lithological studies were processed in the Building Materials and Soil Testing Laboratory of the State Office of Transport of Schleswig-Holstein in Kiel and the State Laboratory of Schleswig-Holstein (division 5, Environmental Monitoring in Neumünster).

The sediment sequence of the Garding-2 core is divided into eight lithological units, which are named Garding lithological units (GLUs). The odd numbers represent coarse-grained units, which are mainly composed of sand and coarser sediments, and the even numbers represent fine-grained units, which are mainly composed of silt and finer sediments. 154 samples for biostratigraphical and 201 samples for geochemical studies were taken from these fine-grained units and from the bottom part of GLU-1 (between 240.00 m and 238.00 m) with 10–90 cm sampling intervals. The sampling interval can be larger, up to about 10 m, in the middle of coarser sediments (Fig. 2a).

Pollen extraction was conducted based on standard methods used at the Palynology Laboratory of the Institute of Ecology at the Leuphana University of Lüneburg. Carbonate was removed from about 7–10 g of sediment samples with the help of 10 % hydrochloric acid (HCl) and then treated in potassium hydroxide (KOH). The organic compounds were separated by sodium polytungstate ($Na_6[H_2W_{12}O_{40}]$) and treated with acetic acid (CH_3COOH). Acetolysis was conducted using a solution of hydrogen sulphide (H_2SO_4) and acetic anhydride ($[CH_3CO]_2O$) to remove additional organic material and darken the palynomorphs (Faegri & Iversen 1989, Moore et al. 1991). Parts of the extracted residue were embedded on microscope slides in glycerin, and palynomorphs were identified using the reference collection of the Palynology Laboratory in Lüneburg and the atlases of Moore et al. (1991), Beug (2004) and Faegri & Iversen (1989, 1993). The Cerealia-type pollen is of wild grasses and was separated from other grass species by metric measurements of the grain and pore besides a detailed observation of the wall structures (Beug 2004). The pollen sum (100 %) was calculated by summing the AP and NAP of dry land taxa, excluding Cyperaceae, aquatic and reworked taxa as well as spores of cryptogams. The TILIA software package (Tilia, Tilia Graph and Tilia View) was used to calculate pollen percentages and to create pollen diagrams (Grimm 1990; Figs. 4a–c). Cluster analysis with square root transformation (implicit dissimilarity coefficient of Edwards and Cavalli-Sforza chord distance; Grimm 1987) on pollen sum data and conventional interpretation of the pollen diagram were used to subdivide every lithological unit into local pollen assemblage zones (LPAZ) based on the distribution and variation of the dominant taxa.

Carbonate content was measured using a Scheibler apparatus. Soluble salt content was determined with an EC meter (VDLUFA 1991). pH values were measured with a pH meter in a 1:2.5 0.01 mol/l calcium chloride solution (Urban 2002), and the carbon (C), hydrogen (H) and nitrogen (N) values were determined with a CHNS/O 2400 series II analyser of PerkinElmer. The geochemical analyses were carried out in the soil laboratory of the Institute of Ecology of Leuphana University of Lüneburg where the residue of all samples is stored as well. Results of geochemical properties such as pH values and carbonate content (Figs. 5a–d) were analysed in accordance with the classification of Ad-Hoc-Arbeitsgruppe-Boden (2005), while the soluble salt content was classified after Plaster (2009) and the resulting C/N ratios were interpreted based on the work of Meyers (1994) and Thornton & McManus (1994).

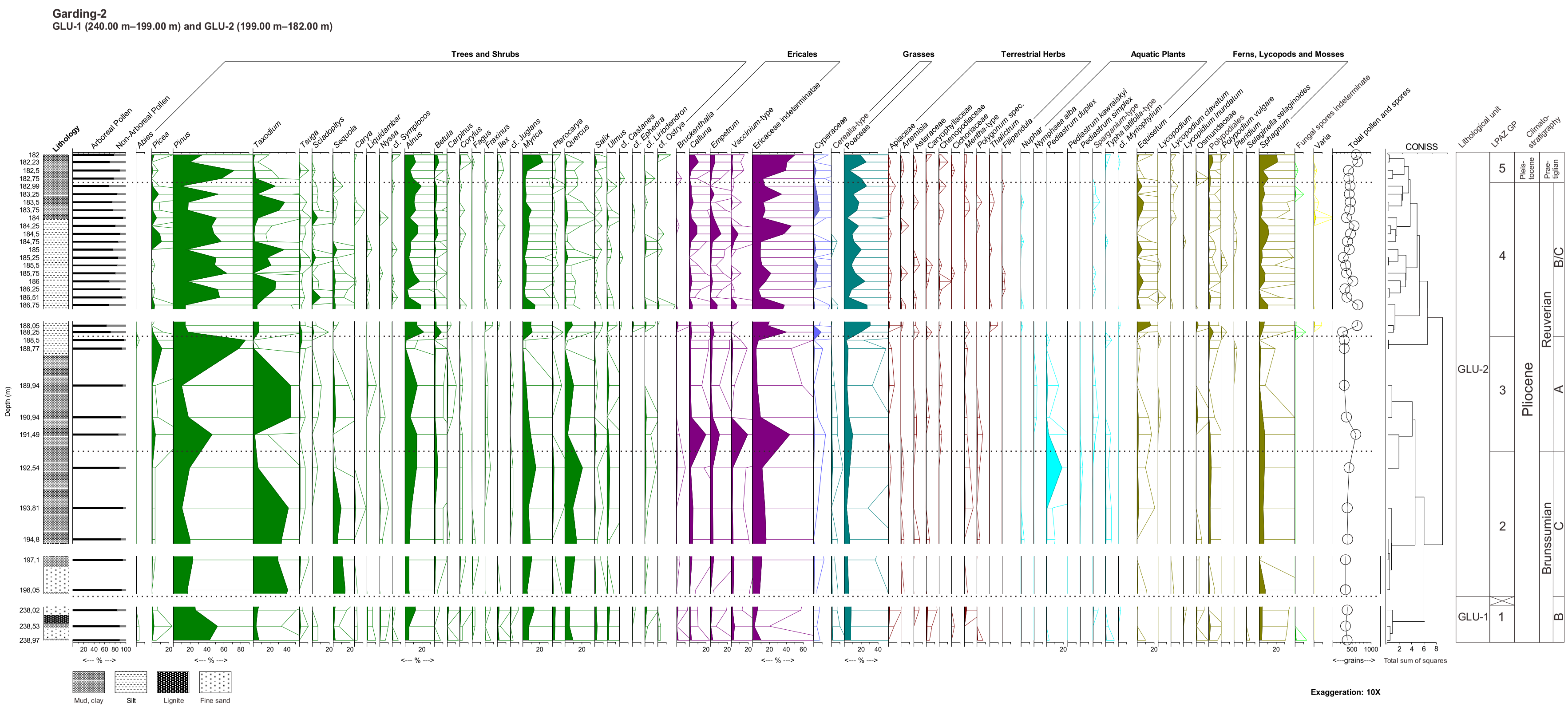

(a)

Fig. 4: Pollen diagrams of the Garding-2 core, showing local pollen assemblage zones (LPAZ) as well as their biostratigraphic correlation of GLU-1 to GLU-7. **(a)** GLU-1 and GLU-2. **(b)** GLU-4 and GLU-5. **(c)** GLU-6 and lower GLU-7.

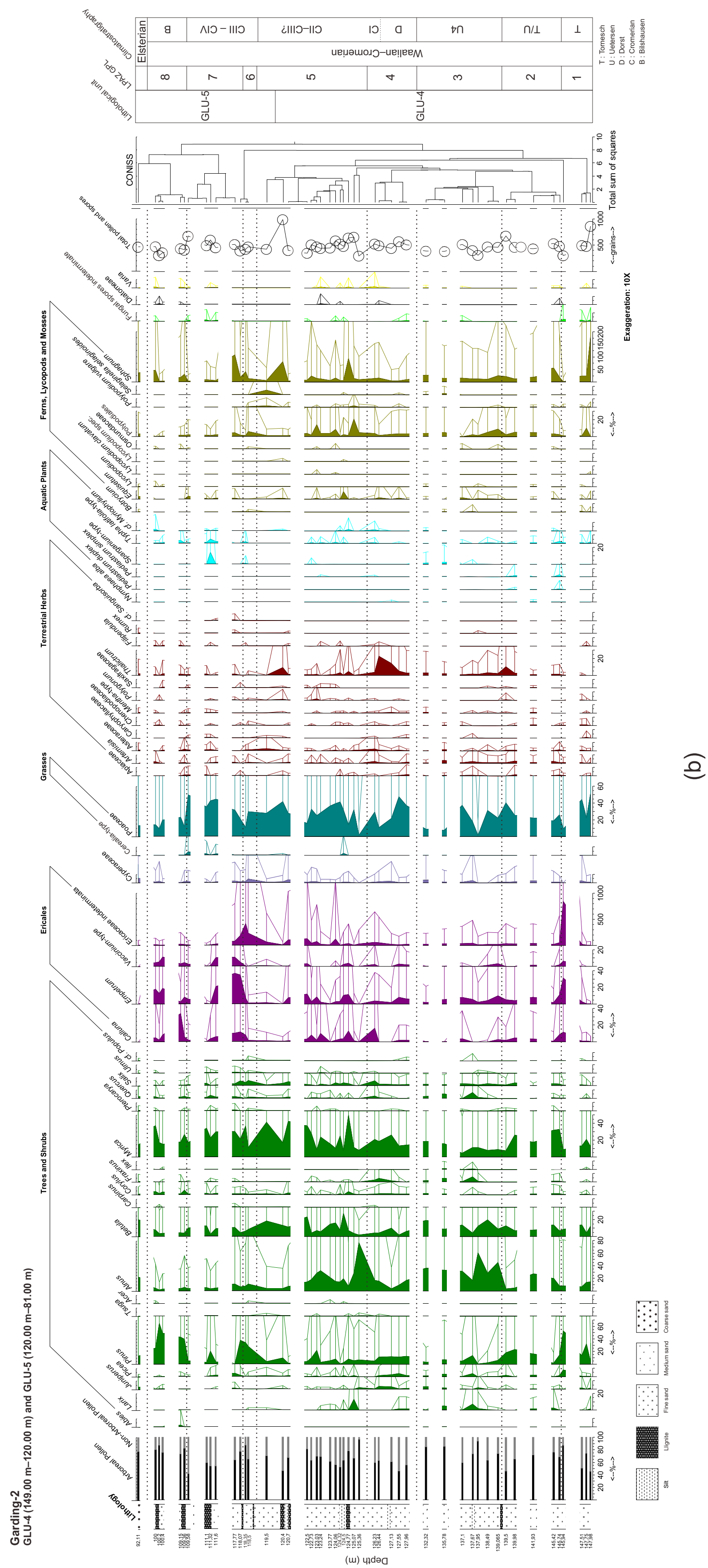
Garding-2
GLU-4 (149.00 m–120.00 m) and GLU-5 (120.00 m–81.00 m)
Trees and Shrubs
Ericales
Grasses
Terrestrial Herbs
Aquatic Plants
Ferns, Lycopods and Mosses
CONISS
Total sum of squares
Exaggeration: 10X
Waalian–Cromerian
Elsterian
(b)

Fig. 4: cont.

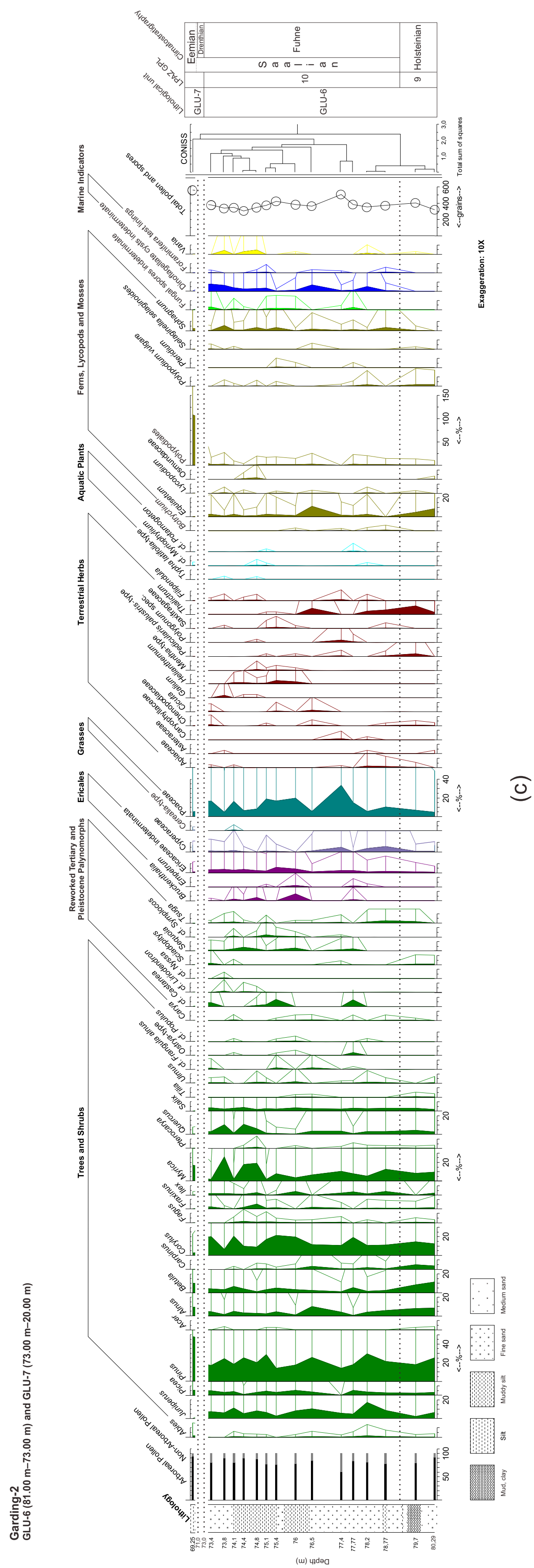

(c)

Fig. 4: cont.

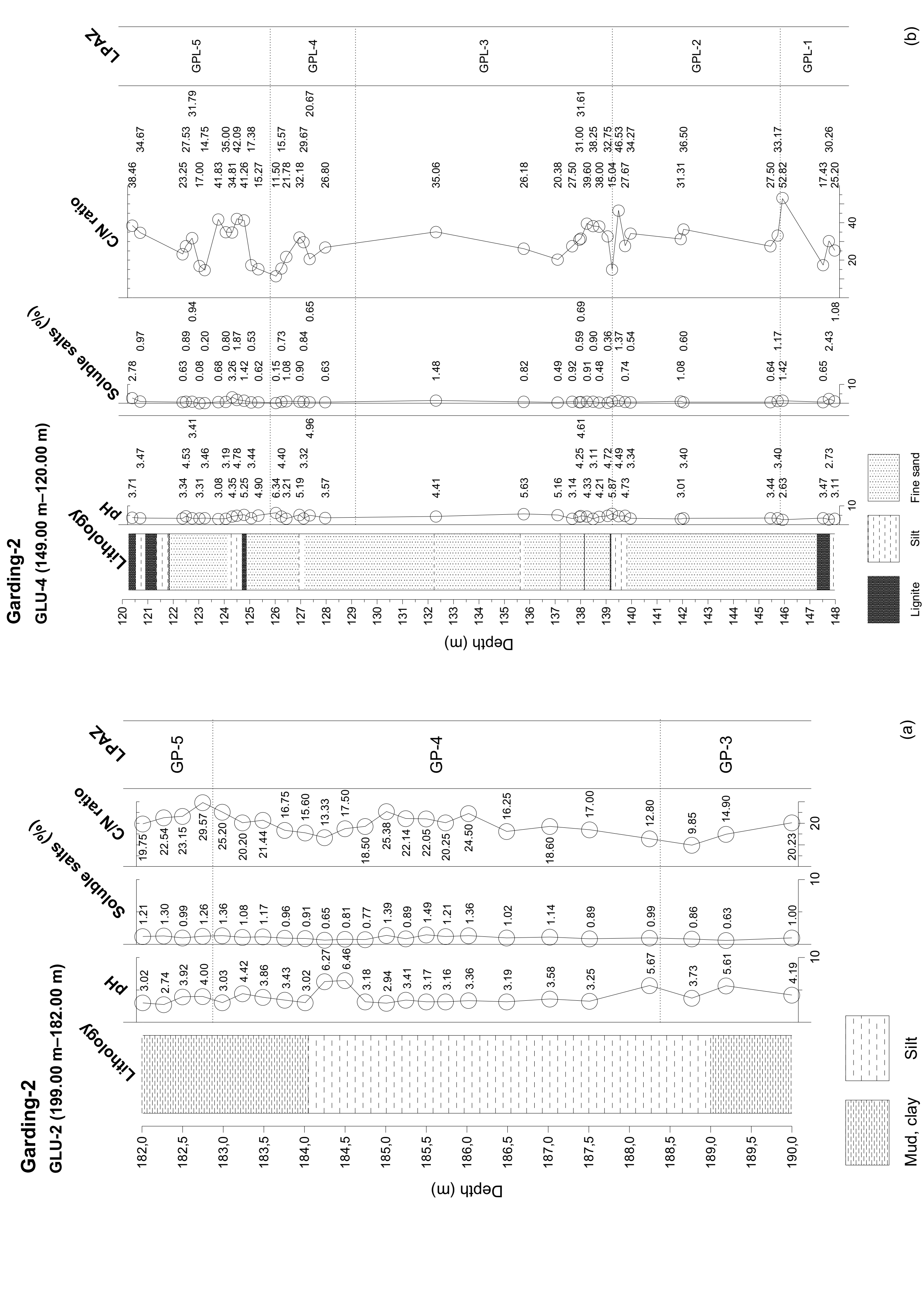

Fig. 5: Results of geochemical analyses of the Garding-2 core indicating pH, soluble salt content, C/N ratios and carbonate content. (**a**) GLU-2. (**b**) GLU-4. (**c**) GLU-5. (**d**) GLU-6.

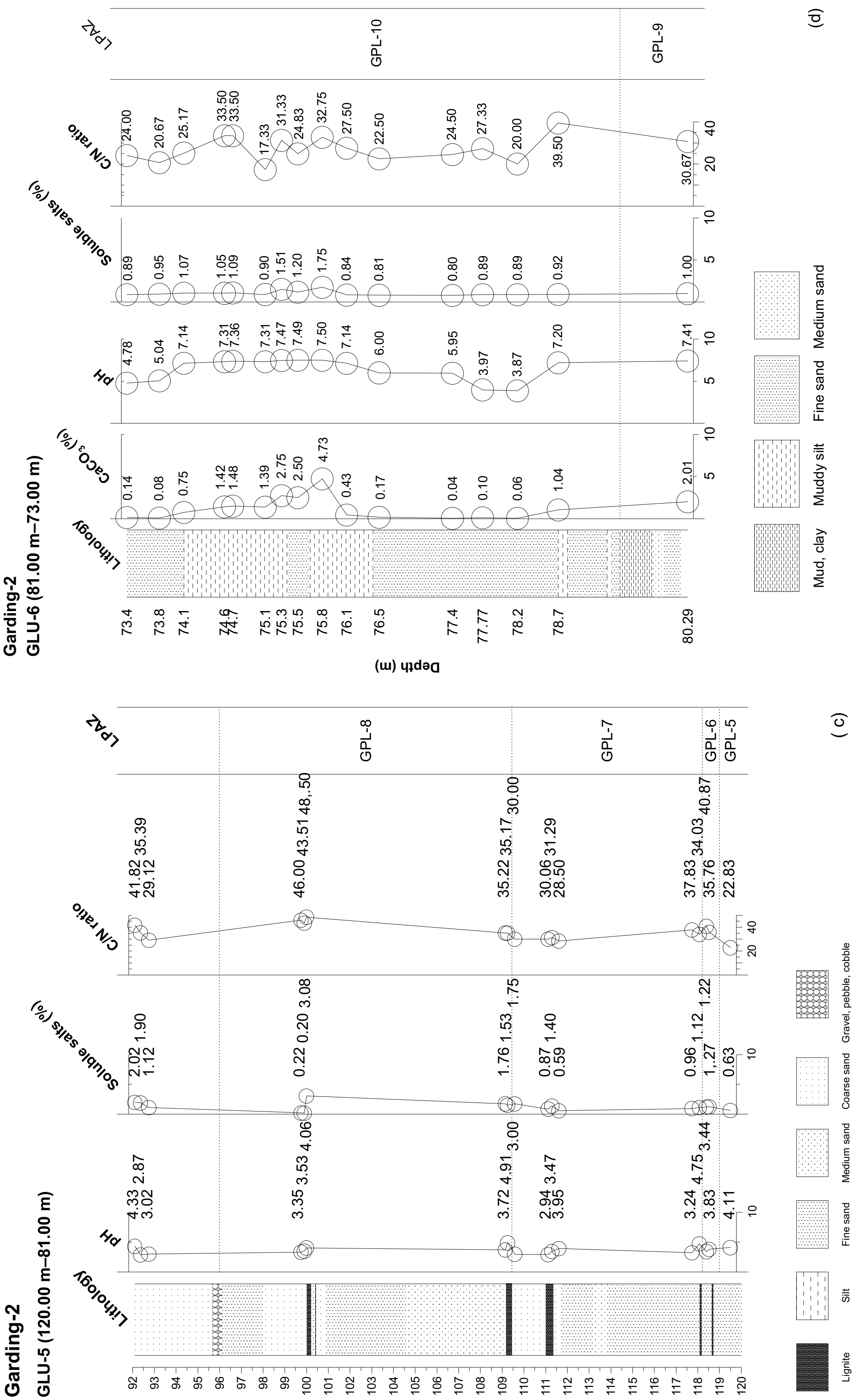
Garding-2
GLU-5 (120.00 m–81.00 m)
Lithology
pH
Soluble salts (%)
C/N ratio
LPAZ
Depth (m)
GPL-8
GPL-7
GPL-6
GPL-5
(c)
Lignite
Silt
Fine sand
Medium sand
Coarse sand
Gravel, pebble, cobble
Garding-2
GLU-6 (81.00 m–73.00 m)
Lithology
CaCO3 (%)
pH
Soluble salts (%)
C/N ratio
LPAZ
Depth (m)
GPL-10
GPL-9
(d)
Mud, clay
Muddy silt
Fine sand
Medium sand

Fig. 5: cont.

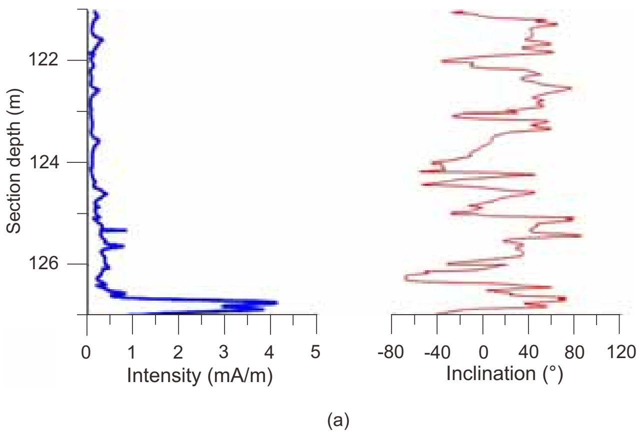

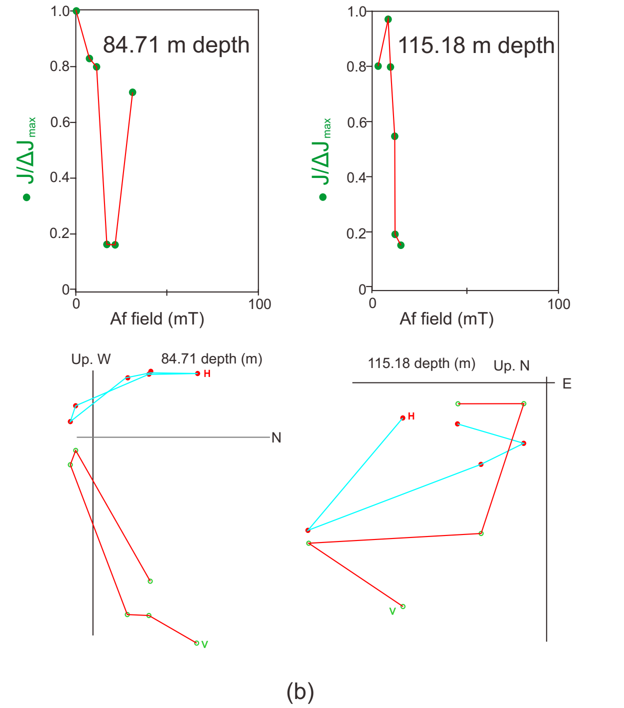

Fig. 6: (**a**) Intensity and inclination of magnetisation vector measured on full cores between 121.00 and 127.00 m, showing extremely low intensity and chaotic wiggles in inclination, which is due to a low quality record of EMF. (**b**) Intensity decay and Zijderveld diagrams, identifying low coercivity and highly chaotic behaviour of the remanence signal measured on single sample (oriented in borehole direction). These examples demonstrate magnetostratigraphy and cannot provide a solid chronostratigraphical framework for the Garding-2 core.

A detailed description of the optically stimulated luminescence (OSL) and radiocarbon dating methods can be found in Zhang et al. (2014). The authors have applied these methods to the upper 26 m of the Garding-2 core and the results for the upper 20 m of Holocene sediments show an excellent agreement. However, the numerical dating method of OSL has limitations when determining the age of older sediments. The upper dating limit of OSL depends on luminescence properties of the minerals such as quartz and feldspar, and the dose rate of the sample (Wintle 2008, Rhodes 2011). Roskosch et al. (2015) dated fluvial sediments ranging in age from MIS 4 to MIS 12 from Lower Saxony and yielded good agreement with geological estimation up to about 450 ka before present. In order to set up a more reliable chronological framework in the older part of the core, palaeomagnetic studies were carried out.

Two tools were used to measure bulk susceptibility on material from the boreholes (Figs. 2a, b). A susceptibility probe was used to measure the bulk susceptibility in the borehole at intervals of 1 cm and with a sensitivity of 1×10^{-5} SI. The second tool, a long-core susceptibility logger from Magnon GmbH, was used to measure bulk susceptibility of cores (5–13 cm in diameter) up to 0.5 cm in distance with a sensitivity of 1×10^{-6} SI. Both the magnetic susceptibility of the core and of the rocks surrounding the drill could be measured.

In addition to the susceptibility measurements, a full core measurement of natural remanent magnetisation (NRM) at intervals of 1 cm was conducted using a 2G cryogenic magnetometer (Rolf 2000). Alternating field coils (peak fields 15 mT) were installed in the cryogenic magnetometer to demagnetise drill-induced remanences. The full core measurements were performed to get an initial overview of the quality of remanence acquisition. Detection of sediment sections of primary reversed or normal magnetic polarity (magnetostratigraphy) requires isolating stable remanences called characteristic remanent magnetisation (ChRM). This is not possible on full cores, so discrete samples were used (cubes with 2 cm edge length or cylinders 2.54 cm in diameter) on selected core sections with magnetic signals proper for demagnetisation-experiments. Samples were demagnetised more thoroughly using the single sample alternating field demagnetiser (AFD) Magnon MI AFD 300, which is an alternating field (AF) demagnetiser for the static demagnetisation of rock specimens in peak fields of up to 300 mT.

4. Results

4.1 Lithology

The lower part of the core, between approximately 240.00 and 199.00 m (GLU-1), mainly consists of fine sand, with some medium to coarse sand and silt layers (Fig. 2a). Some of these sediments are slightly humic. Most of them also contain lignite and considerable amounts of mica. There are numerous intercalated layers of lignite, lignite-clay and of clay or silt. The predominant colours are beige-brown-grey. The sediments are completely free of carbonate. Genetically, these sediments are classified as fluvial sediments, which are likely deposited during the Pliocene.

Between approximately 199.00 and 182.00 m (GLU-2), silty clays, clayey silts and muds are dominant and usually contain elongated lenses of peat and mica. Thin coarse to fine sand layers are frequent. The muds, clays and silts are dark grey to black in colour and free of calcium carbonate. These sediments indicate swamp or boggy environments and were still likely deposited during the Pliocene. The sediments of GLU-2 are non-saline to slightly saline (0.63–1.49 %) with pH values below 7 and vary from 2.7–6.5 (extremely to slightly acidic). C/N ratios are relatively narrow, 9.9–29.6 (Fig. 5a), typical for estuary and terrestrial organic matter origin.

Between approximately 182.00 and 149.00 m (GLU-3), medium sands with partially humic fine sands dominate, with subsequent layers of significant coarse sands, accompanied in addition by medium-sized sand and gravel, and fine sand with some medium-sized sand. Occasional streaks of sand with humic layers, mud and peats, as well as layers of lignite, clay and silt were observed. The entire sequence is clearly stratified, brown to grey in colour and completely free of calcium carbonate. Genetically, the depositional environment has changed to fluvial-limnic conditions. Thick organic layers in the upper part of this section represent a transition to the overlying sequence. This sequence is considered as a part of the early Quaternary deposits.

From approximately 149.00–120.00 m below the surface (GLU-4), fine sands are dominant, but often contain some medium-sized sand. Intercalated humic sands, humus streaks and layers of mud, peat and lignite can be observed. There are also numerous thin layers of silt and clay (Fig. 2a). The deposits are usually grey to brown and are completely free of calcium carbonate. The sediments of GLU-4 show variations of the C/N ratios between 11.5 and 52.8 indicating estuary to terrestrial origin of the organic matter. The salinity of the sediments varies between non-saline (0.08 %) and moderately saline (3.26 %), and the pH values are within a range of 2.6 (extremely acidic) and 6.3 (slightly acidic) (Fig. 5b). This sequence indicates a limnic to slightly low energy fluviatile depositional environment, with short intervals of peat formation.

Between 120.00 and 81.00 m (GLU-5), fine to coarse sands are predominant, which also contain silt and medium-sized sand (Fig. 2a). In addition, they mostly contain small amounts of mica. Up to 100.00 m below the surface, numerous intercalated layers of organic silt and peaty organic silt occur. Above 100.00 m mainly coarse-grained sand was found. The sediments are beige, brown and grey in colour and the entire sequence is carbonate free. Wide C/N ratios (22.8–48.5) of terrestrial organic matter origin are observed in this lithological unit. The sediments also show very strong to strongly acidic pH values (2.9–4.9). Values of the soluble salt content range from 0.2 to 3.08 %, indicating non-saline to moderate saline sediments (Fig. 5c). Between 89.00 and 85.50 m, calcareous dark grey to blackish grey till of gravel and gravelly coarse sand occurs. This till is homogeneous and strongly compacted, with occasional thin layers of light grey clay or silt. Up to 82.00 m depth, another till, which has very similar characteristics to the underlying one, occurs. The subsequent fine to coarse sands are regarded as glaciofluvial sediments. The majority of GLU-5 is assigned to the Elsterian Glaciation.

In GLU-6, between 81.00 and 73.00 m, there is a massive package of almost 8 m thick sands, silts and muds with minor intercalated fine sands, under- and overlain by 1.5 m thick layers of fine to coarse sand with little humus. In GLU-6, lignite and mica are abundant, which are possibly reworked from the Tertiary sediments. The deposits are grey to brown and characterised by minimum (0.04 %) to moderate (4.73 %) calcium carbonate. The C/N ratios are slightly narrower than in the lithological unit before, ranging between 17.3 and 39.5, but still suggesting terrestrial organic matter origin. Non-saline to slightly saline sediments are observed, while pH values show very strongly acidic (3.9) to very slightly alkaline (7.5) conditions (Fig. 5d).

Between 73.00 and 20.00 m below the surface (GLU-7), sandy sediments are dominant. The bottom of this unit consists of 2 m of sandy till between 73.00 and 71.00 m. This layer is composed of medium to coarse sand with gravels and larger rock fragments (up to >9 cm) and is assigned to the Drenthian Glaciation. This classification is likely because of the stratigraphical position of this layer with respect to the underlying Elsterian till and the absence of the uniform petrography rich in silt, clay and chalk, characteristic of the younger Warthian Glaciation. Besides, the Warthian ice advance is expected to have extended far to the east of the drilling location. On top of the till, there are layers of fine to coarse sands, parts of which contain accessory silt or gravelly sand. The sand is intercalated by layers of lignite and peat, which are probably reworked, and humic sand at 69.33–69.02 m, 62.13–62.08 m, 47.00–46.27 m and 26.12–26.10 m. The sequence is beige-grey-brown in colour and decalcified. Between 49.55 and 48.84 m, glaciofluvial sediments of coarse sand and gravel (up to >3 cm) were deposited. A layer of medium sand with gravel of flint (up to 5 cm) is found between 27.80 and 27.75 m. Genetically, the major part of GLU-7 is related to fluvial deposits of the Weichselian. From 35.00–20.00 m below the surface, fine sands are dominant, in which silty to clayey layers, as well as layers with accessory medium to coarse sand, were also found. The transition from Weichselian to Holocene is unclear.

Between 20 m and the surface (GLU-8), brackish and marine deposits are found; these were fine-grained sandy, silty and clayey sediments, intercalated by thin peat beds. These sediments contain mica, mollusc fragments and lignite. A single layer, which contains a concentration of mollusc fragments, occurs. The deposits are grey in colour and are entirely calcareous. Geochemical studies of GLU-8 show variations in carbonate and soluble salt contents and in C/N ratios. Slightly acidic to slightly alkaline conditions were also found in this unit (Proborukmi & Urban 2017, this issue). Zhang et al. (2014) have dated and divided the uppermost 26 m sediment of the Garding-2 core into six units, which range from offshore to terrestrial facies.

4.2 Magnetic susceptibility and polarity

The susceptibility measurements of the Garding-2 core are presented in Fig. 2a. Borehole and core susceptibility values agree, suggesting that the core most likely represents the geological conditions in the Garding area. An offset of ca. 700×10^{-6} SI is found between the borehole probe and the core values: this was device specific and recalibrated. For better visibility, the offset is not recalculated in the plotted data. The core is characterised by a background signal with very low susceptibility values ($<10^{-5}$ SI) due to sandy, silty sediments. In some segments the background is superimposed by sharp peaks (spikes) with increased susceptibility values up to more than 10^{-3} SI (Fig. 2a). Based on its susceptibility characteristics (Fig. 2b), the Garding-2 core could be subdivided into seven susceptibility units (SU).

SU I (240.00–201.00 m) comprises most parts of GLU-1. It is characterised by low values (mean: 19×10^{-6} SI) with a few moderate spikes to less than 90×10^{-6} SI. At SU II (between 201.00 and 182.00 m), which includes the upper part of GLU-1 and GLU-2, a fivefold increased mean value (100×10^{-6} SI) and pronouncedly higher spikes are observed.

In the light of the susceptibility measurements, SU III is defined by its greater thickness (182.00–89.00 m), and comprises three lithological units, GLU-3, GLU-4 and most of GLU-5 (Fig. 2a). This is the longest part of the drill profile with unified characteristic, showing only little scatter in susceptibility values and being characterised by a relatively uniform mean value (18×10^{-6} SI). The lowermost part of this range shares the same basic characteristics but with higher spike values (510×10^{-6} SI). At 181.00–180.00 m, extremely high susceptibility values occur but these are caused by a geophone embedded in the sediment, which was lost during VSP measurements. To avoid an extremely broad susceptibility abscissa, these values were neglected (Fig. 2a). At 89.00 m, a sharp increase of susceptibility background (mean value 307×10^{-6} SI) and spike values ($>2000 \times 10^{-6}$ SI) are detected.

SU IV (89.00–68.00 m) is correlated with the upper part of GLU-5, GLU-6 and the beginning of GLU-7. This susceptibility unit indicates higher background susceptibility, which is interbedded by two intervals of the highest background susceptibility between about 89.00 and 80.00 m and between around 73.00 and 69.00 m (Fig. 2). At SU V, which comprises most of GLU-7 and the beginning of GLU-8 between 68.00 and 17.00 m, lower background intensity and very scattered susceptibility signals are indicated, with some peaks between 50.00 and 40.00 m (Fig. 2a). SU VI (between 17.00 and 10.00 m) comprises almost the first half of GLU-8 and is characterised by slightly higher background susceptibility. The uppermost unit, SU VII (10.00 m–top of the core), includes the upper half of GLU-8 and shows moderate to low scatter values. The variation in the magnetic susceptibility correlates well with depth and depends strongly on the lithology.

However, the coarse-grained sand dominated sediments of the Garding-2 core are not very suitable to record palaeodirection and the intensity of the EMF. Unfortunately, the palaeomagnetic measurements on the full cores indeed proved to be unsuitable, showing scattered intensity and direction of the NRM, even on small sections (within one metre or less; Fig. 6a). This behaviour is not typical for EMF and may only be controlled by changing the amount and distribution of dia-, para- and ferromagnetic minerals. Normal magnetic polarity is found in the more silty parts of the core (71.00–80.00 m and 180.00–200.00 m). Without any further chronostratigraphic information, this result does not improve the geochronological framework for this core. Although there was a clear inverse polarity signal at some parts within these normal-magnetised silty sections, the parts with negative polarity could at best be assigned to the Matuyama Chron. This then implies that the parts above the negative polarity section can be assigned as Brunhes Chron and the parts below as Jaramillo Subchron or Gauss Chron. This interpretation is most likely correct but remains speculative. To test this working hypothesis, small oriented cubes from these silty sections were collected. AF samples, which were demagnetised and analysed using both Zijderveld plots (Zijderveld 1967) and the principal component analyses (PCA; after Kirschvink 1980) embedded in the “Palmag” program (Maier & Bachtadse 1994), did not confirm such an inverse polarity. The samples show no useful demagnetisation behaviour, and therefore no useful palaeodirection (Figs. 6a, b). Thus a chrono-stratigraphical framework cannot be provided for the Garding-2 core using magnetostratigraphy. So, in this case, estimations of the age rely mainly on palynological evidence and lithological description of typical deposits, such as the kaolin sand and the assignment of Elsterian and Saalian till. Other important chronological evidence such as superposition and unconformities should be also taken into account. For the younger deposits, OSL and AMS ^{14}C methods play important roles in defining the age of the sediments, and therefore detailed palynological and geochemical analyses were carried out in these depth intervals in more detail (Proborukmi & Urban 2017, this issue).

4.3 Palynology

4.3.1 GLU-1

GLU-1 is represented by the three lowermost samples (238.97–238.02 m) in LPAZ GP-1 (238.97–199.00 m). These samples are grouped in the lowermost third order of the CONISS calculation for GLU-1 and GLU-2 (Fig. 4a). The samples are characterised by high percentages of AP, mainly of *Pinus*, *Quercus*, *Alnus* and *Myrica*, with few *Abies* and *Picea*. Little amounts of Tertiary taxa like *Taxodium*, *Nyssa*, *Liquidambar, Sequoia* and cf. *Symplocos* as well as *Carya* and *Sciadopitys* can be found up to GLU-2. Aquatic and marine indicator taxa are absent, while riparian taxa such as *Salix*, *Ulmus* and *Pterocarya* as well as backswamp taxa such as *Taxodium*, *Nyssa* and *Sequoia* are present. The upper part of GLU-1 (238.00–199.00 m) is dominated by coarse-grained sediments, therefore no samples were taken for palynological analysis.

4.3.2 GLU-2

This lithological unit is divided into four LPAZ: GP-2, GP-3, GP-4 and GP-5, which show relatively similar compositions of pollen taxa (Fig. 4a). CONISS subdivisions show some incoherencies with the conventional interpretation in defining the clusters for GLU-2. This is likely caused by sampling gaps, especially at the transition from GLU-1 to GLU-2.

At the base of LPAZ GP-2 (199.00–192.00 m), amounts of *Taxodium* and *Quercus* increase, while *Pinus* decreases. Tertiary taxa still occur, with notable percentages of *Sequoia*. In this pollen zone, Polypodiales slightly increase, with high percentages of *Pediastrum duplex* at the top of the zone. At the beginning of LPAZ GP-3 (192.00 m–188.38 m), the percentages of *Picea* and *Taxodium* increase, while those of *Sequoia*, *Quercus* and *Myrica* decrease. Ericaceae and Poaceae increase at first and then decrease towards the top of the zone, while records of *Pinus* and *Picea* show an opposite behaviour. The next pollen zone, LPAZ GP-4 (188.38–182.87 m), is characterised by increased frequencies of *Picea* and higher percentages of total NAP, Tertiary taxa, grasses and Ericales, as well as terrestrial herbs, *Equisetum*, Polypodiales and *Sphagnum*, while thermophilous taxa such as *Quercus*, *Ulmus*, *Corylus*, *Fraxinus* and *Carpinus* decrease towards the top of the zone.

In LPAZ GP-5 (182.87–182.00 m), typical Tertiary taxa such as *Carya*, cf. *Symplocos*, *Liquidambar*, *Nyssa* and *Sequoia* are very rare or even entirely absent. *Picea* and *Taxodium* decrease significantly together with declining percentages of some thermophilous deciduous taxa such as *Fagus*, *Fraxinus, Quercus* and *Ulmus*, while *Myrica*, Ericaceae, Polypodiales and *Sphagnum* increase. In GLU-2, foraminifera test linings and dinoflagellate cysts indeterminate are absent.

4.3.3 GLU-3

GLU-3 is dominated by coarse to medium sand and therefore this lithological unit has not been sampled for palynological analyses (Fig. 2a).

4.3.4 GLU-4 and GLU-5

GLU-4 is divided into four LPAZ: GPL-1, GPL-2, GPL-3 and GPL-4, with the upper part of GPL-4 overlapping with the subsequent GLU-5. GLU-5 is divided into four LPAZ: GPL-5, GPL-6, GPL-7 and GPL-8 and a single sample at 92.11 m (Fig. 4b). The upper part of GLU-5 (92.10–81.00 m) is mainly composed of coarse sand and for this reason, no samples were taken for palynological analyses (Fig. 2a).

GLU-4 includes almost all parts of the first CONISS big subcluster. Although there are some gaps between sampling intervals, cluster analysis shows distinct clustering for LPAZ GPL-1 up to LPAZ GPL-8.

LPAZ GPL-1 (148.00–145.84 m) is composed of four samples, which are characterised by high amounts of NAP, mainly represented by relatively high percentages of Poaceae. The AP taxa are composed mainly by *Pinus*, *Alnus*, *Betula*, *Quercus*, *Salix* and *Picea*, with low percentages of *Juniperus* and *Larix*. At the top of the zone, increasing amounts of *Pinus* and Ericaceae can be observed.

LPAZ GPL-2 (145.84–139.25 m) shows relatively similar characteristics as LPAZ GPL-3, with higher percentages of *Quercus*, terrestrial herbs and aquatic taxa, while *Betula*, *Alnus* and *Myrica* are important components of the arboreal taxa. Percentages of *Pinus* and *Picea* increase towards the top of the zone.

In LPAZ GPL-3 (139.25–129.15 m), increased amounts of AP are reflected mainly by high percentages of *Alnus*, *Betula*, *Quercus*, *Picea* and *Fraxinus*, together with other riparian taxa such as *Salix*, *Pterocarya* and *Ulmus*. Peaks of *Quercus* and *Fraxinus* are found in this zone. Towards the top of this pollen zone, amounts of *Pinus*, *Picea*, *Quercus*, *Fraxinus*, Ericales and Poaceae decrease, while *Larix*, *Selaginella selaginoides*, *Thalictrum* and *Artemisia* increase.

LPAZ GPL-4 (129.15–125.8 m) is characterised by high amounts of NAP, which is mainly composed of *Thalictrum* and Poaceae. Percentages of the AP are very low as indicated by low values mainly of *Pinus*, *Picea*, *Alnus*, *Betula*, *Pterocarya* and *Quercus*. *Tsuga* is found at the top of this zone, and there are low percentages of *Carpinus* and *Ulmus*.

The AP spectra of LPAZ GPL-5 (125.80–119.00 m) show high values of *Alnus*, *Betula*, *Myrica* and *Salix* and decreased percentages of *Quercus* and *Fraxinus*, while *Ulmus*, *Corylus* and *Tsuga* became more frequent. Occurrence of the last taxon is terminated at the top of this pollen zone and there are higher values for *Selaginella selaginoides*, Polypodiales and *Sphagnum*.

LPAZ GPL-6 (119.00–118.20 m) is characterised by high percentages of *Pinus* and Ericaceae indeterminate at the top of the zone, while grasses and heliophilous herbs decrease. *Ulmus* occurs in low percentages together with *Myrica*, *Betula*, *Alnus, Salix*, *Picea*, *Quercus*, *Corylus* and *Pterocarya*.

LPAZ GPL-7 (118.20–109.45 m) is characterised by high percentages of *Pinus* at its base, which is succeeded by relatively higher amounts of *Quercus*, *Salix* and *Myrica*. Percentages of *Empetrum*, *Calluna* and *Sphagnum* decrease, while grasses and NAP increase towards the transition to the next pollen zone.

In LPAZ GPL-8 (109.45–96.00 m), percentages of AP, especially shrubs, increase significantly. High amounts of *Pinus* and *Myrica* and increased percentages of *Pterocarya, Corylus* and *Ulmus* are characteristic of this zone. *Abies* and *Carpinus* occur rarely with low percentages.

The single sample at 92.11 m reveals a quite similar AP assemblage to LPAZ GPL-8, except that *Abies* and *Carpinus* are missing. *Betula*, *Alnus* and *Myrica* are important components. Amounts of Ericales and grasses are drastically reduced, while total NAP and Cyperaceae increase. Aquatic taxa are absent in this zone.

In both GLU-4 and GLU-5, Tertiary and Early Pleistocene taxa such as *Liquidambar*, *Nyssa*, *Carya*, *Taxodium*, *Sequoia*, *Symplocos* and *Sciadopitys*, as well as marine indicators such as dinoflagellate cysts indeterminate, foraminifera test linings are absent (Fig. 4b).

4.3.5 GLU-6

CONISS indicates that there are two big clusters within GLU-6. The first one is composed of the four lowermost samples and the second one includes the rest of the samples of LPAZ GPL-10 and the single sample of GLU-7 (Fig. 4c). Taking the second order cycle, GLU-6 should be divided into three pollen zones, between 81.00 and 79.20 m, between 79.20 and 78.00 m and between 78.00 and 73.00 m. The last two zones that are suggested by CONISS however were manually combined and only form one zone. This discrepancy was based on the consideration of the reworked, aquatic and marine taxa as important for the conventional interpretation of this section, but they were not included in the clustering calculation, to be compatible with the cluster analyses of the other sections of Garding-2. Hence, GLU-6 is subdivided into two pollen zones, LPAZ GPL-9 (81.00–79.20 m) and LPAZ GPL-10 (79.20–73.00 m). The AP percentages are relatively high in GLU-6 in comparison with GLU-4 and GLU-5. The AP composition of LPAZ GP-9 and LPAZ GP-10 is relatively similar, except that there are almost no reworked palynomorphs or marine indicator taxa such as dinoflagellate cysts indeterminate and foraminifera test linings found in LPAZ GP-9. The reworked palynomorphs such as *Carya*, cf. *Nyssa, Sequoia, Tsuga, Sciadopitys*, cf. *Symplocos* and cf. *Castanea* are mainly embedded in the redeposited Tertiary and younger Pleistocene sediments. The AP spectra of these pollen zones are dominated by *Pinus* and *Corylus* and the shrub *Myrica*. *Quercus*, *Ulmus*, *Tilia*, *Fraxinus*, *Abies*, *Picea*, *Carpinus*, *Fagus* and *Pterocarya* occur in low amounts throughout these pollen zones (Fig. 4c). The percentages of Ericales, Cyperaceae, Poaceae and the total NAP of LPAZ GPL-10 are higher than in LPAZ GPL-9. *Selaginella selaginoides* occurs in both pollen zones.

4.3.6 GLU-7

GLU-7 is composed of a massive sand layer; however, one peaty sample was taken at 69.25 m. This sample contains high percentages of AP, which is dominated by *Pinus*, *Picea*, *Betula* and *Alnus* and the shrub *Myrica*. *Quercus* and *Abies* occur in low amounts. *Pterocarya*, foraminifera test linings and dinoflagellate cysts indeterminate are absent in this sample, while amounts of Ericaceae and *Sphagnum* are low (Fig. 4c).

4.3.7 GLU-8

The youngest GLU-8 is investigated in detail by Proborukmi & Urban (2017, this issue). In summary, most part of this sequence, from 15.97 m upwards, shows low constant values of *Ulmus* and low amounts of *Fagus* and *Carpinus*, until the top of the unit. There are no indications of intensive human activities such as occurrences of cultivated cereals and high percentages of *Plantago lanceolata*-type and *Rumex ecetosa*-type in this section.

5. Discussion

5.1 Pliocene

A Pliocene sediment sequence is found at the base of the Garding-2 core up to 182.87 m. This sequence is composed of two lithological units, GLU-1 and GLU-2. Palynological investigations of these lithological units show occurrences of *Carya* and *Sciadopitys* suggesting that GLU-1 and GLU-2 cannot be younger than the Tiglian Complex (Zagwijn 1960, 1963, 1992, Urban 1978a, 1978b). Co-occurrences of *Sciadopitys*, *Carya*, *Liquidambar* and *Symplocos* are as well characteristic for this sequence, similar to the records observed in the Lower Rhine Basin, the Netherlands and in Schleswig-Holstein (Northern Germany) during the Late Pliocene (Zagwijn 1963, Menke 1975, Menke 1976a, Urban 1978a, 1978b, Urban in Arias et al. 1984). A tentative stratigraphical correlation of this sediment sequence with the Brunssumian and Reuverian is proposed. The Brunssumian sequence of the Garding-2 core shows more lignite layers compared to the Reuverian sequence as also indicated in the research drill core Oldenswort (OLW) (Stephan 2002). In this drill core, a sequence of Brunssumian and Reuverian deposits was found between 250.50 and 140.20 m. The Brunssumian layer is composed of carbonate free silt, clay and brown coal with some plant remains changing into coarser sediments with less organic remains towards the transition to the Reuverian (Stephan 2002). In Garding-2, this transition is marked by a change from coarser fluvial sediments into finer swampy sediments, while this transition is not clear in the Oldenswort 9 core (Menke 1975).

5.1.1 Brunssumian B

In LPAZ GP-1 (GLU-1), percentages of *Pterocarya*, *Liquidambar*, *Nyssa*, *Alnus* and *Myrica* are higher compared to LPAZ GP-2 (Fig. 4a). Based on these findings, this pollen zone can be correlated with the Brunssumian B of the Oldenswort sequence (Menke 1975). Occurrences of Osmundaceae, *Myrica* and *Lycopodium inundatum*, which were typical for the climatic conditions of the Late Pliocene, point to mild winters as also observed during the Brunssumian at Oldenswort (Menke 1975). Palynological analyses at LPAZ GP-1 also indicate that the sediments of GLU-1 were deposited in a fresh water environment with riparian and backswamp elements as *Nyssa*, *Myrica, Alnus* and *Pterocary* (Fig. 4a) characterising those stands. This interpretation of the depositional environment is supported by the dominance of carbonate-free sands, indicating strong fluvial activities, with intercalations of lignite, clay, silty and peaty layers, which are also characterised by low values of bulk susceptibility in SU I and in the first 2 m of SU II (Fig. 2a).

5.1.2 Brunssumian C

Palynological analysis of LPAZ GP-2 shows a predominance of conifers of swampy stands, especially of *Sequoia* (Fig. 4a), indicating distinct similarities with the youngest part of the Brunssumian C (Zagwijn 1960, Andrew & West 1977), which is also revealed in the pollen spectra from Oldenswort and Bouwberg (Zagwijn 1960, Menke 1975). *Taxodium*, *Sequoia* and *Quercus* were the main components of the backswamp forest, which together with *Alnus*, *Myrica*, *Sphagnum* and aquatic taxa are indicative of a riparian vegetation and point to the existence of nearby raised bogs (Fig. 4a). The co-occurrence of deciduous thermophilous taxa such as *Corylus* and *Ulmus* (Fig. 4a) gives evidence for a relatively warm period. This interpretation is supported by the domination of silty clay and clayey silt layers in GLU-2 that agrees with the higher susceptibility values, which correspond to SU II (Fig. 2a) and LPAZ GP-2, GP-3, GP-4 and GP-5 respectively. Geochemical analyses also confirm that a high terrestrial input characterises GLU-2 (Fig. 5a). Widening of the C/N ratios to >20 (Meyers & Ishiwatari 1993, Meyers 1994) is indicative of residual input of vascular terrestrial plants, which increase the acidity of the environment, while non-saline to slightly saline and non-calcareous sediments demonstrate disconnection of the basin from salt-water resources throughout GLU-2.

5.1.3 Reuverian A

LPAZ GP-3 (192.00–191.00 m) shows the distribution of conifer-dominated forests (Fig. 4a). *Alnus* and *Quercus* are the major deciduous trees, whereas the conifer-dominated forests are composed of *Abies*, *Picea*, *Pinus*, *Taxodium* and *Tsuga*. These forests had replaced the swampy elements. This supports a tentative correlation of this zone with Reuverian A (Zagwijn 1960, Menke 1975). The environmental conditions were slightly cooler and landscape became more open, indicated by higher percentages of Ericaceae, Asteraceae and Chenopodiaceae and non-calcareous sandy sediments at the top of the zone. In this late phase of the LPAZ GP-3, *Taxodium* retreats, while *Pinus*, *Picea* and *Alnus*, as the main components of the forest, as well as *Quercus* and *Myrica* expand.

5.1.4 Reuverian B

Pollen assemblages of LPAZ GP-4 (188.38–182.87 m) suggest a tentative correlation with the Reuverian B (Menke 1975). Towards the top of the zone, climatic conditions deteriorate, as indicated by higher amounts of Ericaceae and total NAP, while thermophilous as well as Tertiary taxa decrease. In this zone, forests composed of *Pinus*, *Picea* and *Alnus* occur in a backswamp setting with high percentages of *Taxodium*, *Sphagnum* and *Myrica*, as well as continuous occurrences of *Sequoia*, Polypodiales and a few *Nyssa* (Fig. 4a). Lithological descriptions indicate domination of silt and clayey sediments of terrestrial origin (C/N ratios between 12.8 and 25.2). Boggy environmental conditions, which are indicated by the dominance of *Myrica*, Ericaceae and *Sphagnum*, develop towards the top of the zone. The differentiation between Reuverian B and C in Garding is hardly recognisable as has also been discussed by Menke (1975) for Oldenswort. The Garding sequence therefore might as well include part of the Reuverian C around the transition to the Praetiglian.

5.2 Quaternary

In the Garding-2 core, the Quaternary sediments include the last 6 lithological units, GLU-3 to GLU-8 from 182.00 m depth onwards.

5.2.1 Early Pleistocene

5.2.1.1 Praetiglian

The pollen record of LPAZ GP-5 (Fig. 4a) shows distinct similarities to pollen assemblages of the Meinweg and Oldenswort profiles at the Pliocene-Pleistocene transition, and is correlated with the Praetiglian (Zagwijn 1960, Menke 1975). Therefore, the boundary between LPAZ GP-4 and LPAZ GP-5 at 182.87 m is defined as the Tertiary-Quaternary boundary in the Garding-2 core. An open environment under colder conditions is suggested by the decrease of AP and thermophilous taxa, while Ericaceae and heliophilous herbs increase. Pliocene marker taxa are rarely found or are even completely absent. Higher percentages of *Myrica*, *Sphagnum* and Polypodiales point to the development of raised bogs. The deposition of silt and clay with rich terrestrial organic matter, together with very acid to extremely acid environmental conditions, and a widening of the C/N ratios (Fig. 5a) all point to an increase of undecomposed biomass under deteriorating climatic conditions. The same indications are recorded in the Praetiglian deposits of the Lieth and Oldenswort profiles, which are dominated by sand and silt with higher organic matter content and together with palynological results show the development of peat bogs in the area (Menke 1975, Stephan 2002).

The subsequent deposits of GLU-3 are mostly composed of coarse-grained sediments with coarse sand as the main sedimentary facies. This is also shown by the low susceptibility values (Fig. 2a) and therefore GLU-3 probably still belongs to the Praetiglian cold period of the Early Pleistocene. Extremely high susceptibility values between 181.00 m and 180.00 m, where the lost geophone was found, have not been considered. Small differences in susceptibility in this unit may be due to different amounts of accessory minerals. Some streaks of sand with humic layers, peaty organic silt and peat are also found in this lithological unit (Fig. 2a) and represent fluvial, limnic and telmatic depositional environments.

5.2.1.2 Waalian–Bavelian

GLU-4 can at best be correlated with sections of the Waalian (Hahne et al. 2008), the Bavelian (Urban 1997), or with an Early Middle Pleistocene warm period (Menke & Behre 1973, Knipping 2008). The stratigraphical position of this unit, as well as the absence of Tertiary and Early Pleistocene taxa (such as *Sciadopitys*, *Sequoia*, *Carya*, *Nyssa*), indicate that a correlation with the Tiglian warm phase is unlikely. *Pterocarya* exists throughout this lithological unit suggesting that the sediments are not likely younger than the Holsteinian (Litt et al. 2007, Reille et al. 1998).

The sediments of GLU-4 are mainly composed of coarse-grained sediments of medium to coarse sand, which is also reflected by the relatively low values of magnetic susceptibility (Fig. 2a). Nevertheless, some higher susceptibility values are observed in GLU-4 indicating the intercalation of finer grained deposits, from which the pollen samples were taken.

The fine-grained deposits of this lithological unit are frequently composed of mud and clay layers, intercalated by humic sand, peat and lignite. These intercalated sediments suggest some periods of peat formation under limnic to fluvial conditions with low transportation activity. Extremely to slightly acidic pH of the estuary, respectively terrestrial organic matter origin, support the genetic interpretation of the sediments.

LPAZ GPL-1 at the bottom of GLU-4 suggests a tentative correlation with the Tornesch Interglacial of the Waalian (Menke 1975, Litt et al. 2007). This pollen zone shows a sparsely wooded phase with *Quercus*, *Pinus*, *Picea*, *Alnus*, *Betula* and *Myrica* under temperate conditions (Fig. 4b). The occurrence of *Larix* indicates relatively dry conditions. Palynological characteristics of the subsequent LPAZ GPL-2 suggest that this zone might tentatively be correlated with the end of the Tornesch Interglacial of the Waalian period (Menke 1975, 1976a), or with the beginning of the Uetersen warm period of the Bavelian (Menke 1975). This zone shows a relatively cool to transitional period documented by riparian forests dominated by *Betula*, *Myrica* and *Alnus* and an expansion of coniferous forests composed of *Pinus* and *Picea* towards the top of the zone (Fig. 4b). The association of the heliophytes, *Artemisia*, Asteraceae, Chenopodiaceae and *Larix* indicates a dryer period. An extreme increase of Ericaceae suggests local formation of raised bogs. Wide C/N ratios (Fig. 5b) point to a high input of organic matter of terrestrial origin, which is also reflected by high acidity of the sediments.

Pollen assemblage of LPAZ GPL-3 likely indicates a continuation of the warm period, which is tentatively correlated with the Uetersen Interglacial of the Bavelian Complex (Menke 1975). This zone shows high percentages of *Quercus*, *Fraxinus* and *Picea*, with continuous occurrence of *Pinus* and *Corylus* indicating a thermal optimum of an interglacial (Fig. 4b), which might tentatively be correlated with zone U4 of the Uetersen Interglacial (Menke 1975). Relatively high percentages of *Thalictrum*, *Artemisia* and *Larix* at the end of this pollen zone indicate an increase of aridity and opening of the landscape. *Selaginella selaginoides* occurs up to the beginning of the next pollen zone indicating local moist and azonal cool conditions. Wide C/N ratios and high acidity (Fig. 5b) are most likely caused by intense organic matter input from vascular plants.

The subsequent LPAZ GPL-4 is tentatively correlated with the last cold period of the Bavelian, Dorst (Zagwijn & De Jong 1984, Müller 1992, Litt et al. 2007, Deutsche Stratigraphische Kommission 2016). Sediments of this pollen zone are deposited on top of coarse-grained sediments, and characterised by very high percentages of NAP, such as Poaceae, *Thalictrum*, *Artemisia* and Asteraceae, occurrence of *Selaginella selaginoides* and rather low amounts of thermophilous taxa, indicating a cold period (Fig. 4b). The occurrence of *Larix* suggests rather dry climatic conditions. Riparian forest and shrubland characterised by *Myrica*, *Betula*, *Salix* and *Alnus* occur during this cold phase. Compared to the previous zones, C/N ratios are narrower and pH values are higher indicating less input from vascular plants and minor leaching of basic ions such as calcium, potassium and magnesium that would have been caused by the dry and cool climatic conditions. Waalian to Bavelian (Pinneberg) sediments were also recognised in Lieth (Menke 1975), while they are missing in Oldenswort (Stephan 2002). In Oldenswort, Elsterian deposits were found on top of Praetiglian sediments between about 99.45 and 73.10 m depth (Stephan 2002).

At the top of LPAZ GPL-4, from 126.44 m onwards, percentages of *Quercus*, *Fraxinus* and *Tsuga* increase and *Ulmus* and *Carpinus* occur, indicating considerably warmer climatic conditions. This section might be correlated to the first interglacial of the Cromerian Complex, the Osterholz Interglacial (Grüger 1968, Müller 1986, 1992). *Eucommia*, which is still present with remarkable amounts in this first Cromerian Interglacial at some sites (Grüger 1968, Müller 1986, Homann & Lepper 1994) and became extinct in Europe hence forward (Hahne et al. 1994), has not been found in the entire Plio–Pleistocene pollen sequence of Garding. Menke (1975) however describes the occurrence of *Eucommia* in the Lieth section for Early Pleistocene interglacials.

5.2.2 Middle Pleistocene

5.2.2.1 Cromerian

Most of the subsequent LPAZ GPL-5 (125.80–119.00 m) belongs to GLU-4. Only the top 1 m (at 120.00–119.00 m) of this zone is part of GLU-5 (Figs. 2a, 4b). In GLU-5, a facies of coarse-grained sediments intercalated into medium to coarse sands is predominant, which explains the low values of magnetic susceptibility (Fig. 2a). These sediments, especially the sequence above 100.00 m depth, are strongly acidic and show organic matter of terrestrial origin, which indicates stronger fluvial activities compared to GLU-4. However, some finer grained sediments and peaty layers can yet be found in GLU-5, mainly below 100.00 m depth, which were taken for palynological analyses.

The last occurrence of *Tsuga*, in the entire Garding pollen record at 119.50 m, between GLU-4 and GLU-5 can be taken as a marker horizon for correlation. In the Gorleben section, *Tsuga* occurs at the end of the second Cromerian Interglacial and is even present with low values in the third Cromerian Interglacial (Müller 1992). The same holds true for *Eucommia*, which is present in Gorleben until the second interglacial correlated by Müller (1992) with the Hunteburg Interglacial (Hahne et al. 1994). The author did not comment on the occurrences of *Tsuga* and *Eucommia* in the Gorleben sequence younger than the Cromer I Interglacial, therefore these pollen findings might not be interpreted as reworked. Based on the results of the Gorleben section, inter alia regional differentiation seems to be taken into consideration when arguing about the last occurrence of certain taxa and biostratigraphical conclusions. Hence, a biostratigraphical correlation of LPAZ GLP-5 with either the Cromerian II or III has been left open.

In the Netherlands, the first Cromerian Interglacial, the Waardenburg, which is correlated with the Osterholz Interglacial, is magnetically reversed (Zagwijn et al. 1971). The same holds true for the interglacial of Sohlingen (Hohmann & Lepper 1994), a correlative of the Osterholz Interglacial (Fromm 1994). The Brunhes-Matuyama boundary is placed between the first and the second Cromerian Interglacial in the Netherlands (Zagwijn et al. 1971). Litt et al. (2007) are discussing the second Cromerian Interglacial, the Hunteburg, which is also magnetically reversed, as either still being placed into the Matuyama Chron or as falling into the reversed Lishi Event of the Brunhes Chron (Fromm 1994).

Demagnetisation experiments were performed to test the suitability of the sediments in GLU-4 and GLU-5 as a record of information about the ancient earth magnetic field (EMF) and to evaluate any patterns that are related to the regional stratigraphic framework. An oriented sample at 115.18 m was taken but the outcome was rather a failure, as shown by the chaotic behaviour of the magnetisation vectors in the Zijderveld diagram (Fig. 6b). As the palaeomagnetic signal shows no useful palaeodirections in GLU-4 and GLU-5 (Figs. 6a, b), interpretations of magnetic polarity and palaeomagnetic dating cannot be used to confirm the palynological interpretation of the Early to Middle Pleistocene transition between GLU-4 and GLU-5. Consequently, the dating of both lithological units will be based only on the palynological records.

LPAZ GPL-6 is represented by two samples characterised by an expansion of a *Pinus*-dominated forest. Acidic conditions and wide C/N ratios (over 20) reveal an intense biomass development (Fig. 5c) caused by accumulation of organic matter. The organic matter was derived mostly from vascular plants rich in carbon and poor in nitrogen. This zone also shows occurrences of riparian and thermophilous taxa, such as *Ulmus*, *Salix*, *Pterocarya* and *Quercus* and *Corylus* respectively, as well as decreases of grasses and heliophilous herbs such as *Artemisia*, Asteraceae, Chenopodiaceae and *Thalictrum*, which indicate a slightly warmer period, most likely corresponding to a Cromerian warm period. It is difficult to assign this zone to a specific interglacial period within the Cromerian Complex (Müller 1992) because there is not enough palynological evidence and a lack of numerical dating. However, because of its stratigraphical position above the last occurrence of *Tsuga*, this zone might represent the third Cromerian interglacial or even be younger.

Ericaceae, grasses, Asteraceae, *Thalictrum*, *Artemisia* and *Myrica* dominate the bottom of the succeeding LPAZ GPL-7 (Fig. 4b), indicating the development of a colder period in an open landscape. High percentages of *Sphagnum* show an increase of humidity and the development of raised bogs at the beginning of this zone. Towards the top of the zone, riparian forest elements such as *Myrica*, *Salix* and *Quercus* increase again (Fig. 4b). Wide C/N ratios indicate higher input of organic matter, probably of terrestrial provenance (Fig. 5c). The changes of environmental conditions throughout this zone are typical for the warm periods of the younger Cromerian, which has also been observed in the Gorleben section (Müller 1992). As mentioned before, a detailed correlation of this pollen zone to one of the specific substages of the Cromerian Complex is also problematic, because of the limited availability of fine-grained sediments in this unit. Nevertheless, this zone likely represents a transition from a relatively cooler towards a warmer period evidenced by the next pollen zone.

The subsequent LPAZ GPL-8 shows co-occurrences of high and increased percentages of *Pinus* and *Picea* respectively, with low amounts of *Quercus*, *Fraxinus*, *Betula* and *Corylus*, and scattered occurrences of *Abies* and *Carpinus* (Fig. 4b). This feature is characteristic of younger Cromerian warm periods (Zagwijn 1992, Bittmann & Müller 1996, Gaudzinski et al. 1996), and shows similarities with the beginning of the Bilshausen or Rhume Interglacial of section d of the drilling Bilshausen 1/78 (Müller 1992). The continuous presence of *Myrica*, Ericaceae, and *Sphagnum*, occurrences of *Salix* and *Typha latifolia* and an absence of carbonate in the sediments are evidencing fresh water wetland environments. Large supplies of terrestrial organic matter are evidenced by low pH values and very wide C/N ratios (Fig. 5c).

5.2.2.2 Elsterian

A single sample at 92.11 m shows a relatively cool period characterised mainly by riparian boggy arboreal taxa such as *Betula*, *Alnus* and *Myrica* (Fig. 4b). Wide C/N ratios and very low pH values (Fig. 5c) indicate a high input of organic matter. This sample belongs to GLU-5, especially the coarser grained sediments that were deposited above 100.00 m depth. This sequence mainly belongs to SU IV and shows higher susceptibility values, with very high peaks (Fig. 2a). There is a sharp increase of magnetic susceptibility at about 89.00 m. It might be caused by external material from the drilling process, but, as it is not only seen in the core measurements, this reason is unlikely. Therefore, it is more probable that this spike is caused by sediments with higher magnetic susceptibility brought from elsewhere by rivers or glaciers. Thus, this spike likely indicates mixed sediment sources, in this case till. From the stratigraphical position, the sediments of the single sample at 92.11 m and the subsequent GLU-5 were deposited above the Cromerian deposits and therefore an Elsterian age is suggested for this sediment sequence. This confirms the first solid Elsterian till between the spike (89.00 m and 85.50 m). The overlying sediments are composed of glaciofluvial fine to coarse sand. Between 85.50 and 82.00 m, another till with quite similar petrographical characteristics occurs. This till is marked by a large susceptibility spike at about 83.00–82.00 m. In general, this sequence represents interbedded glaciofluvial sediments and tills of the Elsterian Glaciation. Elsterian tills were also found in Oldenswort, which show comparable characteristics with the Elsterian tills in Garding-2, very sandy layers with sandy or silty fine sand streaks and fragments (Stephan 2002).

5.2.2.3 Holsteinian–Saalian

A sequence of alternating sand, silt and organic layers of GLU-6 is found on top of the Elsterian tills of GLU-5. This lithological unit is characterised by fine-grained sediments showing lower susceptibility values. The sediments of GLU-6 have been deposited on top of a hiatus. Occurrences of Tertiary and Early Pleistocene palynomorphs suggest intense reworking activity (Fig. 7). GLU-6 consists of two pollen zones, LPAZ GPL-9 and LPAZ GPL-10.

The occurrence of *Fagus* and *Pterocarya* in the mixed-deciduous forest assemblage of LPAZ GPL-9 (Fig. 4c) is characteristic for the late Holsteinian (Müller 1974, Erd 1970, De Beaulieu et al. 2001). Low percentages of *Abies* and *Carpinus* and the absence of *Buxus* also suggest that this zone can be correlated with pollen zone XIII of Müller (1974). This pollen zone shows the termination of the interglacial indicated by a retreat of thermophilous trees, while amounts of *Pinus* are still relatively high. Percentages of NAP (mainly of Poaceae), Cyperaceae and Ericales increase towards LPAZ GPL-10 indicating climatic deterioration (Fig. 4c). These characteristics are also found in zone V of the Holsteinian marine deposits at Hamburg-Hummelsbüttel (Hallik 1960, Linke & Hallik 1993) and the MM IV, MM V and MM VI assemblage zones in the Bossel section of Geyh & Müller (2005).

Compared to LPAZ GPL-9, LPAZ GPL-10 is composed of coarser grained sediments and contains higher percentages of NAP, especially Poaceae. Ericales and *Helianthemum* as well as occurrences of *Selaginella selaginoides,* pointing to subarctic conditions at the onset of the Fuhne cold period at the beginning of the Saalian Complex (Dücker 1969, Urban et al. 1988, Litt et al. 2007). *Selaginella selaginoides* is also found in the previous zone indicating a transition towards cooler conditions. Increased amounts of reworked palynomorphs and marine taxa occur from about 77.77 m upwards (LPAZ GPL-10) pointing to landscape instability and strong reworking activities. In contrast, moderately wide C/N ratios in this zone suggest that the autochthonous organic matter derived mainly from terrestrial origin. Swampy environmental conditions are indicated by high percentages of *Myrica*, Polypodiales and *Sphagnum*. This evidence suggests that the marine indicator taxa were also reworked, likely from the Holsteinian marine sediments, and were deposited together with reworked material from the Tertiary and Pleistocene.

The subsequent GLU-7 is dominated by sand and coarser sediments. The first 2 m of the sediment between 73.00 and 71.00 m, are made of till, which show extreme peaks of magnetic susceptibility. As the Warthian and the subsequent Weichselian glaciers never reached this area, and based on this argument and the stratigraphical position of this till that is younger than the Fuhne Stadial, it is assigned to the Drenthian. Litt et al. (2007) and the Deutsche Stratigraphische Kommission (2016) correlate the Drenthian with MIS 6. The Drenthian Glaciation has eroded a considerable part of the Lower Saalian sediments of the Garding drilling, which must mainly belong to the Wacken/Dömnitz warm period of MIS 7 (Deutsche Stratigraphische Kommission 2016). Correlable Saalian deposits are found in Oldenswort between 73.10 and 36.65 m, which are characterised by meltwater sands and till between 73.10 and 68.30 m (Stephan 2002).

5.2.3. Late Pleistocene

A single sample was taken from GLU-7, at 69.25 m, from a thin peat layer above the Drenthian till. The underlying Drenthian till and absence of Holsteinian marker taxa (Grüger 1983, De Beaulieu et al. 1994, 2001, Field et al. 2000, Litt et al. 2007, Hrynowiecka-Czmielewska 2010, Pidek et al. 2011), suggest a correlation of this single sample with the Eemian Interglacial. This sample indicates late interglacial conditions with a *Pinus-Picea-Abies* assemblage that corresponds to the zone VI of Menke & Tynni (1984). Low percentages of Poaceae and NAP (Fig. 4c) indicate a densely forested environment. Marine influence is less significant, while brackish to fresh water swampy environmental conditions developed, indicated by *Myrica*, Polypodiales, cf. *Myriophyllum* and *Sphagnum* pointing to peat growth after the Eemian transgression. In Oldenswort, only reworked marine Eemian sediments are found intercalated into Weichselian deposits (Stephan 2002). Nevertheless, the information from this single sample is not sufficient to represent the whole lithological unit and to support a correlation to an established interglacial period from its pollen assemblage.

Peaks of magnetic susceptibility, between 50.00 and 48.00 m characterise the coarse sands and gravel (>3 cm grain size) between 49.55–48.84 m. Above the Saalian deposits, the susceptibility signal shows a lower background intensity that is very scattered. There are alternations of fluvial and glaciofluvial units, as indicated by intercalation of fine sands and thin layers of clayey silt between 35.00 and 20.00 m. Based on these characteristics and on OSL dating at the top of GLU-7 (Zhang et al. 2014), this deposit can be assigned to the late Weichselian. The subsequent erosion during the late glacial period and the later Holocene marine transgressional phase are believed to be the major causes of a hiatus on top of this lithological unit (Fig. 7).

5.2.4 Holocene

The Holocene deposits of GLU-8 are found in the top 20 m of the core. This sequence developed under shallow marine to backshore environmental conditions and is OSL- and ^{14}C dated to 8.3–1.5 ka (Zhang et al. 2014, Proborukmi & Urban 2017, this issue). Similar Holocene deposits were also found in Oldenswort between 19.60 m and the surface (Stephan 2002), which show relatively identical thickness and lithology as those of the Garding-2 core. In Garding-2, a hiatus occurs at the bottom of this sequence, which might have comprised most of the Atlantic and the early Subboreal eroded deposits. In the subsequent Subboreal and Subatlantic deposits, indications for increased anthropogenic activities as well as the expansion of *Fagus* and *Carpinus* are not recorded in the pollen diagram, which was likely caused by frequent erosion and redeposition that are common in this area.

6. Conclusion

The Garding-2 core consists of 240 m Tertiary to Quaternary sediments and reveals climatic and environmental changes in the coastal area of northwestern Germany (Fig. 7). The dating problem of the sediments older than about 450 ka makes it difficult to establish a solid stratigraphical framework of the core. However, palynological and lithological analyses provide considerable results of the climate, stratigraphy and environmental conditions of the Garding-2 core.

Brunssumian and Reuverian sediments were deposited before the onset of a strong cooling at 182.87 m depth, which marks the Pliocene-Pleistocene boundary, above which the sediments are correlated with the Praetiglian. The subsequent sediments indicate layers of the Waalian and Bavelian Complex and of probably the first, and the end of the second or third interglacial of the Cromerian Complex marked by the last occurrence of *Tsuga* at 119.50 m depth. Three thin younger interglacial layers are identified between 119.00 and 96.00 m. Climatic deterioration of the early Elsterian Glaciation is evidenced following the last thin interglacial layer at 109.45–96.00 m, which is likely correlated to the Cromerian V, the Bilshausen Interglacial. The beginning of this cooling is recorded in a single sample at 92.11 m, while the Elsterian Glacial deposits are indicated by two tills at 89.00–85.50 m and at 85.50–82.00 m depth. Late Holsteinian deposits of zone XIII (Müller 1974) are represented by a clayey layer above 80.29 m. The Drenthian glaciers, whose till is found between 73.00 and 71.00 m, have eroded most of the Lower Saalian. Eemian peat is found in the subsequent layer at 69.25 m. This layer is then overlain by late Weichselian and Holocene sediments. Most of the biostratigraphic and particularly lithological findings are in agreement with the sequences of Oldenswort and Lieth (Menke 1975) of the nearer vicinity. This allows long distance correlation, which provides the basis for the classification of the Garding-2 sequence, as the palaeomagnetic and OSL dating were mainly unsuccessful.

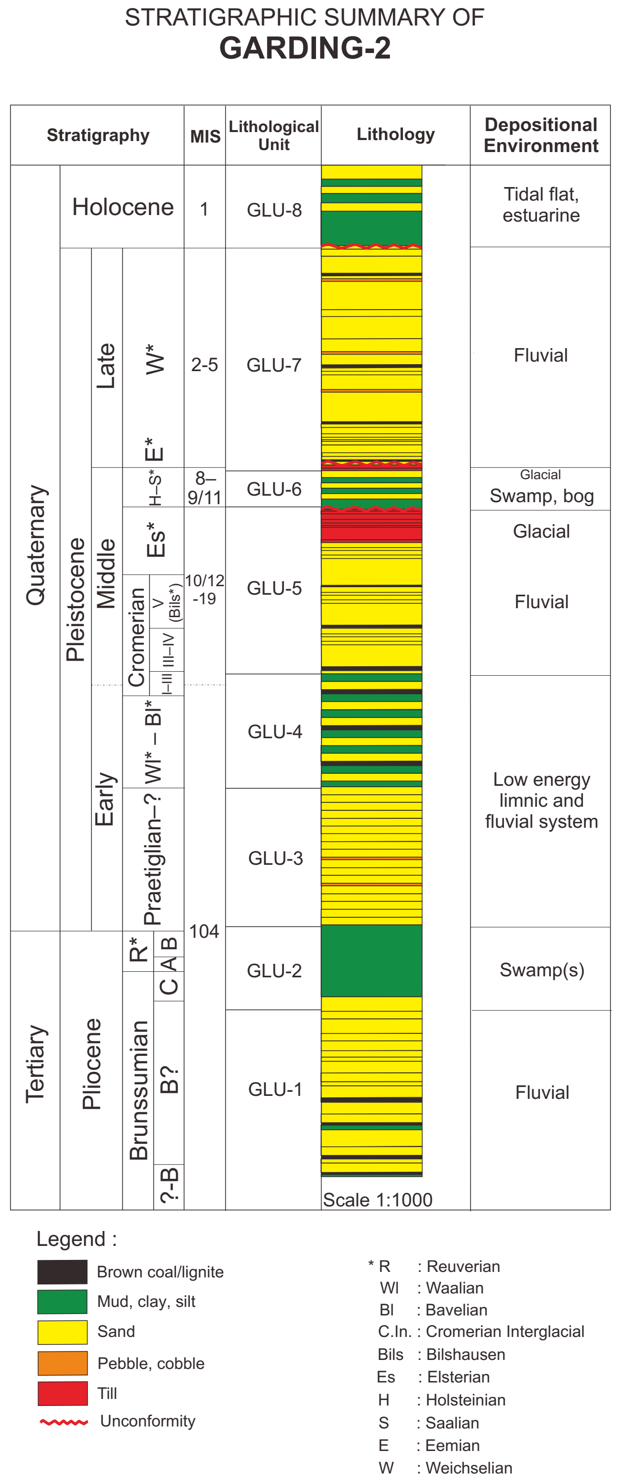

Fig. 7: Summary of the Garding-2 core findings, showing chronostratigraphy, lithology and depositional environment of each lithological unit and its correlation to the established MIS framework.

7. Acknowledgements

We would like to sincerely thank the Directorate General of Indonesian Higher Education (Dikti), the German Academic Exchange Service (DAAD) and International Office of Leuphana University of Lüneburg for the scholarship, as well as Leuphana University of Lüneburg for Small Research Project Funding, that supported this research. We are indebted to Mario Tucci, Emilio Torres, Sabine Hansen and Frank Krüger for their help and assistance in sampling, laboratory work and pollen diagram improvements, Kathrin Worm and Lena Wallbrecht from LIAG for laboratory assistance in rock and palaeomagnetic measurements, Thomas Grelle and LIAG logging team for borehole measurements (susceptibility), Peter Kershaw for his valuable advice and Micha Edlich (Writing Center for Academic English, Leuphana University of Lüneburg) for his English review. We would like to express our gratitude to Jaqueline Strahl (Cottbus) and Hans-Jürgen Stephan (Kiel) for their detailed and constructive comments and suggestions, which considerably helped to improve the manuscript.

8. References

Ad-Hoc-Arbeitsgruppe Boden (2005): Bodenkundliche Kartieranleitung: 438 p., Stuttgart (Schweizerbart).
Andrew, R. & West, R.G. (1977): Pollen spectra from Pliocene crag at Orford, Suffolk. – New Phytol., 78 (3): 709–714.
Arias, C., Bigazzi, G., Bonadonna, F., Brunnacker, K. & Urban, B. (1984): Correlation of Plio-Pleistocene deposits of the Lower Rhine Basin (north-west Germany) and the Valle Ricca pits (Central Italy). – Quatern. Sci. Rev., 3 (1): 73–89.
Baldschuhn, R., Best, G. & Kockel, F. (1991): Inversion tectonics in the North-west German basin. – In: Spencer, A.M. (ed.): Generation, accumulation, and production of Europe's hydrocarbons. – Spec. Publ. Eur. Assoc. Petroleum Geosci., 1: 149–159.
Baldschuhn, R., Binot, F., Fleig, S. & Kockel, F. (2001): Geotektonischer Atlas von Nordwest-Deutschland und dem deutschen Nordsee-Sektors – Strukturen, Strukturentwicklung, Paläogeographie. – Geol. Jb., A 153: 88 p.
Bassinot, F.C., Labeyrie, L.D., Vincent, E., Quidelleur, X., Shackleton, N.J. & Lancelot, Y. (1994): The astronomical theory of climate and the age of the Brunhes-Matuyama magnetic reversal. – Earth Planet. Sci. Lett., 126: 91–108.
Behre, K.-E. (1989): Biostratigraphy of the last glacial period in Europe. – Quatern. Sci. Rev., 8 (1): 25–44.
Behre, K.-E. (1991): Veränderungen von Landschaft und Umwelt in der Wesermarsch in den vergangenen Jahrtausenden. – Archäolog. Mitt. Nordwestdeutschland, 5: 33–36.
Behre, K.-E. (2003): Eine neue Meeresspiegelkurve für die südliche Nordsee – Transgressionen und Regressionen in den letzten 10.000 Jahren. – Probl. Küstenforsch. Südl. Nordseegebiet, 28: 9–63.
Behre, K.-E. (2004): Coastal development, sea-level change and settlement history during the later Holocene in the Clay District of Lower Saxony (Niedersachsen), northern Germany. – Quatern. Int., 112 (1): 37–53.
Behre, K.-E. (2007): Evidence for Mesolithic agriculture in and around central Europe? – Veget. Hist. Archaeobot., 16 (2): 203–219.
Behre, K.-E. & Lade, U. (1986): Eine Folge von Eem und 4 Weichsel-Interstadialen in Oerel/Niedersachsen und ihr Vegetationsablauf. – Eiszeitalter u. Gegenwart, 36: 11–36.
Benda, L. (1995): Das Quartär Deutschlands: 408 p., Berlin (Borntraeger).
Beug, H.J. (2004): Leitfaden der Pollenbestimmung, für Mitteleuropa und angrenzende Gebiete: 542 p., München (Pfeil).
Birks, H.J.B. & Birks, H.H. (2008): Biological responses to rapid climate change at the Younger Dryas-Holocene transition at Kråkenes, western Norway. – Holocene, 18 (1): 19–30.
Bittmann, F. & Müller, H. (1996): The Kärlich Interglacial site and its correlation with the Bilshausen sequence. – In: Turner, C. (ed.): The Early Middle Pleistocene in Europe: 187–193, Rotterdam (Balkema).
Bock, W., Menke, B., Strehl, E. & Ziemus, H. (1985): Neue Funde des Weichsel-Spätglazials in Schleswig-Holstein. – Eiszeitalter u. Gegenwart, 35: 161–180.
Bos, J.A.A. (2001): Lateglacial and Early Holocene vegetation history of the northern Wetterau and the Amöneburger Basin (Hessen), central Germany. – Rev. Palaeobot. Palynol., 115 (3–4): 177–204.
Brauer, A., Endres, C. & Negendank, J.F.W. (1999): Lateglacial calendar year chronology based on annually laminated sediments from Lake Meerfelder Maar, Germany. – Quatern. Int., 61 (1): 17–25.
Brauer, A., Allen, J.R.M., Mingram, J., Dulski, P., Wulf, S. & Huntley, B. (2007): Evidence for last interglacial chronology and environmental change from Southern Europe. – Proc. Nat. Acad. Sci. USA, 104 (2): 450–455.
Cande, S.C. & Kent, D.V. (1995): Revised calibration of the geomagnetic polarity time scale for the Late Cretaceous and Cenozoic. – J. Geophys. Res., 100 (B4): 6093–6095.
Candy, I., Schreve, D.C., Sherriff, J. & Tye, G.J. (2014): Marine isotope stage 11: Palaeoclimates, palaeoenvironments and its role as an analogue for the current interglacial. – Earth-Sci. Rev., 128: 18–51.
Caspers, G., Merkt, J., Müller, H. & Freund, H. (2002): The Eemian Interglaciation in Northwestern Germany. – Quatern. Res., 58 (1): 49–52.
Cepek, A.G. (1967): Stand und Probleme der Quartärstratigraphie im Nordteil der DDR. – Ber. Dt. Ges. Geol. Wiss., A 12 (3–4): 375–404.
Channell, J.E.T., Curtis, J.H. & Flower, B.P. (2004): The Matuyama-Brunhes boundary interval (500–900 ka) in North Atlantic drift sediments. – Geophys. J. Int., 158 (2): 489–505.
Cohen, K.M. & Gibbard, P.L. (2016): Global chronostratigraphical correlation table for the last 2.7 million years v. 2016a. International Commission on Stratigraphy. – Available online: http://www.stratigraphy.org/index.php/ics-chart-timescale (accessed 9 February 2017).
De Beaulieu, J.L., Eicher, U. & Monjuvent, G. (1994): Reconstruction of Middle Pleistocene palaeoenvironments based on pollen and stable isotope investigations at Val-de-Lans, Isère, France. – Veget. Hist. Archaeobot., 3: 127–142.
De Beaulieu, J.L., Andrieu-Ponel, V., Reille, M., Grüger, E., Tzedakis, C. & Svobodova, H. (2001): Correlation between the Velay pollen sequence and the Pleistocene stratigraphy from central Europe. – Quatern. Sci. Rev., 20 (16): 1593–1602.
De Klerk, P. (2002): Changing vegetation patterns in the Endinger Bruch area (Vorpommern, NE Germany) during the Weichse-

lian Lateglacial and Early Holocene. – Rev. Palaeobot. Palynol., 119: 275–309.
Deutsche Stratigraphische Kommission (2016): Stratigraphischen Tabelle von Deutschland 2016. – Available online: https://subkommissionquartaer.wordpress.com/estd2002-quartaer/ (accessed 11 January 2017).
Diehl, M. (2007): Palynologie und Sedimentologie der Interglazialprofile Döttingen, Bonstorf, Munster and Bilshausen. – Ph.D. thesis, Univ. Mainz: 310 p.
Dücker, A. (1969): Der Ablauf der Holstein-Warmzeit in Westholstein. – Eiszeitalter u. Gegenwart, 20: 46–57.
Ehlers, J. (1987): Die Entstehung des Kaolinsandes von Sylt. – In: Von Hacht, U. (ed.): Fossilien von Sylt, II: 249–267, Hamburg (Von Hacht).
Ehlers, J. & Linke, G. (1989): The origin of deep buried channels of Elsterian age in Northwest Germany. – J. Quatern. Sci., 4 (3): 255–265.
Ehlers, J., Meyer, K.-D. & Stephan, H.-J. (1984): The pre-Weichselian glaciations of North-West Europe. – Quatern. Sci. Rev., 3 (1): 1–40.
Ehlers, J., Eissmann, L., Lippstreu, L., Stephan, H.-J. & Wansa, S. (2004): Pleistocene glaciations of North Germany. – In: Ehlers, J. & Gibbard, P.L. (ed.): Quaternary glaciations – extent and chronology. Part I: Europe. – Dev. Quaternary Sci., 2: 135–146.
Ehlers, J., Grube, A., Stephan, H.J. & Wansa, S. (2011): Pleistocene glaciations of North Germany – new results. – In: Ehlers, J., Gibbard, P.L. & Hughes, P.D. (ed.): Quaternary glaciations – extent and chronology, a closer look. – Dev. Quaternary Sci., 15: 149–162.
Eissmann, L. (2002): Quaternary geology of eastern Germany (Saxony, Saxon-Anhalt, South Brandenburg, Thuringia), type area of the Elsterian and Saalian stages in Europe. – Quatern. Sci. Rev., 21: 1275–1346.
Eissmann, L. (2004): Reduced to the maximum: Mitteleuropäisches Quartär im Spiegel hochverdichteter geologischer Schnitte. – Mauritiana, 19: 1–16.
Eissmann, L. & Müller, A. (1979): Leitlinien der Quartärentwicklung im norddeutschen Tiefland. – Z. Geol. Wiss. Berlin, 7 (4): 451–462.
Erd, K. (1970): Pollen-analytical classification of the Middle Pleistocene in the German Democratic Republic. – Palaeogeogr., Palaeoclimatol., Palaeoecol., 8: 129–145.
Erd, K. (1973): Vegetationsentwicklung und Biostratigraphie der Dömnitz-Warmzeit (Fuhne/Saale) im Profil von Pritzwalk/Prignitz. – Abh. Zentr. Geol. Inst., 18: 9–48.
Erd, K., Palme, H. & Präger, F. (1987): Holsteininterglaziale Ablagerungen von Rossendorf bei Dresden. – Z. Geol. Wiss., 15 (3): 281–295.
Faegri, K. & Iversen, J. (1989): Textbook of pollen analysis; 4th ed.: 328 p., New York (Wiley).
Faegri, K. & Iversen, J. (1993): Bestimmungsschlüssel für die Nordwesteuropäische Pollenflora: 85 p., Jena (Fischer).
Field, M.H., De Beaulieu, J.L., Guiot, J. & Ponel, P. (2000): Middle Pleistocene deposits at La Côte, Val de Lans, Isère department, France: plant macrofossil, palynological and fossil insect investigations. – Palaeogeogr., Palaeoclimatol., Palaeoecol., 159: 53–83.
Firbas, F. (1949): Spät- und nacheiszeitliche Waldgeschichte Mitteleuropas nördlich der Alpen; Band 1: Allgemeine Waldgeschichte: 480 p., Jena (Fischer).
Frechen, M., Buness, H., Grube, A., Königer, P., Sirocko, F., Urban, B. & Wiederhold, H. (2011): The Garding drilling project – unravelling the Quaternary record in Northern Germany by means of palynology, geology and applied geophysics. – 71st annual meeting Dt. Geophys. Ges., Cologne, Germany, 21–24 February 2011.
Frenzel, B. (1973): On the Pleistocene vegetation history. – Eiszeitalter u. Gegenwart, 23: 321–332.
Frisch, U. & Kockel, F. (1999): Quantification of Early Cimmerian movements in Northwest Germany. – In: Bachmann, G.H. & Lerche, I. (ed.): Epicontinental Triassic. Vol. 1. – Zbl. Geol. Paläontol., T. 1, 1998 (7–8): 571–600.
Fromm, K. (1994): Paläomagnetische Bestimmungen an Quartärsedimenten in Nordwest-Deutschland. – Geol. Jb., A 134: 229–257.
Gaudzinski, S., Bittmann, F., Boenigk, W., Frechen, M. & Van Kolfschoten, T. (1996): Palaeoecology and archaeology of the Kärlich-Seeufer open-air site (Middle Pleistocene) in the Central Rhineland, Germany. – Quatern. Res., 46: 319–334.
Geyh, M.A. & Krbetschek, M. (2012): Zum radiometrischen Alter des Holstein-Interglazials. In: K.-E. Behre (ed.): Die chronologische Einordnung der paläolithischen Fundstellen von Schöningen. – V. d. Röm. -Germ. Zentralmu., 1: 151–170.
Geyh, M.A. & Müller, H. (2005): Numerical ^{230}Th/U dating and a palynological review of the Holsteinian/Hoxnian Interglacial. – Quatern. Sci. Rev., 24: 1861–1872.
Gibbard, P.L. & Cohen, K.M. (2008): Global chronostratigraphical correlation table for the last 2.7 million years. – Episodes, 31 (2): 243–247.
Gibbard, P.L., West, R.G., Zagwijn, W.H., Balson, P.S., Burger, A.W., Funnell, B.M., Jeffery, D.H., De Jong, J., Van Kolfschoten, T., Lister, A.M., Meijer, T., Norton, P.E.P., Preece, R.C., Rose, J., Stuart, A.J., Whiteman, C.A. & Zalasiewicz, J.A. (1991): Early and Early Middle Pleistocene correlations in the southern North Sea Basin. – Quatern. Sci. Rev., 10: 23–52.
Graham, A.G.C., Stoker, M.S., Lonergan, L., Bradwell, T. & Stewart, M.A. (2011): The Pleistocene glaciations of the North Sea basin. – In: Ehlers, J. & Gibbard, P.L. (ed.): Quaternary glaciations – extent and chronology; 2nd ed.: 261–278, Amsterdam (Elsevier).
Grimm, E.C. (1987): CONISS: a FORTRAN 77 program for stratigraphically constrained cluster analysis by the method of incremental sum of squares. – Comput. Geosci., 13 (1): 13–35.
Grimm, E.C. (1990): Tilia, Tiliagraph & Tiliaview. PC spreadsheet and graphics software for pollen data. Available at: http://www.geo.arizona.edu/palynology/geos581/tiliaview.html (accessed 26 November 2013).
Grube, A. (2011): Schichtansprache der Forschungsbohrung Garding-2. – Landesamt für Landwirtschaft, Umwelt und ländliche Räume, Flintbek [unpubl.].
Grüger, E. (1968): Vegetationsgeschichtliche Untersuchungen an cromerzeitlichen Ablagerungen im nördlichen Randgebiet der deutschen Mittelgebirge. – Eiszeitalter u. Gegenwart, 18: 204–235.
Grüger, E. (1983): Untersuchungen zur Gliederung und Vegetationsgeschichte des Mittelpleistozäns am Samerberg in Oberbayern. – Geol. Bavarica, 84: 21–40.
Grüger, E. (1989): Stratigraphy of the last interglacial/glacial cycle in Germany. – Quatern. Int., 3: 69–79.
Hahne, J., Mengeling, H., Merkt, J. & Gramann, F. (1994): Die Hunteburg-Warmzeit („Cromer-Komplex“) und Ablagerungen der Elster-, Saale- und Weichsel-Kaltzeit in der Forschungsbohrung Hunteburg GE 58 bei Osnabrück. – In: Meyer, K.-D. (ed.): Neuere Untersuchungen an Interglazialen in Niedersachsen. – Geol. Jb., A 134: 117–166.

Hahne, J., Ellwanger, D. & Stritzke, R. (2008): Evidence for a Waalian thermomer pollen record from the research borehole Heidelberg UniNord, Upper Rhine Graben, Baden-Württemberg. – Eiszeitalter u. Gegenwart, 57 (3–4): 403–410.
Hallik, R. (1960): Die Vegetationsentwicklung der Holstein-Warmzeit in Nordwestdeutschland und die Altersstellung der Kieselgurlager der südlichen Lüneburger Heide. – Z. Dt. Geol. Ges., 112: 326–333.
Head, M.J. & Gibbard, P.L. (2005): Early-Middle Pleistocene transitions: an overview and recommendation for the defining boundary. – Geol. Soc. London, Spec. Publ., 247: 1–18.
Head, M.J., Pillans, B. & Farquhar, S.A. (2008): The Early–Middle Pleistocene transition: characterization and proposed guide for the defining boundary. – Episodes, 31 (2): 255–259.
Hinsch, W. (1974): Das Tertiär im Untergrund von Schleswig-Holstein (Das Nordwestdeutsche Tertiärbecken, Beitrag 5). – Geol. Jb., A 24: 34 p.
Hinsch, W. (1991): Karte des präquartären Untergrundes von Schleswig-Holstein 1: 200.000. – Kiel (Geolog. Landesamt Schleswig-Holstein).
Höfle, H.-C., Merkt, J. & Müller , H. (1985): Die Ausbreitung des Eem-Meeres in Nordwestdeutschland. – Eiszeitalter u. Gegenwart, 35: 49–59.
Homann, M. & Lepper, J. (1994): Das Cromer-Profil von Sohlingen (Süd-Niedersachsen). – Geol. Jb., A 134: 211–228.
Hrynowiecka-Czmielewska, A. (2010): History of vegetation and climate of the Mazovian (Holsteinian) Interglacial and the Liviecian (Saalian) Glaciation on the basis of pollen analysis of palaeolake sediments from Nowiny Żukowskie, SE Poland. – Acta Palaeobot., 50 (1): 17–54.
Hrynowiecka, A. & Szymczyk, A. (2011): Comprehensive palaeobotanical studies of lacustrine-peat bog sediments from the Mazovian/Holsteinian interglacial at the site of Nowiny Żukowskie (SE Poland) – preliminary study. – Bull. Geogr., Phys. Geogr. Ser., 4: 21–46.
Jerz, H. & Linke, G. (1987): Arbeitsergebnisse der Subkommission für Europäische Quartärstratigraphie: Typusregion des Holstein-Interglazials (Berichte der SEQS 8). – Eiszeitalter u. Gegenwart, 37: 145–148.
Kirschvink, J.L. (1980): The least-squares line and plane and the analysis of palaeomagnetic data. – Geophys. J. Int., 62 (3): 699–718.
Kleinmann, A., Müller, H., Lepper, J. & Waas, D. (2011): Nachtigall: a continental sediment and pollen sequence of the Saalian Complex in NW-Germany and its relationship to the MIS-framework. – Quatern. Int., 241: 97–110.
Knipping, M. (2008): Early and Middle Pleistocene pollen assemblage of deep core drillings in the northern Upper Rhine Graben, Germany. – Geol. Mijnbouw, 87 (1): 51–65.
Knoth, W. (1964): Zur Kenntnis der pleistozänen Mittelterrassen der Saale und Mulde nördlich von Halle. – Geologie, 13: 598–616.
Koutsodendris, A., Müller, U.C., Pross, J., Brauer, A., Kotthoff, U. & Lotter, A.F. (2010): Vegetation dynamics and climate variability during the Holsteinian interglacial based on a pollen record from Dethlingen (northern Germany). – Quatern. Sci. Rev., 29: 3298–3307.
Kukla, G.J., Bender, M.L., De Beaulieu, J.L., Bond, G., Broecker, W.S., Cleveringa, P., Gavin, J.E., Herbert, T.D., Imbrie, J., Jouzel, J., Keigwin, L.D., Knudsen, K.-L., McManus, J.F., Merkt, J., Muhs, D.R., Müller, H., Poore, R.Z., Porter, S.C., Seret, G., Shackleton, N.J., Turner, C., Tzedakis, P.C. & Winograd, I.J. (2002): Last interglacial climates. – Quatern. Res., 58: 2–13.
Kuneš, P., Kjærsgaard-Sørensen, M., Buylaert, J.-P., Murray, A.S., Houmark-Nielsen, M. & Odgaard, B.V. (2013): A new Middle Pleistocene interglacial record from Denmark: chronostratigraphic correlation, palaeovegetation and fire dynamics. – Boreas, 42: 596–612.
Kunz, A., Urban, B. & Tsukamoto, S. (2017): Chronological investigations of Pleistocene interglacial, glacial and aeolian deposits from Schöningen (Germany) using post-IR IRSL dating and pollen analysis. – Z. Dt. Ges. Geowiss., 168 (1): 81–104 (this issue); DOI: 10.1127/zdgg/2016/0080.
Linke, G. & Hallik, R. (1993): Die pollenanalytischen Ergebnisse der Bohrungen Hamburg-Dockenhuden (qho 4), Wedel (qho 2) und Hamburg-Billbrook. – In: Benda, L. (ed.): Holstein-Interglazial. – Geol. Jb., A 138: 169–184.
Litt, T. & Gibbard, P. (2008): A proposal for the Global Stratotype Section and Point (GSSP) for the Middle/Upper (Late) Pleistocene Subseries Boundary (Quaternary System/Period). – Episodes, 31 (2): 260–263.
Litt, T. & Stebich, M. (1999): Bio- and chronostratigraphy of the Lateglacial in the Eifel region, Germany. – Quatern. Int., 61 (1): 5–16.
Litt, T., Brauer, A., Goslar, T., Merkt, J., Bałaga, K., Müller, H., Ralska-Jasiewiczowa, M., Stebich, M. & Negendank, J.F.W. (2001): Correlation and synchronisation of Lateglacial continental sequences in northern central Europe based on annually laminated lacustrine sediments. – Quatern. Sci. Rev., 20: 1233–1249.
Litt, T., Behre, K.-E., Meyer, K.-D., Stephan, H.-J. & Wansa, S. (2007): Stratigraphische Begriffe für das Quartär des norddeutschen Vereisungsgebietes. – In: Litt, T. (ed.): Stratigraphie von Deutschland – Quartär. – Eiszeitalter u. Gegenwart, 56 (1–2): 7–65.
Litt, T., Schmincke, H.U., Frechen, M. & Schlüchter, C. (2008): Quaternary. – In: McCann, T. (ed.): Geology of Central Europe. Vol. 2: Mesozoic and Cenozoic: 1287–1340, London (Geol. Soc. London).
Litt, T., Schölzel, C., Kühl, N. & Brauer, A. (2009): Vegetation and climate history in the Westeifel Volcanic Field (Germany) during the past 11 000 years based on annually laminated lacustrine maar sediments. – Boreas, 38 (4): 679–690.
Magri, D. (2010): Persistence of tree taxa in Europe and Quaternary climate changes. – Quatern. Int., 219: 145–151.
Maier, F.J. & Bachtadse, V. (1994): PALMAG. Paleomagnetic data analysis software package. – Department of Earth and Environmental Sci., Univ. Munich.
Meng, S., Börner, A., Strahl, J. & Thieke, H. U. (2009): Bio- und lithostratigraphische Untersuchungen an limnisch-fluviatilen Sedimenten aus dem Eem-Interglazial im unteren Peenetal (NE-Deutschland). – Brandenburg. Geowiss. Beitr., 16 (2): 63–78.
Menke, B. (1968a): Beiträge zur Biostratigraphie des Mittelpleistozäns in Norddeutschland. – Meyniana, 18: 35–42.
Menke, B. (1968b): Das Spätglazial von Glüsing. – Eiszeitalter u. Gegenwart, 19: 73–84.
Menke, B. (1968c): Ein Beitrag zur pflanzensoziologischen Auswertung von Pollendiagrammen, zur Kenntnis früherer Pflanzengesellschaften in den Marschenrandgebieten der schleswigholsteinischen Westküste und zur Anwendung auf die Frage der Küstenentwicklung. – Mitt. Florist. Soziol. Arbeitsgemeinschaft, N. F., 13: 195–223.
Menke, B. (1970): Ergebnisse der Pollenanalyse zur Pleistozän-Stratigraphie und zur Pliozän-Pleistozän-Grenze in Schleswig-Holstein. – Eiszeitalter u. Gegenwart, 21: 5–21.

Menke, B. (1972): Wann begann die Eiszeit? – Umschau Wiss. Techn., 72 (7): 214–218.
Menke, B. (1975): Vegetationsgeschichte und Florenstratigraphie Nordwestdeutschlands im Pliozän und Frühquartär. Mit einem Beitrag zur Biostratigraphie des Weichselfrühglazials. – Geol. Jb., A 26: 3–151.
Menke, B. (1976a): Pliozäne und ältestquartäre Sporen- und Pollenflora von Schleswig-Holstein. – Geol. Jb., A 32: 196 p.
Menke, B. (1976b): Befunde und Überlegungen zum nacheiszeitlichen Meeresspiegelanstieg (Dithmarschen und Eiderstedt, Schleswig-Holstein). – Probl. Küstenforsch. Südl. Nordseegebiet, 11: 145–161.
Menke, B. & Behre, K.-E. (1973): History of vegetation and biostratigraphy. – Eiszeitalter u. Gegenwart, 23: 251–267.
Menke, B. & Tynni, R. (1984): Das Eem-Interglazial und das Weichselfrühglazial von Redderstall/Dithmarschen und ihre Bedeutung für die mitteleuropäische Jungpleistozän-Gliederung. – Geol. Jb., A 76: 120 p.
Merkt, J. & Müller, H. (1999): Varve chronology and palynology of the Lateglacial in Northwest Germany from lacustrine sediments of Hämelsee in Lower Saxony. – Quatern. Int., 61: 41–59.
Meyers, P.A. (1994): Preservation of elemental and isotopic source identification of sedimentary organic matter. – Chem. Geol., 114: 289–302.
Meyers, P.A. & Ishiwatari, R. (1993): Lacustrine organic geochemistry – an overview of indicators of organic matter sources and diagenesis in lake sediments. – Org. Geochem., 20 (7): 867–900.
Mohr, M., Kukla, P.A., Urai, J.L. & Bresser, G. (2005): Multiphase salt tectonic evolution in NW Germany: seismic interpretation and retro-deformation. – Int. J. Earth Sci., 94: 917–940.
Moore, P.D., Webb, J.A. & Collinson, M.E. (1991): Pollen analysis; 2nd ed.: 216 p., Oxford (Blackwell).
Müller, H. (1974): Pollenanalytische Untersuchungen und Jahresschichtenzählungen an der holstein-zeitlichen Kieselgur von Munster-Breloh. – Geol. Jb., A 21: 107–140.
Müller, H. (1986): Altquartäre Sedimente im Deckgebirge des Salzstockes Gorleben. – Z. Dt. Geol. Ges., 137: 85–95.
Müller, H. (1992): Climatic changes during and at the end of the interglacials of the Cromerian Complex. – In: Kukla, G.J. & Went, E. (ed.): Start of a glacial: 51–70, Springer (Heidelberg).
Müller, H. & Höfle, H.-C. (1994): Die Holstein-Interglazialvorkommen bei Bossel westlich von Stade und Wanhöden nördlich Bremerhaven. – Geol. Jb., A 134: 71 – 116.
Müller, U. (2004): Alt- und Mittel-Pleistozän; Jung-Pleistozän–Eem-Warmzeit bis Weichsel-Hochglazial. – In: Katzung, G. (ed.): Geologie von Mecklenburg-Vorpommern: 226– 242, Stuttgart (Schweizerbart).
Nelle, O. & Dörfler, W. (2008): A summary of the late- and postglacial vegetation history of Schleswig-Holstein. – In: Dengler, J., Dolnik, C. & Trepel, M. (ed.): Flora, vegetation and nature conservation from Schleswig-Holstein to South America – Festschrift for Klaus Dierßen on occasion of his 60th birthday. – Mitt. Arbeitsgem. Geobot. Schleswig-Holstein Hamb., 65: 45–68.
Nitychoruk, J., Bińka, K., Hoefs, J., Ruppert, H. & Schneider, J. (2005): Climate reconstruction for the Holsteinian interglacial in eastern Poland and its comparison with isotopic data from Marine Isotope Stage 11. – Quatern. Sci. Rev., 24: 631–644.
Partridge, T.C. (1997): Reassessment of the position of the Plio-Pleistocene boundary: is there a case for lowering it to the Gauss-Matuyama palaeomagnetic reversal? – Quatern. Int., 40: 5–10.
Pidek, I.A., Terpiłowski, S. & Małek, M. (2011): Succession of the Mazovian Interglacial near Luków (E. Poland): palynostratigraphic and palaeogeographic approach. – Geologija, 53 (1): 27–35.
Pillans, B. & Naish, T. (2004): Viewpoint defining the Quaternary. – Quatern. Sci. Rev., 23: 2271–2282.
Pirazzoli, P.A. (1991): World atlas of Holocene sea-level changes: 300 p., Amsterdam (Elsevier).
Plaster, E.J. (2009): Soil science and management; 5th ed.: 495 p., Delmar (Cengage Learning).
Proborukmi, M.S. & Urban, B. (2017): Palaeoenvironmental investigations of the Holocene sedimentary record of the Garding-2 research drill core, northwestern Germany. – Z. Dt. Ges. Geowiss., 168 (1): 39–51 (this issue).
Pross, J. & Klotz, S. (2002): Palaeotemperature calculations from the Praetiglian/Tiglian (Plio-Pleistocene) pollen record of Lieth, northern Germany: implications for the climatic evolution of NW Europe. – Global Planet. Change, 34: 253–267.
Reille, M., Andrieu, V., De Beaulieu, J.L., Guenet, P. & Goeury, C. (1998): A long pollen record from Lac du Bouchet, Massif Central, France, for the period ca. 325–100 ka BP (OIS 9c to OIS 5e). – Quatern. Sci. Rev., 17: 1107–1123.
Rhodes, E.J. (2011): Optically stimulated luminescence dating of sediments over the past 20,000 years. – Annu. Rev. Earth Planet. Sci., 39: 461–488.
Richmond, G.M. (1996): The INQUA-approved provisional Lower-Middle Pleistocene boundary. – In: Turner, C. (ed.): The Early–Middle Pleistocene in Europe: 319–327, Rotterdam (Balkema).
Rolf, C. (2000): Das Kryogenmagnetometer im Magnetiklabor Grubenhagen. – Geol. Jb., E 52: 161–188.
Roskosch, J., Winsemann, J., Polom, U., Brandes, C., Tsukamoto, S., Weitkamp, A., Bartholomäus, W.A., Henningsen, D. & Frechen, M. (2015): Luminescence dating of ice-marginal deposits in northern Germany: evidence for repeated glaciations during the Middle Pleistocene (MIS 12 to MIS 6). – Boreas, 44 (1): 103–126.
Scheidt, S., Hambach, U. & Rolf, C. (2015): A consistent magnetic polarity stratigraphy of late Neogene to Quaternary fluvial sediments from the Heidelberg Basin (Germany): a new time frame for the Plio–Pleistocene palaeoclimatic evolution of the Rhine Basin. – Global Planet. Change, 127: 103–116.
Shackleton, N.J., Berger, A. & Peltier, W.R. (1990): An alternative astronomical calibration of the lower Pleistocene timescale based on ODP Site 677. – Trans. Roy. Soc. Edinb., Earth Environm. Sci., 81: 251–261.
Sirocko, F., Dietrich, S., Veres, D., Grootes, P.M., Schaber-Mohr, K., Seelos, K., Nadeau, M.-J., Kromer, B., Rothacker, L., Röhner, M., Krbetschek, M., Appleby, P., Hambach, U., Rolf, C., Sudo, M. & Grim, S. (2013): Multi-proxy dating of Holocene maar lakes and Pleistocene dry maar sediments in the Eifel, Germany. – Quatern. Sci. Rev., 62: 56–76.
Stephan, H.-J. (2002): Forschungsbohrung Oldenswort (OLW). – Landesamt für Natur und Umwelt, Abteilung Geologie/Boden [unpubl.].
Stephan, H.-J. (2014): Climato-stratigraphic subdivision of the Pleistocene in Schleswig-Holstein, Germany and adjoining areas. – Eiszeitalter u. Gegenwart, 63 (1): 3–18.
Stephan, H.-J. & Menke, B. (1993): Das Pleistozän in Schleswig-Holstein. – Geolog. Landesamt Schleswig Holstein, 3: 19–62.

Stephan, H.-J., Urban, B., Lüttig, G., Menke, B. & Sierralta, M. (2011): Palynologische, petrographische und geochronologische Untersuchungen an Ablagerungen der Leck-Warmzeit (spätes Mittelpleistozän) und begleitender Sedimente. – Geol. Jb., A 160: 80 p.

Streif, H. (2004): Sedimentary record of Pleistocene and Holocene marine inundations along the North Sea coast of Lower Saxony, Germany. – Quatern. Int., 112 (1): 3–28.

Suc, J.-P., Bertini, A., Leroy, S.A.G. & Suballyova, D. (1997): Towards the lowering of the Pliocene-Pleistocene boundary to the Gauss-Matuyama reversal. – Quatern. Int., 40: 37–42.

Thornton, S.F. & McManus, J. (1994): Application of organic carbon and nitrogen stable isotope and C/N ratios as source indicators of organic matter provenance in estuarine systems: evidence from the Tay Estuary. – Estuar. Coast. Shelf Sci., 38: 219–233.

Turner, C. (1998): Volcanic maars, long Quaternary sequence and the work of the INQUA subcommission on European Quaternary stratigraphy. – Quatern. Int., 47: 41–49.

Urban, B. (1978a): Vegetationsgeschichtliche Untersuchungen zur Gliederung des Altquartärs der Niederrheinischen Bucht. – Ph.D. thesis, Geolog. Inst. Univ. Köln: 165 p.

Urban, B. (1978b): The interglacial of Frechen I/Rheinland – a section of the Tiglian A-type. – Geol. Mijnbouw, 57 (3): 401–406.

Urban, B. (1983): Biostratigraphic correlation of the Kärlich Interglacial, Northwestern Germany. – Boreas, 12 (2): 83–90.

Urban, B. (1995): Younger Middle Pleistocene interglacials (Holsteinian, Reinsdorf, Schöningen) in the Schöningen open cast lignite mine (Eastern Lower Saxony/Germany). – Meded. Rijks Geolog. Dienst, 52: 175–186.

Urban, B. (1997): Grundzüge der eiszeitlichen Klima- und Vegetationsgeschichte in Mitteleuropa. – In: Wagner, G.A. & Beinhauer, K.W. (ed.): *Homo heidelbergensis* von Mauer – Das Auftreten des Menschen in Mitteleuropa: 241–265, Heidelberg (Universitätsverl. C. Winter).

Urban, B. (2002): Manual for analysis of soil and related materials. – In: Kunst, S., Kruse, T. & Burmester, A. (ed.): Sustainable water and soil management: 321–370, Berlin (Springer).

Urban, B. (2007): Quartäre Vegetations- und Klimaentwicklung im Tagebau Schöningen. – In: Thieme, H. (ed.): Die Schöninger Speere: Mensch und Jagd vor 400.000 Jahren: 66–75, Stuttgart (Theiss).

Urban, B., Thieme, H. & Elsner, H. (1988): Biostratigraphie, quartärgeologische und urgeschichtliche Befunde aus dem Tagebau "Schöningen", Ldkr. Helmstedt. – Z. Dt. Geol. Ges., 139: 123–154.

Urban, B., Sierralta, M. & Frechen, M. (2011): New evidence for vegetation development and timing of Upper Middle Pleistocene interglacials in Northern Germany and tentative correlations. – Quatern. Int., 241: 125–142.

Van der Plicht, J., Van Geel, B., Bohncke, S.J.P., Bos, J.A.A., Blaauw, M., Speranza, A.O.M., Muscheler, R. & Björck, S. (2004): The Preboreal climate reversal and a subsequent solar-forced climate shift. – J. Quatern. Sci., 19 (3): 263–269.

VDLUFA (1991): Methodenbuch; Band 1: Die Untersuchung der Böden: 1570 p., Darmstadt (VDLUFA-Verl.).

Von Hacht, U. (1987): Fossilien von Sylt, II: 325 p., Hamburg (Von Hacht).

Wiethold, J. (1998): Studien zur jüngeren postglazialen Vegetations- und Siedlungsgeschichte im östlichen Schleswig-Holstein. – Ph.D. thesis, Univ. Kiel : 365 p.

Winn, K., Glos, R., Averdieck, F.-R. & Erlenkeuser, H. (2000): On the age of the marine Eem in northwestern Germany. – Geologos, 5: 41–56.

Wintle, A.G. (2008): Luminescence dating: where it has been and where it is going. – Boreas, 37: 471–482.

Zagwijn, W.H. (1960): Aspects of the Pliocene and Early Pleistocene vegetation in the Netherlands. – Meded. Geol. Sticht., C-III (5): 1–78.

Zagwijn, W.H. (1963): Pollen-analytic investigations in the Tiglian of the Netherlands. – Meded. Geol. Sticht., 16: 49–71.

Zagwijn, W.H. (1973): Pollen-analytic studies of Holsteinian and Saalian beds in the Northern Netherlands. – Meded. Rijks Geol. Dienst, 24: 139–156.

Zagwijn, W.H. (1974): Vegetation, climate and radiocarbon datings in the Late Pleistocene of The Netherlands. Part II: Middle Weichselian. – Meded. Rijks Geol. Dienst, 25: 101–110.

Zagwijn, W.H. (1992): The beginning of the Ice Age in Europe and its major subdivision. – Quatern. Sci. Rev., 11: 583–591.

Zagwijn, W.H. (1994): Reconstruction of climate change during the Holocene in western and central Europe based on pollen records of indicator species. – Veget. Hist. Archaeobot., 3: 65–88.

Zagwijn, W.H. (1996): An analysis of Eemian climate in Western and Central Europe. – Quatern. Sci. Rev., 15: 451–469.

Zagwijn, W.H. & De Jong, J. (1984): Die Interglaziale von Bavel und Leerdam und ihre stratigraphische Stellung im niederländischen Früh-Pleistozän. – Meded. Rijks Geolog. Dienst, 37: 155–169.

Zagwijn, W.H., Van Montfrans, H.M. & Zandstra, J.G. (1971): Subdivision of the "Cromerian" in the Netherlands: pollen-analysis, palaeomagnetism and sedimentary petrology. – Geol. Mijnbow, 50: 41–58.

Zhang, J., Tsukamoto, S., Grube, A. & Frechen, M. (2014): OSL and ^{14}C chronologies of a Holocene sedimentary record (Garding-2 core) from the German North Sea coast. – Boreas, 43 (4): 856–868.

Zijderveld, J.D.A. (1967): A. C. demagnetization of rocks: analysis of results. – In: Collinson, D.W., Creer, K.M. & Runcorn, S.K. (ed.): Methods in palaeomagnetism: 254–286, Amsterdam (Elsevier).

http://www.worldatlas.com/webimage/countrys/eu.htm (accessed 1 March 2013).

https://maps.google.de (accessed 7 December 2012).

Manuscript received: 08.12.2016
Accepted for publication: 02.02.2017

Paper II

Palaeoenvironmental investigations of the Holocene sedimentary record of the Garding-2 research drill core, northwestern Germany

Reprinted from: Maria Sekar Proborukmi, Brigitte Urban (2017). Palaeoenvironmental investigations of the Holocene sedimentary record of the Garding-2 research drill core, northwestern Germany. Zeitschrift der Deutschen Gesellschaft für Geowissenschaften (German Journal of Geology) 168 (1), 39–51. DOI: 10.1127/zdgg/2017/0098.

Z. Dt. Ges. Geowiss. (German J. Geol.), **168 (1)**, p. 39–51, 3 figs., 1 table
Published online January 2017 **Article**

Palaeoenvironmental investigations of the Holocene sedimentary record of the Garding-2 research drill core, northwestern Germany

Maria Sekar Proborukmi & Brigitte Urban*

Proborukmi, M.S. & Urban, B. (2017): Palaeoenvironmental investigations of the Holocene sedimentary record of the Garding-2 research drill core, northwestern Germany. – Z. Dt. Ges. Geowiss., 168: 39–51, Stuttgart.

Abstract: A 20 m section of calcareous, fine- to coarse-grained Holocene sediments forming the upper part of the Garding-2 core, taken near Garding on the Eiderstedt Peninsula in Northwest Germany, has been analysed for pollen and for its sedimentological and geochemical characteristics to reconstruct the Holocene environmental history of this coastal area.

The studied sediment sequence was deposited above an unconformity at 20 m depth formed by major erosion due to the rapid sea-level rise in the Early Holocene. A thin layer of marine sediments at the base, possibly correlating to the late Atlantic, is unconformably overlain by marine-tidal flat deposits up to 11.00 m depth. The Subboreal age of these deposits is evidenced by the first occurrence of *Fagus* at 15.97 m, which is OSL-dated, at 16.22 m, to about 3130 ± 260 BP (Zhang et al. 2014) and *Carpinus* at 15.03 m. The *Ulmus* decline, a palynological characteristic marking the Atlantic to Subboreal transition in northwestern Europe, is not revealed in the pollen sequence. *Ulmus* shows low values throughout the entire pollen diagram. It is therefore assumed that late Atlantic transitional sediments were eroded in Garding-2.

Sandy sediments between about 11.00 m and the top of the sequence are palynologically characterised by increased representation of local salt marsh, dune and tidal flat vegetation, indicated by the abundance of Poaceae, Cerealia-type pollen, probably derived mainly from wild grasses, and increased percentages of Ericaceae, Cyperaceae and Chenopodiaceae. These upper deposits are AMS ^{14}C-dated to 2790 ± 20 BP (at 11.41 m) and 1820 ± 50 BP (at 2.70 m; Zhang et al. 2014) suggesting an early Subatlantic age. Due to regional features and peculiarities of the coastal environment, significant anthropogenic impact on landscape as well as the expansion of *Fagus* and *Carpinus*, characteristic for the Subboreal to Subatlantic transition at about 2700 BP in Northern Germany, are not clearly reflected in the pollen diagram.

Keywords: Holocene, palynology, sedimentology, coastal environments, Eiderstedt Peninsula, Northwest Germany

1. Introduction

Coastal areas play an important role in palaeoenvironmental studies as they offer insights into the dynamic interaction between land and sea that causes significant changes and effects on coastal geology, geomorphology, vegetation and human settlement. Several studies have been carried out on the development of the coastal North Sea area during the Holocene (Overbeck 1934, Wiermann 1962, Menke 1968, 1969, 1986, Behre et al. 1979, Falk 2001, Behre 2003, 2005, 2007a, 2007b, Streif 2004, Vink et al. 2007, Bungenstock & Weerts 2010, Zhang et al. 2014). In the coastal area of the northern North Sea, periods of regression and transgression due to climatic changes as well as tectonic activities and glacio- or hydro-isostatic movements (Falk 2001, Kiden et al. 2002, Vink et al. 2007 and references therein) largely control these changes. During the Last Glacial Maximum, sea level in the German North Sea area was about 100 m (Jelgersma 1961, Wieland 1990, Behre 1991) or 130 m (Streif 2004, Behre 2005) below its present-day level. The transgression of the North Sea that started at around 18 000 BP led to multiple phases of sea-level rise and inundation (Jelgersma 1979, Cameron et al. 1993, Streif 2004) and was interrupted by some stagnant and regression phases (Menke 1968, Behre 1991, Streif 2004) related to variations in the rate of sea-level rise and sediment supply (Streif 2004). Behre (2007a) established a new sea-level curve for the southern North Sea, which indicates the same sea-level movements as proposed by Streif (2004) but in more detail, incorporating a large number of radiometric dates. However, this general curve should be used cautiously for comparison with individual records along the coastal area of the North Sea, as there are significant local variations in the degree of sediment compaction, tides, hydrological setting and palaeogeography (Vink et al. 2007, Bungenstock & Weerts 2010).

*Address of the authors: Institute of Ecology, Subject Area Landscape Change, Leuphana University of Lüneburg, Scharnhorststraße 1, C.13, 21335 Lüneburg, Germany / Maria.S.Proborukmi@stud.leuphana.de; b.urban@leuphana.de.

www.schweizerbart.de
DOI: 10.1127/zdgg/2017/0098
1860-1804/0098 $ 6.30

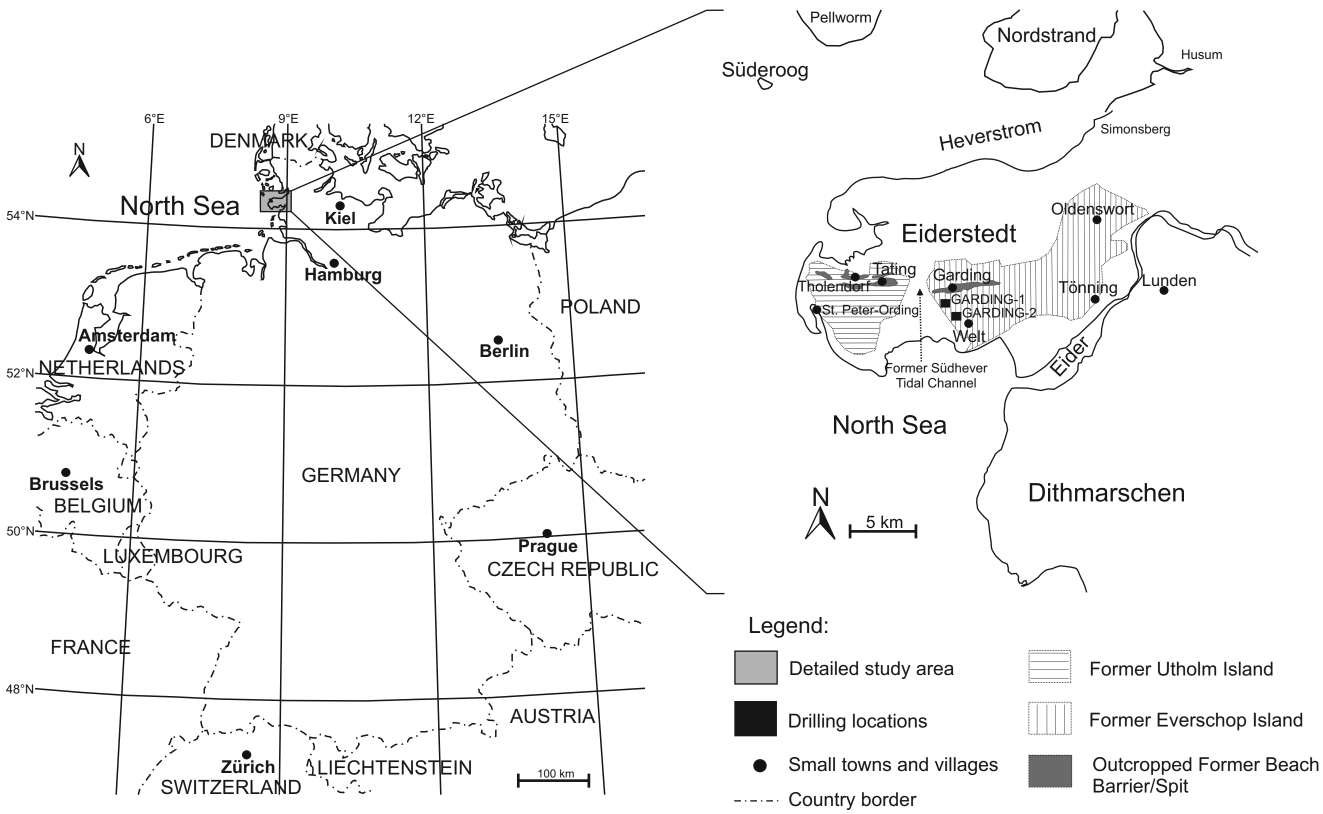

Fig. 1: Location of the Garding-1 and Garding-2 drill cores on the Eiderstedt Peninsula, Schleswig-Holstein (modified from http://www.worldatlas.com/webimage/countrys/eu.htm and https://maps.google.de).

However, the number of available palaeoecological data sets with which to construct a solid biostratigraphical framework of the regional Holocene coastal and Pleistocene climatic development of western Schleswig-Holstein is limited. To redress this deficiency, studies of the Neogene–Quaternary development of the Eiderstedt Peninsula (Fig. 1) have been carried out within a joint research-drilling project of Leibniz Institute of Applied Geophysics (LIAG – Hannover), State Agency for Agriculture, Environment and Rural Areas (LLUR – Flintbek) Leuphana University of Lüneburg and Johannes Gutenberg University Mainz since 2011 (Proborukmi et al. 2017, this volume).

One recent important outcome of this project is the establishment of the chronological framework and depositional history of the 16,000 years sedimentary record of the Garding-2 core (Zhang et al. 2014) using OSL and AMS ^{14}C dating. Following this paper, the Eiderstedt Peninsula was dominated by an estuarine system between 16,000 BP and about 13,000 BP. A prominent depositional hiatus occurred between about 13,000 BP and 8300 BP, most likely caused by the transgressing sea. Holocene sediments have been deposited at Garding since around 8300 BP, still under rising sea level, until about 3000 BP (Zhang et al. 2014). During this period, offshore sediments accumulated at the site. Between 3000 BP and 2000 BP, the sea level stabilised and tidal flat deposits accumulated at a very high rate. Between 2000 BP and about 1500 BP, a sandy beach layer formed and terrestrial clastic material was deposited after this period. Construction of local dikes, which probably started around the 11th century AD, affected this sea regression (Behre et al. 1979, Kühn & Panten 1989, Zhang et al. 2014). Related to this comprehensive chronological framework, our investigations focused on the reconstruction of the local and regional palaeoenvironment from palynological, lithological and geochemical characterisation of the Holocene sediments. The pollen data, in comparison with other well-dated Holocene pollen sequences from Schleswig-Holstein (Wiermann 1962, Menke 1968, 1969, 1986, Wiethold 1998, Barber et al. 2004, Nelle & Dörfler 2008), provide further time control to the established chronology and depositional history of the Garding-2 sequence of Zhang et al. (2014).

The regional and local coastal development highlights that sea level rose during the rapid transgression phase at about 7500–7000 BC (Behre & Menke 1969). The shallow water table in the coastal area caused formation of mires and an associated peat layer, which can be found in certain places along the North Sea, known as the “basis” peat (Behre 2003, 2007a). This layer becomes thinner towards the hinterland, and has been dated to 7500–7000 BC in the southern Dogger Bank (Behre & Menke 1969) and to about 7000 BC in Lower Saxony (Streif 2004). The “basis” peat layer with maximal thickness of 80–100 cm was also found in an early Holocene sequence in the western part of the Eiderstedt Peninsula (Falk 2001), but it is missing in the Garding-2 sequence.

At about 5000 BC (Behre et al. 1979), the Eider River flowed in southern Eiderstedt towards the Wadden Sea and a barrier system started to form in Eiderstedt and the Dithmarschen area in Schleswig-Holstein (Fig. 1) (Falk 2001). In the western part of Eiderstedt, E–W and NW–SE trending barrier systems formed, composed of eroded material from the former islands of the present Süderoog and Heverstrom areas, while parts of the Tholendorf, Garding and St. Peter barrier systems were covered by dunes (Meier 2004). The long Garding barrier system has protected hinterland areas from sea intrusion since about 2500 BP (Meier 2004) and these barrier systems formation processes have contributed substantially to the changes in coastal morphology within the study area. According to Falk (2001), sediment sources of Eiderstedt derive from reworked Pleistocene deposits of the upland areas in the north (“Geestkerne”) and from the bulldozing effect of the sea transporting sands from the north and northwest. Presently, the current runs parallel to the coast from north to south and deposits sandy material from the islands of Sylt through Amrun to Eiderstedt.

The oldest settlements in the German North Sea marshes are no older than Bronze Age, about 1000 BC (Behre 1991). This area was subsequently abandoned between 300 BC and 100 BC, most probably related to the Dunkirk Ib transgression at about 400 BC–150 BC (Behre 2003, 2007a). This marine transgression had influenced the mainland of Eiderstedt and the Eider River. At the time of Christ’s birth, sea level retreated (Falk 2001). Colonisation in the area of Dithmarschen and along the Eider River started about 100 AD, and about 200 AD on the west Eiderstedt beach barriers near Tating. These settlers created and lived on dwelling mounds (“Wurten”/“Terpen”), while others inhabited dunes on the Eiderstedt Peninsula to survive the occasional storm floods and the rising sea level (Menke 1969). Since approximately 1100 AD, the inhabitants around the study area started to build dikes to protect their settlement areas from storm floods and seawater intrusions during high tides causing changes in sedimentation processes, patterns and local morphological features (Behre et al. 1979, Behre 1991, Hoselmann & Streif 2004, Ahrend 2006). The Eiderstedt Peninsula area was originally composed of two main islands, Everschop (Harden Everschop) and Utholm, separated by the Südhever tidal channel (Panten et al. 2013; Fig. 1). However, dike building on the Südhever tidal channel area caused a merging of both islands in 1213 and development of the present-day peninsula (Ehlers 1988).

2. Site characteristics and geological setting of Garding-1 and Garding-2 drill cores

Garding-1 and Garding-2 drillings are geologically located in the Garding Trough, developed on the western flank of the Oldenswort North salt dome (Proborukmi et al. 2017, this volume). An extensional stress regime of the Cimmerian Orogeny, during late Triassic, caused a rifting of the North Sea and Ems area, which led to a diapirism of the Keuper evaporite (Frisch & Kockel 1999, Baldschuhn et al. 2001) and formation of the trough. This process was reactivated by the Subhercynian tectonic inversion during the Late Cretaceous and Early Cenozoic (Baldschuhn et al. 1991, 2001), which deepened the trough and trapped sediments since the Tertiary (Mohr et al. 2005). During the Quaternary, the western part of Schleswig-Holstein has been glaciated at least twice, during the Elsterian and the Saalian, but the Weichselian glaciers did not reach the study area (Gibbard 2007, Stephan 2014). The present-day landscape of the Eiderstedt Peninsula is dominated by mudflats, marshlands or sand dunes and dikes in the coastal area, with some barrier islands along the northwestern coast and in the vicinity of the Eider Estuary. At Garding and Tating, the landmass is characterised mainly by raised bogs and former beach ridges (“Strandwälle”; Panten et al. 2013; Fig. 1). Marshes, river estuaries and floodplains are covered by fluvisols (Nelle & Dörfler 2008), which are used as pasture or for arable agriculture. The natural vegetation of the marshes and floodplains of the Eiderstedt Peninsula is characterised by the northwest European salt marsh vegetation such as *Puccinellia maritima*, *Juncus gerardii*, *Salicornia* spp., *Suaeda maritima* and *Elytrigia atherica* (Esselink et al. 2009), whereas the inland vegetation is characterised by oak-ash forests (*Quercus robur*, *Fraxinus excelsior*) or ash-elm forests (*Fraxinus excelsior*, *Ulmus minor*), partly accompanied by *Alnus glutinosa* and additional elements of the natural vegetation of the diked and non-saline marshland (Bohn et al. 2000, Nelle & Dörfler 2008). The annual mean temperature is between 8 and 8.5 °C with annual precipitation between 900 and 1000 mm in the central part and between 600 and 700 mm in the eastern part of Schleswig-Holstein (Nelle & Dörfler 2008).

The Garding-2 drill core is situated at 08°46’35.22” E and 54°18’13.74” N, about 700 m to the south of the exploration drilling Garding-1. It is named after the village of Garding, which is located approximately 3 km north of the drilling points, near the village of Welt on the Eiderstedt Peninsula (Fig. 1). A 40 m sequence of alternating sand and clayey layers was obtained from the first exploration drill core Garding-1. Numerical dating results of the Garding-1 core suggest a Holocene age for the entire sequence (Kunz et al. 2009, 2010). The OSL dating indicates an age of ~10 ka at 35 m and of ~4 ka at 15 m below the surface, while AMS ^{14}C dating of *Cardiidae* specimen shells shows an age of 7590±40 BP at 27 m below the surface (Kunz et al. 2009, 2010). The pollen spectra between 16 and 17 m depth include *Fagus* and *Carpinus*, pointing to a Subboreal age.

3. Material and methods

The entire Garding-2 core consists of a 240 m thick sediment sequence (Proborukmi et al. 2017, this volume). The top 20 m sediments are composed of alternating layers of calcareous fine-grained sand, silt and clay, with some intercalated

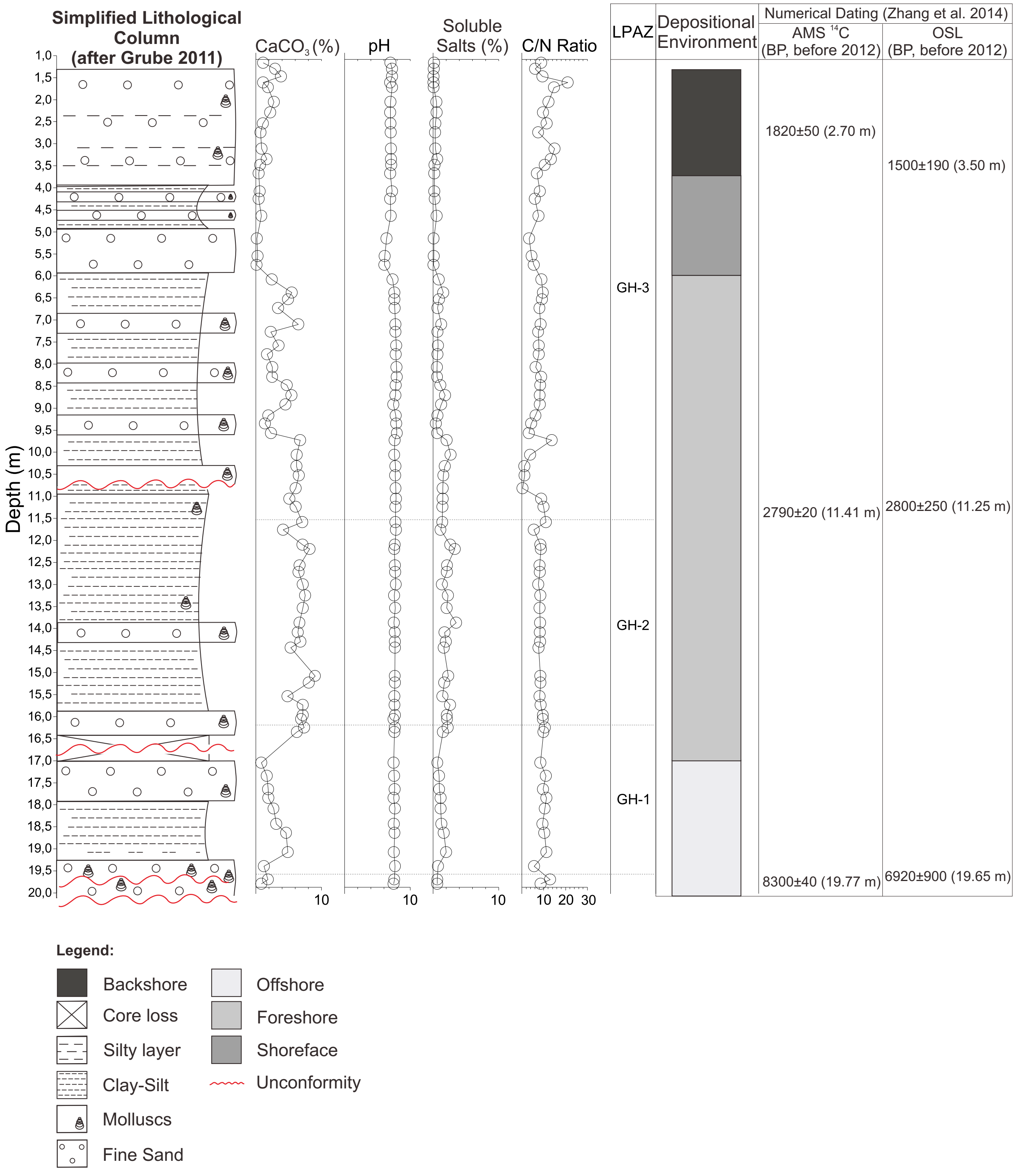

Fig. 2: Summary of lithological and geochemical analyses, including carbonate content, pH, C/N ratio and soluble salt content, and interpretation of the depositional environments of the top 20 m Holocene section of the Garding-2 core. Important dating results of Zhang et al. (2014) are included.

organic-rich and mollusc-rich layers (Fig. 2). Lithological descriptions of the top 20 m of the Garding-2 core have been taken from Grube (2011). The sediment colour was determined by means of the Munsell Color Chart 2009 (Munsell Color 2009). The chronological age model based on OSL and Accelerator Mass Spectrometry (AMS) ^{14}C dating, established by Zhang et al. (2014), was adopted as the geochronological frame for this study. The results of OSL and AMS ^{14}C dating are reported in the format of years before 2012 (Zhang et al. 2014). BC ages based on ^{14}C dating taken from other references were therefore also converted to BP with 2012 as the reference year, to be comparable.

Within the Holocene interval, between 1 m and 20 m depth, 53 samples were taken for palynological analysis every 30–40 cm, with up to 1.18 m sample spacing in unsuitable sandy sediments (at about 6.00–5.00 m) and even very narrow spacing, of about 10 cm, between approximately 10.00 and 9.50 m, where the transition from finer to coarser sediments is observed. In addition, 74 samples were taken for carbonate content, pH, soluble salt content and C/N ratio measurements every 10–70 cm.

Approximately 7 g of each sample were treated by standard palynological methods (Faegri & Iversen 1989, Moore et al. 1991) in the Laboratory of Palynology of the Institute of Ecology of Leuphana University of Lüneburg. Carbonate content was determined by treatment with 10 % HCl and dispersion undertaken with 10 % KOH. Organic matter was separated from the inorganic matrix by the heavy liquid sodium polytungstate ($3Na_2WO_4.9WO_3.H_2O$). Acetolysis was conducted to dissolve cellulose and darken the palynomorphs to improve taxon determination (Faegri & Iversen 1989, Moore et al. 1991). The prepared residues were embedded in glycerine on up to three 24 x 32 mm slides per sample and analysed for pollen and non-pollen palynomorphs. Pollen and spores were identified using the atlases of Faegri & Iversen (1989, 1993), Moore et al. (1991), Beug (2004) and the reference collection of the Laboratory of Palynology of the Institute of Ecology of Leuphana University of Lüneburg. Between 350 and 375 pollen grains per sample of arboreal pollen (AP) taxa, excluding *Corylus*, were counted in order to form a statistically solid basis for total pollen calculation. The pollen sum (100 %) was based on these AP taxa. Pollen calculations and diagram construction were performed using the software packages Tilia, Tilia Graph and Tilia View (Grimm 1990). A combination of conventional observation of major changes within the pollen diagram and the stratigraphically constrained cluster analysis, CONISS, provided by Tilia were conducted to determine the local pollen assemblage zones (LPAZ) of the 20 m sediment sequence (Grimm 1987). Square root transformation (implicit dissimilarity coefficient of Edwards and Cavalli-Sforza's chord distance) was chosen to process the pollen data, which were based on the sum of AP taxa excluding *Corylus* and pollen of non-arboreal dry land taxa (NAP).

Palynological analysis, especially of pollen spectra of transitional marine sediments, is strongly influenced by fluvial and marine pollen dispersal as well as transportation and sedimentation processes (Heusser 1988). Therefore, pollen records from these areas show the principal characteristics of the continental (inland) sources (Robertsson 1982 and references therein), which relate to the permanent drainage area (Heusser 1998), mixed with coastal vegetation of the region (Heusser 1998). Consequently, according to Robertsson (1982) there are limitations to palynological interpretation of the marine minerogenic sediments, including low frequency of pollen grains, erosion, redeposition and irregular pollen transport mechanisms. However, the author suggested that the reworked palynomorphs of the sediments from older ages are valuable for identifying erosion and sediment source. Secondary sedimentation processes such as oxidation, bioturbation and diagenesis should also be considered in the interpretation (Heusser 1998).

The inner test linings of foraminifera and dinoflagellate cysts were obtained together with extracted pollen and spores by standard palynological treatments and they were used to further characterise marine influence and near shore environments during the time of sediment deposition (Müller 1959, Mathison & Chmura 1995, De Vernal 2009). Foraminifera test lining is an organic component between the cytoplasm and the internal surface of the foraminifera test, which is made of chitin derivatives, protein, polysaccharides and even lignin. Although most parts of the foraminifera tests, which are composed by calcium carbonate, are dissolved in the preparation process, the inner linings are resistant to acid and therefore can still be found after standard palynological treatment (Concheyro et al. 2014). On the other hand, dinoflagellate cysts are mainly composed of very resistant organic matter, similar to the sporopollenin of palynomorphs (De Vernal 2009) and therefore their presence is more likely. The summary percentages of the foraminifera test linings are presented together with percentages of dinoflagellate cysts in the pollen diagram (Fig. 3).

Carbonate content was measured by gasometrical calculation using a Scheibler apparatus (Urban 2002). The soluble salt content (electric conductivity) was determined by an EC meter according to the standard of VDLUFA (1991). The pH value was measured in a 1:2.5 0.01 mol/l $CaCl_2$ suspension and C, H and N values were determined by a CHNS/O 2400 Series II Analyser (Perkin Elmer) using the standard procedure of the laboratory of the Institute of Ecology at Leuphana University of Lüneburg. For classification of the geochemical properties such as pH, carbonate contents and soluble salts, Ad-Hoc-Arbeitsgruppe-Boden (2005) and Urban (2002) were followed, while the classification of sources of organic matter expressed by the C/N ratio was derived from Meyers (1994) and Thornton & McManus (1994).

4. Results

4.1 Lithology and geochemistry

The top 20 m section of the Garding-2 core is composed mainly of fine sand with alternating layers of calcareous clay and silt and some organic-rich and mollusc-rich layers (Fig. 2). Marine sediments contain little to moderate carbonate,

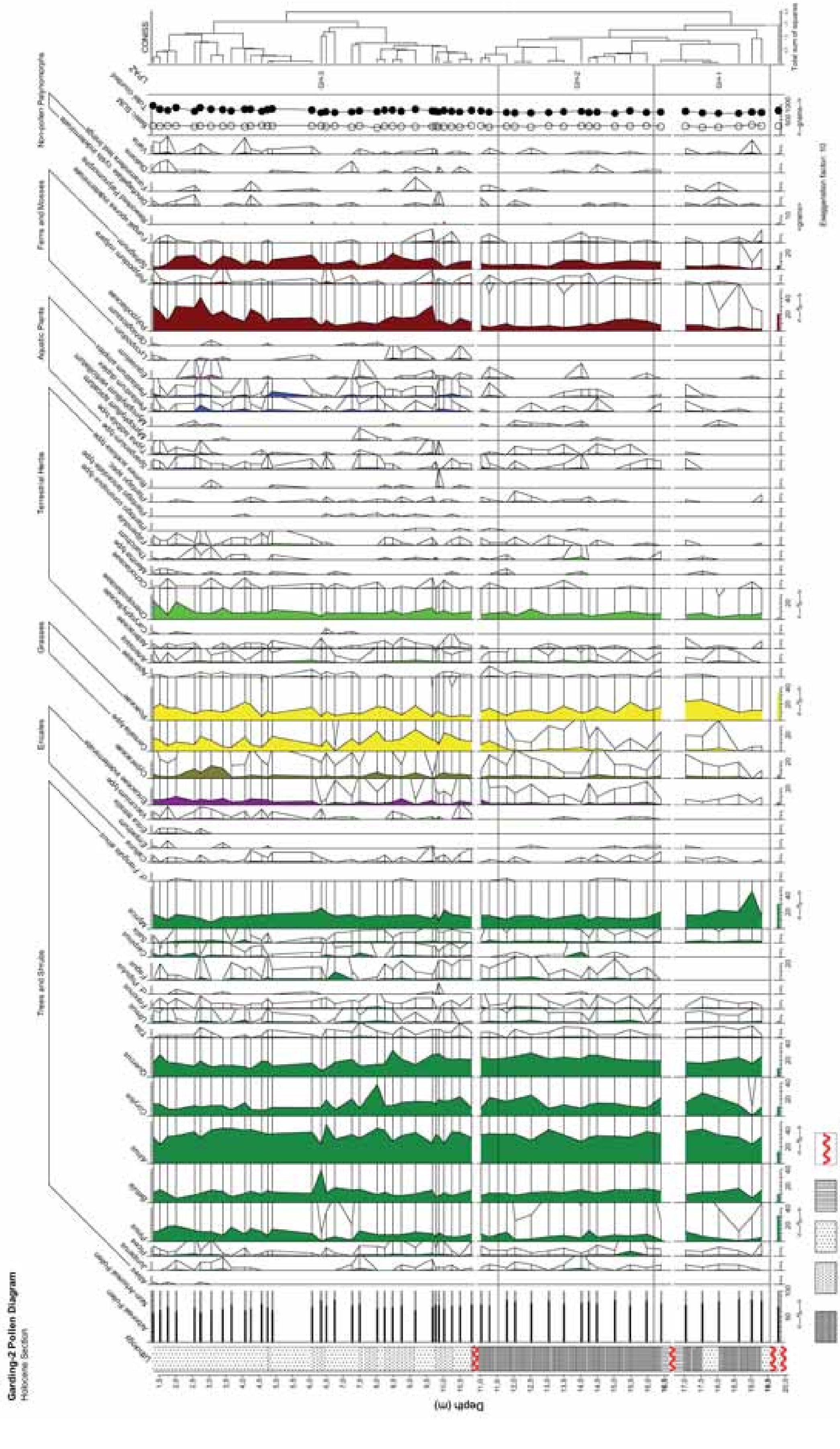

Fig. 3: Pollen diagram of the top 20 m Holocene section of the Garding-2 core, showing vegetation development and division of local pollen assemblage zones (LPAZ) based on the combinations of cluster analyses and conventional interpretation.

low to high salinity with slightly alkaline pH and narrow C/N ratios are found at about 19.80–17.00 m depth. These sediments are characterised by very dark to dark greenish-grey (N 3/0 to 10GY 4/1) calcareous fine sand, which contains abundant mollusc shells between 19.80 and 19.30 m. At 19.30–18.00 m, very dark greenish-grey (10Y 3/1) calcareous fine sand layers intercalated into calcareous grey clayey silt are found and overlain by a layer of very dark greenish-grey (10Y 3/1) calcareous fine sand at 18.00–17.00 m (Fig. 2).

Transitional to marine fine-grained sediments dominate the core between 17.00 and 6.00 m, which is characterised by intercalation of very dark to greenish-grey (N 3/0 to 10Y 3/1) calcareous clay and grey (N 5/0) calcareous fine sand layers with mica mixtures. This sequence displays fine stratification of sandy and clayey sediments that is typical for tidal flat deposits (Zhang et al. 2014). A section of core was lost between 17.00 and 16.45 m. Moderate to substantial carbonate contents, slightly alkaline pH, high to very high salinity and very narrow C/N ratios characterise the samples between the top of the core loss, at 16.45 m, and 11.00 m. The sediments at 11.00–6.00 m show more frequent sandy layers, little to moderate carbonate content, very slightly to slightly alkaline pH, very low to very high salinity and very narrow C/N ratios (Fig. 2).

Sand-dominated marine to transitional deposits are found between 6.00 and 3.72 m. Massive dark to dark bluish-grey (5Y 4/1 to 5PB 4/1) calcareous fine sand occurs between 6.00 and 5.00 m, which is overlain by a sequence of interbedded very dark to dark greenish-grey (10Y 3/1 to 10Y 4/1) calcareous fine sand and silt between 5.00 and 3.72 m. The samples between 6.00 and 3.72 m show relatively similar values for each geochemical property compared to sediments at 11.00–6.00 m (Fig. 2).

A layer of dark greenish- to dark grey (10Y 4/1 to N 4/0) backshore calcareous silty fine sand was observed between 3.72 and 1.30 m. Variations of carbonate content and C/N ratio can be observed in this sequence, with more distinct changes from 2.60 m upwards. The samples within this depth interval show 0.44–3.83 % carbonate content, slightly to very slightly alkaline pH, very low to low salinity and the highest C/N ratios in the core (Fig. 2).

4.2 Palynology

Palynological results are presented in a pollen diagram (Fig. 3), which is subdivided into three LPAZs. The sample at 19.80 m could not be grouped with the closest LPAZ above and is presented as a single sample.

4.2.1 Single sample at 19.80 m

This sample is dominated by *Pinus*, Poaceae and *Myrica*, with the first two taxa achieving highest percentages of the diagram. By contrast, values of *Alnus* and *Quercus* are notably low, while Chenopodiaceae values are the lowest recorded (Fig. 3). There are a few *Pediastrum duplex*, *Pediastrum simplex*, dinoflagellate cysts indeterminate and foraminifera test linings recorded. Percentages of Polypodiaceae are relatively high, while those of *Sphagnum* are low. Redeposited pollen of *Tsuga diversifolia* is present.

4.2.2 LPAZ GH-1 (19.56 m–16.19 m)

This zone is characterised by higher values of *Alnus*, *Corylus* and *Quercus*, while *Myrica* declines after an early peak and percentages of *Pinus* are lower compared to the sample below. *Picea* is recorded from this zone onwards, reaching values up to 1.6 % in LPAZ GH-1 (Fig. 3). Percentages of NAP are significantly lower than in the basal sample but are also mainly composed of Poaceae with single occurrences of *Mentha*-type, *Thalictrum*, *Filipendula*, *Plantago* spec. and *Rumex acetosa*-type, as well as low amounts of Ericaceae, Cerealia-type and Cyperaceae. Polypodiaceae percentages are much reduced, while *Sphagnum* values are marginally lower. Percentages of aquatic taxa are low but increase slightly towards the top of the zone, while dinoflagellate cysts indeterminate and foraminifera test linings occur throughout the zone.

4.2.3 LPAZ GH-2 (16.19 m–11.53 m)

The base of this zone is defined on the first occurrence of *Fagus* that then has consistently low values through the zone. The only other significant AP feature is the first appearance of *Carpinus* at 15.03 m and its subsequent occasional representation through the zone (Fig. 3). Terrestrial herbs and aquatic taxa have increased in diversity and abundance, with the most notable increases in *Filipendula* and *Plantago* spec. within the herbs and *Sparganium*-type, *Typha latifolia*-type, *Myriophyllum verticillatum*, *Pediastrum duplex* and *Pediastrum simplex* within the aquatic taxa. There are also increased values of Polypodiaceae and *Sphagnum* in this zone. Reworked pollen of *Tsuga diversifolia* is found at 13.05 m.

4.2.4 LPAZ GH-3 (11.53 m–1.33 m)

The base of this zone is defined on a major sustained increase in Cerealia-type pollen at 11.53 m depth below an unconformity of unknown age. This increase plus the first occurrences of *Plantago lanceolata*-type and *Rumex acetosa*-type pollen are the most characteristic NAP changes of this zone, though Cyperaceae and Chenopodicaeae achieve highest values for the core near and at the top of the diagram, respectively. There are also higher values for Ericaceae taxa, especially *Calluna*, continued increases in aquatic pollen as well as Polypodiaceae and *Sphagnum*, while *Lycopodium* and *Ophioglossum* are restricted to the zone. There are few notable features in the AP, but *Pinus* is observed to increase towards the top of the core (Fig. 3). There are single occurrences of *Abies* pollen at the top of the zone, from 2.74 m onwards. Reworked pollen are notable with *Carya* (at 8.25 m), *Pterocarya* (at 4.08 m, 6.08 m, 6.76 m), *Symplocos* (at 7.27 m, 9.77 m, 10.03 m), *Taxodium* (at 3.41 m) and

Tsuga diversifolia (at 10.03 m) recorded within the zone. Scattered dinoflagellate cysts indeterminate and foraminifera test linings persist throughout this zone.

5. Discussion

Interpretation of the pollen spectra has to take into account that all samples are from marine and brackish deposits. These sediments are mixed compared to modern tidal flats and are partly eroded and redeposited. According to characteristic features that can be observed in other Holocene pollen diagrams of western Schleswig-Holstein, it is obvious that, in particular, the arboreal pollen curves are smoothed in the Garding pollen record. Consequently, the zonation of the pollen diagram and its interpretation are based largely on those regional changes, which are most significant in the Holocene vegetation history of Northern Germany, particularly of western Schleswig-Holstein.

At the base of the Garding-2 Holocene section, at around 20 m depth, a hiatus dated to approximately 13,000 to 8300 BP occurs. Above this hiatus, a shell-rich layer between 19.85 and 19.30 m was deposited. This layer marks the onset of marine sedimentation at the site around 8300 BP (Zhang et al. 2014), which is likely related to the major transgression of the early Holocene. Therefore, the hiatus at the bottom of the section corresponds strongly to erosion caused by the early Holocene transgression.

The single sample at 19.80 m shows pollen of *Tsuga diversifolia*, derived from Early Pleistocene deposits, which indicates sediment reworking. These deposits are most likely eroded by sea intrusion and transported from the north and northwest hinterland (Falk 2001). This transgression was characterised by high-velocity currents followed by relative lower energy inflow indicating open marine environments in the study area. This interpretation of a marine depositional environment at 19.80 m is supported by the occurrence of dinoflagellate cysts indeterminate and foraminifera test linings as well as a narrow C/N ratio.

The tree pollen spectrum at 19.80 m reveals a mixed pollen assemblage, which is characterised by high amounts of *Pinus* and moderate values of *Betula*. Beside those taxa, the AP are mainly composed of *Corylus, Alnus, Quercus*, *Ulmus* and *Tilia,* which are all present with moderate amounts (Fig. 3, Table 1). This assemblage suggests an Atlantic age for the sediments, which would be supported by the numerical age determination of ~8300 BP (Zhang et al. 2014). Low amounts and even absence of heliophilous herbs such as Asteraceae, *Artemisia*, Caryophyllaceae, Chenopodiaceae, *Thalictrum* and *Filipendula* might relate to unfavourable and unstable ecological conditions for an expansion of the local marsh vegetation. Elements of swamps and peat bogs such as Polypodiaceae, *Sphagnum* and *Myrica* indicate paludification in the surrounding area at the beginning of the sea intrusion that is also indicated in the area near Eider at about 7512–7012 BP (5500–5000 BC; Menke 1968). This single sample reveals a mixed pollen spectrum, which might best be correlated with Zone VI to VII (Firbas 1949) and Zone VIII^{WD} (Overbeck 1975). The erosional surface between the single sample at 19.80 m and LPAZ GH-1 is dated to ~7000 BP (Zhang et al. 2014) and was most likely formed by the continuation of the course of the early Holocene transgression.

After ~7000 BP (Zhang et al. 2014), the first principal cluster between 19.56 and 11.53 m is characterised by relatively constant values of *Quercus*, *Ulmus*, *Tilia*, *Fraxinus*, *Alnus*, *Betula* and *Corylus* (Fig. 3). This principal cluster is then subdivided into two zones, LPAZ GH-1 and LPAZ GH-2, based on the increased amounts of total NAP, which are represented mostly by terrestrial herbs, and the beginning of *Fagus* and *Carpinus* occurrences in LPAZ GH-2 (Table 1).

The transition from the Atlantic to the Subboreal period, zone VII to VIII (Firbas 1949) and zone VIII^{WD} to IX^{WD} (Overbeck 1975), is usually defined palynostratigraphically by the elm decline, which is known from most of the mid-Holocene pollen records of Northwest Europe (Overbeck 1975, Wiethold 1998, Dörfler 2000, Parker et al. 2002, Kalis et al. 2003). At Lake Belau, Schleswig-Holstein, new chronological results based on varve counting and AMS ^{14}C dating date the elm decline to about 5780 cal. BP (Dörfler et al. 2012) when constant low values of elm were achieved. The end of the elm decline at Lake Belau corresponds with the empirical boundary of *Fagus*. Constant low percentages of *Ulmus* and the first occurrence of *Fagus* are reflected in Subboreal pollen spectra of sediments from the Tholendorf beach ridge adjacent to Garding (Fig. 1; Menke 1969). The start of the *Fagus* curve in this area was AMS ^{14}C-dated to 4112 BP (2100 BC; Menke 1969) and of *Carpinus* to about 3912 BP (1900 BC). Pollen records of Flögeln V in Lower Saxony (Behre & Kučan 1994) indicate low amounts of *Ulmus* (below 5 %) since the Atlantic period.

In the Garding-2 record, *Fagus* (1.6 %) occurs first at 15.97 m, followed by the appearance of *Carpinus* at 15.03 m. Pollen zone GH-1 already shows low *Ulmus* values, which persists during the following pollen zone. The first occurrence of *Fagus* at the base of LPAZ GH-2 marks the boundary between LPAZ GH-1 and LPAZ GH-2. Those features confirm the Subboreal age for these local pollen assemblage zones and suggest that Late Atlantic transitional sediments were most likely eroded in the Garding-2 core, indicated by the unconformity at the base of LPAZ GH-1. Therefore, LPAZ GH-1 and LPAZ GH-2 are correlated to the zone VIII (Firbas 1949) and zone IX^{WD} (Overbeck 1975) (Table 1).

Zhang et al. (2014) have OSL-dated the sediments around the first occurrence of *Fagus* (15.97 m) in the Garding-2 section, to 3130 ± 260 BP. This age disagrees with the recent age model of Dörfler et al. (2012) for the empirical occurrence of *Fagus* as well as with the age for the first *Fagus* appearance in the Tholendorf record (Menke 1969). This offset might be explained by erosion and redeposition of sediments, which is common in the study area. In the case of intensive erosion, even small differences in depth of dated levels and palynostratigraphic events may represent considerable time spans. Considering these conditions of sedimentation, it is also possible that older sediments containing *Fagus* pollen were eroded, which is also suggested by some reworked pol-

Table 1: Summary of palynological characteristics of the local pollen assemblage zones (LPAZ) and comparison with the established pollen zones of Firbas (1949) and Overbeck (1975) as well as depositional environments and dating results of Zhang et al. (2014).

Depth Range (m)	LPAZ	Palynological Characteristics	Depositional Environment	Pollen Zones		Holocene Zonation (Blytt and Sernander)	Numerical Dating (Zhang et al. 2014)	
				Firbas (1949)	Overbeck (1975)		AMS ^{14}C (BP, before 2012)	OS L (BP, before 2012)
1.33–11.53	GH-3	*Quercus, Alnus, Corylus, Ulmus, Fagus, Carpinus, Tilia, Fraxinus*	Backshore (Dunes)	IX	X^{NWD}	Subatlantic	1820 ± 50 (2.70 m)	
		Increase of salt marsh and dune vegetation, Cyperaceae, Ericaceae					2229 ± 50 (3.50 m)	1500 ± 190 (3.50 m)
		Single grains of *Abies*	Shoreface (Barrier Island, Spit)					
		Increase of Cerealia-type and decrease of Poaceae					2380 ± 30 (4.80 m)	2050 ± 250 (5.25 m)
		Unconformity (between 11.00 and 10.85 m)					2790 ± 20 (11.41 m)	2800 ± 250 (11.25 m)
11.53–16.19	GH-2	*Quercus, Alnus, Ulmus, Tilia, Fraxinus*	Foreshore (Tidal Flat)	VIII	IX^{NWD}	Subboreal		
		First occurrence of ***Fagus*** and ***Carpinus***						2990 ± 25 (13.25 m)
		Increase of terrestrial herbs						
16.19–19.56	GH-1	Unconformity (core loss: 17.00–16.45 m)						**3130 ± 260 (16.22 m)**
		Quercus, Alnus, Corylus, Ulmus, Tilia, Fraxinus	Offshore				4670 ± 40 (17.44 m)	4430 ± 550 (17.25 m)
		Considerable amounts of *Alnus* and *Betula*						
		Increase of *Corylus*, Poaceae and heliophilous herbs						
Unconformity								
19.80–20.00	–	*Quercus, Corylus, Alnus, Tilia, Ulmus*	Offshore	VI–VII	$VIII^{NWD}$	Atlantic	7860 ± 60 (19.61 m)	6920 ± 900 (19.65 m)
		High amounts of *Pinus* and Poaceae					8300 ± 40 (19.77 m)	
		Very low values heliophilous herbs						
Unconformity								13300 ± 220 (20.25 m)

len in LPAZ GH-2 or represented in the core loss at about the top of LPAZ GH-1.

Sediment of LPAZ GH-1 is generally sandy, rich in molluscs, with low to high salinity, little to substantial carbonate content and narrow C/N ratios (Fig. 2), typical for offshore marine deposits. However, the subsequent sediments of LPAZ GH-2 show a domination of fine-grained deposits within the stack of sandy-clayey sediment intercalations, pointing to a tidal flat environment in a foreshore area. The abrupt changes of the depositional environment, from offshore to foreshore, might also be indicated by the occurrence of an unconformity at around the boundary between LPAZ GH-1 and LPAZ GH-2.

The uppermost pollen zone, LPAZ GH-3, is defined by the second principal cluster (Fig. 3). The main characteristics of LPAZ GH-3 are the significant increase of the Cerealia-type curve and the first appearance of *Plantago lanceolata*-type and *Rumex acetosa*-type pollen (Table 1). The Cerealia-type pollen most likely derives from wild grasses such as *Agropyron* spec. and *Ammophila arenaria* of sand dunes, which formed around 2700 BP near Garding (Menke 1969). This is supported by the increased occurrence of the Ericaceae (Fig. 3), which are also commonly distributed in dune areas. Menke (1969) also investigated surface samples at St. Peter-Böhl, Eiderstedt, palynologically. He found similar features of abundant wild grasses and Cyperaceae with considerable amounts of *Calluna*, *Empetrum* and herbs such as Chenopodiaceae, *Glaux*, *Triglochin*, *Lotus*, *Ononis*, *Plantago maritima*, *Plantago coronopus* and *Rumex acetosa*-type in beach ridge area. Salt marsh vegetation existed not far away from the study area, which is evidenced by Chenopodiaceae, most likely including *Atriplex*, *Salicornia europaea*, *Salsola kali* and *Suaeda maritima*, Asteraceae, Cichoriaceae, Apiaceae, *Artemisia*, *Plantago coronopus-type*, *Plantago maritima*, *Ophioglossum* and other herbs. Similar pollen spectra are recorded from the Tholendorf pollen diagram (Menke 1969), which reflect congeneric late Subboreal environmental conditions.

In contrast to the tidal flat deposits that are dominant during LPAZ GH-2, tidal flat sediments at the bottom of LPAZ GH-3 that have higher proportions of sandy fractions point to an area around a tidal channel, indicating the existence of an erosional surface, which probably corresponds to a scour, typical for the base of a tidal channel. This interpretation is supported by high frequencies of reworked Pleistocene pollen grains, which were likely redeposited together with eroded materials from the north (Falk 2001), brought in by the tidal channel. This interpretation might as well explain the increased amounts of redeposited cell remnants of the freshwater algae *Pediastrum*, which is found in the marine sediments of this zone. The beginning of the deposition of the marine sand is found on top of these sandy tidal flat sediments, between 6.00 and 3.72 m. These sediments were dated by Zhang et al. (2014) to about 2380 ± 30 BP, which is likely related to the sandy deposits of Garding and Tholendorf barrier systems (barrier islands and/or spits), in a shoreface setting, that extensively protected the hinterland area of Eiderstedt since about 2500 BP (Meier 2004). Regardless of the dominant local flora, occurrences of constantly low percentages of *Juniperus* throughout the Garding-2 section are noticeable (Fig. 3). According to the composite Holocene pollen diagrams of Central Schleswig-Holstein (Lake Belau and Dosenmoor; Nelle & Dörfler 2008 and references therein), *Juniperus* is regularly recorded from the Preboreal and Subatlantic, while occurrence of *Juniperus* during the Boreal, Atlantic and Subboreal is rare.

Zhang et al. (2014) have OSL-dated the sediments of LPAZ GH-3 to 2800 ± 250 BP at 11.25 m and to 1820 ± 50 BP at the top of the zone, at 2.70 m, suggesting that the sediments of the upper part of LPAZ GH-3 were deposited during the Subatlantic (Wiethold 1998, Urban et al. 2011, Dörfler et al. 2012). The boundary between Subboreal and Subatlantic in northwestern Europe is marked by a slow but constant increase of *Fagus* (>2 %), and slightly later of *Carpinus*, at about 2700 BP (Wiethold 1998, Urban et al. 2011, Dörfler et al. 2012) corresponding to pollen zone IX of Firbas (1949) and pollen zone X^{NWD} of Overbeck (1975). The amounts of *Fagus* and *Carpinus* in LPAZ GH-3 are almost constantly low (below 5.5 %) and the classical Subboreal to Subatlantic transitional features are not observed in the Garding-2 pollen diagram. In Tholendorf (Menke 1969), *Fagus* expands very slightly after 2500 BP up to 10 % and only reaches amounts up to 20 % after about the birth of Christ. Additionally, strong increases of anthropogenic indicators are also not recorded in the topmost sediments of Garding-2; only *Rumex acetosa*-type and *Plantago lanceolata*-type are found with relatively low percentages. This fact might be caused by the less intensive settlement and human activity in the surrounding area, as the inhabitants were forced to occasionally leave the area during this period because of storm floods (Menke 1969), until they started to create dikes at about the 11th century. The occurrence of *Abies* can be interpreted as a result of long distance pollen transport during the strong fir expansion in the low mountain ranges within southern parts of the country (Wiethold 1998: 145 and references therein). Sparse occurrences of *Abies* are also known from the Subboreal sediments of Tholendorf (Menke 1969) as well as from zone 9 of the pollen profile of Lake Belau (Wiethold 1998) during the Bronze Age and therefore are not a good indicator of the Subatlantic.

6. Conclusion

Sediments of the top 20 m of the Garding-2 core provide evidence of Holocene coastal sediments being rapidly deposited during the Subboreal and early Subatlantic. The Early Holocene transgression is marked by an unconformity at the bottom of the section, overlain by a thin Atlantic marine deposit. This transgression also causes another big erosional surface at about 19.60 m. The sediment sequence on top of this erosional surface is subdivided into three local pollen assemblage zones (LPAZ).

The *Ulmus* decline, which is a typical palynological feature of the Atlantic to Subboreal transition in northwestern Europe, is not recorded in Garding. *Ulmus* shows low constant values throughout the whole pollen sequence. Numerical dating at around the first occurrence of *Fagus* indicates an age of 3130 ± 260 BP (at 16.22 m; Zhang et al. 2014) and might suggest that the late Atlantic transitional sediments were eroded in Garding-2. Offshore marine sediments of LPAZ GH-1 were deposited during the Subboreal. An unconformity occurs almost at the top of this zone, which is then overlain by tidal flat sediments of LPAZ GH-2.

Increasing sandy sediments of LPAZ GH-3 are found on top of an unconformity at around the base of this zone. Depositional environment changes from sandy tidal flat, between 11.00 and 6.00 m, to sandy barrier and spit, between 6.00 and 3.72 m, which is followed by development of sand dunes in a backshore environment, between 3.72 m and the top of the core, are also reflected by a significant increase of marsh, dune and tidal flat vegetation at around 2790 ± 20 (Zhang et al. 2014). The age of the onset of this regional feature of coastal development in this zone is in very good agreement with the age of the same events occurring at Tholendorf (Fig. 1), dated to 2800 BP (Menke 1969).

The expansion of *Fagus* and *Carpinus* as well as a rapid increase of anthropogenic indicators, characteristic of the beginning of the Subatlantic at about 2700 BP (Dörfler et al. 2012), are not observed in the Garding-2 core. These features, however, are in good agreement with the regional development during the Subboreal to Subatlantic transition (Menke 1969, 1986) and are supported by the numerical dating of Zhang et al. (2014).

7. Acknowledgements

We would like to sincerely thank the Directorate General of Indonesian Higher Education (Dikti) and the German Academic Exchange Service (DAAD) for the scholarship that supported this research and Mario Tucci, Emilio Torres, Sabine Hansen and Frank Krüger for their assistance in laboratory work. We acknowledge financial support by the Small Research Project Funding of Leuphana University of Lüneburg, which helped setting the research drill preparation. Last but not least we would like to thank Peter Kershaw for the helpful and important suggestions.

8. References

Ad-Hoc-Arbeitsgruppe Boden (2005): Bodenkundliche Kartieranleitung: 438 p., Stuttgart (Schweizerbart).

Ahrendt, V.K. (2006): Ein Beitrag zur holozänen Entwicklung Nordfrieslands. – Die Küste, 71: 1–32.

Baldschuhn, R., Best, G. & Kockel, F. (1991): Inversion tectonics in the North-west German basin. – In: Spencer, A.M. (ed.): Generation, accumulation, and production of Europe's hydrocarbons. – Spec. Publ. Eur. Assoc. Petroleum Geosci., 1: 149–159.

Baldschuhn, R., Binot, F., Fleig, S. & Kockel, F. (2001): Geotektonischer Atlas von Nordwest-Deutschland und dem deutschen Nordsee-Sektors – Strukturen, Strukturentwicklung, Paläogeographie. – Geol. Jb., A 153: 88 p.

Barber, K.E., Chambers, F.M. & Maddy, D. (2004): Late Holocene climatic history of northern Germany and Denmark: peat macrofossil investigations at Dosenmoor, Schleswig-Holstein, and Svanemose, Jutland. – Boreas, 33 (2): 132–144.

Behre, K.-E. (1991): Veränderungen von Landschaft und Umwelt in der Wesermarsch in den vergangenen Jahrtausenden. – Archäol. Mitt. Nordwestdeutschland, 5: 33–36.

Behre, K.-E. (2003): Eine neue Meeresspiegelkurve für die südliche Nordsee – Transgressionen und Regressionen in den letzten 10.000 Jahren. – Probleme der Küstenforschung im Südlichen Nordseegebiet, 28: 9–63.

Behre, K.-E. (2005): Die Botanik als Schlüssel für die Umweltgeschichte: Paläo-Ökologie an der Nordsee. – Biol. Unserer Zeit, 35: 320–330.

Behre, K.-E. (2007a): A new Holocene sea-level curve for the southern North Sea. – Boreas, 36 (1): 82–102.

Behre, K.-E. (2007b): Evidence for Mesolithic agriculture in and around central Europe? – Veget. Hist. Archaeobot., 16 (2): 203–219.

Behre, K.-E. & Kučan, D. (1994): Probleme der Küstenforschung im südlichen Nordseegebiet; Band 21: Die Geschichte der Kulturlandschaft und des Ackerbaus in der Siedlungskammer Flögeln, Niedersachsen, seit der Jungsteinzeit: 227 p., Oldenburg (Isensee).

Behre, K.-E. & Menke, B. (1969): Pollenanalytische Untersuchungen an einem Bohrkern der südlichen Doggerbank. – Beitr. Meereskd., 24 (25): 122–129.

Behre, K.-E., Menke, B. & Streif, H. (1979): The Quaternary geological development of the German part of the North Sea. – In: Oele, E., Schüttenhelm, R.T.E. & Wiggers, A.J. (ed.): The Quaternary history of the North Sea. – Acta Univ. Ups. Symp. Univ. Ups. Annum Quingentesimum Celebrantis, 2: 85–113.

Beug, H.J. (2004): Leitfaden der Pollenbestimmung, für Mitteleuropa und angrenzende Gebiete: 542 p., München (Pfeil).

Bohn, U., Gollub, G. & Hettwer, C. (2000): Karte der natürlichen Vegetation Europas; Maßtab 1: 2 500 000; Legende: 153 p., Bonn (Bundesamt für Naturschutz).

Bungenstock, F. & Weerts, H.J.T. (2010): The high-resolution Holocene sea-level curve for Northwest Germany: global signals, local effects or data-artefacts? – Int. J. Earth Sci., 99 (8): 1687–1706.

Cameron, D., Van Doorn, D., Laban, C. & Streif, H. (1993): Geology of the southern North Sea basin. – In: Hillen, R. & Verhagen, H.J. (ed.): Coastlines of the Southern North Sea: 14–26, New York (American Society of Civil Engineers).

Concheyro, A., Caramés, A., Amenábar, C.R. & Lescano, M. (2014): Nannofossils, foraminifera and microforaminiferal linings in the Cenozoic diamictites of Cape Lamb, Vega Island, Antarctica. – Polish Polar Res., 35 (1): 1–26.

De Vernal, A. (2009): Marine palynology and its use for studying nearshore environments. – IOP Conference Series: Earth Environ. Sci., 5 (1): 012002.

Dörfler, W. (2000): Palynologische Untersuchungen zur Vegetations- und Landschaftsentwicklung von Joldelund, Kr. Nordfriesland. – In: Haffner, A., Jöns, H. & Reichstein, J. (ed.): Frühe Eisengewinnung in Jodelund, Kr. Nordfriesland. – Universitätsforschungen zur Prähistorischen Archäologie, 59: 147–216.

Dörfler, W., Feeser, I., van den Bogaard, C., Dreibrodt, S., Erlenkeuser, H., Kleinmann, A., Merkt, J. & Wiethold, J. (2012): A high-quality annually laminated sequence from Lake Belau, Northern Germany: revised chronology and its implications for

palynological and tephrochronological studies. – Holocene, 22 (12): 1413–1426.
Ehlers, J. (1988): The morphodynamics of the Wadden Sea: 397 p., Rotterdam (Balkema).
Esselink, P., Petersen, J., Arens, S., Bakker, J.P., Bunje, J., Dijkema, K.S., Hecker, N., Hellwig, U., Jensen, A.-V., Kers, A.S., Körber, P., Lammerts, E.J., Stock, M., Veeneklaas, R.M., Vreeken, M. & Wolters, M. (2009): Salt marshes; thematic report No. 8. – In: Marencic, H. & Vlas, J. de (ed.): Quality status report 2009. Wadden-sea ecosystem; No. 25, Wilhelmshaven (Common Wadden Sea Secretariat, Trilateral Monitoring and Assessment Group).
Faegri, K. & Iversen, J. (1989): Textbook of pollen analysis; 4th ed.: 328 p., New York (Wiley).
Faegri, K. & Iversen, J. (1993): Bestimmungsschlüssel für die Nordwesteuropäische Pollenflora: 85 p., Jena (Fischer).
Falk, G.C. (2001): Die Paläogeomorphologie ausgewählter Standorte der schleswig-holsteinischen Nordseeküste im Früh- und Mittelholozän. – Diss., Techn. Univ. Berlin: 171 p.
Firbas, F. (1949): Spät- und nacheiszeitliche Waldgeschichte Mitteleuropas nördlich der Alpen; Band 1: Allgemeine Waldgesichte: 480 p., Jena (Fischer).
Frisch, U. & Kockel, F. (1999): Early Cimmerian movements in Northwest Germany. – Zentralbl. Geol. Palaeontol., Teil I: 571–600.
Gibbard, P. (2007): History of the northwest European rivers during the past three million years. – http://www.qpg.geog.cam.ac.uk/research/projects/nweurorivers/ (accessed 24 September 2014).
Grimm, E.C. (1987): CONISS: a FORTRAN 77 program for stratigraphically constrained cluster analysis by the method of incremental sum of squares. – Comput. Geosci., 13 (1): 13–35.
Grimm, E.C. (1990): Tilia, Tiliagraph & Tiliaview. PC spreadsheet and graphics software for pollen data. – http://www.geo.arizona.edu/palynology/geos581/tiliaview.html (accessed 26 November 2013).
Grube, A. (2011): Schichtansprache der Forschungsbohrung Garding-2. – Landesamt für Landwirtschaft, Umwelt und ländliche Räume, Flintbek (unpubl.).
Heusser, L.E. (1988): Pollen distribution in marine sediments on the continental margin off northern California. – Mar. Geol., 80: 131–147.
Heusser, L.E. (1998): Spores and pollen in the marine realm. – In: Haq, B.U. & Boersma, A. (ed.): Introduction to marine micropaleontology: 327–340, Singapore (Elsevier).
Hoselmann, C. & Streif, H. (2004): Holocene sea-level rise and its effect on the mass balance of coastal deposits. – Quatern. Int., 112 (1): 89–103.
Jelgersma, S. (1961): Mededelingen van de Geologische Stichting; Serie C/VI, 7: Holocene sea level changes in the Netherlands: 100 p., Maastricht (Ernest van Aelst).
Jelgersma, S. (1979): Sea-level changes in the North Sea basin. – In: Oele, E., Schüttenhelm, R.T.E. & Wiggers, A.J. (ed.): The Quaternary history of the North Sea. – Acta Univ. Ups. Symp. Univ. Ups. Annum Quingentesimum Celebrantis, 2: 233–248.
Kalis, A.J., Merkt, J. & Wunderlich, J. (2003): Environmental changes during the Holocene climatic optimum in central Europe – human impact and natural causes. – Quat. Sci. Rev., 22 (1): 33–79.
Kiden, P., Denys, L. & Johnston, P. (2002): Late Quaternary sea-level change and isostatic and tectonic land movements along the Belgian-Dutch North Sea coast: geological data and model results. – J. Quatern. Sci., 17 (5–6): 535–546.
Kühn, H.J. & Panten, A. (1989): Der frühe Deichbau in Nordfriesland: Archäologisch-historische Untersuchungen: 127 p., Bredstedt (Nordfriisk Inst.).
Kunz, A., Urban, B., Grube, A., Sirocko, F. & Frechen, M. (2009): The Garding Trough in northwest Germany: a high resolution record of Quaternary glacial and interglacial cycles for scientific drilling. – Eos Trans. AGU, 90 (52), Fall Meet. Suppl., Abstract: 21-A-1319.
Kunz, A., Urban, B., Grube, A., Sirocko, F. & Frechen, M. (2010): The Garding Trough in northwest Germany: a high resolution record of Quaternary glacial and interglacial cycles for scientific drilling. – In: Hoppe, A., Röhling, H.-G. & Schüth, C. (ed.): GeoDarmstadt 2010 – Geowissenschaften sichern Zukunft. – Schriftenr. Dt. Ges. Geowiss., 68: 624 p.
Mathison, S.W. & Chmura, G.L. (1995): Utility of microforaminifera test linings in palynological preparations. – Palynology, 19 (1): 77–84.
Meier, D. (2004): Man and environment in the marsh area of Schleswig-Holstein from Roman until Medieval times. – Quatern. Int., 112 (1): 55–69.
Menke, B. (1968): Ein Beitrag zur pflanzensoziologischen Auswertung von Pollendiagrammen, zur Kenntnis früherer Pflanzengesellschaften in den Marschenrandgebieten der schleswig-holsteinischen Westküste und zur Anwendung auf die Frage der Küstenentwicklung. – Mitt. Florist. Soziol. Arbeitsgemeinschaft N.F., 13: 195–223.
Menke, B. (1969): Vegetationskundliche und vegetationsgeschichtliche Untersuchungen an Strandwällen. – Mitt. Florist. Soziol. Arbeitsgemeinschaft N.F., 14: 95–120.
Menke, B. (1986): Beiträge zur Entwicklung des Holozäns im Raum Husum-Simonsberg/Nordfriesland. – Offa, 43: 265–272.
Meyers, P.A. (1994): Preservation of elemental and isotopic source identification of sedimentary organic matter. – Chem. Geol., 114 (3–4): 289–302.
Mohr, M., Kukla, P.A., Urai, J.L. & Bresser, G. (2005): Multiphase salt tectonic evolution in NW Germany: seismic interpretation and retro-deformation. – Geol. Rundsch., 94: 917–940.
Moore, P.D., Webb, J.A. & Collinson, M.E. (1991): Pollen analysis; 2nd ed.: 216 p., Oxford (Blackwell).
Müller, J. (1959): Palynology of Recent Orinoco delta and shelf sediments: reports of the Orinoco Shelf expedition; vol. 5. – Micropaleontology, 5 (1): 1–32.
Munsell Color (2009): Munsell soil-color chart, Michigan (Munsell color x.rite).
Nelle, O. & Dörfler, W. (2008): A summary of the late- and post-glacial vegetation history of Schleswig-Holstein. – In: Dengler, J., Dolnik, C. & Trepel, M. (ed.): Flora, vegetation and nature conservation from Schleswig-Holstein to South America. Festschrift for Klaus Dierßen on occasion of his 60th birthday. – Mitt. Arbeitsgem. Geobot. Schleswig-Holstein und Hamburg, 65: 45–68.
Overbeck, F. (1934): Bisherige Ergebnisse der botanischen Moorforschung zur Frage der Küstensenkung an der deutschen Nordsee. – Abh. Naturwiss. Ver. Bremen, 29 (1–2): 48–73.
Overbeck, F. (1975): Botanisch-geologische Moorkunde, unter besonderer Berücksichtigung der Moore Nordwestdeutschlands als Quellen zur Vegetations-, Klima- und Siedlungsgeschichte: 719 p., Neumünster (Wachholtz).
Panten, A., Porada, H.T. & Steensen, T. (2013): Eiderstedt: Eine landeskundliche Bestandsaufnahme im Raum St. Peter-Ording, Garding, Tönning und Friedrichstadt: 388 p., Köln (Böhlau).

Parker, A.G., Goudie, A.S., Anderson, D.E., Robinson, M.A. & Bonsall, C. (2002): A review of the mid-Holocene elm decline in the British Isles. – Prog. Phys. Geogr., 26: 1–45.

Proborukmi, M.S., Urban, B., Frechen, M., Grube, A. & Rolf, C. (2017): Upper Pliocene–Quaternary record of the Garding-2 research drill core, Northwest Germany. – Z. Dt. Ges. Geowiss., 168 (1) 141–167 (this volume).

Robertsson, A.-M. (1982): Pollen. – In: Olausson, E. (ed.): The Pleistocene/Holocene boundary in south-western Sweden. – Sver. Geol. Unders., Upsala, C 794: 224–242.

Stephan, H.-J. (2014): Climato-stratigraphic subdivision of the Pleistocene in Schleswig-Holstein, Germany and adjoining areas. – Eiszeitalter u. Gegenwart, 63 (1): 3–18.

Streif, H. (2004): Sedimentary record of Pleistocene and Holocene marine inundations along the North Sea coast of Lower Saxony, Germany. – Quatern. Int., 112 (1): 3–28.

Thornton, S.F. & McManus, J. (1994): Application of organic carbon and nitrogen stable isotope and C/N ratios as source indicators of organic matter provenance in estuarine systems: evidence from the Tay Estuary. – Estuar. Coast Shelf Sci., 38 (3): 219–233.

Urban, B. (2002): Manual for analysis of soil and related materials. – In: Kunst, S., Kruse, T. & Burmester, A. (ed.): Sustainable water and soil management: 321–370, Berlin (Springer).

Urban, B., Sierralta, M. & Frechen, M. (2011): New evidence for vegetation development and timing of Upper Middle Pleistocene interglacials in Northern Germany and tentative correlations. – Quatern. Int., 241: 125–142.

VDLUFA (1991): Methodenbuch; Band 1: Die Untersuchung der Böden: 1570 p., Darmstadt (VDLUFA-Verl.).

Vink, A., Steffen, H., Reinhardt, L. & Kaufmann, G. (2007): Holocene relative sea-level change, isostatic subsidence and the radial viscosity structure of the mantle of northwest Europe (Belgium, the Netherlands, Germany, southern North Sea). – Quatern. Sci. Rev., 26 (25–28): 3249–3275.

Wieland, P. (1990): Küstenfibel. Ein Abc der Nordseeküste: 152 p., Heide (Boyens & Co.).

Wiermann, R. (1962): Botanisch-moorkundliche Untersuchungen in Nordfriesland. – Meyniana, 12: 97–146.

Wiethold, J. (1998): Studien zur jüngeren postglazialen Vegetations- und Siedlungsgeschichte im östlichen Schleswig-Holstein. – Diss., Univ. Kiel: 365 p.

Zhang, J., Tsukamoto, S., Grube, A. & Frechen, M. (2014): OSL and ^{14}C chronologies of a Holocene sedimentary record (Garding-2 core) from the German North Sea coast. – Boreas, 43 (4): 856–868. http://www.worldatlas.com/webimage/countrys/eu.htm (accessed 1 March 2013); https://maps.google.de (accessed 7 December 2012).

http://www.worldatlas.com/webimage/countrys/eu.htm (accessed 1 March 2013).

https://maps.google.de (accessed 7 December 2012).

Manuscript received: 08.09.2016
Accepted for publication: 14.11.2016

Paper III

Evidence for climatic changes around the Matuyama-Brunhes Boundary (MBB) inferred from a multi-proxy palaeoenvironmental study of the GBY#2 core, Jordan River Valley, Israel

Maria Sekar Proborukmi, Brigitte Urban, Steffen Mischke, Henk K. Mienis, Yoel Melamed, Guillaume Dupont-Nivet, Fred Jourdan, Naama Goren-Inbar (2018). Evidence for climatic changes around the Matuyama-Brunhes Boundary (MBB) inferred from a multi-proxy palaeoenvironmental study of the GBY#2 core, Jordan River Valley, Israel. Palaeogeography, Palaeoclimatology, Palaeoecology 489 (C), 166–185. DOI: 10.1016/j.palaeo.2017.10.007.

Palaeogeography, Palaeoclimatology, Palaeoecology 489 (2018) 166–185

Contents lists available at ScienceDirect

Palaeogeography, Palaeoclimatology, Palaeoecology

journal homepage: www.elsevier.com/locate/palaeo

Evidence for climatic changes around the Matuyama-Brunhes Boundary (MBB) inferred from a multi-proxy palaeoenvironmental study of the GBY#2 core, Jordan River Valley, Israel

Maria Sekar Proborukmi[a,*], Brigitte Urban[a], Steffen Mischke[b], Henk K. Mienis[c], Yoel Melamed[d], Guillaume Dupont-Nivet[e,f], Fred Jourdan[g], Naama Goren-Inbar[h]

[a] Institute of Ecology, Subject Area Landscape Change, Leuphana University Lüneburg, Scharnhorststraße 1, 21335 Lüneburg, Germany
[b] Faculty of Earth Sciences, University of Iceland, Sturlugata 7, Askja, 101, Reykjavik, Iceland
[c] National Natural History Collections, Hebrew University of Jerusalem, Edmond J. Safra Campus, Jerusalem 9190401, Israel
[d] The Mina and Everard Goodman Faculty of Life Sciences, Bar-Ilan University, Ramat-Gan 5290002, Israel
[e] UMR-CNRS 6118 OSUR-Geosciences Rennes, Université de Rennes 1, Campus de Beaulieu Bat. 15, 35042 Rennes Cedex, France
[f] Institute of Earth and Environmental Sciences, University of Potsdam, Karl Liebknecht Str. 24-25, 14476 Potsdam-Golm, Germany
[g] Western Australian Argon Isotope Facility, Department of Applied Geology, John de Laeter Centre for Isotope Research, Curtin University, GPO Box U1987, Perth, WA 6845, Australia
[h] Institute of Archaeology, Hebrew University of Jerusalem, Mount Scopus, Jerusalem 9190501, Israel

ARTICLE INFO

Keywords:
Hula Basin
Levant
Hominins
Pollen record
Plant macro-remains

ABSTRACT

The Acheulian site of Gesher Benot Ya'aqov (GBY) in the Upper Jordan Valley revealed important data on environment and material culture, as well as evidence for hominin behavioural and cognitive patterns documented at the margins of the Hula Palaeo-lake. A 50 m long core (GBY#2) drilled at the archaeological site has provided a long Pleistocene geological, environmental and climatological record, which expands the existing knowledge of hominin-habitat relationships. Bracketed by two basalt flows dated by $^{40}Ar/^{39}Ar$ and based on the identification of the Matuyama-Brunhes Boundary (MBB) and correlation with the GBY excavation site, the sedimentary sequence provides the climatic history around the MBB. Multi-proxy data including pollen and non-pollen palynomorphs, macro-botanical remains, molluscs and ostracods provide evidence for lake and lake-margin environments during Marine Isotope Stages (MIS) 20 and 19. Semi-moist conditions were followed by a pronounced dry phase during MIS 20, and warm and moist conditions with *Quercus-Pistacia* woodlands prevailed during MIS 19. In contrast to the reconstructed climate change from relatively dry to moister conditions, the depositional environment developed from an open-water lake during MIS 20 to a lake margin environment in MIS 19. Generally shallower conditions at the core site in MIS 19 resulted from the progradation of the lake shore due to the filling of the basin. Micro-charcoal analysis suggests a likelihood of human-induced fire in some parts of the core, which can be correlated with artefact-containing layers of the GBY excavation site. The Hula Palaeo-lake region provided an ideal niche for hominins and other vertebrates during global glacial-interglacial climate fluctuations at the end of the Early Pleistocene.

1. Introduction

The Acheulian site of Gesher Benot Ya'aqov (GBY) is located within the Jordan River Valley, through which hominins diffused from Africa to Eurasia (Goren-Inbar and Saragusti, 1996; Goren-Inbar et al., 2000, 2004), at the southern margin of the Lake Hula, which was drained in the 1950s. This site, and particularly its recent excavations, have yielded well-preserved archaeological evidence of the Acheulian culture such as handaxes, cleavers and flakes of basalt, flint and limestone (Alperson-Afil et al., 2009; Goren-Inbar and Saragusti, 1996; Goren-Inbar and Sharon, 2006; Goren-Inbar et al., 1992, 2000, in press; Sharon et al., 2011), as well as wood artefacts associated with an elephant (*Palaeoloxodon antiquus*) skull (Goren-Inbar et al., 1994). The lake sediments in this site were dated to MIS 20–18 (Goren-Inbar et al., 2000; Melamed et al., 2016), including the Matuyama-Brunhes Boundary (MBB) at 780 ka (Head and Gibbard, 2005) during MIS 19

* Corresponding author.
E-mail addresses: Maria.S.Proborukmi@stud.leuphana.de (M.S. Proborukmi), b.urban@leuphana.de (B. Urban), smi@hi.is (S. Mischke), mienis@netzer.org.il (H.K. Mienis), Guillaume.dupont-nivet@univ-rennes1.fr (G. Dupont-Nivet), F.Jourdan@curtin.edu.au (F. Jourdan), naama.g@mail.huji.ac.il (N. Goren-Inbar).

http://dx.doi.org/10.1016/j.palaeo.2017.10.007
Received 16 June 2017; Received in revised form 1 October 2017; Accepted 9 October 2017
Available online 16 October 2017

(Lisiecki and Raymo, 2005). The Acheulian material culture remains of GBY are assigned to the African Large Flake Acheulian Tradition (Sharon, 2007), which is characterised by modification of handaxes and cleavers made on large flakes. The Acheulian lithic assemblages were produced on basalt, limestone and flint, each of the raw materials being selected for the production or utilization of particular pre-planned artefacts. In addition, the stratigraphic/sedimentological analyses of the depositional archive and the multiple archaeological occurrences which appear along it clearly demonstrate that the Acheulian material culture, as well as the evidence for controlled fire, did not change along the diachronic sequence. Furthermore, the 15 very rich super-positioned archaeological horizons, with an estimated duration of 50 ka, demonstrate similar technology and typology, a continuing tradition which is expressed in the lithic assemblages. The multidisciplinary research of the GBY sedimentary sequence and the diverse archaeological and biological remains embedded in it provides us with a large data set that allows detailed reconstruction of the varied environment and its biological components. The geomorphological reconstruction is that of a narrow embayment located south of a freshwater lake in a sedimentary and volcanic terrain (Belitzky, 2002; Feibel, 2001, 2004). The quality of the water in the drainage basin was dictated by the sedimentary and volcanic rocks that surround the Hula Basin (Spiro et al., 2009, 2011) and generally resemble those of the present day. The existence of lake, lake margin and terrestrial habitats enabled the survival of many organisms which inhabited this region from the Early Pleistocene to the Holocene, with minimal species extinction (Ashkenazi et al., 2005, 2010; Mienis and Ashkenazi, 2011; Mischke et al., 2014a; Rabinovich and Biton, 2011; Rosenfeld et al., 2004; Zohar et al., 2014). These palaeoenvironmental conditions are documented by the presence of aquatic submerged taxa such as ostracods, molluscs, fish, crabs and an array of amphibians (as above and Biton et al., 2013, 2016) and a rich Mediterranean flora (Goren-Inbar et al., 2002a, 2002b) including macro- and micro-botanical remains (Kislev and Melamed, 2011; Van Zeist and Bottema, 2009). It was in this setting that the GBY hominins left the remains of their activities, from which particular behavioural patterns are readable. It has been shown that the hominins were very mobile on the landscape, of which they possessed extensive knowledge expressed in the selection pattern of the different raw materials and their transportation into the lake margin sites. Thick basalt slabs were transformed into large cores for the production of bifaces (Goren-Inbar, 2011), thin slabs were used as anvils (Goren-Inbar et al., 2015), small flint pebbles were transformed into an array of retouched tools including evidence for hafting (Alperson-Afil and Goren-Inbar, 2016) and limestone pebbles were meticulously selected for use as percussors (Alperson-Afil and Goren-Inbar, 2015). Carcasses of medium-sized and large mammals were processed on the lake margin, leaving various recognizable patterns of bone damage (particular on deer bones) indicating consumption of meat, brain and bone marrow (Rabinovich and Biton, 2011; Rabinovich et al., 2008). Large fish were consumed and their remains were found clustered spatially in several archaeological horizons (Zohar et al., 2014). The presence of the lake also made available a wide variety of food plants; Melamed et al. (2016) identified 9148 plant remains of 55 taxa including nuts, fruits, seeds, vegetables and plants with underground storage organs. Among these, staple plant remains and all-season food plant species were abundantly found in archaeological layers, indicating year-round occupations. Evidence of the use of fire and of particular stone tools in the processing of unpalatable foods, point to the hominins' expertise in dealing with these foods and an adaptation to a Eurasian diet that would have enhanced their survival during the further dispersal into Eurasia (Melamed et al., 2016). Most of these data derived from the rich sites located above the MBB, where although the particular behavioural patterns differ between Acheulian archaeological horizons, the material culture remains are consistently similar to each other in their techno-morpho-typological characteristics, pointing to a strong and continuous tradition displaying cognitively advanced hominin abilities (Goren-Inbar et al., in press), during MIS 18. They also show that the GBY hominins were present for a long duration in the Hula Valley and that they knowingly exploited their environment, which provided them with a stable and wide spectrum of subsistence sources. In order to extend our knowledge of the Early–Middle Pleistocene transition (Head and Gibbard, 2005), in 2006 we drilled a core designated GBY#2 from the GBY archaeological site (Fig. 1) and initiated a study of the sediment of this core.

The research objectives of this study were to analyse the depositional processes and to reconstruct palaeoenvironments during the Early–Middle Pleistocene transition, when hominins diffused along the Upper Jordan Valley. The perceived outcomes of this multi-proxy study were to enhance the biostratigraphic framework of the area and provide a better understanding of the interaction between climatic changes and environmental conditions during the recorded period.

2. Regional setting

2.1. Location

Excavations of the Acheulian site of GBY were located on the eastern bank of the Jordan River, about 4 km to the south of the recent Lake Hula at ITM E 200417 m and N 767274 m, on the margin of the Hula Palaeo-lake in northern Israel (Goren-Inbar et al., 2000). The drilling point of the GBY#2 core was located at the eastern end of the current southern bridge, some 300 m north of the GBY excavation site, at ITM E 259080 m and N 768450 m (Fig. 1).

2.2. Geological setting

The GBY site is located at the major transform fault of the Dead Sea Rift that connects the spreading area of the Red Sea to the Zagros-Taurus zone. Along this plate boundary, the Arabian Plate shows a sinistral displacement from the African Plate, which has been active since the Neogene (Belitzky, 2001, 2002). The GBY#2 core site is situated in the complex Quaternary tectonic setting of the pull-apart Hula Basin (Belitzky, 2002). The Hula Basin belongs to the North Jordan Valley geomorphological unit, which is elevated ca. 70 m above sea level and intersected by the Jordan River through the deeply incised narrow basaltic canyon downstream of GBY (Horowitz, 1979).

The Benot Ya'akov Formation is exposed along a narrow valley at the Jordan River bank, which extends for about 1 km to the south and about 1.5 km to the north of the Benot Ya'aqov Bridge (Horowitz, 1973), mainly due to erosion of the Jordan River and recent drainage operations (Goren-Inbar et al., 1992). Palaeomagnetic investigations of the GBY excavation site (Goren-Inbar et al., 2000) and other important archaeological, geological and geochronological studies of the same section (Goren-Inbar et al., 2000, 2002b; Spiro et al., 2009) have demonstrated that this formation was developed at ca. 800–700 ka, during MIS 20–18 (Feibel, 2009, personal communication; Goren-Inbar et al., 2000). These results point to older ages than those indicated by previous studies, which concluded that the Benot Ya'akov Formation is composed of Rissian (ca. MIS 10–6) sediments (Horowitz, 1973, 1975, 1979). Cenozoic volcanic rocks are also common in the local stratigraphy (Horowitz, 1979). The GBY excavation shows that the Benot Ya'akov Formation is composed of fluvio-lacustrine sedimentary rocks showing three dominant lithofacies: beach (coquina, sand and gravel), shallow lacustrine (calcareous mud) and fluvial channel (conglomerate) (Feibel, 2004; Feibel, 2001; Goren-Inbar et al., in press). The depositional record demonstrates excellent preservation and high diversity of floral remains and faunal fossils in addition to revealing outstanding archaeological remains of the Acheulian culture (Goren-Inbar and Sharon, 2006; Goren-Inbar et al., 1992, 2000, 2002a, 2002b; Van Zeist and Bottema, 2009).

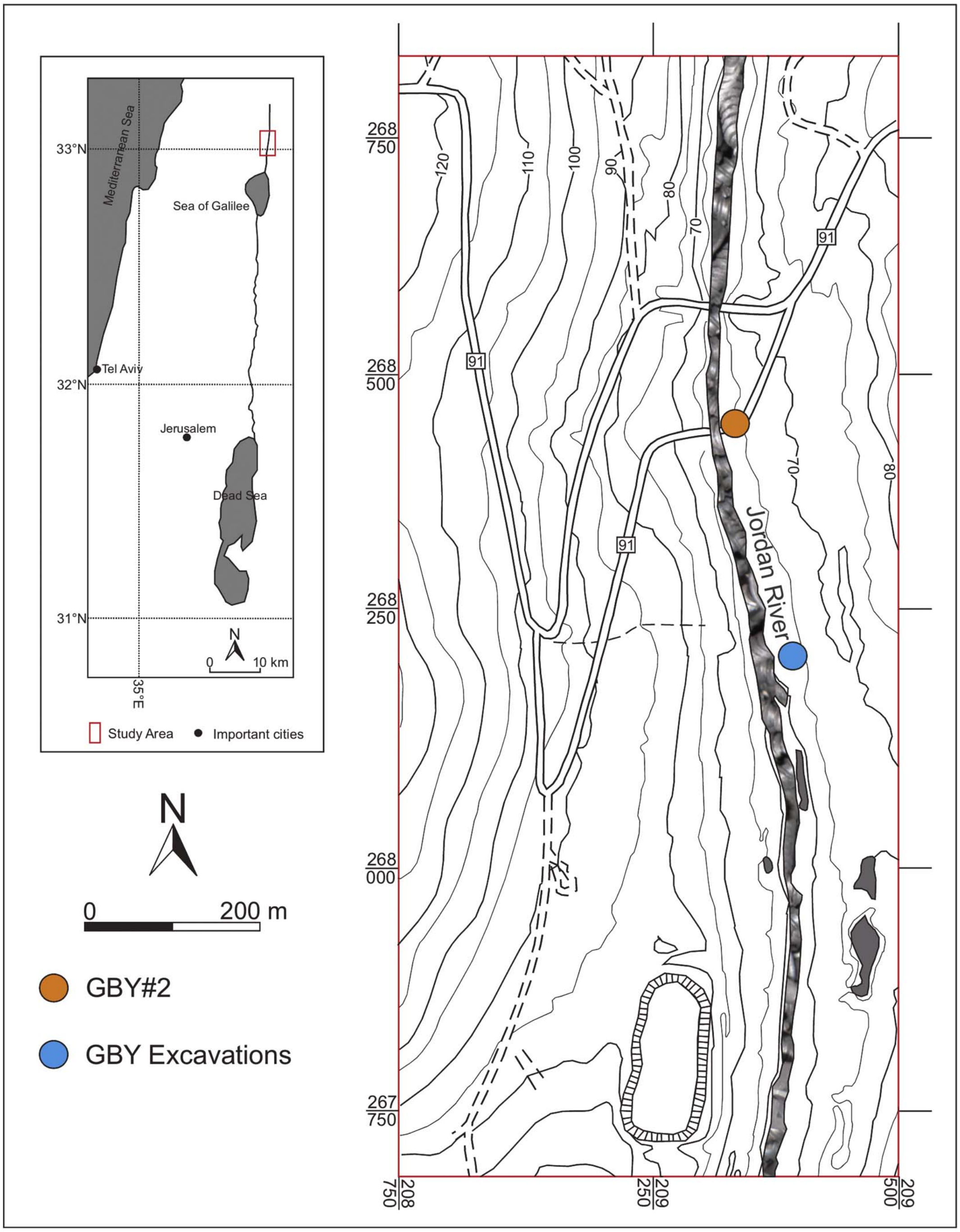

Fig. 1. Location map of the GBY site (after Horowitz, 1987) including position of the GBY excavation (after Goren-Inbar et al., 1992; Van Zeist and Bottema, 2009) and GBY#2 core drilling points.

2.3. Climate and vegetation

The GBY area is dominated by a Mediterranean climate with cool, wet winters and hot, dry summers and a mean annual temperature of 21 °C (Van Zeist and Bottema, 2009; Van Zeist et al., 2009). Referring to the vegetation map of the Middle East (Frey and Kürschner, 1989), the potential natural vegetation around the study area is dominated by Eu-Mediterranean vegetation composed mainly of evergreen species. Below 300 m altitude, a Ceratonio-Pistacion lentisci maquis dominates. At higher altitudes, a Quercion calliprini belt is found up to 1200 m. Open woodland dominated by *Quercus ithaburensis* originally covered a broad area of northern Israel below 500 m altitude. Danin (1992) suggests a vegetation map of Israel, which shows savannoid Mediterranean vegetation in the vicinity of the GBY#2 core site. According to Zohary (1982), the alluvial plain is surrounded by semi-steppe chamaephytic and hemicryptophytic shrublands. Although trees are rare in this environment, *Pistacia atlantica* and *Quercus ithaburensis* dominate the semi-steppe forests, which usually occur together with or are replaced by the main shrubland communities of *Ziziphus lotus* or *Ziziphus spina-christi*.

3. Material and methods

3.1. Lithological investigations

The 50 m sequence of the GBY#2 core is composed of sediments about 23 m thick intercalated between two basalt layers, the underlying

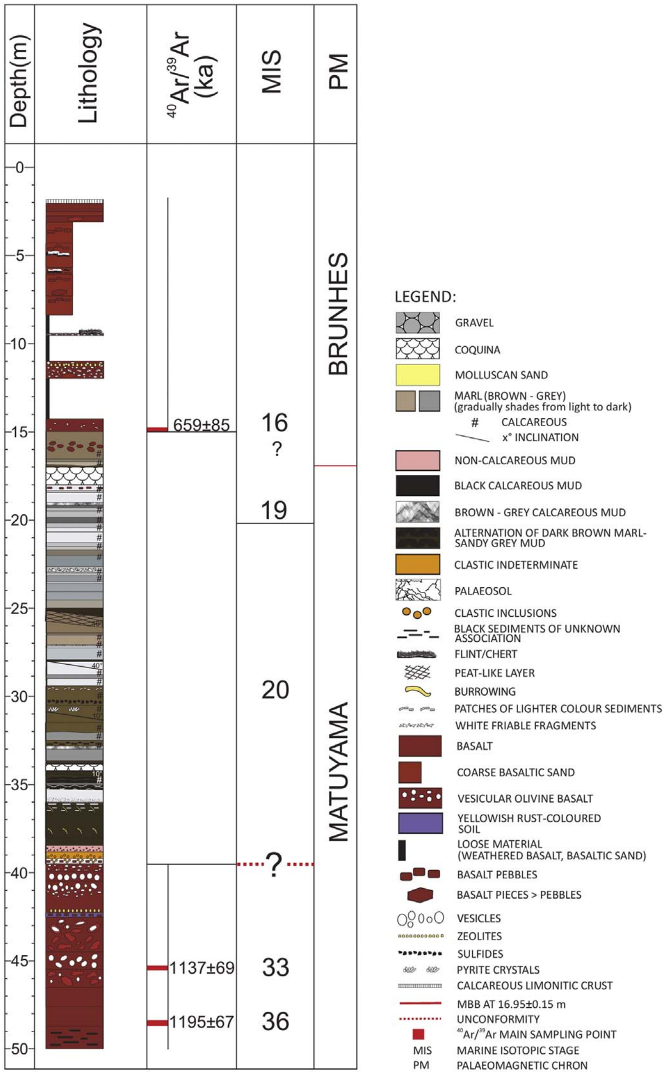

Lithological column is modified from Spiro and Sharon (unpublished report, 2008)

Fig. 2. Lithological composition of the GBY#2 core (Spiro and Sharon, unpublished report, 2008), $^{40}Ar/^{39}Ar$ dating results, MIS subdivision and palaeomagnetic chrons.

basalt between ca. 50.00 and 39.50 m and the overlying basalt between ca. 16.50 and 1.00 m (Fig. 2). Based on the detailed lithological observations and descriptions of the core (Spiro and Sharon, 2008) (Fig. 2), larger and smaller pieces of basalt are found from 50.00 m onwards, containing denser and larger vesicles towards 39.50 m (Fig. 3A). Between about 42.50 and 39.50 m, basalts weathered in various degrees are identified. The overlying sediments between 39.50 and 36.10 m are composed of calcareous marl with clastic mixtures at the bottom succeeded by dark brown marl showing bioturbation at 36.96 m. At 36.10–32.60 m, there are more sandy sediments which are often rich in well-preserved mollusc shells and shell fragments (Fig. 3B). Marls, calcareous marls and sandy marls with shells and shell fragments alternate.

The sediments between 32.60 and 28.00 m are mainly composed of dark brown to grey calcareous marl with mixtures of sand and mollusc fragments in thin sandy lenses at about 31.80 m, while a thin peat layer occurs at approximately 28.70 m. Between 28.00 and 25.30 m, a sequence of calcareous marl, marl, sandy marl with gastropod shells (Fig. 3C) and brown calcareous marl rich in small wood fragments was deposited. This sequence is overlaid by brown marl and a thin peaty layer. Lithology of the subsequent sediments, between 25.30 and 20.15 m, includes layers of peat, dark brown marl and grey sandy marl, which again are overlaid by a massive calcareous marl layer (Fig. 3D)

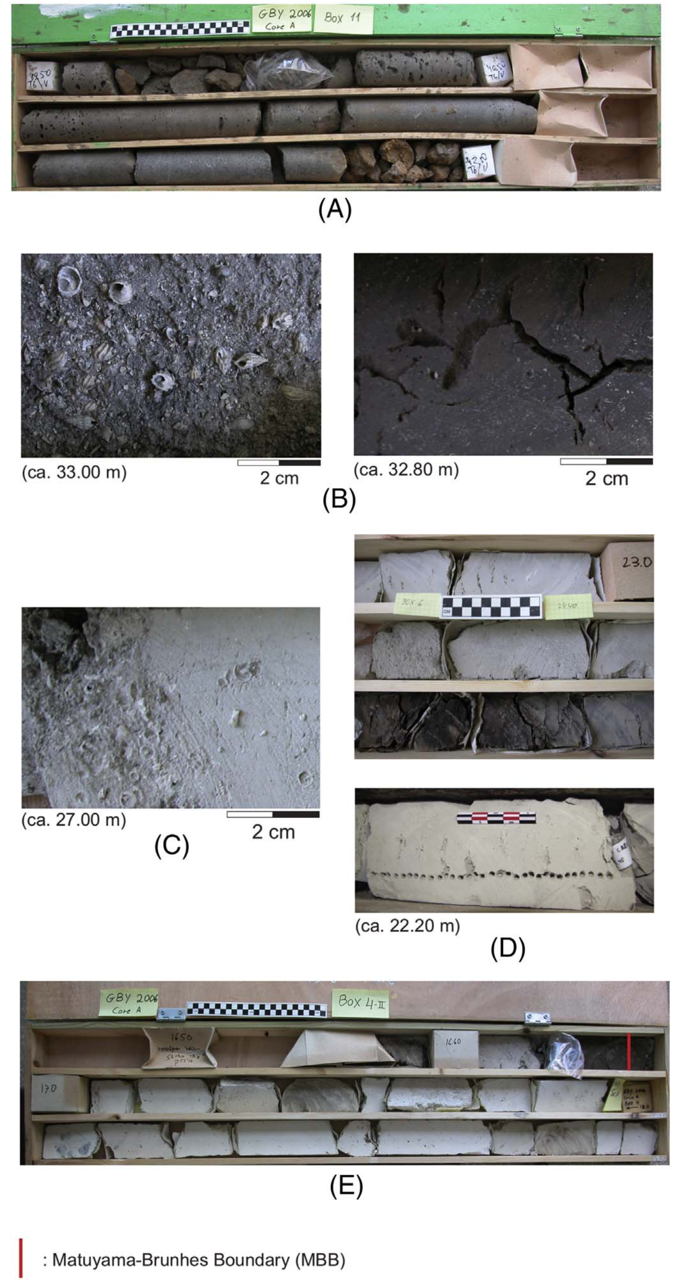

Fig. 3. Photographs of the GBY#2 core section showing: (A) underlying basalt between ca. 39.50 and 42.50 m, (B) grey sandy marl containing mollusc shells and bioclasts at ca. 33.00 m and brown calcareous mud with dispersed mollusc shells at ca. 32.80 m, (C) transition from grey mollusc-rich to brown sandy marl at ca. 27.00 m, (D) above: transition from brown marl to low density peat in the lowermost row, changes from sandy sediment to light grey marl in the middle row and massive light grey calcareous marl in the topmost row; below: light grey calcareous marl with sparse and poorly preserved molluscs at ca. 22.20 m, (E) light grey calcareous marl with mollusc shells between ca. 19.00 and 16.90 m. (For interpretation of the references to colour in this figure legend, the reader is referred to the web version of this article.)

that shows poor preservation of mollusc and is often sterile. Between 20.15 and 16.80 m, sediments are composed of massive calcareous marl with mollusc shells and fragments (Fig. 3E). Core loss occurred between 16.60 and 15.00 m; only loose basalt pieces and calcareous marl with mollusc fragments are found. Loose pieces of weathered basalts compose the lithological sequence at 15.00–8.30 m. From 8.30 to about 3.10 m, coarse basaltic sands are found below a large piece of basalt, which is overlaid by a limonitic crust at about 2.00–1.80 m.

3.2. $^{40}Ar/^{39}Ar$ dating

We selected three fresh samples from depths of about 48.30, 45.30 and 14.90 m for $^{40}Ar/^{39}Ar$ dating (Fig. 2) and carefully hand-picked 300 mg of unaltered groundmass chips for each sample. The chips were further leached in diluted HF for 1 min and then thoroughly rinsed with distilled water in an ultrasonic cleaner.

Samples were loaded into two large wells of one aluminium disc, 1.9 cm in diameter and 0.3 cm deep. These wells were bracketed by small wells that included Fish Canyon sanidine (FCs) used as a neutron fluence monitor for which an age of 28.294 ± 0.036 Ma (1σ) was adopted (Renne et al., 2011). The discs were Cd-shielded (to minimize undesirable nuclear interference reactions) and irradiated for 2 h in the Hamilton McMaster University (Canada) nuclear reactor in position 5C. The mean J-values computed from standard grains within the small pits and determined as the average and standard deviation of J-values of the small wells for each irradiation disc are given along with the raw data in Supplementary Tables A.1.1–3. Mass discrimination is given in the supplementary table for each sample and was monitored using an automated air pipette and calculated relative to an air ratio of 298.56 ± 0.31 (Lee et al., 2006). The correction factors for interfering isotopes were $(^{39}Ar/^{37}Ar)_{Ca} = 7.30 \times 10^{-4}$ (± 11%), $(^{36}Ar/^{37}Ar)_{Ca} = 2.82 \times 10^{-4}$ (± 1%) and $(^{40}Ar/^{39}Ar)_K = 6.76 \times 10^{-4}$ (± 32%) for the McMaster reactor and (39Ar/37Ar)Ca = 7.06 × 10–4 (± 7%), (36Ar/37Ar)Ca = 2.81 × 10–4 (± 3%) and (40Ar/39Ar)K = 6.76 × 10–4 (± 10%) for the USGS TRIGA reactor.

The $^{40}Ar/^{39}Ar$ analyses were performed at the Western Australian Argon Isotope Facility at Curtin University. The three samples were step-heated in a double vacuum high frequency Pond Engineering© furnace. The gas was purified in a stainless steel extraction line using two AP10 and one GP50 SAES getters and a liquid nitrogen condensation trap. Ar isotopes were measured in static mode using a MAP 215-50 mass spectrometer (resolution of ~400; sensitivity of 4×10^{-14} mol/V) with a Balzers SEV 217 electron multiplier using 9 to 10 cycles of peak-hopping.

The data acquisition was performed with the Argus program written by M.O. McWilliams and run under a LabView environment. The raw data were processed using the ArArCALC software (Koppers, 2002) and the ages have been calculated using the decay constants recommended by Renne et al. (2011). Blanks were monitored every 3 to 4 steps and typical ^{40}Ar blanks range from 1×10^{-16} to 2×10^{-16} mol. Ar isotopic data corrected for blank, mass discrimination and radioactive decay are given in Supplementary Tables A.1.1–3. Individual errors in Supplementary Tables A.1.1–3 are given at the 1σ level. Our criteria for the determination of plateaus are as follows: they must include at least 70% of ^{39}Ar and they must be distributed over a minimum of 3 consecutive steps agreeing at the 95% confidence level and satisfying a probability of fit (P) of at least 0.05. Plateau ages (Fig. 2, Supp. Fig. B.1) are given at the 2σ level and are calculated using the mean of all plateau steps, each weighted by the inverse variance of their individual analytical error. Inverse isochrons include the maximum number of steps with a probability of fit ≥ 0.05. S-factors showing the spread along the inverse isochron (Jourdan et al., 2009) and $^{40}Ar/^{36}Ar$ intercept values are provided. All sources of uncertainties are included in the calculation.

3.3. Palaeomagnetism

A first set of 20 pilot palaeomagnetic samples was taken at targeted stratigraphic intervals of ca. 100 cm. This pilot sampling was later complemented by a second set of 10 samples at stratigraphic intervals of ca. 30 cm upon determining the approximate position of the targeted paleomagnetic reversal following the analysis of the pilot samples (Table 1). The sampling positions were determined at a precision of centimetres with respect to the surface reference level of the GBY#2 core. For the first set of 20 pilot samples, standard 2.5-cm-diameter cylindrical palaeomagnetic cores were taken from the GBY#2 core-halves with an electric drill mounted with a diamond-coated bit and cooled with water or air depending on the lithological properties. The second set of samples consisted of cubes carved into soft sediments using non-magnetic blades. The samples were oriented perpendicular to the up-down orientation of the GBY#2 core. Because of the random rotations of the GBY#2 core segments during drilling, the declination of the samples with respect to North could not be determined.

Palaeomagnetic analyses were performed in the shielded environment of the Rennes University palaeo-archaeomagnetic laboratory. The Natural Remanent Magnetization (NRM) was measured using a 2G Enterprises DC SQUID cryogenic magnetometer. The NRM was demagnetized stepwise using either the 2G in-line degausser for Alternating Field (AF) demagnetization or an MMTD shielded oven for thermal demagnetization. Demagnetization paths were interpreted on vector end-point diagrams and stereographic projections to isolate magnetic components and identify the Characteristic Remanent Magnetizations (ChRM) (Dupont-Nivet et al., 2008) (Fig. 4).

3.4. Palynology

From the sediments of the GBY#2 core, 41 palynological samples were taken. This sampling was mostly conducted at intervals of 5 to 75 cm. Samples were not collected from the calcareous marl between 32.50 and 29.90 m, the sandy marl between 26.65 and 25.40 m or the calcareous marl between 25.40 and 20.40 m, due to the expected poor preservation of pollen.

Carbonates were removed from about 7–10 g sediment per sample with 10% HCl. The residues were then treated in KOH and the organic compounds were separated from the inorganic ones by $Na_6[H_2W_{12}O_{40}]$. The organic remains were subsequently treated with CH_3COOH. Non-palynomorph organic remains were removed by acetolysis using H_2SO_4 and $[CH_3CO]_2O$ solution. The extracted palynomorphs were stained during this process to ease later microscopic identification (Faegri and Iversen, 1989; Moore et al., 1991). The extracted residues were mounted in glycerine and palynomorphs were identified to the family, genus or species level depending on the pollen type and preservation status, using pollen atlases (Beug, 2004, 2015; Faegri and Iversen, 1989; Moore et al., 1991; Reille, 1995, 1998, 1999) and the reference collections of the Palynology Laboratory of the Institute of Ecology, Leuphana University of Lüneburg.

At least 300 grains of arboreal pollen (AP) were counted per sample and a minimum of 350 grains of total AP and non-arboreal pollen (NAP) were counted from samples that contained very little AP. At least 100 pollen grains were counted from the samples that are particularly poor in pollen. Pollen and spores of Cyperaceae, cryptogams, aquatic taxa and the locally over-represented palynomorphs such as cf. *Solanum dulcamara*, *Primula clusiana*-type and *Mentha*-type were excluded from the basic sum (the sum of AP and NAP). Pollen percentages were calculated and the pollen diagram was plotted using the TILIA software package (Grimm, 1990). The actual percentages are represented by closed curves in colour and the 10 times exaggeration of the actual percentage values is represented by open curves with depth bars, to make the low-values taxa that occur in high frequencies more noticeable. Taxa that occur in very low frequencies and percentages were excluded from the pollen diagram and are presented separately (Table 2). The varia group is composed of unknown, respectively indeterminable NAP. Micro-charcoal particles smaller than 100 μm encountered during pollen counting were also counted and represented by an individual semi-log curve for each 24 × 32 mm slide. A combination of cluster analysis (CONISS) (Grimm, 1987) and conventional interpretation was used to define Local Pollen Assemblage Zones (LPAZ).

The aridity index, the (*Artemisia* + Amaranthaceae)/Poaceae or (Ar + Am)/P ratio, was calculated after Cour and Duzer (1978) and Fowell et al. (2003), where *Artemisia* and Amaranthaceae are characteristic of dry steppic environments, whereas Poaceae represent relatively moister

Table 1
Palaeomagnetism measurements of the GBY#2 core.

Depth (m)	Rock	Demag	Dec (°)	Inc (°)	Int (mA/m)	MAD (°)	Line	Q	Pol
11.20	Basalt	AF	20.5	32.0	763,898	1.0	Free	1	N
14.90	Basalt	AF	50.2	29.2	1,213,246	0.4	Free	1	N
16.80	Sediments	Th	191.1	70.9	2043	5.5	Free	1	N
REVERSAL									
17.10	Sediments	Th	109.6	− 64.0	7245	5.6	Forced	2	R
17.40	Sediments	Th	No interpretable result						?
17.85	Sediments	Th	340.5	− 59.0	1023	7.9	Free	2	R
18.35	Sediments	Th	47.0	− 39.5	1804	5.1	Free	1	R
18.65	Sediments	Th	65.7	− 37.0	2238	7.6	Forced	2	R
18.90	Sediments	Th	No interpretable result						?
19.05	Sediments	Th	30.8	− 32.2	5432	24.7	Forced	3	?
19.40	Sediments	Th	92.2	− 55.1	3318	8.4	Forced	2	R
19.65	Sediments	Th	189.5	− 48.9	7067	3.0	Free	1	R
19.90	Sediments	Th	172.4	− 26.8	7824	8.3	Free	1	R
20.25	Sediments	Th	301.7	− 54.7	3452	11.6	Free	1	R
20.75	Sediments	Th	240.8	− 29.2	5934	4.4	Free	1	R
21.40	Sediments	Th	282.6	− 54.3	2270	10.2	Free	1	R
23.20	Sediments	Th	225.2	− 55.7	4102	3.8	Free	1	R
26.20	Sediments	Th	1.8	− 30.5	1128	9.0	Free	1	R
27.90	Sediments	Th	305.0	− 42.6	2875	5.4	Free	1	R
28.80	Sediments	Th	No interpretable result						?
31.30	Sediments	Th	No interpretable result						?
33.60	Sediments	Th	No interpretable result						?
36.70	Sediments	Th	No interpretable result						?
38.70	Sediments	Th	No interpretable result						?
40.50	Basalt	AF	29.1	− 59.3	1,520,806	1.7	Free	1	R
41.50	Basalt	AF	323.8	− 17.7	106,401	1.6	Free	1	R
42.30	Basalt	AF	198.6	− 62.2	267,214	0.8	Free	1	R
44.10	Basalt	AF	339.3	− 47.7	2,033,559	0.3	Free	1	R
45.00	Basalt	AF	312.7	− 43.8	1,598,266	0.6	Free	1	R
46.50	Basalt	AF	2.2	− 44.5	1,014,902	1.1	Free	1	R
48.60	Basalt	AF	288.6	− 62.6	965,181	0.7	Free	1	R

Depth in m below surface, Rock: rock type, Demag: demagnetization procedure applied (AF: alternating field, Th: thermal), Dec: declination of interpreted ChRM direction, Inc.: inclination of interpreted ChRM direction, Int: intensity of ChRM direction, MAD: Maximum Angular Deviation on line fit performed to determine ChRM direction, Line: type of line fit applied (free or forced to the origin), Q: quality of direction and polarity determination (1: reliable direction and polarity, 2: reliable polarity but unreliable direction, 3: unreliable polarity and direction), Pol: Polarity determination (N: normal, R: reversed,?: undetermined).

conditions of steppe, shrub-steppe and woodlands that are more or less similar to the distribution of vegetation around the study area (Danin, 1992; Van Zeist and Bottema, 1991; Van Zeist et al., 2009). The Amaranthaceae family is composed mainly of the Chenopodiaceae subfamily, which was formerly grouped as a separate family. Grass pollen cannot be further determined except for Cerealia-type pollen, which can be separated by grain size (> 37 μm) (Beug, 2015). At the GBY site, Cerealia-type pollen might have originated from wild cereals and grass species such as *Aegilops* (Van Zeist and Bottema, 2009), part of the local marsh and understory vegetation of the *Quercus ithaburensis-Pistacia terebinthus* woodland (Van Zeist and Bottema, 2009).

The (Ar + Am)/P curve and other climate-related signals, such as the AP/NAP ratio, representation of *Ephedra fragilis*-type pollen and the *Cedrus* curve (Figs. 5 and 6) were used to construct and interpret the palaeoclimatic cycles. Species of *Ephedra* are found in deserts, semi-deserts, desert steppes or seasonally dry habitats (Ickert-Bond and Renner, 2016). In the GBY#2 core, only pollen of *Ephedra fragilis*-type has been found, perhaps deriving from *Ephedra aphylla*, which is currently distributed in the Upper Jordan Valley (Danin, 2003), or from *Ephedra foeminea*, which is a common species of the Mediterranean maquis. *Cedrus* indicates higher humidity that is likely related to an increase in precipitation or a cooler Mediterranean climate (Van Zeist and Bottema, 2009). These authors also argue that this taxon was probably a component of the altitudinal montane belt.

3.5. Plant macro-remains

Samples for macro-botanical analyses were obtained from the same depths as the pollen samples. A total of 20 small-volume samples (40–107 cm^3), from between 38.70 and 16.60 m at intervals of 20 cm to 2.2 m, were analysed (Fig. 7). A list of macro-botanical counts is found in Supplementary Table A.2. Quantitative comparison between the percentages of plant macro-remains and the mean pollen percentages (Van Zeist and Bottema, 2009) was conducted mainly to assess local environmental conditions and possible factors that influence the distribution of vegetation. The percentage calculations of the macro-remains were based on the total macro-remains found in the sample excluding indeterminate taxa, *Stratiotes intermedius*, *Azolla* cf. *filiculoides* and *Salvinia* sp. (Fig. 8), while the mean pollen percentages were calculated based on the percentage sum of each taxon with respect to the total AP, divided by the total number of the analysed samples. For a better comparison with the pollen data, some macro-remain taxa were grouped into the respective family.

3.6. Molluscs and ostracods

At the same depths as the pollen samples, 39 samples were taken for mollusc and ostracod analyses based on the sediment types and expected good preservation. Molluscs and ostracods were extracted from the sediments using the detergent soaking method (Snyder and Huber, 1996). About 5–7 g of samples were treated in detergent solution for 24 h and washed under flowing water using a standard sieve number 270 (63 μm). The retained material was dried at 105 °C for three to five hours. Fossils were picked and preserved in vials. Well-preserved molluscs were identified to species level and recorded as presence-absence data (Fig. 9). In addition, all mollusc shells were counted and mostly identified to genus level due to the poor preservation of some of the counted specimens. The ostracod valves were all counted and identified

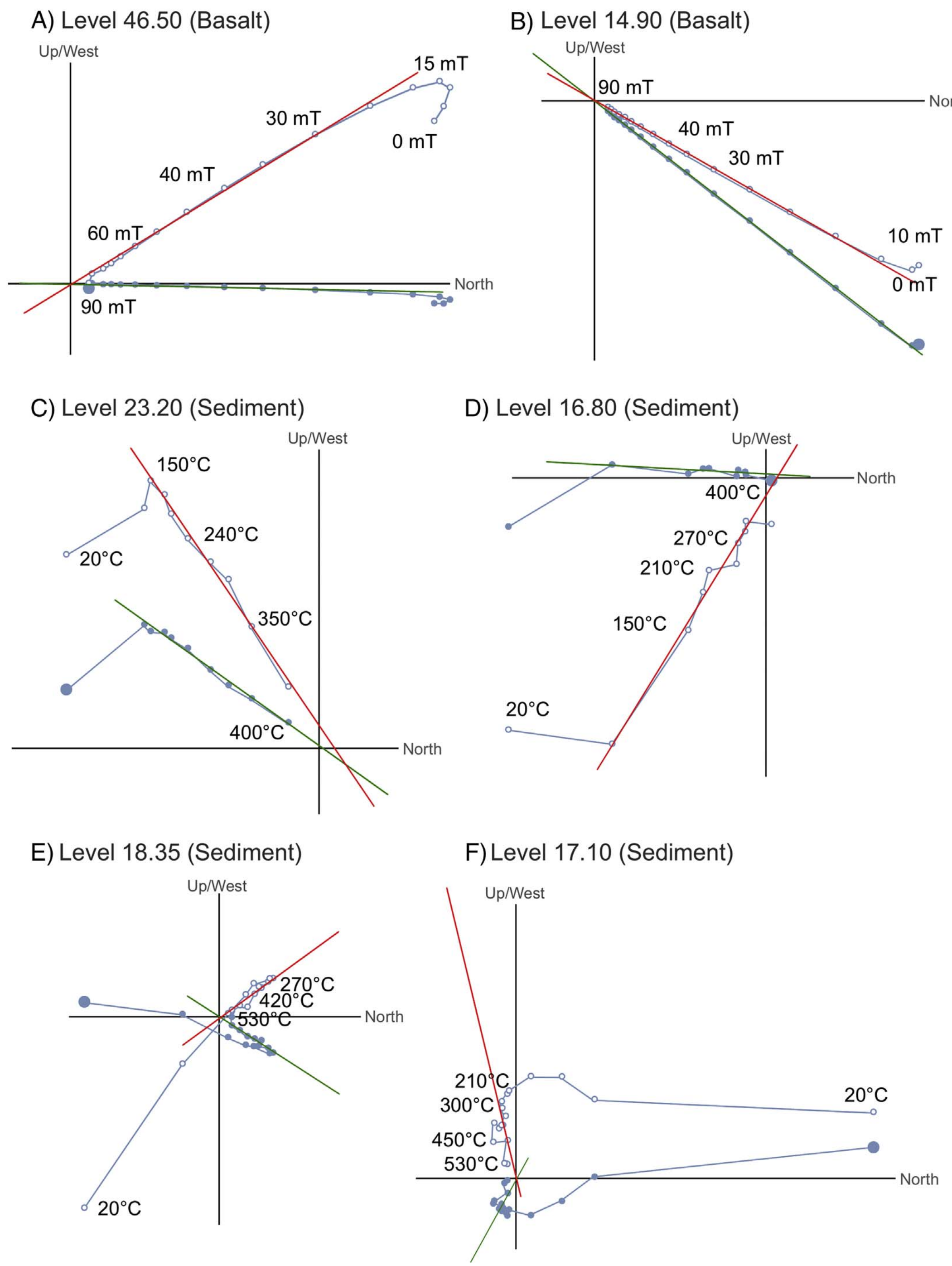

Fig. 4. Typical demagnetization diagrams. Full (open) symbols are vector projections of the Natural Remanent Magnetization (NRM) in the horizontal (vertical) plane. Line fits are indicated by green (red) lines on the horizontal (vertical) plane. (A) and (B) show alternating field demagnetizations of basaltic samples. (C), (D), (E) and (F) show thermal demagnetizations of sedimentary samples. Note the secondary low temperature component (LTC) well separated from the high temperature component (HTC) in (E) and overlapping the HTC in (F) where the line fit was forced through the origin. (For interpretation of the references to colour in this figure legend, the reader is referred to the web version of this article.)

to species level apart from two specimens of *Ilyocypris* sp. A list of mollusc and ostracod counts is found in Supplementary Table A.3.

4. Results

4.1. $^{40}Ar/^{39}Ar$ dating

Samples from the underlying basalt, GBYH2–48.30 and GBYH2–45.30, yielded well-defined plateau ages of 1195 ± 67 ka (MSWD = 1.19; P = 0.30) and 1137 ± 69 ka (MSWD = 0.47; P = 0.90) respectively (Fig. 2, Supp. Fig. B.1). Inverse isochron plots for those two samples yielded ages of 1024 ± 183 ka ($^{40}Ar/^{36}Ar$ = 319 ± 22) and 1097 ± 165 ka ($^{40}Ar/^{36}Ar$ = 303 ± 18) indistinguishable from the plateau ages within error and with trapped $^{40}Ar/^{36}Ar$ values indistinguishable from the atmospheric composition of 298.6 ± 0.1 (Lee et al., 2006) adopted in this study. We interpret the two plateau ages of 1195 ± 67 and 1137 ± 69 ka as indicating the eruption ages of these basalts. A sample from the overlying basalt, GBY14.9, yielded a much younger plateau age of 659 ± 85 ka (MSWD = 0.66; P = 0.81) (Fig. 2, Supp. Fig. B.1) and an inverse isochron age of 638 ± 118 ka ($^{40}Ar/^{36}Ar$ = 299.8 ± 2.4). We interpret the plateau age of 659 ± 85 ka as indicating the eruption age of this basalt.

Table 2
Percentages of taxa that are not included in the GBY#2 pollen diagram in relation to the Local Pollen Assemblage Zones (LPAZ).

Depth (m)	LPAZ	Pollen taxon											
		cf. *Ziziphus spina-christi*	*Pimpinella*-type	*Anthemis*	Brassicaceae	*Papaver rhoeas*-type	*Polygonum aviculare*	Ranunculaceae	Saxifragaceae	*Scabiosa palestina*-type	*Ammi majus*	*Ferula*-type	*Pediastrum duplex*
17.10	GBY#2-5	0.6	–	–	–	–	–	–	–	–	–	–	–
17.85		–	–	–	1.3	–	–	–	–	0.8	–	–	–
18.35		–	–	–	–	0.7	–	–	–	0.7	–	0.7	–
18.90		–	–	–	–	–	–	0.7	–	0.9	0.2	–	–
19.05		–	–	–	–	–	–	–	–	0.2	–	–	–
19.90		–	–	–	–	–	–	–	–	–	1.1	–	–
20.40	GBY#2-4	–	1.6	1.4	–	–	0.2	0.5	0.7	–	–	0.5	–
25.40		–	1.1	–	–	0.2		0.2	1.1	–	–	–	–
27.00		–	–	–	–	–	–	–	–	–	0.9	0.9	–
28.25	GBY#2-3	–	–	–	–	–	–	–	–	–	0.3	–	–
28.50		–	–	–	–	–	0.6	–	–	–	14.4	–	–
29.00		0.4	–	–	–	–	0.7	–	–	–	1.1	–	–
29.20		–	–	–	–	–	0.2	–	–	–		12	–
29.45		–	–	–	–	–		–	0.7	–	–	–	–
29.90		–	0.4	–	–	–	–	–	–	–	–	–	–
32.50		–	–	–	–	1	–	–	–	–	–	–	–
34.00	GBY#2-2	–	–	–	–	1	–	–	–	–	–	–	–
35.10		–	–	–	1	–	–	–	–	–	–	–	–
38.30	GBY#2-1	–	0.5	–	–	–	–	–	–	–	–	–	–
39.10		–	0.1	–	–	–	–	–	–	0.1	–	–	–
39.30		–	–	0.2	–	–	–	–	–	–	–	–	0.2
39.40		–	–	–	–	–	–	–	–	–	–	–	1

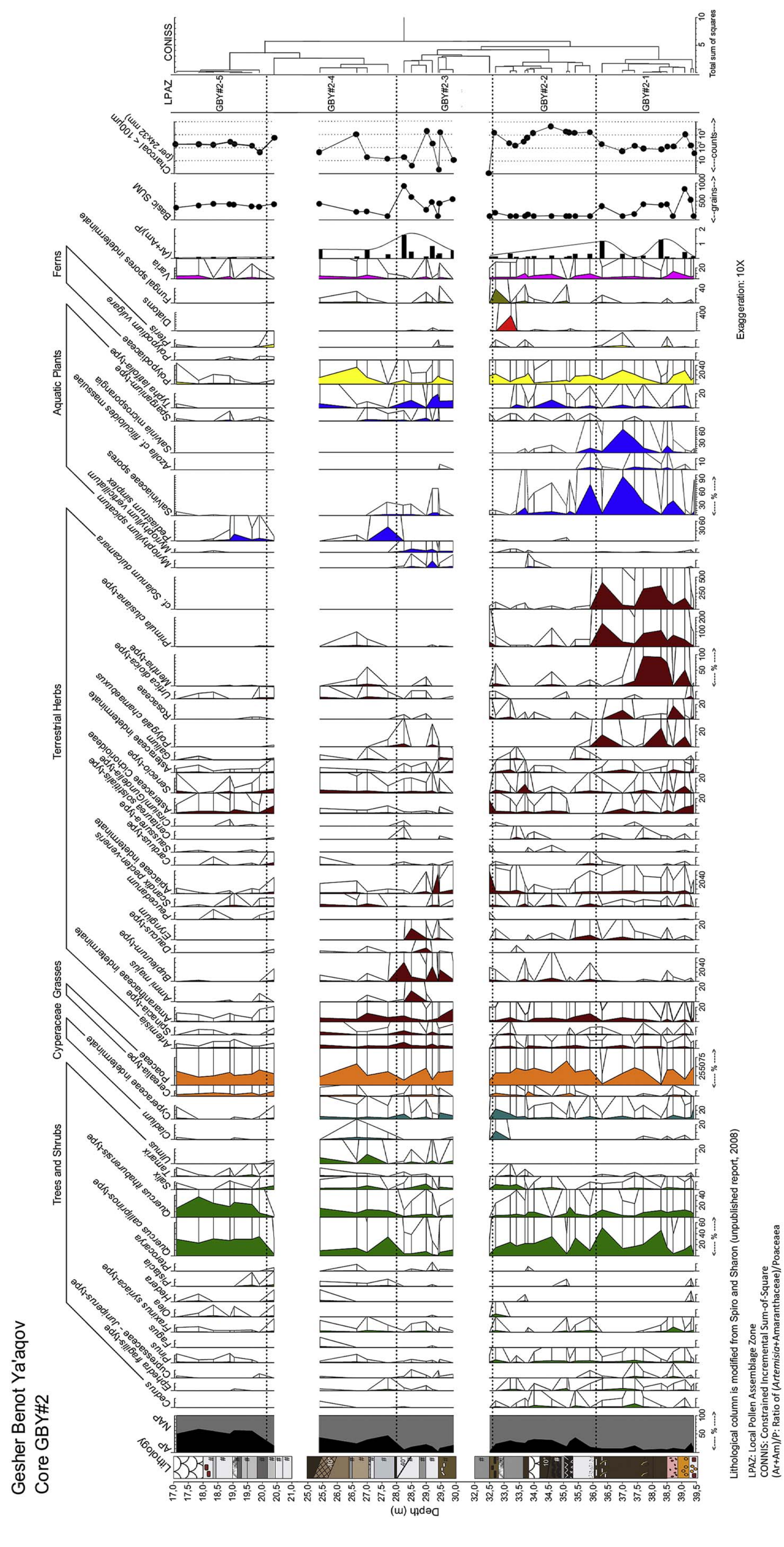

Fig. 5. Pollen diagram of the GBY#2 section between 39.50 and 17.00 m. The diagram is divided into five Local Pollen Assemblage Zones (LPAZ), based on the cluster analyses (CONISS) and conventional interpretation. For a detailed description of the lithological symbols see Fig. 2.

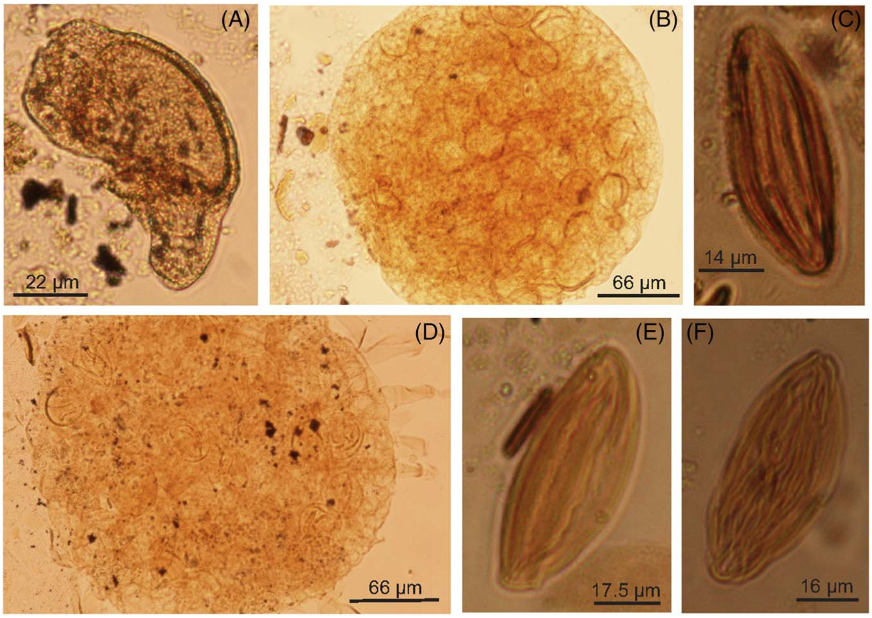

Fig. 6. Pollen of: (A) *Cedrus* at 37.40 m, (B) *Salvinia* massulae at 35.90 m, (C) *Ephedra fragilis*-type at 29.20 m, (D) *Azolla filiculoides* massulae at 35.90 m, (E–F) *Ephedra fragilis*-type at 28.25 m. Total magnification: 400 ×.

4.2. Palaeomagnetism

Pilot samples were stepwise demagnetized in detail with thermal as well as AF treatments in order to determine characteristic demagnetization behaviour and the best demagnetization procedure for each lithological section. Basaltic samples yielded excellent AF demagnetization of most of the NRM linearly pointing towards the origin (Fig. 4). All basaltic samples were thus demagnetized by AF treatments using the following 17 steps (0, 5, 10, 15, 20, 25, 30, 35, 40, 45, 50, 55, 60, 65, 70, 80, 90 mT). For all these samples, after occasional removal of a low coercivity component (LCC) below 15 mT, the unblocking spectrum indicates a higher coercivity component (HCC) with a relatively soft magnetic mineralogy such as magnetite typical of basalts.

For detrital sediments, thermal treatment yielded better demagnetization paths than AF and was therefore used for all subsequent analyses. Samples were demagnetized until reaching the origin using thermal treatment with the following steps (20, 100, 150, 180, 210, 240, 270, 300, 330, 360, 390, 420, 480, 510, 530, 550, 570 °C). Initial NRM has generally low intensities (Table 1) but demagnetization paths decay in linear fashion towards the origin, usually following two distinct ChRM components (Fig. 4). A low-temperature component (LTC) is typically demagnetized between about 20 and 250 °C. A high-temperature component (HTC) decays between about 250 and 400 °C, sometimes extending up to 550 °C. However, in some samples, the HTC was poorly preserved, sometimes partially overprinted by the overlapping LTC, such that they did not yield reliable directions.

The LCC and LTC are found exclusively with a normal polarity orientation (based on inclination alone because of the absence of orientation on the GBY core), while the higher coercivity and HTC show normal and reverse polarity. This clearly identifies the low coercivity and LTC as a normal overprint and suggests a primary magnetization for the HTC. In a majority of samples, the HTC is well expressed, enabling straightforward isolation of normal or reversed polarity inclinations.

ChRM directions were calculated using least square analysis (Kirschvink, 1980) on a minimum of four consecutive steps of the HTC. Line fits were not anchored to the origin except for four demagnetizations. ChRM directions have a Maximum Angular Deviation (MAD) below 25° for sediments (average of 6.6°) and below 2° for basalts (average of 0.6°).

Normal and reversed polarity directions were clearly identified on the HTC with linear decay extending through several temperature steps up to 400–450 °C (quality-1 directions, Table 1) for 19 samples. There are three samples with a clear reversed polarity, but the directions are less reliable (quality-2 directions) because of directional scatter and/or LTC overlap on HTC resulting in directions slightly divergent from ideal univectorial decay towards the origin. Unreliable direction (quality-3 directions) is identified in one sample and no interpretable results could be obtained from seven other samples. In these samples, polarity determination is ambiguous due to weak magnetization, scattered direction and a strong normal polarity LTC extending up to 450 °C partially or fully overprinting the HTC. The resulting set of 23 quality-1 and -2 ChRM directions provides reliable palaeomagnetic polarity throughout the sampled section. The polarity determination relied mainly on the inclination of the remanent magnetization expected at 50° at this latitude and is in good agreement with the average 39° inclinations for sediments and 44° for basalts. The slightly lower values in sediments probably reflect inclination shallowing due to depositional and post-depositional processes such as compaction.

Based on these results, a reversal is clearly indicated between the 17.10 and 16.80 m level (positioned at 16.95 ± 0.15 m). This does not correspond to a lithological transition between the basalt and the clastic sediments that might be associated with a hiatus in the record. Instead, the reversal lies within the clastic sediments, suggesting there is no large depositional gap associated with the reversal (Figs. 2 and 10).

4.3. Palynology

Based on the cluster analysis combined with conventional interpretation, the pollen diagram of the GBY#2 sediments, between 39.50 and 17.00 m, is subdivided into five LPAZ, LPAZ GBY#2-1–GBY#2-5 (Fig. 5).

LPAZ GBY#2-1 (39.50–36.10 m) includes ten samples in the bottommost second-order cluster (Fig. 5). AP is composed mainly of *Quercus calliprinos*-type, *Quercus ithaburensis*-type and *Cedrus*, which has a first peak (C1) at 37.40 m (Figs. 6A and 10). Cupressaceae-*Juniperus*-type and *Ephedra fragilis*-type are well represented. NAP is dominated by *Mentha*-type, *Primula clusiana*-type and cf. *Solanum dulcamara* and is further characterised by low amounts of Asteraceae and Apiaceae and *Azolla* cf. *filiculoides* massulae, while microspores and microsporangia of *Salvinia* are extremely abundant. The (Ar + Am)/P ratios and microcharcoal are relatively low in this zone (Fig. 5).

The next second-order cluster of 11 samples (36.10–28.00 m) is subdivided into two third-order clusters, LPAZ GBY#2-2

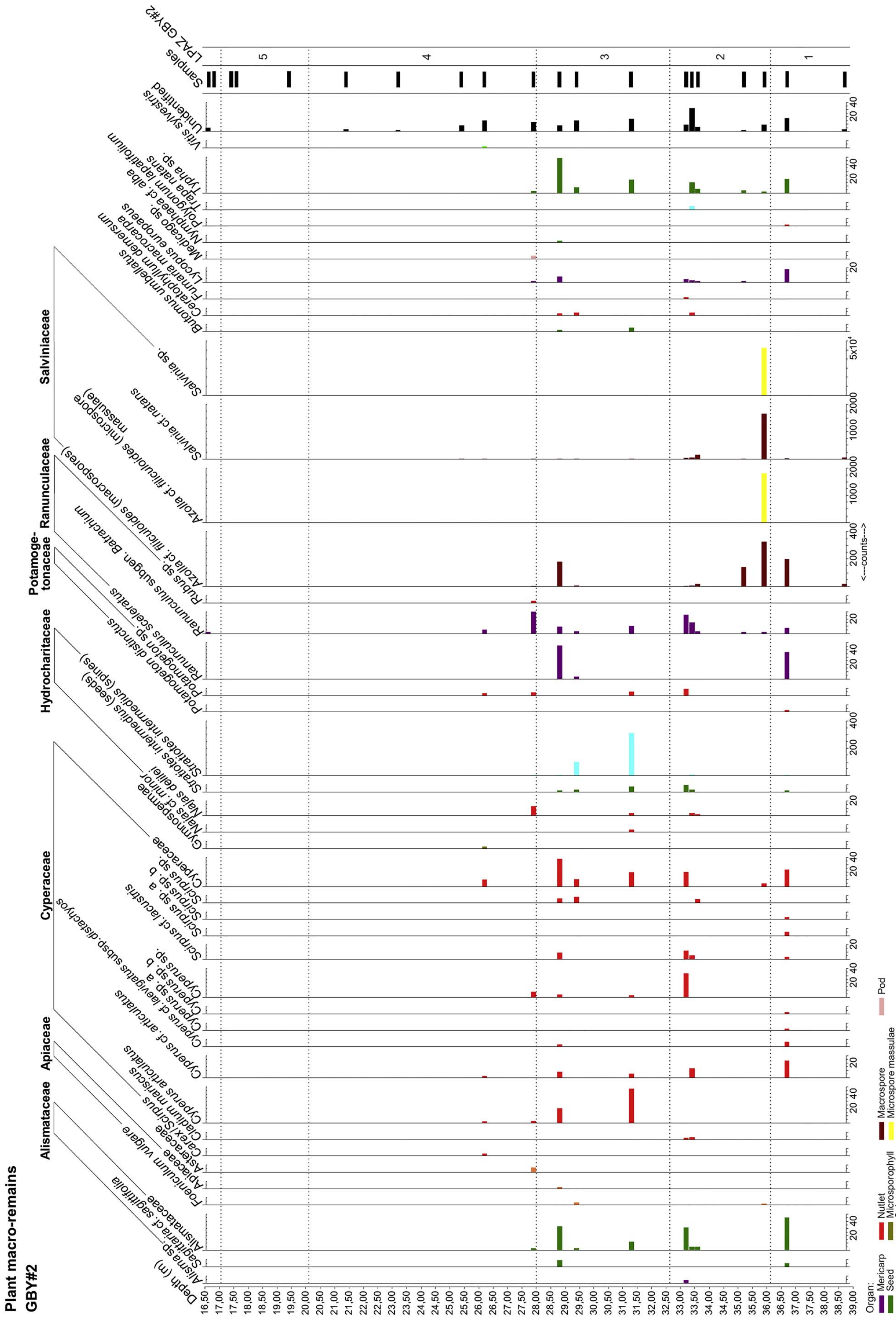

Fig. 7. Plant macro-remains of the GBY#2 core and their occurrence in relation to the Local Pollen Assemblage Zones (LPAZ).

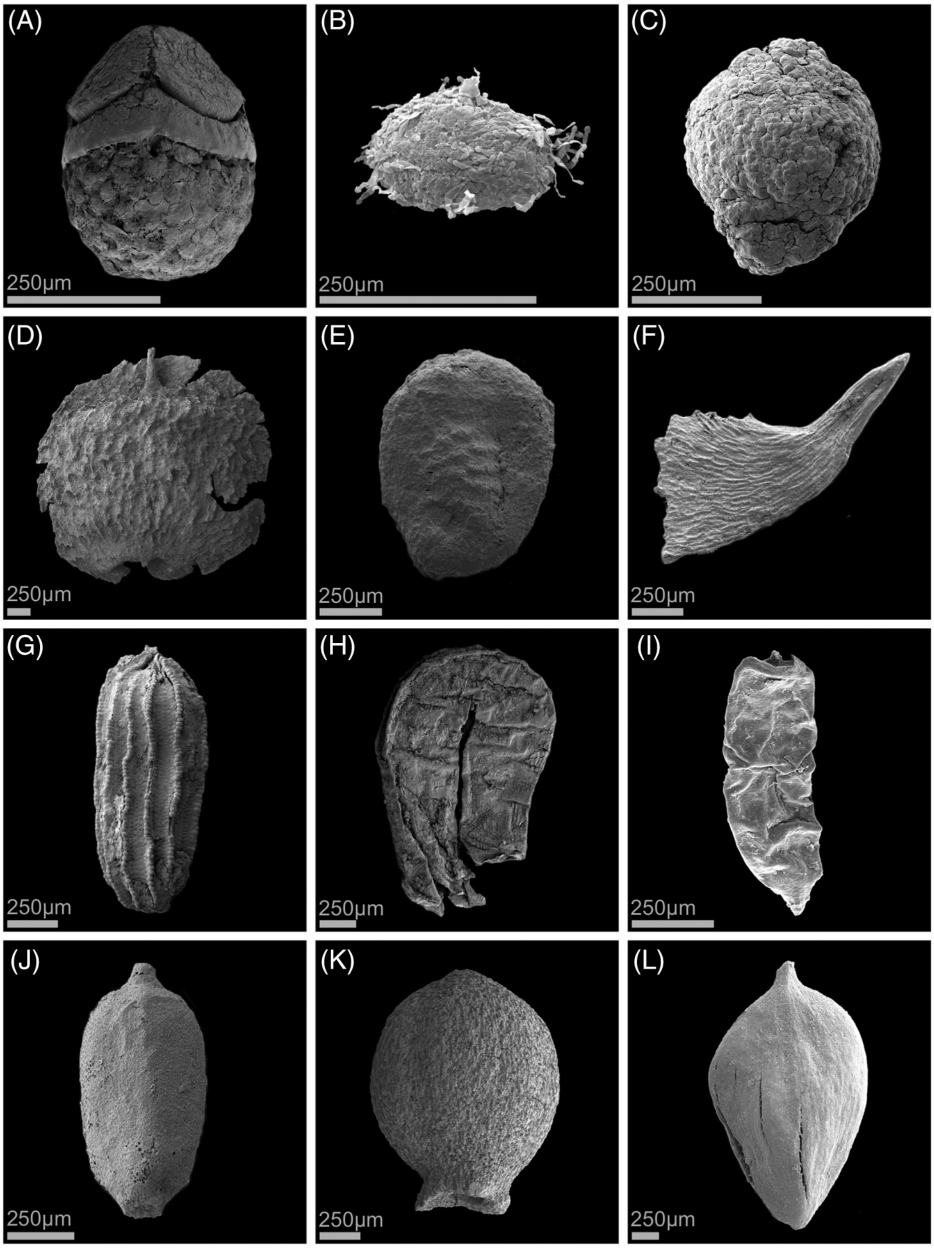

Fig. 8. Plant macro-remains: (A) *Azola* cf. *filiculoides* macrospore in side view at 36.70 m, (B) *Azola* cf. *filiculoides* microspore massulae in side view at 35.90 m, (C) *Salvinia* cf. *natans* macrospore in side view at 28.80 m, (D) *Fumaria macrocarpa* nutlet valve in dorsal view at 36.70 m, (E) *Ranunculus sceleratus* seed in side view at 36.70 m, (F) *Stratiotes* cf. *intermedius* spine in side view at 31.03 m, (G) *Butomus umbellatus* seed in side view at 28.80 m, (H) *Sagittaria* cf. *sagittifolia* flattened seed in side view at 36.70 m, (I) *Typha* cf. *domingensis* seed in side view at 28.80 m, (J) *Cyperus* cf. *articulatus* nutlet in dorsal view at 31.30 m, (K) *Cladium mariscus* nutlet in side view at 33.20 m, (L) *Scirpus* cf. *lacustris* nutlet in dorsal view at 36.70 m.

(36.10–32.60 m) and LPAZ GBY#2-3 (32.60–28.00 m). In LPAZ GBY#2-2, percentages of AP increase. *Salix*, *Cladium* and Cyperaceae indeterminate also increase towards the top of the zone, while *Ephedra fragilis*-type (Fig. 6C, E and F) decreases. Percentages of *Cedrus* slightly decrease but still show a small peak (C2) at 34.00 m (Figs. 5 and 10). Grasses are relatively abundant, in contrast to decreasing abundances of aquatic taxa. In this zone, the last peak of *Salvinia* (PS), both of microspores and microsporangia, occurs at 35.90 m (Figs. 5, 6B and 10). Amaranthaceae, *Artemisia*, Asteraceae and Apiaceae are important components of NAP, while amounts of *Mentha*-type, *Primula clusiana*-type and cf. *Solanum dulcamara* are markedly lower. The (Ar + Am)/P ratios are relatively low, between 0.03 and 0.33. This zone shows the highest amounts of micro-charcoal and diatoms (Fig. 5) in the entire profile.

LPAZ GBY#2-3 (32.60–28.00 m) consists of seven samples and is characterised by relatively low percentages of AP. Percentages of *Ephedra fragilis*-type are low, while values of Poaceae and Cyperaceae are relatively high. High percentages of Amaranthaceae (at 29.90 m) and *Artemisia* (at 28.25 m) form the first maximum (AA1, Figs. 5 and 10). Values of the (Ar + Am)/P ratios are relatively high and vary between 0.10 and 1.62. *Myriophyllum verticillatum*, *Myriophyllum spicatum* and some *Salvinia* microspores and microsporangia dominate the aquatic plant spectrum. Amounts of micro-charcoal are lower compared to LPAZ GBY#2-2 (Fig. 5). Although this zone includes about 2.6 m interval (32.49–29.90 m) without samples at the base, cluster analysis indicates high similarities of all samples in this zone.

LPAZ GBY#2-4 (28.00–20.15 m) is composed of five samples in the third second-order cluster, characterised by relatively high percentages of AP. *Cedrus* values are low, *Ephedra fragilis*-type reaches up to 2% and percentages of grasses are relatively high. The aquatic taxa are dominated by *Pediastrum simplex* at the base, while *Typha latifolia*-type characterises the top of this zone. The (Ar + Am)/P ratios are relatively high, while micro-charcoal yielded low values (Fig. 5). Both conventional and cluster analyses indicate similarities between every sample in this zone.

LPAZ GBY#2–5 (20.15 – 17.10 m) includes seven samples of the fourth second-order cluster, which is characterised by high percentages of AP with occurrences of some *Pistacia* and *Olea* (Fig. 5). Percentages of Cyperaceae and *Ephedra fragilis*-type are very low, while percentages of Poaceae and Cerealia-type are relatively high. Asteraceae, Amaranthaceae

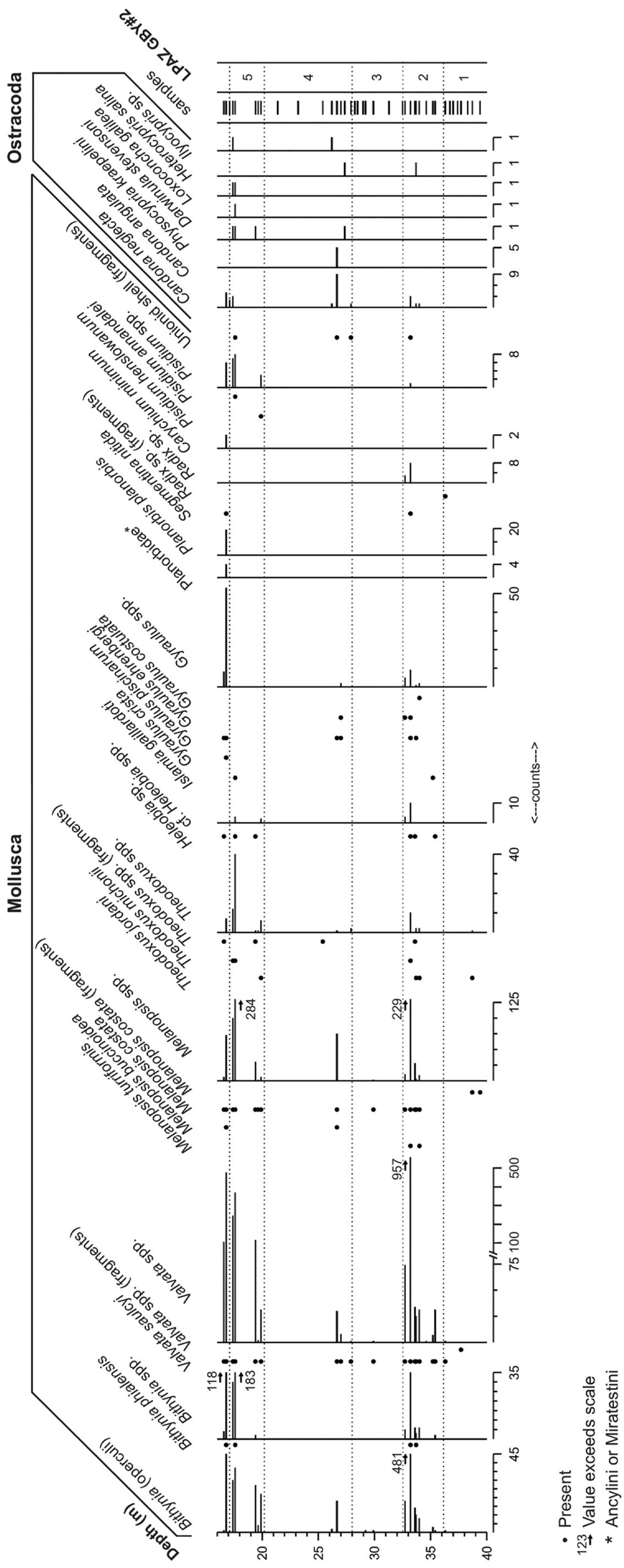

Fig. 9. Mollusc remains and ostracod valves in the GBY#2 core. The data are presented as presence-absence data (dots, mostly for mollusc identified to species level) and quantitative data (absolute count numbers as bars, mostly for taxa identified to genus level including less well preserved specimen not identified to species level).

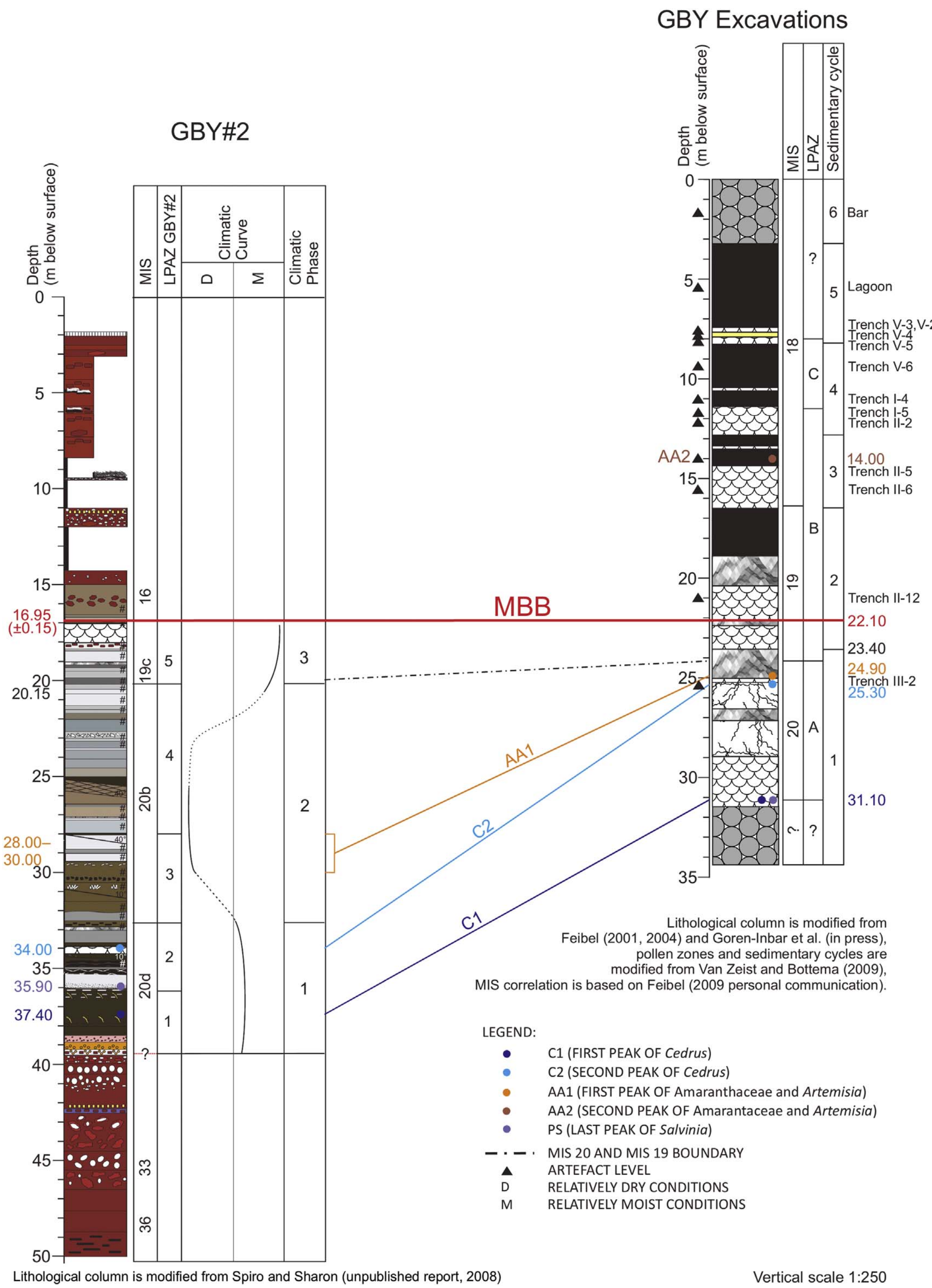

Fig. 10. Correlation between the sequence of the GBY excavation (modified from Feibel, 2001, 2004, 2009 personal communication; Van Zeist and Bottema, 2009; Goren-Inbar et al., in press) in the southern part of the GBY site and the GBY#2 core (modified from Spiro and Sharon, unpublished report, 2008) in the northern part of the archaeological site. The Matuyama-Brunhes Boundary (MBB) is the chronological reference for the correlation. The three other correlation lines are based on common palynological characteristics of both pollen profiles: C1 (first peak of *Cedrus*), C2 (second peak of *Cedrus*) and AA1 (first peak of Amaranthaceae and *Artemisia*). The last peak of *Salvinia* is indicated at 31.10 m in the excavation record and at 35.90 m in the GBY#2 core. For further explanations see Fig. 5 and for a detailed description of the lithological symbols see Fig. 2.

and Apiaceae dominate the NAP spectrum, though in low amounts, and *Cedrus* is absent. *Pediastrum simplex* and *Sparganium*-type compose the bulk of the aquatic taxa spectrum. The (Ar + Am)/P ratio and counts of micro-charcoal are very low.

4.4. Plant macro-remains

Plant macro-remains are mostly found in sediment layers between 38.70 and 26.20 m depth (Fig. 7). They are dominated by *Azolla* cf. *filiculoides* (Fig. 8A and B), *Salvinia* cf. *natans* and *Salvinia* sp. between

38.70 and 33.20 m and at 28.80 m. Remains of these two taxa occur together with low numbers of Alismataceae, Cyperaceae (Fig. 8J and K), *Foeniculum vulgare*, *Fumaria macrocarpa* (Fig. 8D), *Lycopus europaeus*, *Najas delilei*, *Polygonum lapatifolium*, *Potamogeton* sp., *Ranunculus* subgen. *Batrachium*, *Scirpus* cf. *lacustris* (Fig. 8L), *Scirpus* sp., seeds of *Stratiotes intermedius*, *Trapa natans* and *Typha* sp. between 38.70 and 33.20 m. Between 33.20 and 26.20 m, numbers of macrospores and massulae (respectively microsporangia) of *Azolla* cf. *filiculoides*, *Salvinia* cf. *natans* (Fig. 8C) and *Salvinia* sp. are lower, but remains of other taxa including Apiaceae, Asteraceae, Cyperaceae, Gymnospermae indeterminate, Ranunculaceae and aquatic taxa such as Alismataceae and *Trapa natans* (Fig. 7) are more abundant compared to the sediments between 38.70 and 33.20 m. From 25.40 m to the top of the sediment sequence, the number of plant macro-remains declines; only a few remains of *Ranunculus* subgen. *Batrachium* together with macrospores and microsporangia of *Salvinia* cf. *natans* and *Salvinia* sp. are found (Fig. 7).

Percentages of the mean pollen, non-pollen palynomorphs and plant macro-remains of *Cladium*, Asteraceae, Cyperaceae, Ranunculaceae, Apiaceae, *Salvinia* microsporangia and *Typha* sp. are always more or less proportional (Table 3). Exceptions are Apiaceae and *Typha latifolia*-type, which have a much higher mean pollen proportion, and Ranunculaceae and *Salvinia*, which have much lower mean pollen and microspore proportions (Table 3).

Taxa recorded by the macro-remains are in good accordance with the corresponding taxa of the pollen record in the lower part of the sequence. In LPAZ GBY#2-1, macro-remains of reed-swamp and marsh taxa such as *Ranunculus sceleratus*, *Typha* sp. and Cyperaceae are abundant. These are found together with freshwater taxa, mainly Salviniaceae, which reach their highest values in LPAZ GBY#2-2. Reed-swamp and marsh taxa, especially Cyperaceae, begin to expand in LPAZ GBY#2-3, while these and other macro-remains of wetland and aquatic taxa strongly decrease or even disappear completely in LPAZ GBY#2-4 and LPAZ GBY#2-5. The near absence of plant macro-remains in the upper ca. 10 m of the section contrasts markedly with the abundance of pollen.

Table 3
Comparison between plant macro-remains and mean pollen percentages of the GBY#2 core.

Taxa	Plant macro-remains (%)	Taxa and pollen-types	Mean pollen/spores/non-pollen palynomorphs (%)
Alismataceae	3.62		
Apiaceae	0.05	Apiaceae	94.84
Asteraceae	0.15	Asteraceae	31.40
Azolla cf. *filiculoides* (M)	46.35	*Azolla* cf. *filiculoides* (M)	0.87
Butomus umbellatus	0.18		
Ceratophyllum demersum	0.21		
Cladium mariscus	0.13	*Cladium*	1.37
Cyperaceae	8.22	Cyperaceae indeterminate	21.28
Fumaria macrocarpa	0.05		
Gymnospermae	0.05		
Lycopus europaeus	1.00		
Medicago sp.	0.10		
Najas cf. *minor*	0.08		
Najas delilei	0.54		
Nymphaea cf. *alba*	0.05		
Polygonum lapatifolium	0.05		
Potamogeton distinctus	0.05		
Potamogeton sp.	0.54		
Ranunculaceae	5.16	Ranunculaceae	0.09
Rubus sp.	0.05		
Salvinia (Ms)	1333.74	*Salvinia* (Ms)	13.87
Stratiotes intermedius	0.67		
Trapa natans	0.13		
Typha sp.	3.21	*Typha latifolia*-type	21.80
Vitis sylvestris	0.00		

M: Massulae; Ms.: Microsporangia.

4.5. Molluscs and ostracods

Almost 5000 mollusc shells and operculi and 41 ostracod valves were recorded from GBY#2. In LPAZ GBY#2–1, shells are very rare and ostracod valves are absent. Fragments of *Melanopsis costata* were recorded at 39.40 and 38.70 m; a shell of *Theodoxus jordani* was also recorded at 38.70 m. Fragments of *Valvata* and *Radix* were found at 37.70 and 36.30 m respectively; a shell of *Valvata saulcyi* and an operculum of *Bithynia* were also found at 36.30 m (Fig. 9). Between 36.10 and 32.60 m (LPAZ GBY#2-2), shells of *Valvata* (*Valvata saulcyi* and possibly poorly preserved specimens of other species) reach high abundances, with a maximum of 957 at 33.20 m. *Bithynia* operculi and *Melanopsis* shells (*Melanopsis* spp. including *M. costata* and *M. turriformis*) are also very abundant in this part of the core. Shells of *Bithynia* (including *B. phialensis*), *Gyraulus* (including *G. piscinarum*, *G. ehrenbergi* and *G. costulata*) and *Theodoxus* (including *T. jordani* and *T. michonii*) were also recorded relatively frequently. Valves of the two ostracods *Candona neglecta* and *Heterocypris salina* were recorded between 34.00 and 33.20 m (Fig. 9). The sediments between 32.60 and 28.00 m (LPAZ GBY#2–3) contained only two *Bithynia* operculi and one shell of *Valvata saulcyi* and *Melanopsis costata* respectively, while ostracod valves are absent. Shells of *Melanopsis* (including *M. costata* and *M. buccinoidea*), *Valvata* (including *V. saulcyi*), *Theodoxus* and *Gyraulus* (including *G. piscinarum* and *G. ehrenbergi*), fragments of unionid shells and *Bithynia* operculi were recorded in the sediments between 28.00 and 20.15 m (LPAZ GBY#2–4). Valves of *Candona neglecta*, *C. angulata*, *Physocypria kraepelini*, *Ilyocypris* sp. and *Heterocypris salina* were also recorded (Fig. 9). The abundance and diversity of mollusc shells are high in the uppermost sediments between 20.15 and 17.10 m (LPAZ GBY#2–5) and are comparable to those of LPAZ GBY#2-2 (Fig. 9); most abundant are shells of *Valvata*, *Melanopsis* and *Bithynia*, and *Bithynia* operculi. Ostracod valves of *Candona neglecta*, *Physocypria kraepelini*, *Darwinula stevensoni*, *Loxoconcha galilea* and *Ilyocypris* sp. were recovered from the uppermost sediments (Fig. 9).

4.6. Amphibia and micromammals

An undetermined phalanx of an amphibian as well as a metapodial and a femur of undetermined micromammals were found at 33.20 m in LPAZ GBY#2-2.

5. Discussion

The GBY#2 core represents one of the first coring campaigns that were conducted at archaeological sites. This core provided a variety of suitable materials for multi-proxy palaeoenvironmental study and dating, establishing environmental and chronological constraints. The MBB, which is recognised in the GBY excavation sediments, was also found at the top of the GBY#2 core. Consequently, the MBB can be used as a chronological reference for correlation, relating the older parts of the GBY excavation sequence to the sediments of the GBY#2 core. The effects of climatic changes on depositional environments and lake-level fluctuations at the GBY#2 core site and its correlation with the wider area of the GBY excavation and other Eastern Mediterranean records around the MBB have been the main focus.

5.1. Assessment of the pollen and plant macro-remain record of the GBY#2 core

The plant macro-remain record of the GBY#2 core (Fig. 7) shows fewer aquatic taxa in comparison to the GBY excavation (Goren-Inbar et al., 2002a; Melamed et al., 2011, 2016 Table S4). This record reveals no evidence of woody plants but shows dominance of Cyperaceae and *Typha* sp. (Fig. 7). These plants grow at the lake margin or in surrounding marsh and wetlands, from which plant remains are not widely transported. On the other hand, the pollen record (Fig. 5) reflects both the local and the regional vegetation. The local vegetation is represented mainly by aquatic taxa, lake-margin marshland taxa of Cyperaceae and *Typha latifolia*-type and riverine woody taxa such as *Salix*, *Tamarix* and *Ulmus*. Macro-remains of *Cyperus* are relatively abundant and may have dominated the reed community of the Hula Palaeo-lake, rather than *Phragmites*, as was the case during the Holocene (Payne and Gophen, 2012). This suggests that the grass pollen derived mainly from the surrounding woodland and steppe environments that were temporarily distributed in the study area, as is also indicated by relatively high abundances of *Quercus calliprinos*-type and *Quercus ithaburensis*-type, and occurrence of *Artemisia*, *Ephedra fragilis*-type and Amaranthaceae pollen. There are no macro-botanical remains of *Cedrus*, while the pollen is found mainly in LPAZ GBY#2-1 and GBY#2-2, marking long-distance transport by wind (Van Zeist and Bottema, 2009). Presently, *Cedrus* is native only to Lebanon (Van Zeist and Bottema, 2009) or farther afield in Cyprus and Turkey (Biltekin et al., 2015; Goren-Inbar et al., 2002b). Therefore, taxa that are found in both the pollen and the macro-remain records can predominantly be considered as components of the local vegetation.

Mean pollen percentages and the plant macro-remain percentages of the local taxa such as *Cladium*, Asteraceae and Cyperaceae show mainly proportional ratios (Table 3). On the other hand, the mean pollen percentages of Apiaceae and Asteraceae are higher compared to the macro-remain percentages (Table 3), demonstrating over-representation. Apiaceae and Asteraceae are insect-pollinated families with low pollen production and poor pollen dispersal. Therefore, their occurrence may indicate relatively abundant occurrences at the location, or that their pollen was more resistant than other pollen. In contrast, mean percentages of Ranunculaceae and *Salvinia* macro-remains show higher values than the mean pollen and spore percentages respectively, suggesting under-representation. Ranunculaceae are insect-pollinated and low pollen producers, while *Salvinia* is a floating fern whose spores are easily transported by water. It is also possible that Ranunculaceae pollen and *Salvinia* spores are less resistant to weathering than others. Macro-remains of some taxa such as *Lycopus europaeus*, *Medicago* sp., *Najas* cf. *minor*, *Najas delilei* and *Trapa natans* are found but have left no pollen traces, showing very limited distribution (Table 3). However, other factors such as pollen production, resistance and transport mechanisms should also be taken into account.

5.2. Micro-charcoal

Previous studies pointing to low frequencies of heavily burned item that are normally produced by lightning, peat burning and volcanism as well as clustered fire-damaged micro-artefacts possibly indicating hearths (Alperson-Afil, 2008; Alperson-Afil and Goren-Inbar, 2010; Alperson-Afil et al., 2009; Goren-Inbar et al., 2004) suggest that the occurrence of fire around the GBY site was caused by human activities rather than natural agents. In the GBY#2 core, relatively high micro-charcoal counts are found in LPAZ GBY#2-1 and GBY#2-3. The highest frequency occurs between 35.20 and 34.60 m (LPAZ GBY#2-2) (Fig. 5), perhaps resulting from hominin activities since the inferred relatively moist conditions would have prevented spontaneous burning and volcanism was no longer affecting the region. This possibility is supported by evidence of processing of unpalatable foods, including roasting, by hominins at the GBY site (Melamed et al., 2016). Furthermore, this layer likely corresponds to Layer III-2 (25.80–25.10 m) of the GBY excavation site, in which stone artefacts were found (Fig. 10) (Goren-Inbar et al., in press). Although only small numbers of artefacts were recovered from the oldest sediments of the GBY excavation, which were deposited below the MBB, there are definite artefacts such as small flints. These findings indicate that the Acheulian culture was already present in the GBY site in MIS 20 (Goren-Inbar et al., in press). In LPAZ GBY#2-4 and GBY#2-5 the counts of micro-charcoal are relatively low (Fig. 5), pointing to a lower intensity of burning in the study area. Whether the burning in these LPAZs was induced by human (Alperson-Afil, 2008; Alperson-Afil and Goren-Inbar, 2010; Goren-Inbar et al., 1992, 2004) or natural agents remains speculative.

5.3. Palaeoenvironmental reconstruction of the GBY#2 core

Calcareous marl and marls of LPAZ GBY#2-1 represent typical lacustrine sediments indicative of open-water lake environments (Figs. 5 and 7), an interpretation underlined by the dominance of *Azolla* cf. *filiculoides*, *Salvinia* cf. *natans* and *Salvinia* sp. The lithological change from calcareous marl to marl and the subsequent decreased abundance of aquatic taxa (Fig. 5) suggest that the depositional environment changed slightly to shallower conditions from approximately 38.30 m upwards. Van Zeist and Bottema (2009) suggested that the vegetation of the Upper Jordan Valley did not experience strong changes related to the glacial-interglacial fluctuations of the Early Pleistocene. However, the impacts of climatic changes are specifically marked by fluctuations in the arboreal vegetation record and the spread of steppe-like vegetation. In LPAZ GBY#2-1, relatively high amounts of *Quercus calliprinos*-type and grasses, low percentages of *Cedrus*, *Artemisia*, Amaranthaceae indeterminate and *Ephedra fragilis*-type and relatively low aridity indices (Fig. 5) suggest semi-moist conditions with a potential mean annual precipitation between 600 and 800 mm (Quézel and Médail, 2003; Suc and Popescu, 2005). However, pollen counts of Poaceae and Amaranthaceae of the GBY#2 may also include taxa of local marshes and drier woodland stands, and the aridity index may vary from place to place in different geographic areas (El-Moslimany, 1990; Herzschuh, 2007). Moreover, the relatively moist conditions of LPAZ GBY#2-1 were probably related to a decrease in temperature (Van Zeist and Bottema, 2009).

After its highest stand recorded in LPAZ GBY#2-1, the lake level dropped, producing an even shallower depositional environment characteristic of a lake-margin or lakeshore-near setting in LPAZ GBY#2-2, which is concluded for the subsequent sediments of the upper LPAZ GBY#2-2 (from about 33.50 m) from the deposition of sandy material containing abundant diatoms tests, well-preserved mollusc shells of different taxa and very low amounts or even absence of pollen of aquatic taxa (Fig. 5). The occurrence of Cyprinidae remains at 33.20 m suggests that the lake was relatively shallow, with a maximum depth of 5 m (Zohar et al., 2014). Additionally, higher percentages of riparian woody taxa (Fig. 5) provide evidence for riparian stands close to the lake margin, as shown by their present-day distribution along many rivers in Israel (Danin, 1992). This interpretation is supported by the occurrence of amphibian, micromammalian and ostracod remains; among ostracods, *Candona neglecta* is able to tolerate significantly drained environments (Rosenfeld et al., 2004; Wagner, 1957) and *Heterocypris salina* commonly inhabits temporary oligohaline – mesohaline water bodies (Mischke et al., 2014b; Rosenfeld et al., 2004) (Fig. 9). The occurrence of *Heterocypris salina* in the GBY record is also indicative of small water bodies such as ponds and swamps with increased evaporative enrichment of dissolved salts situated close to the lake, or slightly brackish springs in the vicinity of the drilling site, which are also observed today (Mienis and Ashkenazi, 2011; Mischke et al., 2014a; Spiro et al., 2011). Compared to LPAZ GBY#2-1, slightly higher humidity is indicated in the pollen record of LPAZ GBY#2-2, while relatively cool conditions seem to have continued throughout this zone (Fig. 5). Cooler conditions than today are possibly also indicated by the presence of *Candona neglecta* valves (Mischke et al., 2014a) (Fig. 9). Fish skeletal elements of Cyprinidae taxa including *Luciobarbus longiceps* and *Carasobarbus canis*, native to the Lake Hula and also indicative of lower water temperatures suitable for their breeding, were found at 33.20 m. Therefore, LPAZ GBY#2-1 and GBY#2-2 are characteristic of the semi-moist climatic phase 1 of the GBY#2 core (Figs. 5 and 10). On the whole, from LPAZ GBY#2-1 to GBY#2-2 the depositional environment became shallower, which likely corresponds to the transition to the arid climatic phase 2. In LPAZ GBY#2-2, the overall diversity of biological remains is relatively high.

The fine-grained sediments of LPAZ GBY#2-3 are mixed with sand and mollusc fragments at the base of the zone (Fig. 2), indicating that higher-energy depositional conditions at the lake margin persisted to about 31.80 m. The subsequent sediments of massive calcareous marl between 31.80 and 28.00 m indicate a slightly deeper environment, which is supported by the occurrence of the submerged species *Myriophyllum verticillatum* and *Myriophyllum spicatum*. As conditions became progressively drier (climatic phase 2), the development of a slightly deeper depositional environment is probably related to a climatically induced lower sedimentation rate. Overall, sediments of LPAZ GBY#2-3 contain remains of marsh vegetation (Figs. 5 and 7) pointing to swampy conditions, similar to present-day shallow bays and swamps in the Hula Plain (Dimentman et al., 1992; Zohary and Orshansky, 1947). Progressively warmer environmental conditions characterise the youngest part of LPAZ GBY#2-3 (Fig. 5).

The deposition of marl and occurrence of several aquatic plant taxa in LPAZ GBY#2-4 indicate that open-water conditions persisted up to about 25.40 m. The subsequent thin peat layer at about 25.30 m points to a phase of terrestrialisation, which likely represents a short-term drop in water level. Thereafter, the sediment type changes to marl and calcareous marl up to 20.15 m (Figs. 2 and 3C), which again likely indicates a slightly deeper lake environment. This interpretation cannot be supported by pollen or plant macrofossil evidence due to the sampling gap. However, remains of Cyprinidae at 23.20, 21.50 and 21.40 m point to a lake environment < 5 m deep (Zohar et al., 2014). Overall assessment of the findings may suggest that the water depth increased in this zone from about 25.30 m, probably corresponding to the transition to the moister climatic phase 3. LPAZ GBY#2-3 and GBY#2-4 have been classified as dry but relatively warm periods and assigned to climatic phase 2 (Fig. 10). However, for the overall interpretation of LPAZ GBY#2-4 the sampling gap needs to be considered (Fig. 5).

LPAZ GBY#2-5 is characterised by calcareous marl (Fig. 3D), which was likely deposited under shallow water conditions with a maximum depth of 5 m, indicated by remains of Cyprinidae (*Luciobarbus/Carasobarbus*) (Zohar et al., 2014) and abundant molluscs and ostracods. The occurrence of ostracod valves of five taxa in the middle of the zone probably points to a variety of micro-habitats in shallow water conditions, while coquina deposits in the upper part of the zone and the lack of ostracod valves in the uppermost sample probably resulted from the accumulation of shells at or near the beach of the lake. Similar to LPAZ GBY#2-2 and GBY#2-4, the shallow depositional environment in LPAZ GBY#2-5 is probably the result of a higher sedimentation rate. The pollen record of LPAZ GBY#2-5 shows high percentages of AP (mainly of *Quercus ithaburensis*-type and *Quercus calliprinos*-type), high values of grasses and very low values of steppic elements and aridity index (Fig. 5), suggesting rather moist environmental conditions. This zone characterises the moist and warm climatic phase 3 with denser forest at the end of the GBY#2 core section (Fig. 10).

In summary, the depositional environment of the GBY#2 core record reflects a trend of shallowing, subsequent to the deposition of LPAZ GBY#2-2, with two phases of slightly deeper depositional conditions at the end of LPAZ GBY#2-3 and GBY#2-4. Similar shallowing depositional conditions are also described for the beginning of a second-order sedimentary cycle of the GBY excavation (Van Zeist and Bottema, 2009). Considering the age of the overlying basalt (1137 ± 69 ka, Figs. 2 and 3A), which probably corresponds to MIS 33, an unconformity can be deduced at the bottom of the sediment sequence of GBY#2. Consequently, this unconformity occurs somewhere between about MIS 32 and 21.

5.4. Correlation of the palynological and other proxy records of the GBY#2 core with the GBY excavation site

The pollen diagram of the GBY excavation site is based on 25 samples (Van Zeist and Bottema, 2009) that are subdivided into pollen zones GBY A, B and C, based mainly on the *Cedrus* curve. In zone A, two small *Cedrus* peaks mark an increase in humidity, whereas *Cedrus* values are low to very low in pollen zone B. A peak in Amaranthaceae and *Artemisia* in zone A and another maximum in zone B (Fig. 10), as well as coinciding minima of Poaceae, are indicative of increased dryness (Van Zeist and Bottema, 2009). The chronological reference for correlation, the MBB, corresponds to the base of pollen zone B at a depth of 22.10 m (Van Zeist and Bottema, 2009), and hence zone A was assigned to MIS 20 and bottom part of zone B to MIS 19. In the GBY#2 core, the MBB is located at a depth of 16.95 ± 0.15 m (Table 1). Due to the higher resolution of the time-equivalent GBY#2 pollen spectra indicative of warm and moist interglacial conditions, the boundary between MIS 20 and 19 in the GBY excavation record has been modified (Fig. 10). Pollen zone C, which is assigned to MIS 18, is again characterised by increases in *Cedrus* and *Quercus ithaburensis*-type pointing to higher humidity.

The entire pollen record of the GBY#2 core is therefore correlated with pollen zone A (samples 1–7) and samples 8 and 9 of pollen zone B of the excavation record (Van Zeist and Bottema, 2009). As the pollen record of the GBY#2 core has a much higher resolution and represents a thicker sequence compared to the excavation site, palynological correlation is difficult. In zone A of the excavation record, *Cedrus* shows two different peaks that are correlated with lines C1 and C2 in the GBY#2 pollen diagram (Fig. 10). It has been suggested by Van Zeist and Bottema (2009) that *Cedrus* may not have been present in the area during phases represented by the older parts of the pollen diagram (zone A). Nevertheless, findings of macro-remains (Goren-Inbar et al., 2002b) and relatively high percentages of *Cedrus* pollen at the top of the GBY excavation (Layers V-5 and V-6) (Picard, 1965; Van Zeist and Bottema, 2009) suggest that *Cedrus* occurred around the GBY site during MIS 18 (zone C) or that the pollen was transported by wind from Lebanon (Van Zeist and Bottema, 2009). Analysis of the taphonomy of the wood remains suggests that *Cedrus* pollen was brought into the Benot Ya'aqov embayment (and into the present Jordan River) from western and north-western areas (Goren-Inbar et al., 2002b).

Between correlation line C2 and the MBB, only a thin sediment layer in the GBY excavation site (25.30–22.10 m) can be correlated with the much thicker sequence of the GBY#2 core (34.00–17.10 m) (Fig. 10). This might suggest that the GBY#2 drilling point is located closer to the basin depocenter compared to the GBY excavation.

The AA1 (Van Zeist and Bottema, 2009) and findings of lentic molluscs and hygrophilous land snails in most of cycle 1 of the GBY excavation (Mienis and Ashkenazi, 2011), indicating very dry conditions, can be correlated with the GBY#2 core sequence between about 30.00 and 28.00 m (Fig. 10). Van Zeist and Bottema (2009) identified a second maximum of Amaranthaceae and *Artemisia* (AA2), which is not recorded in the GBY#2 core due to its higher position above the MBB. However, the post-MBB basalt of the GBY#2 core, dated to ca. 0.66 Ma, can be correlated with the exposed basalt flow of the "North of Bridge Acheulian" (NBA) site, about 500 m north of the Benot Ya'aqov Bridge (Sharon et al., 2010). According to these authors, samples of the basalt flow below the Acheulian archaeological horizon were $^{40}Ar/^{39}Ar$ dated to 658 ± 15 ka (mean age), and Acheulian tools similar to those of the GBY excavation were found in this archaeological horizon. Together with the dating results presented here, the NBA can be allocated to the same Acheulian entity as that revealed in the GBY excavation (Sharon et al., 2011).

Looking at the aquatic flora, particularly high percentages of *Salvinia* occur at the bottom of both pollen diagrams and in the plant macro-remains record of GBY#2, while this taxon strongly decreases towards the top of the corresponding sediment sections (pollen zone A and GBY#2-2). The last peak of *Salvinia* microspores and microsporangia at 35.90 m in the GBY#2 pollen sequence and sample 5 of the excavation profile (Van Zeist and Bottema, 2009) can therefore be taken as another significant reference point (PS) (Fig. 10).

According to Mienis and Ashkenazi (2011), the PS line in the GBY excavation profile also coincides with the maximum abundance of lentic Basommatophora and hygrophilous land snails including embryonic forms of the Planorbidae family, indicating nutrient-rich conditions of a lacustrine ecosystem. Changes of water depth, water quality and climatic conditions caused a dramatic decrease of these taxa between about 26.50 m and the MBB. The same authors suggest that the pre-MBB sediments at the GBY excavation site were deposited during cool climatic conditions, referring mainly to the occurrence of the Palaearctic mollusc *Carychium minimum* and the oxygen isotope analysis of *Candona neglecta* (Rosenfeld et al., 2004). They also propose that the lake level changed from high levels at the bottom of the sediment sequence (34.30–31.20 m) to lower levels representing a shallower depositional environment in the subsequent sediment cycle 1 and the beginning of cycle 2 (Fig. 10). This interpretation corresponds to drier and cooler environmental conditions related to climatic phases 1 and 2 of the GBY#2 core during MIS 20. The study of Mienis and Ashkenazi (2011) also suggests that the post-MBB sediments of the GBY excavation site indicate a short warm phase (between about 18.90 and 16.50 m), which may relate to the warm climatic phase 3 of the GBY#2 core starting shortly before the MBB. The data from the core and the excavation site are not in agreement with regard to the timing of the onset of the warm climatic phase: in the GBY#2 record this coincided with the transition from MIS 20 to 19, while in the GBY excavation record it occurred later, at the beginning of MIS 19. This discrepancy, however, can be explained by the much higher sampling resolution of the palynological study of the GBY#2 core, which provides new evidence for a modification of the MIS subdivision of the GBY excavation record.

5.5. Comparison with other Mediterranean palaeoclimatic records

There are only a few pollen records in the Eastern Mediterranean spanning a time interval comparable to the GBY record, between 900 and 700 ka. Joannin et al. (2007) have stated that in the Early and Middle Pleistocene Tsampika section of Rhodes (Greece) between MIS 20 and 17, cold and arid (glacial) climatic conditions are characterised by the herbaceous taxa *Artemisia*, Asteraceae and Asteroidae, while warmer and moister (interglacial) phases are characterised by taxa such as *Quercus*, *Cedrus* and *Abies*. Langgut (2008) presents similar observations for a south-eastern Mediterranean marine sequence during the last 90 ka. The investigation showed that percentages of *Artemisia* were high during the late Pleistocene cold glacial stages and *Quercus* pollen (*calliprinos*-type) showed higher values during the moister and warmer Holocene. Similar features were observed in the GBY#2 record for the pronounced dry and slightly cooler climatic phase 2 (Fig. 10) within MIS 20, when AP had drastically decreased and NAP were dominated by *Artemisia*, *Asteraceae* and Amaranthaceae. Subsequently, *Quercus calliprinos*-type, *Quercus ithaburensis*-type, *Pistacia* and *Olea* were again characteristic of a relatively warm and moist climate during MIS 19.

Maiorano et al. (2016) have published a multi-proxy record of the Montalbano Jonico section of the Early–Middle Pleistocene transition which reflects interglacial conditions lasting for about 10.6 ka during MIS 19c. MIS 19c was characterised in southern Italy by warm, oligotrophic surface waters with forest expansion, consistent occurrence of woody taxa and moderate abundance of herbaceous ones, suggesting warm and humid conditions prevailing on land. Almogi-Labin (2011) has recalculated the GBY excavation site pollen record of Van Zeist and Bottema (2009) by removing Poaceae and other NAP from the basic sum of pollen following Tzedakis et al. (2006) and plotting the new AP curve against the $\delta^{18}O$ values of ostracods and the inferred salinity values that are deduced from the ostracod assemblage (Mischke et al., 2010). Although the resolution of the pollen record of Van Zeist and Bottema (2009) is very low, Almogi-Labin (2011) stated that during MIS 19, shortly before the MBB, values of AP were relatively low and the lake level was rather low as well.

The pollen record of Tenaghi Philippon (Tzedakis et al., 2006) indicates the occurrence of forests during the temperate phase of MIS 19, with *Quercus* prevailing among the high AP percentages, and very low percentages of AP during the preceding glacial period of MIS 20, which corresponds to the GBY#2 record. However, at Tenaghi Philippon, the MBB is located in MIS 20 rather than in MIS 19. This discrepancy, due to the maintenance of remanent magnetisation, has frequently been described for long terrestrial records (Tzedakis et al., 2006; Zhou and Shackleton, 1999). Therefore, an adjustment is required for this deviation. With regard to the GBY#2 record, the adjustment of the MBB to MIS 19 was established successfully.

In our study of the GBY#2 records we have amplified and specified the climatic characterisation of MIS 20 and 19 in the Upper Jordan Valley and can show that the climatic conditions shortly before the MBB (773 ka; Channell et al., 2004) during interglacial stage MIS 19 were moist and warm, reflected by a high amount of AP (cycle 2, Fig. 10). Our inferences of a relatively low lake level and lake-margin conditions at the GBY#2 location are in agreement with the findings of other authors.

6. Conclusions

Changes in the depositional environment from open freshwater to shallower lake-margin environments were influenced by an interaction between climatic conditions and variations in sediment supply. Evidence for possible human use of fire is detected in LPAZ GBY#2-2 near the lakeshore of the Hula Palaeo-lake, which can be correlated with artefact-containing layers of the GBY excavation site. Concerning the deposition of the sediments of LPAZ GBY#2-2, mollusc analysis for the core sediments and the correlating sediments of the GBY excavation sequence indicates abundant freshwater lentic species that, in association with macrophytes, point to a relatively shallow freshwater ecosystem with high nutrient content.

The MBB, which falls within MIS 19, is represented in the GBY excavation as well as in the GBY#2 record. Post-MBB sediments of MIS 19 and 18 are represented only in the excavation record. Palynological results of the pre-MBB GBY#2 record indicate at least three climatic phases, based mainly on *Cedrus* and AP curves, aridity indices and taxa of steppic elements as well as lithological changes. This interpretation is supported by evidence of molluscs, ostracods and fish and their ecological implications. Based on these proxies and the correlation with the established MIS framework of the GBY excavation and the palaeomagnetic investigations, the sediments of the semi-moist climatic phase 1 in the GBY#2 core correspond to MIS 20d, and the sediments of the cold and dry climatic phase 2 to the glacial period of MIS 20b. The sediments of the younger part of the sequence were deposited shortly before the MBB (phase 3) and imply a pronounced change of the vegetation to *Quercus calliprinos*-, *Quercus ithaburensis*- and *Pistacia*-rich woodlands, representing the warm and moist MIS 19c.

Supplementary data to this article can be found online at https://doi.org/10.1016/j.palaeo.2017.10.007.

Acknowledgments

The authors thank the Israel Antiquities Authority for financing and supervising the drilling of GBY#2 and, in particular, Ofer Marder and Chamoudi Khalaily. Gonen Sharon handled the maintenance and storage of the core and participated in its initial description and sampling. Some of the research aspects were conducted thanks to a grant awarded to N.G.-I. by the Israel Science Foundation [Grant No. 300/06] for the Center of Excellence Project entitled 'The Effect of Climate Change on the Environment and Hominins of the Upper Jordan Valley between ca.

800Ka and 700Ka ago as a Basis for Prediction of Future Scenarios'. Baruch Spiro was nominated by N.G.-I. to be in charge of describing the core, cutting it into two halves for archiving and sampling. He was also the sole person responsible for sampling and distributing the samples among the multidisciplinary researchers. Thanks go to Mara Goldstein for her study of the malacology, to Irit Zohar for the ichthyological analysis, to Rebecca Biton for the macro-mammal analysis and to Alexandra Sumner for the illustration of the GBY#2 core. Thanks are due also to the directors of the Institute of Archaeology, Benny Sekay and Smadar Pustilnik, for their continuous support and understanding. Abraham Starinsky of the Institute of Earth Sciences coordinated some of the administrative aspects and we thank him for his academic and psychological support. M.S.P. and B.U. wish to thank the Directorate General of Indonesian Higher Education (Dikti) and the German Academic Exchange Service (DAAD) for the scholarship to support this research, Mario Tucci and Sabine Hansen for their help and discussion concerning laboratory treatments and pollen diagram preparation and Peter Kershaw for his constructive and valuable advice. G.D.-N. acknowledges funding from EU Career Integration Grant 'HIRESDAT' [Project No. 294282]. Finally, the authors would like to thank Jean-Pierre Suc and an anonymous reviewer for their valuable comments on the manuscript.

References

Almogi-Labin, A., 2011. The paleoclimate of the eastern Mediterranean during the transition from Early to Mid Pleistocene (900 to 700 ka) based on marine and non-marine records: an integrated overview. J. Hum. Evol. 60, 428–436. http://dx.doi.org/10.1016/j.jhevol.2010.03.007.

Alperson-Afil, N., 2008. Continual fire-making by hominins at Gesher Benot Ya'aqov, Israel. Quat. Sci. Rev. 27, 1733–1739. http://dx.doi.org/10.1016/j.quascirev.2008.06.009.

Alperson-Afil, N., Goren-Inbar, N., 2010. The Acheulian Site of Gesher Benot Ya'aqov Volume II: Ancient Flames and Controlled Use of Fire. Springer, New York.

Alperson-Afil, N., Goren-Inbar, N., 2015. Scarce but significant: the limestone component of the Acheulian lithic assemblages of Gesher Benot Ya'aqov, Israel. In: Haidle, M.N., Conard, N., Bolus, M. (Eds.), The Nature of Culture. Vertebrate Paleobiology and Paleoanthropology. Vol. X. Springer, New York, pp. 41–56.

Alperson-Afil, N., Goren-Inbar, N., 2016. Acheulian hafting: proximal modification of small flint flakes at Gesher Benot Ya'aqov, Israel. Quat. Int. 411, 34–43.

Alperson-Afil, N., Sharon, G., Kislev, M., Melamed, Y., Zohar, I., Ashkenazi, S., Rabinovich, R., Biton, R., Werker, E., Hartman, G., Feibel, C., Goren-Inbar, N., 2009. Spatial organization of hominin activities at Gesher Benot Ya'aqov, Israel. Science 326, 1677–1680. http://dx.doi.org/10.1126/science.1180695.

Ashkenazi, S., Motro, U., Goren-Inbar, N., Biton, R., Rabinovich, R., 2005. New morphometric parameters for assessment of body size in the fossil freshwater crab assemblage from the Acheulian site of Gesher Benot Ya'aqov, Israel. J. Archaeol. Sci. 32, 675–689. http://dx.doi.org/10.1016/j.jas.2004.12.003.

Ashkenazi, S., Klass, K., Mienis, H.K., Spiro, B., Abel, R., 2010. Fossil embryos and adult Viviparidae from the Early-Middle Pleistocene of Gesher Benot Ya'aqov, Israel: ecology, longevity and fecundity. Lethaia 43, 116–127. http://dx.doi.org/10.1111/j.1502-3931.2009.00178.x.

Belitzky, S., 2001. The morphotectonic structure of the lower Jordan Valley – an active segment of the Dead Sea rift. Stephan Mueller Spec. Publ. Ser. 2, 95–103. http://dx.doi.org/10.5194/smsps-2-95-2002.

Belitzky, S., 2002. The structure and morphotectonics of the Gesher Benot Ya'aqov area, northern Dead Sea rift, Israel. Quat. Res. 58, 372–380. http://dx.doi.org/10.1006/qres.2002.2347.

Beug, H.-J., 2004. Leitfaden der Pollenbestimmung, für Mitteleuropa und angrenzende Gebiete. Verlag Dr, Friedrich Pfeil, München.

Beug, H.-J., 2015. Leitfaden der Pollenbestimmung, für Mitteleuropa und angrenzende Gebiete, second ed. Verlag Dr. Friedrich Pfeil, München.

Biltekin, D., Popescu, S.-M., Suc, J.-P., Quézel, P., Jiménez-Moreno, G., Yavuz, N., Çağatay, M.N., 2015. Anatolia: a long-time plant refuge area documented by pollen records over the last 23 million years. Rev. Palaeobot. Palynol. 215, 1–22.

Biton, R., Geffen, E., Vences, M., Cohen, O., Bailon, S., Rabinovich, R., et al., 2013. The rediscovered Hula painted frog is a living fossil. Nat. Commun. 4, 1959. http://dx.doi.org/10.1038/ncomms2959.

Biton, R., Boistel, R., Rabinovich, R., Gafny, S., Bailon, S., 2016. Osteological observations on the Alytid Anura Latonia nigriventer with comments on functional morphology, biogeography, and evolutionary history. J. Morphol. 227 (9), 1131–1145.

Channell, J.E.T., Curtis, J.H., Flower, B.P., 2004. The Matuyama-Brunhes boundary interval (500–900 ka) in North Atlantic drift sediments. Geophys. J. Int. 158, 489–505. http://dx.doi.org/10.1111/j.1365-246X.2004.02329.x.

Cour, P., Duzer, D., 1978. La signification climatique, édaphique et sédimentologique des rapports entre taxons en analyse pollinique. Ann. Mines Belgique 7–8, 155–164.

Danin, A., 1992. Flora and vegetation of Israel and adjacent areas. Bocconea 18–42.

Danin, A., 2003. Flora of Israel Online [WWW Document]. http://flora.org.il/en/plants/, Accessed date: 12 October 2016.

Dimentman, C., Bromley, H.J., Por, F.D., 1992. Lake Hula. Reconstruction of the Fauna and Hydrobiology of the Lost Lake. The Israel Academy of Sciences and Humanities, Jerusalem.

Dupont-Nivet, G., Sier, M., Campisano, C.J., Arrowsmith, J.R., DiMaggio, E., Reed, K., Lockwood, C., Franke, C., Hüsing, S., 2008. Magnetostratigraphy of the eastern Hadar Basin (Ledi-Geraru research area, Ethiopia) and implications for hominin paleoenvironments. In: Quade, J., Wynn, J.G. (Eds.), The Geology of Early Humans in the Horn of Africa: Geological Society of America Special Paper 446. The Geological Society of America, Boulder-Colorado, pp. 67–85. http://dx.doi.org/10.1130/2008.2446(03).

El-Moslimany, A.P., 1990. Ecological significance of common nonarboreal pollen: examples from drylands of the Middle East. Rev. Palaeobot. Palynol. 64, 343–350. http://dx.doi.org/10.1016/0034-6667(90)90150-H.

Faegri, K., Iversen, J., 1989. Textbook of Pollen Analysis, fourth ed. John Wiley and Sons, New York.

Feibel, C., 2009. personal communication.

Feibel, C.S., 2001. Archaeological sediments in lake margin environments. In: Stein, J.K., Farrand, W.R. (Eds.), Sediments in Archaeological Context. The University of Utah Press, Salt Lake City, pp. 127–148.

Feibel, C.S., 2004. Quaternary lake margins of the Levant Rift Valley. In: Goren-Inbar, N., Speth, J.D. (Eds.), Human Paleoecology in the Levantine Corridor. Oxbow Books, Oxford, pp. 21–36.

Fowell, S.J.B., Hansen, C.S., Peck, J.A., Khosbayar, P., Ganbold, E., 2003. Mid to late Holocene climate evolution of the Lake Telmen Basin, north central Mongolia, based on palynological data. Quat. Res. 59, 353–363.

Frey, W., Kürschner, H., 1989. Tübinger Atlas des Vorderen Orients, Karte A VI 1, Vorderer Orient. Vegetation 1:8000000. Dr. Ludwig Reichert Verlag, Wiesbaden.

Goren-Inbar, N., 2011. Culture and cognition in the Acheulian industry – a case study from Gesher Benot Ya'aqov. Philos. Trans. R. Soc. B 366 (1567), 1038–1049.

Goren-Inbar, N., Saragusti, I., 1996. An Acheulian biface assemblage from Gesher Benot Ya'aqov, Israel: indications of African affinities. J. Field Archaeol. 23, 15–30. http://dx.doi.org/10.2307/530606.

Goren-Inbar, N., Sharon, G., 2006. Invisible handaxes and visible Acheulian biface technology at Gesher Benot Ya'aqov, Israel. In: Goren-Inbar, N., Sharon, G. (Eds.), Axe Age: Acheulian Tool-Making from Quarry to Discard. Equinox Publishing Ltd., London, pp. 105–129.

Goren-Inbar, N., Belitzky, S., Verosub, K.L., Werker, E., Kislev, M.E., Heimann, A., Carmi, I., Rosenfeld, A., 1992. New discoveries at the Middle Pleistocene Acheulian site of Benot Ya'aqov, Israel. Quat. Res. 38, 117–128.

Goren-Inbar, N., Lister, A., Werker, E., Chech, M., 1994. A butchered elephant skull and associated artifacts from the Acheulian site of Gesher Benot Ya'aqov, Israel. Paléorient 20, 99–112. http://dx.doi.org/10.3406/paleo.1994.4604.

Goren-Inbar, N., Feibel, C.S., Verosub, K.L., Melamed, Y., Kislev, M.E., Tchernov, E., Saragusti, I., 2000. Pleistocene milestones on the out-of-Africa corridor at Gesher Benot Ya'aqov, Israel. Science 289, 944–947. http://dx.doi.org/10.1126/science.289.5481.944.

Goren-Inbar, N., Sharon, G., Melamed, Y., Kislev, M., 2002a. Nuts, nut cracking, and pitted stones at Gesher Benot Ya'aqov, Israel. Proc. Natl. Acad. Sci. U. S. A. 99, 2455–2460. http://dx.doi.org/10.1073/pnas.032570499.

Goren-Inbar, N., Werker, E., Feibel, C.S., 2002b. The Acheulian Site of Gesher Benot Ya'aqov, Israel, I the Wood Assemblage. Oxbow Books, Oxford.

Goren-Inbar, N., Alperson, N., Kislev, M.E., Simchoni, O., Melamed, Y., Ben-Nun, A., Werker, E., 2004. Evidence of hominin control of fire at Gesher Benot Ya'aqov, Israel. Science 304, 725–727. http://dx.doi.org/10.1126/science.1095443.

Goren-Inbar, N., Alperson-Afil, N., Sharon, G., Herzlinger, G., 2015. A new type of anvil in the Acheulian of Gesher Benot Ya'aqov, Israel. Philos. Trans. R. Soc. B 370 (1682), 20140353. http://dx.doi.org/10.1098/rstb.2014.0353.

Goren-Inbar, N., Alperson-Afil, N., Sharon, G., Herzlinger, G., 2017;al., in press. The Acheulian Site of Gesher Benot Ya'aqov: The Lithic Assemblages. Springer, Dordrecht (in press).

Grimm, E.C., 1987. CONISS: a Fortran 77 program for stratigraphically constrained cluster analysis by the method of incremental sum of squares. Comput. Geosci. 13, 13–35.

Grimm, E.C., 1990. Tilia, Tiliagraph & Tiliaview. PC spreadsheet and graphics software for pollen data. INQUA working group on data-handling methods. Newsletter 4, 5–7.

Head, M.J., Gibbard, P.L., 2005. Early-Middle Pleistocene transitions: an overview and recommendation for the defining boundary. Geol. Soc. Lond. Spec. Publ. 247, 1–18. http://dx.doi.org/10.1144/GSL.SP.2005.247.01.01.

Herzschuh, U., 2007. Reliability of pollen ratios for environmental reconstructions on the Tibetan Plateau. J. Biogeogr. 34, 1265–1273. http://dx.doi.org/10.1111/j.1365-2699.2006.01680.x.

Horowitz, A., 1973. Development of the Hula Basin, Israel. Isr. J. Earth Sci. 22, 107–139.

Horowitz, A., 1975. The quaternary stratigraphy and paleogeography of Israel. Paléorient 3, 47–100. http://dx.doi.org/10.3406/paleo.1975.4190.

Horowitz, A., 1979. The Quaternary of Israel. Academic Press, New York.

Horowitz, A., 1987. Palynological evidence for the age and rate of sedimentation along the Dead Sea rift, and structural implications. Tectonophysics 141, 107–115.

Ickert-Bond, S.M., Renner, S.S., 2016. The Gnetales: recent insights on their morphology, reproductive biology, chromosome numbers, biogeography, and divergence times. J. Syst. Evol. 54, 1–16. http://dx.doi.org/10.1111/jse.12190.

Joannin, S., Cornée, J.-J., Moissette, P., Suc, J.-P., Koskeridou, E., Lécuyer, C., Buisine, C., Kouli, K., Ferry, S., 2007. Changes in vegetation and marine environments in the eastern Mediterranean (Rhodes, Greece) during the Early and Middle Pleistocene. J. Geol. Soc. Lond. 164, 1119–1131.

Jourdan, F., Renne, P.R., Reimold, W.U., 2009. An appraisal of the ages of terrestrial

impact structures. Earth Planet. Sci. Lett. 286, 1–13. http://dx.doi.org/10.1016/j.epsl.2009.07.009.
Kirschvink, J.L., 1980. The least-squares line and plane and the analysis of palaeomagnetic data. Geophys. J. Int. 62, 699–718. http://dx.doi.org/10.1111/j.1365-246X.1980.tb02601.x.
Kislev, M., Melamed, Y., 2011. The first archaeobotanical record of environmental change and hominin diet in the out-of-Africa corridor during the Lower to Upper Paleolithic. In: Center of Excellence Project No. 858/09.
Koppers, A.A.P., 2002. ArArCALC-software for $^{40}Ar/^{39}Ar$ age calculations. Comput. Geosci. 28, 605–619.
Langgut, D., 2008. Late Quaternary palynological sequences from the Eastern Mediterranean Sea. In: Report GSI/16/08. Geological Survey of Israel.
Lee, J.-Y., Marti, K., Severinghaus, J.P., Kawamura, K., Yoo, H.-S., Lee, J.B., Kim, J.S., 2006. A redetermination of the isotopic abundance of atmospheric Ar. Geochim. Cosmochim. Acta 70, 4507–4512.
Lisiecki, L.E., Raymo, M.E., 2005. A Pliocene-Pleistocene stack of 57 globally distributed benthic d18O records. Paleoceanography 20, PA1003. http://dx.doi.org/10.1029/2004PA001071.
Maiorano, P., Bertini, A., Capolongo, D., Eramo, G., Gallicchio, S., Girone, A., Pinto, D., Toti, F., Ventruti, G., Marino, M., 2016. Climate signatures through marine isotope stage 19 in the Montalbano Jonico section (southern Italy): a land–sea perspective. Palaeogeogr. Palaeoclimatol. Palaeoecol. 461, 341–361. http://dx.doi.org/10.1016/j.palaeo.2016.08.029.
Melamed, Y., Kislev, M., Weiss, E., Simchoni, O., 2011. Extinction of water plants in the Hula Valley: evidence for climate change. J. Hum. Evol. 60 (4), 320–327. http://dx.doi.org/10.1016/j.jhevol.2010.07.025.
Melamed, Yoel, Kislev, M.E., Geffen, E., Lev-Yadun, S., Goren-Inbar, N., 2016. The plant component of an Acheulian diet at Gesher Benot Ya'aqov, Israel. Proc. Natl. Acad. Sci. U. S. A. 113 (51), 14674–14679.
Mienis, H.K., Ashkenazi, S., 2011. Lentic Basommatophora molluscs and hygrophilous land snails as indicators of habitat and climate in the Early-Middle Pleistocene (0.78 Ma) at the site of Gesher Benot Ya'aqov (GBY), Israel. J. Hum. Evol. 60, 328–340. http://dx.doi.org/10.1016/j.jhevol.2010.03.009.
Mischke, S., Almogi-Labin, A., Ortal, R., Rosenfeld, A., Schwab, M.J., Boomer, I., 2010. Quantitative reconstruction of lake conductivity in the quaternary of the near east (Israel) using ostracods. J. Paleolimnol. 43, 667–688. http://dx.doi.org/10.1007/s10933-009-9359-y.
Mischke, S., Ashkenazi, S., Almogi-Labin, A., Goren-Inbar, N., 2014a. Ostracod evidence for the Acheulian environment of the ancient Hula Lake (Levant) during the Early-Mid Pleistocene transition. Palaeogeogr. Palaeoclimatol. Palaeoecol. 412, 148–159. http://dx.doi.org/10.1016/j.palaeo.2014.07.036.
Mischke, S., Almogi-Labin, A., Al-Saqarat, B., Rosenfeld, A., Elyashiv, H., Boomer, I., Stein, M., Lev, L., Ito, E., 2014b. An expanded ostracod-based conductivity transfer function for climate reconstruction in the Levant. Quat. Sci. Rev. 93, 91–105. http://dx.doi.org/10.1016/j.quascirev.2014.04.004.
Moore, P.D., Webb, J.A., Collinson, M.E., 1991. Pollen Analysis, second ed. Blackwell Scintific Publications, Oxford.
Payne, R., Gophen, M., 2012. The hula peatland: past, present and future (foreword). Mires Peat 9.
Picard, L., 1965. The geological evolution of the quaternary in the central-northern Jordan graben. American Geol. Soc. Spec. Pap. 84, 337–366.
Quézel, P., Médail, F., 2003. Ecologie et biogéographie des forêts du bassin méditerranéen. vol. 572 Elsevier, Paris.
Rabinovich, R., Biton, R., 2011. The Early-Middle Pleistocene faunal assemblages of Gesher Benot Ya'aqov: inter-site variability. J. Hum. Evol. 60, 357–374. http://dx.doi.org/10.1016/j.jhevol.2010.12.002.
Rabinovich, R., Gaudzinski, S., Goren-Inbar, N., 2008. Systematic butchering of fallow deer (Dama) at the Early Middle Pleistocene Acheulian site of Gesher Benot Ya'aqov, (Israel). J. Hum. Evol. 54, 134–149.
Reille, M., 1995. Pollen et spores d'Europe et d'Afrique du Nord: Supplément 1. Laboratoire de Botanique Historique et Palynologie, Marseille.
Reille, M., 1998. Pollen et spores d'Europe et d'Afrique du Nord: Supplément 2. Laboratoire de Botanique Historique et Palynologie, Marseille.
Reille, M., 1999. Pollen et spores d'Europe et d'Afrique du Nord: Index. Laboratoire de Botanique Historique et Palynologie, Marseille.
Renne, P.R., Balco, G., Ludwig, K.R., Mundil, R., Min, K., 2011. Response to the comment by W.H. Schwarz et al. on "joint determination of K-40 decay constants and Ar-40*/K-40 for the fish canyon sanidine standard, and improved accuracy for Ar-40/Ar-39 geochronology" by PR Renne et al. (2010). Geochim. Cosmochim. Acta 75, 5097–5100.
Rosenfeld, A., Nathan, Y., Feibel, C.S., Schilman, B., Halicz, L., Goren-Inbar, N., Siman-Tov, R., 2004. Palaeoenvironment of the Acheulian Gesher Benot Ya'aqov Pleistocene lacustrine strata, northern Israel - lithology, ostracod assemblages and ostracod shell geochemistry. J. Afr. Earth Sci. 38, 169–181. http://dx.doi.org/10.1016/j.jafrearsci.2003.10.008.
Sharon, G., 2007. Acheulian Large Flake Industries: Technology, Chronology, and Significance. BAR International Series, Oxford.
Sharon, G., Feibel, F., Alperson-Afil, N., Harlavan, Y., Feraud, G., Ashkenazi, S., Rabinovich, R., 2010. New evidence for the northern Dead Sea rift Acheulian. PaleoAnthropology 2010, 79–99. http://dx.doi.org/10.4207/PA.2010.ART35.
Sharon, G., Alperson-Afil, N., Goren-Inbar, N., 2011. Cultural conservatism and variability in the Acheulian sequence of Gesher Benot Ya'aqov. J. Hum. Evol. 60, 387–397. http://dx.doi.org/10.1016/j.jhevol.2009.11.012.
Snyder, S.W., Huber, B.T., 1996. Preparation Techniques for Use of Foraminifera in the Classroom [WWW Document]. http://www.ucmp.berkeley.edu/fosrec/Snyder&Huber.html, Accessed date: 3 March 2010.
Spiro, B., Sharon, G., 2008. Preliminary report on the handling, sampling and storing of the geological core #2-2006 from Gesher Benot Ya'aqov. In: Unpublished Project Report (IAA Project 37782-0).
Spiro, B., Ashkenazi, S., Mienis, H.K., Melamed, Y., Feibel, C., Delgado, A., Starinsky, A., 2009. Climate variability in the Upper Jordan Valley around 0.78 Ma, inferences from time-series stable isotopes of Viviparidae, supported by mollusc and plant palaeoecology. Palaeogeogr. Palaeoclimatol. Palaeoecol. 282, 32–44. http://dx.doi.org/10.1016/j.palaeo.2009.08.005.
Spiro, B., Ashkenazi, S., Starinsky, A., Katz, A., 2011. Strontium isotopes in Melanopsis sp. as indicators of variation in hydrology and climate in the Upper Jordan Valley during the Early–Middle Pleistocene, and wider implications. J. Hum. Evol. 60, 407–416.
Suc, J.-P., Popescu, S.-M., 2005. Pollen records and climatic cycles in the North Mediterranean region. In: Head, M.J., Gibbard, P.L. (Eds.), Early–Middle Pleistocene Transitions: The Land–Ocean Evidence. Geological Society of Londonpp. 147–158. http://dx.doi.org/10.1144/GSL.SP.2005.247.01.08.
Tzedakis, P.C., Hooghiemstra, H., Pälike, H., 2006. The last 1.35 million years at Tenaghi Philippon: revised chronostratigraphy and long-term vegetation trends. Quat. Sci. Rev. 25, 3416–3430.
Van Zeist, W., Bottema, S., 1991. Late Quaternary vegetation of the Near East. Beihefte zum Tübinger Atlas des Vorderen Orients. Reihe A (Naturwissenschaften) Nr. 18. Dr. Ludwig Reichert Verlag, Wiesbaden.
Van Zeist, W., Bottema, S., 2009. A palynological study of the Acheulian site of Gesher Benot Ya'aqov, Israel. Veg. Hist. Archaeobotany 18, 105–121. http://dx.doi.org/10.1007/s00334-008-0167-5.
Van Zeist, W., Baruch, U., Bottema, S., 2009. Holocene palaeoecology of the Hula area, northeastern Israel. In: Kaptijn, E., Petit, L.P. (Eds.), A Timeless Vale. Archaeological and Related Essays on the Jordan Valley in Honour of Gerrit van Der Kooij on the Occasion of His Sixty-fifth Birthday. Leiden University Press, Leiden, pp. 29–64.
Wagner, C.W., 1957. Sur les ostracodes du Quaternaire récent des Pays-Bas et leur utilisation dans l'étude géologique des dépôts Holocènes. Mouton & Co., 'S-Gravenhage.
Zhou, L.P., Shackleton, N.J., 1999. Misleading positions of geomagnetic reversal boundaries in Eurasian loess and implications for correlation between continental and marine sedimentary sequences. Earth Planet. Sci. Lett. 168, 117–130.
Zohar, I., Goren, M., Goren-Inbar, N., 2014. Fish and ancient lakes in the Dead Sea rift: the use of fish remains to reconstruct the ichthyofauna of paleo-lake Hula. Palaeogeogr. Palaeoclimatol. Palaeoecol. 405, 28–41. http://dx.doi.org/10.1016/j.palaeo.2014.04.006.
Zohary, M., 1982. Beihefte zum Tübinger Atlas des Vorderen Orients. Reihe A, No. 7: Vegetation of Israel and Adjacent Areas. Dr. Ludwig Reichert Verlag, Wiesbaden.
Zohary, M., Orshansky, G., 1947. The vegetation of the Huleh plain. Palest. J. Bot. 4, 90–104.

Curriculum Vitae

Name : Maria Sekar Proborukmi
Birth- place and date : Yogyakarta and 29th July 1985

Education:

2000–2003	High school, SMU Stella Duce 1, Yogyakarta-Indonesia.
2003–2007	Bachelor of engineering (ST), geological engineering, Institut Teknologi Bandung, Bandung-Indonesia.
2008–2010	Master of science (MSc.), reservoir engineering and petroleum geosciences, École Nationale Supérieure Géologie, Institut National Polytechnique de Lorraine, Nancy-France.
2012–present	PhD student, faculty of Sustainability Science, Leuphana University of Lüneburg, Lüneburg, Germany.